

This electronic thesis or dissertation has been downloaded from the King's Research Portal at <https://kclpure.kcl.ac.uk/portal/>



## Modulation of B Lymphocytes and Antibody Responses to Solid Tumours

Harris, Robert

*Awarding institution:*  
King's College London

The copyright of this thesis rests with the author and no quotation from it or information derived from it may be published without proper acknowledgement.

### END USER LICENCE AGREEMENT



Unless another licence is stated on the immediately following page this work is licensed

under a Creative Commons Attribution-NonCommercial-NoDerivatives 4.0 International

licence. <https://creativecommons.org/licenses/by-nc-nd/4.0/>

You are free to copy, distribute and transmit the work

Under the following conditions:

- Attribution: You must attribute the work in the manner specified by the author (but not in any way that suggests that they endorse you or your use of the work).
- Non Commercial: You may not use this work for commercial purposes.
- No Derivative Works - You may not alter, transform, or build upon this work.

Any of these conditions can be waived if you receive permission from the author. Your fair dealings and other rights are in no way affected by the above.

### Take down policy

If you believe that this document breaches copyright please contact [librarypure@kcl.ac.uk](mailto:librarypure@kcl.ac.uk) providing details, and we will remove access to the work immediately and investigate your claim.

# **Modulation of B Lymphocytes and Antibody Responses to Solid Tumours**

A Thesis submitted to the Faculty of Life Sciences & Medicine of the University of London for the degree of Doctor of Philosophy

By

**Robert John Harris**

St John's Institute of Dermatology  
School of Basic & Medical Biosciences  
King's College London

December 2021

## **Declaration**

The work herein presented is my own and all experiments, except where acknowledged, were performed by myself.

## **Acknowledgements**

I would first like to express my utmost gratitude to my supervisor Prof. Sophia Karagiannis for her unwavering support, advice, and optimism throughout my PhD. Her encouragement and open door have been a constant throughout the last four years, and I have been lucky to have a supervisor with vast knowledge and insights to guide and challenge me in my research. I would also like to thank my second and third supervisors, Dr. Katie Lacy and Prof. James Spicer, for their advice and critique, and helping to shape my investigations.

I am grateful to members of the Karagiannis lab, both past and present, for their friendship and always being willing to help with a spare reagent or advice on an experiment. I would like to thank Dr. Anthony Cheung and Dr. Silvia Crescioli for helping me to get started in the lab and for their continued support during my PhD journey.

I am grateful to those who have collaborated with me during my PhD and contributed with valuable pieces of data and scientific insights. These include Roman Laddach, whose enthusiasm for computational biology is infectious, and whose rich source of computational insights has facilitated a deeper understanding of the key questions of this Thesis. I also thank Dr. Anita Grigoriadis, Dr. Sophia Tsoka, and Prof. Franca Fraternali for their assistance and scientific expertise, and Dr. Zena Willsmore, Dr. Joseph Ng, Elena Alberts and Dr. Alicia Chenoweth for their advice and pieces of data acknowledged herein.

My thanks also go to members of the BRC flow core, including Dr Anna Rose, Dr Isabel Correa, Leanne Farnan and Rianne Wester, as well as Dr Virginia Silio at the Nikon Imaging Centre, for their help with training and technical expertise.

I have been fortunate to have had access to a steady stream of clinical samples to facilitate my research. This has been made possible by the tenacious work of those at Guy's and St Thomas's NHS Trust (GSTT) Oncology and St John's Institute of Dermatology and Early Phase Clinical Trials Unit, in particular Dr. Sara Lombardi, Anna Black, Dr. Mano Nakamura, Atousa Khiabany, Harriet Gilbert-Jones, and Jitesh Chauhan. I also extend my thanks to all patients and healthy volunteers for whom samples have been analysed in my experiments. Your consent and willingness to contribute to our understanding of immuno-oncology will not be forgotten.

I would also like to express my heartfelt gratitude to my parents and brothers for their continued support, and joyous company throughout the last four years. Lastly, to my partner Zoe, for always being there for me during the best times and the worst, and for providing her patience and understanding as I grappled with my PhD.

## **Abstract**

B lymphocytes (B cells) are widely known to be important players within the context of adaptive immunity and may contribute to immune responses through expression of immunoglobulin (Ig), antigen presentation to CD4<sup>+</sup> and CD8<sup>+</sup> T cells, and production of effector cytokines. Moreover, in patients with solid tumours, initiation of effective humoral immunity may contribute to tumour growth restriction through specific antigen-directed responses. This Thesis investigates the complex and dynamic roles of B cells in immune responses to solid tumours, with specific focus on immunogenic tumours such as melanoma and subsets of breast cancer. Overall, I aimed to identify novel features and biases among circulating and tumour-infiltrating B lymphocyte (TIL-B) populations, to elucidate their roles and functional significance, and to place these findings within the wider context of the adaptive immune response.

In breast cancer, I used flow cytometric, transcriptomic, fluorescence immunohistochemistry (IHC), single-cell RNA-seq and long-read Ig repertoire studies to evaluate isotype-switched and memory B cell subsets, Ig isotype distribution, and clonal expansion profiles within the circulation and lesions of patients. Isotype-switched and activatory B cell signatures were enhanced among breast TIL-B. Quantitative IHC showed that TIL-B frequently form stromal clusters with T lymphocytes (T cells), and single cell transcriptomic analyses suggested that B and T cells in tumours engage in bidirectional crosstalk. TIL-B-rich tumours demonstrated expansion of IgG isotypes, and IgG isotype-switching was found to be positively associated with survival outcomes, especially in the aggressive triple-negative breast cancer (TNBC) subtypes. Long-read Ig repertoire analysis also indicated that B cell clonal expansion was biased towards IgG, showing expansive clonal families with specific variable region gene combinations and

narrow variable region repertoires. Lastly, stronger selection pressure was present in the complementarity determining regions of IgG compared to their clonally related IgA in tumour samples.

In melanoma, I used CyTOF, intracellular cytokine assays, transcriptomic, fluorescence IHC, single-cell RNA-seq and *ex vivo* co-culture analyses to investigate the phenotype and functional significance of cytokine-expressing B cells in patients with melanoma, including regulatory (IL-10 and/or TGF- $\beta$ -expressing) and pro-inflammatory (IFN- $\gamma$  and/or TNF- $\alpha$ -expressing) subsets. Using CyTOF analyses, circulating regulatory B cell populations (IL-10<sup>+</sup> plasmablasts and TGF- $\beta$ <sup>+</sup> naïve B cells) were found to be enhanced in melanoma patients compared with a matched healthy volunteer cohort. In concert, intracellular cytokine assay phenotyping revealed a collapse in TNF- $\alpha$ -expressing B cells in melanoma patient compared to healthy volunteer blood. In concordance, TNF- $\alpha$ -expressing B cells were rare among TIL-B. Contrasting to a sparse TNF- $\alpha$ -expressing B cell population, single-cell RNAseq analyses revealed prominent TGF- $\beta$ -expressing B cell populations in the melanoma tumour microenvironment. CellPhoneDB analyses predicted signaling with Tregs via the immune checkpoint receptor Galectin-9. The less well represented tumour-infiltrating TNF- $\alpha$ -expressing B cells were also predicted to engage in crosstalk with Tregs and may point to potential suppressive activity via TNF- $\alpha$  signaling and the ICOS/ICOSL axis. Lastly, in *ex vivo* co-cultures, patient-derived B cells enhanced the proliferation of autologous T-helper cells, an effect further enhanced with programmed cell death protein 1 (PD-1) blockade, and allowed T-helper cells to express pro-inflammatory Th1 cytokines (IFN- $\gamma$  and TNF- $\alpha$ ). Patient B cells could also induce FOXP3<sup>+</sup> Tregs from conventional T-helper (Tcon) cells in a TGF- $\beta$ -dependent manner.

In summary, my findings have established contrasting immunostimulatory and immunomodulatory roles of B cells in their response to solid tumours. In breast cancer, and particularly in TNBC patients, B cells and their connected functional signatures were associated with improved clinical outcomes. Isotype-switched B cell lineage traits were prevalent and conferred IgG-biased, clonally expanded, and likely antigen-driven humoral responses. In melanoma, my findings point to a dysregulated cytokine-expressing B cell compartment both in the circulation and in melanoma lesions, favouring regulatory as opposed to pro-inflammatory phenotypes. Within the tumour, cytokine-expressing B cells may engage in crosstalk with and promote Tregs. Furthermore, patient B cells can exert a combination of immunostimulatory and immunomodulatory influences upon autologous T-helper cells in *ex vivo* culture including expansion of Tregs.

Overall, my findings have unravelled previously unknown features of B cell responses to melanoma and breast cancer, which could help to inform the development of novel therapeutics.



## Abbreviations

Abbreviation	Meaning
ADCC	Antibody-dependent cellular cytotoxicity
ADCP	Antibody-dependent cellular phagocytosis
AID	Activation-induced cytidine deaminase
AJCC	American Joint Committee on Cancer
Allo-SCT	Allogeneic Stem Cell Transplantation
AMORIS	Apolipoprotein-related MORTality RISK
ANOVA	Analysis of variance
APC	Antigen presenting cell
BCC	Basal cell carcinoma
BCR	B cell receptor
Bm	Memory B cell
Breg	Regulatory B cell
BSA	Bovine serum albumin
CCL	Chemokine (C-C motif) ligand
CD	Cluster of differentiation
CDK	Cyclin-dependent kinases
CDR	Complementarity-determining region
CLA	Cutaneous leucocyte-associated antigen
CM	Central memory
CPI	Checkpoint inhibitor
CTL	Cytotoxic T lymphocyte
CTLA4	Cytotoxic T-Lymphocyte Associated Protein 4
CXCL	Chemokine (C-X-C motif) ligand
DAPI	4',6-diamidino-2-phenylindole
DEG	Differential expression gene
DMEM	Dulbecco's Modified Eagle Medium
DMFS	Distant metastasis-free survival (DMFS)
DMSO	Dimethyl sulfoxide
DNA	Deoxyribonucleic acid
EDTA	Ethylenediaminetetraacetic acid
ELISA	Enzyme-linked immunosorbent assay
EM	Effector memory
ER	Oestrogen receptor
FACS	Fluorescence-activated single cell sorting
FBS	Foetal bovine serum

Abbreviation	Meaning
Fc	Fc-receptor binding region
FC	Fold change
FDA	Food and Drug Administration
FDR	False discovery rate
FFPE	Formalin-fixed, paraffin-embedded
FMO	Fluorescence minus one
FOXP3	Forkhead box P3
FWR	Framework region
GC	Germinal centre
G-CSF	Granulocyte colony stimulating factor
GEx	Gene expression
GO	Gene ontology
GSEA	Gene Set Enrichment Analysis
GSTT	Guy's and St Thomas's NHS Trust
GVHD	Graft versus host disease
HER2	Human epidermal growth factor receptor 2
HLA	Human leukocyte antigen
HR	Hormone receptor
HSC	Hematopoietic stem cell
HV	Healthy volunteer
ICOS	Inducible T-cell co-stimulator
ICOSL	Inducible T-cell co-stimulator ligand
IF	Immunofluorescence
IFN	Interferon
Ig	Immunoglobulin
IHC	Immunohistochemistry
IL	Interleukin
ILB	Innate-like B cell
IM	Immunomodulatory
KCL	King's College London
KM	Kaplan-Meier
LAR	Luminal androgen receptor
LDH	Lactate dehydrogenase
LPS	Lipopolysaccharide
LT	Lymphotoxin
MAPK	Mitogen-activated protein kinase
MDSC	Myeloid-derived suppressor cell
MHC	Major histocompatibility complex
MIF	Macrophage migration inhibitory factor

Abbreviation	Meaning
MISST	Melanoma Immunomodulation and Immune Responses of the Skin Study: A Translational Science Research Protocol
MZ	Marginal zone
NANT	Non-adjacent non-tumour
NICE	National Institute for Health and Care Excellence
NK	Natural killer
NMSC	Non-melanoma skin cancer
NSCLC	Non-small cell lung cancer
ODN	Oligodeoxynucleotide
PB	Plasmablast
PBMC	Peripheral blood mononuclear cell
PBS	Phosphate-buffered saline
PD-1	Programmed cell death protein 1
PD-L1	Programmed death-ligand 1
PMA	Phorbol myristate acetate
pMHCII	MHC-peptide complex
PR	Progesterone receptor
RAG	Recombination-activating gene
RBC	Red blood cell
RNA	Ribonucleic acid
RPMI	Roswell Park Memorial Institute
RT	Room temperature
RT-PCR	Reverse transcription polymerase chain reaction
SCC	Squamous cell carcinoma
SEM	Standard error of mean
SEREX	Serological identification of antigens by recombinant expression cloning
SHM	Somatic hypermutation
SLNB	Sentinel lymph node biopsy
TAA	Tumour-associated antigen
TBS	Tris-buffered saline
TCGA	The Cancer Genome Atlas
Tcon	Conventional T cell
TCR	T cell receptor
TGF	Transforming growth factor
T-I	Thymus Independent Antigen
TIL	Tumour-infiltrating lymphocyte
TIL-B	Tumour-infiltrating B lymphocyte
TIL-T	Tumour-infiltrating T lymphocyte

Abbreviation	Meaning
TLR	Toll-like receptor
TLS	Tertiary lymphoid structure
TME	Tumour microenvironment
TNBC	Triple-negative breast cancer
TNF	Tumour necrosis factor
TNFR	Tumour necrosis factor receptor
TNM	Tumour, Node, Metastasis
TrB	Transitional B cell
Treg	Regulatory T cell
tSNE	t-distributed stochastic neighbour embedding
UMAP	Uniform Manifold Approximation and Projection
VEGF	Vascular endothelial growth factor
WLE	Wide-local excision

## **Table of Contents**

<b>Declaration</b> .....	<b>2</b>
<b>Acknowledgements</b> .....	<b>3</b>
<b>Abstract</b> .....	<b>5</b>
<b>Abbreviations</b> .....	<b>8</b>
<b>List of Figures</b> .....	<b>18</b>
<b>List of Tables</b> .....	<b>22</b>
<b>Chapter 1: Introduction</b> .....	<b>24</b>
1.1 Cancer epidemiology and outlook .....	24
1.1.1 Breast cancer .....	25
1.1.2 Melanoma.....	32
1.1.3 Breast cancer treatment overview .....	36
1.1.3.1 Early (stage I/II) and locally advanced (stage III) breast cancer management .....	37
1.1.3.2 Advanced (stage IV) breast cancer management.....	39
1.1.4 Melanoma treatment overview.....	40
1.1.4.1 Early (stage 0-II) melanoma management.....	40
1.1.4.2 Regional (stage III) and advanced (stage IV) melanoma management ..	41
1.1.5 The future of cancer therapy .....	43
1.2 B cells and their functions in human immunity .....	45
1.2.1 B cell development.....	45
1.2.1.1 Antigen-independent and antigen-dependent B cell development.....	45
1.2.2 B cells as antibody producing cells.....	52
1.2.2.1 Antibody isotype distribution.....	53
1.2.2.2 Functions of antibodies .....	55
1.2.2.2.1 Neutralisation .....	55
1.2.2.2.2 Antibody-dependent cellular cytotoxicity and phagocytosis .....	56
1.2.2.2.3 Complement activation .....	57
1.2.3 B cells as antigen presenting cells.....	57
1.2.4 B cells as cytokine expressors.....	58

1.2.4.1 Regulatory B cells .....	59
1.2.4.1.1 Regulatory B cells in non-cancerous disease .....	61
1.3 Systemic immunity in cancer .....	63
1.3.1 Perturbations of systemic immunity in breast cancer and melanoma .....	63
1.3.2 Systemic immune predictive biomarkers in breast cancer and melanoma ....	66
1.4 The tumour microenvironment .....	69
1.4.1 Th2-bias in the tumour microenvironment .....	70
1.4.2 Tertiary Lymphoid Structures .....	71
1.4.3 Anti- and pro-tumour roles of B cells in different cancers .....	72
1.5 Breast tumour-infiltrating B lymphocytes .....	73
1.6 Melanoma tumour-infiltrating B lymphocytes .....	76
1.6.1 Mechanisms of the humoral immune response and expressed antibody effector functions in melanoma.....	79
1.6.1.1 Antibody expression among melanoma tumour-reactive B cells .....	79
1.6.1.2 IgG4 subclass switching as an immune evasion mechanism .....	84
1.7 Regulatory B cells in cancer .....	86
1.7.1 Regulatory B cells in skin inflammation and cancer .....	87
1.8 Aims and Objectives .....	88
<b>Chapter 2: Materials and Methods .....</b>	<b>91</b>
2.1 Human tissue samples and processing .....	91
2.1.1 General reagents.....	91
2.1.2 Human tissue sample collection.....	91
2.1.3 Serum collection and processing.....	92
2.1.4 Tumour, NANT and normal tissue processing .....	92
2.2 Immune cell isolation.....	93
2.2.1 General reagents.....	93
2.2.2 Antibodies .....	94
2.2.3 Peripheral Blood Mononuclear Cell isolation.....	95
2.2.4 Positive isolation of B and T-helper cells from HV and melanoma patient peripheral blood .....	96
2.2.5 Isolation of purified B and T-helper cells from HV and melanoma patient peripheral blood mononuclear cells by negative selection .....	98
2.3 B cell phenotyping using flow cytometry .....	99

2.3.1 General reagents.....	99
2.3.2 Antibodies .....	100
2.3.3 Phenotyping of memory and isotype-switched B cells from HV and breast cancer patient peripheral blood and breast tissues .....	101
2.3.4 B cell intracellular cytokine phenotyping in HV and melanoma patient peripheral blood, and melanoma tumours .....	103
2.3.4.1 Dimensionality reduction of B cell lineage phenotyping data using the tSNE and FlowSOM Algorithms .....	106
2.3.5 B cell CyTOF phenotyping of HV and melanoma patient peripheral blood	106
2.3.6 Flow cytometry panel optimisations .....	107
2.3.6.1 Compensation of fluorescence spillover .....	107
2.3.6.2 Antibody titrations .....	107
2.3.6.3 Fluorescence minus one .....	108
2.4 Ex vivo B cell functional studies .....	109
2.4.1 General reagents.....	109
2.4.2 Antibodies .....	110
2.4.3 Ex vivo B cell functional studies of melanoma patient circulating B cells .	110
2.4.3.1 Cytokine suppression assay.....	111
2.4.3.2 T-helper cell proliferation assay.....	113
2.4.3.3 Treg induction assay .....	114
2.5 Gene expression and immunoglobulin repertoire profiling .....	115
2.5.1 Bulk gene expression profiling of lymphocyte and lymphoid assembly markers in breast tumours .....	115
2.5.1.1 KM plotter prospective cohort study.....	115
2.5.1.2 CIBERSORT analysis of tumour-infiltrating B lymphocyte subsets ...	116
2.5.2 Single-cell RNA-sequencing (scRNA-seq) analysis of breast cancer circulating and tumour-infiltrating B lymphocytes.....	117
2.5.3 Single-cell RNA-sequencing (scRNA-seq) analysis of melanoma tumour-infiltrating B lymphocytes .....	118
2.5.4 Long-read immunoglobulin repertoire analysis of breast cancer and normal breast tissues .....	119
2.6 Serum antibody isotype profiling.....	120
2.6.1 General reagents.....	120

2.6.2 7-plex antibody isotyping of HV and breast cancer patient serum .....	120
2.6.3 AMORIS analysis of Ig isotype titres in breast cancer patient serum .....	121
2.7 Fluorescence immunohistochemistry .....	121
2.7.1 General reagents .....	121
2.7.2 Antibodies .....	122
2.7.3 Fluorescence immunohistochemistry evaluation of breast TIL-B localisation and immunoglobulin isotype expression.....	123
2.7.3.1 Preparation, antigen retrieval, and staining of FFPE tissues.....	124
2.7.3.2 Quantitative technique for determination of TIL-B densities .....	125
2.7.4 Fluorescence immunohistochemistry evaluation of melanoma tumour- infiltrating IL-10 <sup>+</sup> regulatory and TNF- $\alpha$ <sup>+</sup> inflammatory B cells.....	126
2.7.4.1 Preparation and staining of frozen tissues.....	126
2.8 Statistical methods .....	127

**Chapter 3: B Lymphocyte Subsets, Immunoglobulin Isotype Expression, and  
Clonal Features in Breast Cancer..... 128**

3.1 Introduction .....	128
3.2 Hypothesis, objectives, and published work .....	130
3.2.1 Hypothesis.....	130
3.2.2 Objectives.....	130
3.2.3 Published Work.....	131
3.3 Patient and healthy volunteer cohort characteristics .....	132
3.4 Results .....	133
3.4.1 Collapse in circulating memory B cells contrasts with amplification of intratumoural class-switched memory B cell compartment in breast cancer.....	133
3.4.2 TIL-B signatures and assembly within stromal clusters are elevated in TNBC compared with other breast cancer subtypes.....	140
3.4.3 Breast tumour-infiltrating B lymphocytes are activated via the B Cell Receptor .....	146
3.4.4 IgG <sup>+</sup> B cell densities are elevated in TNBC, and IgG isotype-switching predicts positive survival outcomes in TNBC .....	150
3.4.5 IgG-biased, clonally-expanded, immunoglobulin repertoires in breast cancer .....	160
3.5 Discussion and future directions .....	164



<b>Chapter 4: Phenotype and Functional Significance of Regulatory and Inflammatory B Lymphocytes In Melanoma .....</b>	<b>170</b>
4.1 Introduction .....	170
4.2 Hypothesis and objectives.....	172
4.2.1 Hypothesis.....	172
4.2.2 Objectives.....	173
4.3 Patient and healthy volunteer cohort characteristics.....	174
4.4 Results .....	175
4.4.1 Enrichment in TGF- $\beta$ -expressing naïve B cells and IL-10-expressing plasmablasts contrasts with diminished IFN- $\gamma$ and TNF- $\alpha$ <sup>+</sup> inflammatory B cells in melanoma patient peripheral blood.....	175
4.4.2 Cytokine expression among the whole melanoma patient circulating B cell compartment is preferentially associated with CD27 <sup>+</sup> memory subsets.....	181
4.4.3 TGF- $\beta$ -expressing Bregs infiltrate melanoma patient tumours, while TNF- $\alpha$ -expressing B cells are proportionally lower in the tumour-infiltrating B lymphocyte populations compared to the circulation .....	185
4.4.4 Evidence for associations and crosstalk between B cells and Bregs with T cells in the tumour microenvironment .....	188
4.4.5 Melanoma patient peripheral blood-derived B cells support the proliferation of autologous T-helper cells in ex vivo co-culture, but do not regulate Th1 cytokine expression.....	193
4.4.6 Melanoma patient peripheral blood-derived B cells induce TGF- $\beta$ -mediated differentiation of autologous FOXP3 <sup>+</sup> Tregs from conventional T cells in ex vivo co-culture, and naïve TGF- $\beta$ <sup>+</sup> Bregs associate with unfavourable survival outcomes .....	196
4.5 Discussion and future directions .....	199
<b>Chapter 5: Discussion and Future Directions .....</b>	<b>207</b>
5.1 Introduction .....	207
5.2 The role of circulating and tumour-infiltrating B lymphocytes in breast cancer	208
5.2.1 Evidence for systemic perturbations of humoral immunity and for active roles of B cells in breast cancer .....	209
5.2.2 IgG-biased and clonally skewed profiles in the anti-tumour immune response in breast cancer.....	212

5.2.3 B cells and their functional profiles as prognostic biomarkers in breast cancer .....	215
5.2.4. Graphical summary .....	218
5.3 Cytokine-expressing B cells as complex and dynamic players in systemic and intratumoural immunity of patients with melanoma.....	220
5.3.1 Dysregulation and lineage sources of cytokine-expressing B cells in the peripheral blood of melanoma patients .....	221
5.3.2 An immune dichotomy: Immunostimulatory and immunomodulatory influences of B cells in melanoma .....	225
5.3.3 Graphical summary .....	228
5.4 Concluding remarks .....	230
<b>Appendix .....</b>	<b>234</b>
<b>References .....</b>	<b>270</b>
<b>Articles .....</b>	<b>296</b>

## **List of Figures**

### **Chapter 1: Introduction**

Figure 1.1 Breast cancers can be categorised into five biologically distinct subtypes. ...	27
Figure 1.2 Illustration of the three most common types of skin cancer. ....	32
Figure 1.3 Schematic representation of the early human B cell development hierarchy. ....	46
Figure 1.4 Schematic representation of T cell-independent B cell activation in response to multivalent T-independent (T-I) antigens. ....	48
Figure 1.5 Schematic representation of T cell-dependent B cell activation in response to tumour-associated antigens (TAA). ....	49
Figure 1.6 Overview of the key stages of B cell development following T cell-dependent B cell activation. ....	51
Figure 1.7 Human antibody isotype structure and glycosylation sites. ....	54
Figure 1.8 Landscape of the tumour microenvironment. ....	70
Figure 1.9 Summary of studies to-date analysing the prognostic significance of tumour-infiltrating B lymphocytes in patients with solid tumours. ....	73
Figure 1.10 Melanoma patient peripheral blood B cells produce IgG antibodies to autoantigens ex vivo. ....	81
Figure 1.11 IgG subclass switching, clonal selection and somatic hypermutation among melanoma tumour-infiltrating B lymphocytes. ....	83
Figure 1.12 IgG4 subclass switching as an immune evasion mechanism in patients with melanoma. ....	85

### **Chapter 2: Materials and Methods**

Figure 2.1 Gating strategy and purity check for the positive isolation of CD19 <sup>+</sup> B cells and CD4 <sup>+</sup> T-helper cells from the peripheral blood of healthy volunteers and melanoma patients using the BD FACS Aria II cell sorter. ....	97
---	----

Figure 2.2 Gating strategy for the positive isolation of CD4 <sup>+</sup> CD25 <sup>-/int</sup> CD127 <sup>+</sup> non-Treg (conventional) T cells from the peripheral blood of healthy volunteers and melanoma patients using the BD FACS Aria II cell sorter. ....	98
Figure 2.3 Gating strategy for the detection and quantification of memory and isotype-switched B cell phenotypes in HV and breast cancer patient peripheral blood, and breast tissue.....	102
Figure 2.4 Gating strategy for the detection and quantification of B cell cytokine expression profiles among key B cell subpopulations in HV and melanoma patient peripheral blood, and melanoma tumours.....	104
Figure 2.5 Example antibody titration for optimisation of assay resolution.....	108
Figure 2.6 Schematic representation of ex vivo B cell functional studies of melanoma patient circulating B cells contained within this Thesis.....	111

### **Chapter 3: B Lymphocyte Subsets, Immunoglobulin Isotype Expression, and Clonal Features in Breast Cancer**

Figure 3.1 Flow cytometric analyses reveal reduced circulating CD20 <sup>+</sup> CD27 <sup>+</sup> memory and amplification of breast tumour-infiltrating CD20 <sup>+</sup> CD27 <sup>+</sup> IgD <sup>-</sup> isotype-switched subsets among B cells. ....	135
Figure 3.2 Serum IgG titres are collapsed in breast cancer patients following chemotherapy.....	136
Figure 3.3 Serum immunoglobulin isotype titres do not serve as a predictive marker for breast cancer-related mortality.....	137
Figure 3.4 CD27 <sup>+</sup> expression distribution and GC B cell marker expression across B cell populations analysed by single-cell gene expression and IHC/IF. ....	139
Figure 3.5 B cell infiltration and its positive prognostic value in TNBC.....	141
Figure 3.6 TIL-B, TIL-T and B cell recruitment markers in TNBC.....	143
Figure 3.7 Occurrence of B cells in stromal clusters. ....	146
Figure 3.8 scRNA-seq analysis reveals BCR-driven TIL-B activatory signatures and B cell lineage gene markers predict positive survival outcome.....	148
Figure 3.9 Expression data of genes that positively regulate key B cell functions.....	149
Figure 3.10 IHC staining demonstrate CD20 and IgD expression in normal breast and TNBC tumours.....	151

Figure 3.11 Quantitative fluorescence IHC reveals elevated IgG <sup>+</sup> :IgA <sup>+</sup> ratio within high TIL-B tumours, implicating expansion of IgG <sup>+</sup> B cells within TNBC tumour. microenvironment. ....	152
Figure 3.12 IHC staining demonstrates CD27 expression in isotype-switched TIL-B and presence of both memory/GC B and plasma IgG <sup>+</sup> B cells in TNBC. ....	154
Figure 3.13 Single cell RNA-seq data analysis reveals favor of IgG isotypes in TNBC and isotype-switching gene markers predict positive survival outcome. ....	156
Figure 3.14 IgCH transcripts of CD27 <sup>+</sup> B cells. ....	158
Figure 3.15 Expression data in TNBC of key genes known to positively regulate B cell isotype-switching. ....	159
Figure 3.16 B cell repertoire analyses of immunoglobulin isotype-switching and clonal expansion in breast cancers. ....	161
Figure 3.17 Immunoglobulin repertoire analysis of breast cancer samples. ....	163

## **Chapter 4: Phenotype and Functional Significance of Regulatory and Inflammatory B Lymphocytes In Melanoma**

Figure 4.1 TGF- $\beta$ -expressing naïve B cells and IL-10-expressing plasmablasts are enriched in melanoma patient peripheral blood compared to healthy volunteer peripheral blood. ....	178
Figure 4.2 Flow cytometric gating strategy for the identification of CD19 <sup>+</sup> B cells from peripheral blood mononuclear cells following ex vivo culture. ....	179
Figure 4.3 Flow cytometric evaluations of IL-10, IL-4, IFN- $\gamma$ , TNF- $\alpha$ , and TGF- $\beta$ expressing B cells in melanoma patient and compared to healthy volunteer peripheral blood. ....	180
Figure 4.4 Lineage analysis of B cells expressing each of IL-10, TGF- $\beta$ and TNF- $\alpha$ cytokines show wide phenotypic distribution, with preference towards a CD27 <sup>+</sup> memory phenotype and with TGF- $\beta$ <sup>+</sup> cells routinely non-isotype-switched. ....	183
Figure 4.5 Dimensionality reduction using the tSNE and FlowSOM Algorithms for lineage analysis of B cells expressing each of IL-10, TGF- $\beta$ and TNF- $\alpha$ . ....	184
Figure 4.6 TNF- $\alpha$ -expressing inflammatory B cell subsets are collapsed, while TGF- $\beta$ -expressing subsets are favored in melanoma lesions. ....	186
Figure 4.7 Immunofluorescence studies of melanoma lesions revealed limited presence of TNF- $\alpha$ -expressing, but detectable IL-10-expressing B cells within the metastatic melanoma tumour microenvironment. ....	187

Figure 4.8 Correlation of B and T cell densities in the tumour microenvironment in melanoma. ....	189
Figure 4.9 CellPhoneDB analysis of TGF- $\beta$ + [left] and TNF- $\alpha$ + [right] B cell:T cell predicted communication pathways in the tumour microenvironment. ....	190
Figure 4.10 TGF- $\beta$ and TNF- $\alpha$ -expressing B cells may engage in functional crosstalk with Tcon and Treg cells in the TME. ....	192
Figure 4.11 B cells derived from melanoma patient peripheral blood do not suppress Th1 (IFN- $\gamma$ and TNF- $\alpha$ ) cytokine expression. ....	194
Figure 4.12 B cells derived from melanoma patient peripheral blood enhance the proliferation of autologous T-helper cells ex vivo. ....	195
Figure 4.13 B cells derived from melanoma patient peripheral blood induce a FOXP3+ Treg phenotype from CD25-/-int CD127+ conventional T cells. ....	198

## **Chapter 5: Discussion and Future Directions**

Figure 5.1 Breast tumour-infiltrating B lymphocytes carry an expanding IgG isotype profile in TNBC, which associates with favourable clinical outcomes. ....	218
Figure 5.2 Cytokine-expressing B cells in melanoma are dysregulated in melanoma patient circulation, engage in crosstalk with Tregs in the TME, and engender immunostimulatory and immunomodulatory influences ex vivo. ....	228
Figure 5.3 Graphical summary of the key findings contained within this Thesis, highlighting the contrasting immunostimulatory and immunomodulatory roles of B cells within the context of the immune response to solid tumours. ....	230

## **List of Tables**

Table 1.1 Overview of breast cancer anatomic staging as determined by the TNM criteria. ....	28
Table 1.2 Overview of breast cancer clinical prognostic staging as determined by the anatomic stage, grade, and biomarker status.....	31
Table 1.3 Overview of melanoma staging as determined by the TNM criteria.....	35
Table 1.4 Peripheral immune perturbations observed in breast cancer, melanoma, or both. ....	64
Table 1.5 Peripheral immune predictive biomarkers in breast cancer and melanoma....	67
Table 1.6 List of studies to-date analysing the prognostic significance of tumour-infiltrating B lymphocytes and immunoglobulin expression in breast cancer patients. .	75
Table 1.7 List of studies to-date analysing the prognostic significance of tumour-infiltrating B lymphocytes and immunoglobulin expression in melanoma patients.....	78
Table 2.1 Reagents used for human tissue sample processing. ....	91
Table 2.2 Reagents used for immune cell isolation. ....	93
Table 2.3 In-house produced buffers used for immune cell isolation.....	94
Table 2.4 Antibodies used for immune cell isolation using the BD FACS Aria II cell sorter.....	95
Table 2.5 Reagents used for flow cytometric B cell phenotyping. ....	99
Table 2.6 In-house produced buffers used for flow cytometric B cell phenotyping.....	100
Table 2.7 Antibodies used for flow cytometric B cell phenotyping. ....	100
Table 2.8 Flow cytometry panel for detection and quantification of memory and isotype-switched B cells in healthy volunteer and breast cancer patient peripheral blood, and breast tissue. ....	101
Table 2.9 Flow cytometry panel for detection and quantification of B cell cytokine expression profiles among B cell lineage subpopulations. ....	103
Table 2.10 CyTOF phenotyping panel for identification of IL-10 and TGF- $\beta$ expressing regulatory B cell subsets in HV and melanoma patient peripheral blood.....	107
Table 2.11 Reagents used for ex vivo B cell functional studies. ....	109
Table 2.12 In-house produced buffers for ex vivo B cell functional studies. ....	109
Table 2.13 Antibodies used for ex vivo B cell functional studies. ....	110
Table 2.14 GO annotations for KM plotter prospective cohort study gene sets. ....	116
Table 2.15 Reagents used for serum antibody isotype profiling.....	120
Table 2.16 Reagents used for fluorescence immunohistochemistry evaluations.....	121
Table 2.17 In-house produced buffers used for fluorescence immunohistochemistry evaluations.....	122
Table 2.18 Antibodies used for fluorescence immunohistochemistry evaluations.....	122

Table 2.19 Fluorescence immunohistochemistry staining panels for identification of TILs, naïve B cells, and B cell immunoglobulin isotype expression within the breast TME. ....	124
Table 3.1 Summary of healthy volunteer (control) and breast cancer patient cohorts.	132
Table 4.1 Summary of healthy volunteer (control) and melanoma patient cohorts.....	174
Table 5.1 Summary of the prognostic significance of breast tumour-infiltrating B lymphocyte signatures, as analysed in this Thesis. ....	216



## **Chapter 1: Introduction**

### **1.1 Cancer epidemiology and outlook**

The GLOBOCAN analysis estimated that approximately 19.3 million new cases and a little under 10.0 million cancer-caused deaths occurred in 2020, making cancer a leading cause of morbidity and mortality in the world [1]. The burden of global cancer incidence and mortality is increasing, reflecting aging and expanding populations, as well as changes in risk factors associated with socioeconomic development. In contrast to the global trend, there has been an encouraging overall decline of cancer mortality rates in both men (-6.6%) and women (-4.5%) since 2015 in Europe, although trends have varied according to cancer type [2]. Where favourable trends have been observed, for example in breast and prostate cancers, key drivers have been attributed to improvements in screening, diagnosis and therapeutic strategies [2].

At its basic level, cancer is caused by dysregulation of cell cycle control mediated by mutations in the genetic code of somatic cells. Mutations in cell cycle control genes, such as P53, or proto-oncogenes, such as Ras, can enhance the ability of a cell to survive and proliferate. These genetic errors are known as driver mutations and can be mediated by faulty DNA replication or external environmental stimuli. It has been shown that between one and ten driver mutations are necessary to drive a normal cell to one that is uncontrollably dividing and has become cancerous [3], and the exact number of mutations is dependent upon the cancer type. On average, four driver mutations per individual drive breast carcinogenesis, while melanomas are typically driven by ten driver mutations, the vast majority of which are outside of currently known cancer genes.

Cancerous cells follow a progressive path of clonal selection, and driver mutations accumulate over time. If left unchecked, cancer cells can begin to escape their local confines and immunological surveillance, mediate immune suppression, and engender damaging effects all over the body. However, if clinical detection can be achieved, and we can understand the local and systemic immune response in individual patients and across patient cohorts, then we can rely upon an increasingly sophisticated arsenal of treatments, including immunotherapies, to eliminate and halt the spread of these cells.

Emerging and established immunotherapies in the clinic are heavily dependent upon our knowledge of how the immune system responds to tumour formation and progression, the systematics of the tumour microenvironment and the development of metastatic cancer.

### 1.1.1 Breast cancer

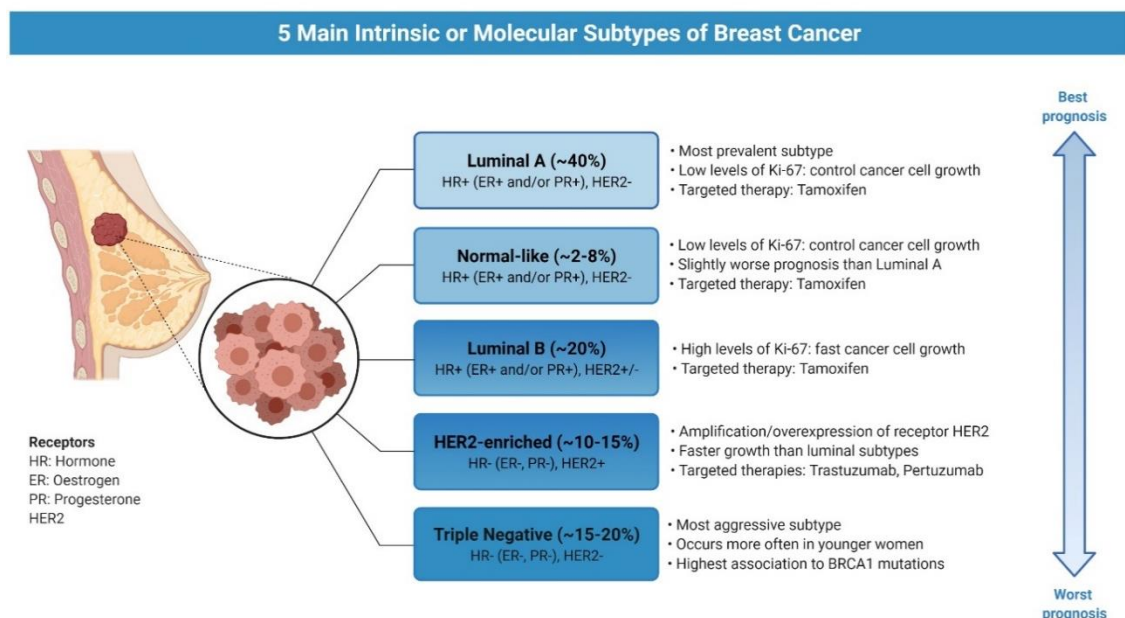
Female breast cancer is the most frequently occurring non-skin cancer globally [1], and cases are on the rise, with a projected 3.2 million cases worldwide per year by 2050 [4]. In 2020 there was an estimated 2.3 million global cases of female breast cancer, and 685,000 deaths, representing a startling increase of 35% and 31%, respectively, compared to cases and deaths in 2012 [1,5]. These increases have been driven in part by socio-economic factors including longer life expectancies, reduced physical activity and delays in childbearing [6], and incidence rates are over three times higher in Western Europe compared to Eastern Africa. On the other hand, breast cancer-related mortality rates have been declining since the early 1990s for women in Europe, driven by advances in

screening, diagnosis, and treatment [2], while there is considerable progress to be made in less developed nations.

Breast cancer is a highly heterogenous disease, taking on a wide range of pathological features, from slow growing to highly aggressive forms, and tumour aetiology can substantially affect survival outcomes [7]. Breast carcinomas represent over 99% of all breast cancers and arise from the epithelium, while sarcomas arise from stromal constituents of the breast. Breast cancers are routinely classified by their morphological characteristics, and subtypes include ductal, lobular, tubular, mucinous, medullary, and adenoid cystic carcinomas, although there is the potential for overlap between these categories, as a single tumour mass may contain malignant cells of diverse origin. The most common form is ductal carcinoma, which represents approximately 80% of breast cancers [8]. Tumours can be further sub-classified by histological grade, and those with higher grade are associated with larger, metastatic tumours.

Breast tumours are also routinely categorised according to their molecular subtype [9]. There are five biologically distinct subtypes which define breast cancers on a molecular level, which are illustrated in **Figure 1.1**. Luminal A and Luminal B which are oestrogen receptor (ER) positive subtypes, human epidermal growth factor receptor 2 (HER2) subtype, basal-like subtype, and normal-like subtype. HER2 and basal-like subtypes are usually aggressive and associated with poor prognosis in a stage-independent manner [10,11]. These subtypes are used for classification in the clinical setting, whereby tumour expression of ER, progesterone receptor (PR) and HER2 are monitored, although these evaluations do not fully recapitulate the intrinsic subtypes, which are based upon a wider range of molecular marker expression [12]. Nonetheless, identification of ER, PR and HER2 expression is key to guiding therapeutic strategies (discussed in Section

1.1.3). Importantly, 15-20% of all breast tumours [13] and 75-80% of basal-like subtype tumours [12] can be defined as ‘triple-negative’, reflecting their lack of ER, PR and HER2 expression. Patients with triple-negative breast cancers (TNBC) are unable to benefit from conventional treatments such as hormonal receptor blocker therapies, or specific targeted therapies such as the anti-HER2 monoclonal antibodies trastuzumab and pertuzumab, and therefore represent a pressing unmet clinical need for new biomarkers and therapies [14].



**Figure 1.1 Breast cancers can be categorised into five biologically distinct subtypes.**

Intrinsic subtypes are grouped according to expression of hormone receptors (oestrogen receptor (ER) and progesterone receptor (PR)) and the receptor tyrosine kinase human epidermal growth factor receptor 2 (HER2). Molecular subtypes determine severity of prognosis and can be used to guide therapeutic strategies. Adapted from “Intrinsic and Molecular Subtypes of Breast Cancer” by BioRender.com [15].

Besides the morphological characteristics, grade, and molecular subtype, breast cancers are classified by stage of tumour progression. The initial transition from *in situ* to invasive phenotype is defined by the loss of myoepithelial cell layer and basement membrane. Overall, breast carcinomas evolve via sequential progression through well-defined stages, beginning with epithelial hyperproliferation, and progressing through *in situ* (stage 0),

early (stage I-II), locally advanced (stage III) and advanced (stage IV) stages [16], the latter involving the spread of cancer cells to distant sites and resulting in diagnosis of metastatic disease [17].

Anatomic stages are clinically defined according to the American Joint Committee on Cancer (AJCC) TNM (tumour-node-metastasis) criteria, which considers the tumour size and spread to the skin or chest wall ('T'), trafficking to nearby lymph nodes ('N'), and metastasis to distant organs ('M') [18]. An overview of breast cancer anatomic staging from stage I to stage IV is illustrated in **Table 1.1**. The anatomic stage at diagnosis substantially influences survival rates (stage I, 98.5%; stage II, 90.2%; stage III, 74.2%; stage IV, 27.5% after 5-years [19]), and breast cancer awareness and screening programmes in Europe and elsewhere have been successful at supporting early detection and ensuring more favourable survival outcomes.

In recent years, sentiment has grown that purely anatomic staging fails to consider important non-anatomic features including tumour grade, hormone receptor status, and HER2 expression, and these key biomarkers, in addition to multigene panels, are now integrated into a clinical prognostic staging protocol [20], an overview of which is provided in **Table 1.2**.

**Table 1.1 Overview of breast cancer anatomic staging as determined by the TNM criteria.** Anatomic stages are determined from stage I to stage IV according to tumour characteristics (T), lymph node involvement (N), and distant metastatic spread (M) [18]. Stage I and II cancer is contained within breast tissue with possible micrometastases. By stage III, primary tumours (when evident) may be large, and cancer may have spread to auxiliary lymph nodes. Stage IV is the final stage, whereby the cancer has spread to distant lymph nodes, or organs such as the brain, lungs, liver, and bones.

Stage (TNM)	Physiological description
IA (T1-N0-M0)	Tumour $\leq$ 20 mm in greatest dimension
IB (T0-N1mi-M0)	No evidence of primary tumour, micrometastases (approximately 200 cells, 0.2 mm - 2.0 mm)
IB (T1-N1mi-M0)	Tumour $\leq$ 20 mm in greatest dimension, micrometastases (approximately 200 cells, 0.2 mm - 2.0 mm)
IIA (T0-N1-M0)	No evidence of primary tumour, micrometastases (approximately 200 cells, 0.2 mm - 2.0 mm)
IIA (T1-N1-M0)	Tumour $\leq$ 20 mm in greatest dimension, micrometastases (approximately 200 cells, 0.2 mm - 2.0 mm)
IIA (T2-N0-M0)	Tumour $>$ 20mm and $\leq$ 50 mm in greatest dimension
IIB (T2-N1-M0)	Tumour $>$ 20mm and $\leq$ 50 mm in greatest dimension, micrometastases (approximately 200 cells, 0.2 mm - 2.0 mm)
IIB (T3-N0-M0)	Tumour $>$ 50 mm in greatest dimension
IIIA (T0-N2-M0)	No evidence of primary tumour, metastases; or metastases in 4-9 axillary lymph nodes; or positive ipsilateral internal mammary lymph nodes by imaging in the absence of axillary lymph node metastasis
IIIA (T1-N2-M0)	Tumour $\leq$ 20 mm in greatest dimension, metastases; or metastases in 4-9 axillary lymph nodes; or positive ipsilateral internal mammary lymph nodes by imaging in the absence of axillary lymph node metastasis
IIIA (T2-N2-M0)	Tumour $>$ 20mm and $\leq$ 50 mm in greatest dimension, metastases; or metastases in 4-9 axillary lymph nodes; or positive ipsilateral internal mammary lymph nodes by imaging in the absence of axillary lymph node metastasis
IIIA (T3-N1-M0)	Tumour $>$ 50 mm in greatest dimension, micrometastases (approximately 200 cells, 0.2 mm - 2.0 mm)

IIIA (T3-N2-M0)	Tumour > 50 mm in greatest dimension, metastases; or metastases in 4-9 axillary lymph nodes; or positive ipsilateral internal mammary lymph nodes by imaging in the absence of axillary lymph node metastasis
IIIB (T4-N0-M0)	Tumour of any size with direct extension to the chest wall and/or to the skin (ulceration or macroscopic nodules); invasion of the dermis alone does not qualify as T4
IIIB (T4-N1-M0)	Tumour of any size with direct extension to the chest wall and/or to the skin (ulceration or macroscopic nodules), micrometastases (approximately 200 cells, 0.2 mm - 2.0 mm
IIIB (T4-N2-M0)	Tumour of any size with direct extension to the chest wall and/or to the skin (ulceration or macroscopic nodules), metastases; or metastases in 4-9 axillary lymph nodes; or positive ipsilateral internal mammary lymph nodes by imaging in the absence of axillary lymph node metastasis
IIIC (Any TN3-M0)	Metastases in 10 or more axillary lymph nodes; or in infraclavicular (Level III axillary) lymph nodes; or positive ipsilateral internal mammary lymph nodes by imaging in the presence of one or more positive Level I, II axillary lymph nodes; or in more than three axillary lymph nodes and micrometastases or macrometastases by sentinel lymph node biopsy (SLNB) in clinically negative ipsilateral internal mammary lymph nodes; or in ipsilateral supraclavicular lymph nodes, metastases greater than 0.2 mm
IV (Any T, Any N, M1)	Any histologically proven metastases in distant organs; or if in nonregional nodes, metastases greater than 0.2 mm

**Table 1.2 Overview of breast cancer clinical prognostic staging as determined by the anatomic stage, grade, and biomarker status.**

Clinical prognostic stage is assigned to all patients regardless of type of therapy administered. ER<sup>-</sup> = estrogen receptor-negative, ER<sup>+</sup> = ER-positive, G = grade, HER2<sup>-</sup> = HER2 negative, HER2<sup>+</sup> = HER2-positive, mi = micrometastasis, PR<sup>-</sup> = progesterone receptor-negative, PR<sup>+</sup> = PR-positive, Tis = in situ.

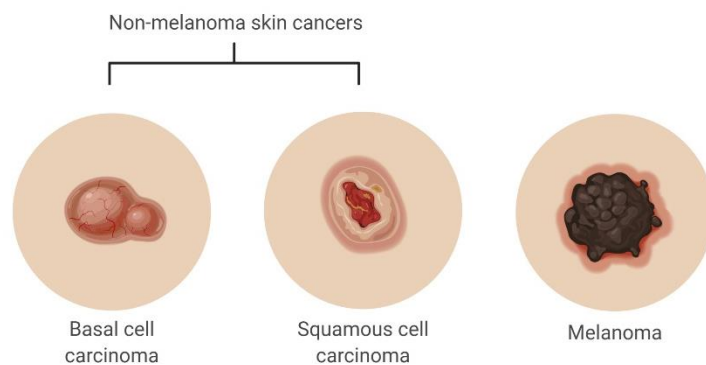
	T1 N0 M0 T0 N1mi M0 T1 N1mi M0			T0 N1 M0 T1 N1 M0 T2 N0 M0			T2 N1 M0 T3 N0 M0			T0 N2 M0 T1 N2 M0 T2 N2 M0 T3 N1 M0 T3 N2 M0			T4 N0 M0 T4 N1 M0 T4 N2 M0		
	G1	G2	G3	G1	G2	G3	G1	G2	G3	G1	G2	G3	G1	G2	G3
HER 2 <sup>+</sup> , ER <sup>+</sup> , PR <sup>+</sup>	IA	IA	IA	IB	IB	IB	IB	IB	IB	IIA	IIA	IIB	III A	III A	III B
HER 2 <sup>+</sup> , ER <sup>+</sup> , PR <sup>-</sup>	IA	IA	IA	IIA	IIA	IIA	IIA	IIA	IIB	III A	III A	III A	III B	III B	III B
HER 2 <sup>+</sup> , ER <sup>-</sup> , PR <sup>+</sup>	IA	IA	IA	IIA	IIA	IIA	IIA	IIA	IIB	III A	III A	III A	III B	III B	III B
HER 2 <sup>+</sup> , ER <sup>-</sup> , PR <sup>-</sup>	IA	IA	IA	IIA	IIA	IIA	IIB	IIB	IIB	III A	III A	III A	III B	III B	III B
HER 2 <sup>-</sup> , ER <sup>+</sup> , PR <sup>+</sup>	IA	IA	IA	IB	IB	IIA	IIA	IIA	IIB	IIA	IIA	III A	III B	III B	III B
HER 2 <sup>-</sup> , ER <sup>+</sup> , PR <sup>-</sup>	IA	IA	IB	IIA	IIA	IIB	IIB	IIB	III A	III A	III A	III B	III B	III B	III C
HER 2 <sup>-</sup> , ER <sup>-</sup> , PR <sup>+</sup>	IA	IA	IB	IIA	IIA	IIB	IIB	IIB	III A	III A	III A	III B	III B	III B	III C
HER 2 <sup>-</sup> , ER <sup>-</sup> , PR <sup>-</sup>	IB	IB	IB	IIA	IIB	IIB	IIB	III B	III B	III B	III B	III C	III C	III C	III C
Anatomic stage	IA			IIA			IIB			IIIA			IIIB		



The new criteria can result in alterations in stage compared to anatomic staging alone, and inclusion of these additional features can provide supplementary prognostic information which confers improved guidance for choice of therapeutic regimens, although anatomic staging is still the main system where biomarker data is unavailable. An additional pathologic prognostic stage is assigned to patients who receive surgery as initial treatment and includes findings at surgery and pathological findings from surgical resection.

### 1.1.2 Melanoma

**Figure 1.2** illustrates the three most common types of skin cancer, which reflect the formation of the skin epidermis: basal cell carcinoma (BCC) and squamous cell carcinoma (SCC) which arises from keratinocytes, and melanoma, a skin cancer arising from melanocytes in the basal layer of the epidermis.



**Figure 1.2 Illustration of the three most common types of skin cancer.**

[Left] basal cell carcinoma (BCC), [middle] squamous cell carcinoma (SCC) and [right] melanoma. Adapted from “Skin Cancer” by BioRender.com [15].

BCC and SCC are the two most common types of non-melanoma skin cancers (NMSC) and are typically associated with a much lower mortality rate (0.05% and 0.7% respectively [21]) than melanoma (8% [22]). NMSC is typically treated within the offices of physicians [23], which makes it difficult for cancer registries to collect accurate incidence information. For example, in the United States alone, the estimated number of unreported cases of NMSC per year is 5.4 million [24], twice as many as the collective number of reported cases for all the other forms of cancer. Despite the large burden of cases, NMSC conferred a small proportion (0.6%) of the total global deaths from cancer in 2020 [1], and the low mortality rate and often unreported nature of NMSC cases means they are regularly excluded from overall cancer incidence and mortality rate surveys.

The propensity to spread across the skin, lymph nodes and distant tissues contributes to higher mortality rates of melanoma compared to NMSC. In 2020, 325,000 new cases of melanoma, and 57,000 melanoma-associated deaths were estimated globally [1]. Melanoma therefore represents an ongoing public health burden, and warrants thorough investigation into early detection, disease mechanics and treatment strategies.

Melanoma derives from the melanin-producing melanocytes, which reside in the basal membrane of the skin epithelium and are guided by keratinocytes in their behaviour and growth [25]. Melanoma cells escape localised keratinocyte control by downregulating E-cadherin and upregulating N-cadherin [26]. Melanoma cells adapt to their new microenvironmental conditions through a complex series of interactions within the tumour stroma, including the activation of growth factors including basic fibroblast growth factor [27] that regulates cell adhesion. Melanoma cells also secrete transforming growth factor beta (TGF- $\beta$ ) which has inhibitory properties on epithelial and several immune cell types [28]. During tumour progression, melanoma cells secrete increasing quantities of vascular endothelial growth factor (VEGF) which promotes angiogenesis

and vasculogenesis and provides the growing tumour mass with oxygen and nutrients for further proliferation. The remodelling of the surrounding tissue is substantial, and the non-malignant cells and extracellular matrix become an integral part of the cancer lesion. It is therefore apt to consider melanoma, and other cancers, as a tissue, not just as individual cancer cells [29].

The first phase of malignancy is the radial growth phase within the basal epidermis and papillary dermis, followed by the vertical growth phase where malignant melanocytes begin to penetrate deeper into the dermis and subcutaneous tissue. By this stage, a substantial tumour has formed at the primary site of tumorigenesis, and localised shedding of tumour cells will inevitably lead to regional and eventually distant metastases if the tumour is left unchecked. Like other cancer types, including breast cancer, early detection is vital for ensuring more favourable survival rates (stage I, 99.6%; stage II, 75.0%; stage III, 67.6%; stage IV, 25.3% after 5-years [19]).

Melanoma staging is therefore critical tool for use in clinical practice and research, and aids in assessment of patient prognosis, allocation of treatment regimen, and trial enrolment [30]. Stages are presently determined using the AJCC TNM criteria, whereby ‘T’ describes tumour thickness and ulceration, ‘N’ describes lymph node involvement, and ‘M’ describes metastasis to distant sites [18,31]. An overview of the TNM criteria for melanoma is illustrated in **Table 1.3**. Stage I and II melanoma is localised to the skin, while stage III melanoma has spread to nearby lymph nodes or skin. By stage IV, the cancer has metastasised to distant sites including lymph nodes and other organs.

**Table 1.3 Overview of melanoma staging as determined by the TNM criteria.**

Stages are determined from stage I to stage IV according to features of the primary tumour (thickness and ulceration), lymph node involvement, and metastasis to distant sites [18].

Stage (TNM)	Physiological description
IA (T1a-N0-M0)	Lesions $\leq 1$ mm in thickness with no evidence of ulceration or metastases
IB (T1b-N0-M0)	Lesions $\leq 1$ mm in thickness with ulceration noted but without lymph node involvement
IB (T1a-N0-M0)	Lesions 1.01-2 mm in thickness without ulceration or lymph node involvement
IIA (T2b-N0-M0)	Melanomas $>1$ mm but $\leq 2$ mm in thickness with no evidence of metastases but with evidence of ulceration
IIA (T3a-N0-M0)	Lesions 2.01-4.0 mm in thickness without ulceration or lymph node involvement
IIB (T3b-N0-M0)	Melanomas 2.01-4 mm in thickness with ulceration but no lymph node involvement
IIB (T4a-N0-M0)	Lesions $>4$ mm in thickness without ulceration or lymph node involvement
IIC (T4b-N0-M0)	Lesions $>4$ mm in thickness with ulceration but no lymph node involvement
IIIA (T1-4a-N1a-M0)	Any-depth lesion, no ulceration, and 1 lymph node positive for micrometastatic
IIIA (T1-4aN2aM0)	Any-depth lesion, no ulceration, but 2-3 lymph nodes positive for micrometastatic
IIIB (T1-4b-N1a-M0)	Any-depth lesion, positive ulceration, and 1 lymph node positive for micrometastasis
IIIB (T1-4b-N2a-M0)	Any-depth lesion, positive ulceration, and 2-3 lymph nodes positive for micrometastasis

IIIB (T1-4a-N1b-M0)	Any-depth lesion, no ulceration, and 1 lymph node positive for macrometastasis
IIIB (T1-4a-N2b-M0)	Any-depth lesion, no ulceration, and 1 lymph node positive for macrometastasis
IIIC (T1-4b-N1b-M0)	Any-depth lesion, positive ulceration, and 1 lymph node positive for macrometastasis
IIIC (T1-4b-N2b-M0)	Any-depth lesion, positive ulceration, and 2-3 lymph nodes positive for macrometastasis
IIIC (N/A)	≥4 metastatic lymph nodes, matted lymph nodes, or in-transit met(s) /satellite(s)
IV, M1a (N/A)	Melanoma metastatic to skin, subcutaneous tissue, or lymph nodes with normal LDH level
IV, M1b (N/A)	Metastatic disease to lungs with normal LDH level
IV, M1c (N/A)	Metastatic disease to all other visceral organs and normal LDH level or any distant disease with elevated LDH level

### 1.1.3 Breast cancer treatment overview

Treatment selection for patients with breast cancer depends upon a number of factors including stage, tumour grade, steroid hormone receptor (HR; consisting of ER and/or PR) and HER2 expression, patient-specific history, and menopausal status.

Potential therapies must pass through a rigorous sequence of clinical trials, demonstrating safety and efficacy in phase I-II trials within small patient cohorts and then expanding

into larger cohorts and being contrasted against existing medicines for specific treatment goals [32].

The following sections summarise the guidelines for management of breast cancer, which are published by the National Institute of Care Excellence (NICE) UK. These guidelines were last updated in July 2018 (early and locally advanced [33]) and August 2017 (advanced [34]), and so omit guidance for recently emerging therapies such as immunotherapies, which are beginning to find clinical utility in breast cancer.

#### 1.1.3.1 Early (stage I/II) and locally advanced (stage III) breast cancer management

Treatment for operable breast cancer involves surgery to the breast and axillary lymph nodes, with or without radiotherapy to reduce local recurrence rates. This may be followed by adjuvant therapy, which includes chemotherapy, endocrine therapy and/or targeted therapies to reduce risk of relapse. The decision to use adjuvant therapy depends upon prognostic and predictive factors, including HR and HER2 status of the primary lesion.

Adjuvant chemotherapy, administered as anthracycline-taxane combination, can significantly reduce the risk of recurrence, independent of nodal status, grade or use alongside endocrine therapy [35]. However, adjuvant chemotherapy use is declining due to efforts to eliminate unnecessary treatments, especially in early-stage patients with favourable tumour features [36], and is currently only recommended for patients who are at enhanced risk of disease recurrence.

The anti-HER2 monoclonal antibody trastuzumab has shown clinical efficacy [37], and is recommended as targeted therapy of choice for HER2-expressing tumours above size

T1c, in combination with surgery, chemotherapy, and radiotherapy. Trastuzumab can also be considered for smaller tumours (*e.g.*, T1a or T1b), depending upon additional patient and prognostic factors.

Signalling via naturally occurring steroid hormone receptors frequently regulates the growth of breast cancers, and HR are overexpressed in up to 70% of breast tumours [38]. Endocrine therapies which block HR signaling were the first targeted therapies developed for breast cancer treatment, and the small molecule endocrine pathway inhibitor tamoxifen is recommended as initial adjuvant endocrine therapy in men and premenopausal women with ER<sup>+</sup> breast cancers [39], although development of resistance is common [40]. In postmenopausal women with ER<sup>+</sup> cancer who are at medium to high risk of recurrence, an aromatase inhibitor, such as anastrozole, is instead recommended as first-line therapy. Bisphosphonate therapy can also be given to postmenopausal women with node-positive breast cancer.

Chemotherapies and endocrine therapies can also be administered in the neoadjuvant setting. Neoadjuvant chemotherapy is recommended to reduce tumour burden in patients with ER<sup>-</sup> tumours and considered for ER<sup>+</sup> cancers. In HER2<sup>+</sup> patients, neoadjuvant chemotherapy is recommended in combination with anti-HER2 monoclonal antibody therapy (trastuzumab and pertuzumab). For patients with TNBC, for whom few systemic treatment options are available, a combination of platinum and anthracycline adjuvant chemotherapy is recommended. Although neoadjuvant chemotherapy induces pathologic complete response in approximately 20% of TNBC patients [41], the remainder may gain resistance or be intrinsically less susceptible [42]. Finally, neoadjuvant endocrine therapy can be considered as an alternative to chemotherapy in postmenopausal women with ER<sup>+</sup> cancer.

### 1.1.3.2 Advanced (stage IV) breast cancer management

Treatment of advanced, late-stage breast cancer depends upon the individual's treatment history, disease severity, and HR and HER2 status. For most ER<sup>+</sup> advanced breast cancers, endocrine therapy is recommended as first-line treatment. Aromatase inhibitors are recommended to postmenopausal women who have no history of endocrine therapy or have undergone tamoxifen treatment. For pre- and peri-menopausal women with ER<sup>+</sup> advanced cancer who have not received tamoxifen treatment, a combination of tamoxifen and ovarian function suppression with gonadotropin-releasing hormone (GnRH) is recommended as first-line treatment. In addition, tamoxifen is offered to men with ER<sup>+</sup> advanced cancer as first-line treatment.

For ER<sup>+</sup> advanced breast cancers which are prospectively life-threatening, or are associated with significant visceral organ involvement, chemotherapy, and subsequent endocrine therapy, is recommended. Trastuzumab is recommended for HER2<sup>+</sup> advanced breast cancers and may be used with or without combination chemotherapy with paclitaxel, depending upon treatment history. Bisphosphonates may also be considered to reduce pain and burden of bone metastases.

Checkpoint inhibitor (CPI) immunotherapies (discussed in more detail in Section 1.1.4.2) are beginning to find clinical utility in advanced breast cancer. In a phase III clinical trial, the combination of the anti-PD-1 monoclonal antibody pembrolizumab plus chemotherapy showed improved progression free survival when compared to chemotherapy alone, in metastatic TNBC patients [43]. In addition, drugs targeting programmed death-ligand 1 (PD-L1) have shown efficacy in patients across a wide range of cancers. The humanized IgG1 anti-PD-L1 monoclonal antibody atezolizumab, in combination with nab-paclitaxel, was the first CPI immunotherapy to be approved for



treatment of PD-L1<sup>+</sup> metastatic TNBC [44], although the manufacturer has since withdrawn the accelerated approval in the US [45]. Recent advances have been also made with the development of CDK4/CDK6 inhibitors, which fit part way between chemotherapeutic agents and targeted therapies, and are approved for the treatment of metastatic HR<sup>+</sup> breast cancer. When used in combination with endocrine therapies they can help to slow tumour growth and confer improved clinical outcomes [46].

#### 1.1.4 Melanoma treatment overview

Treatment selection for patients with melanoma depends upon several factors including staging by the tumour, node and metastasis (TNM) scoring, characteristics of the primary tumour (including the level of dermal invasion, described by the Clark scale and Breslow thickness which identify how deeply the melanoma has gone into the skin, the genetic profile), and patient-specific history [30].

Historically, there has been a paucity of available treatments for malignant melanoma. In the last decade however, there has been an explosion in new therapies, centering around immunotherapeutic and targeted therapeutic approaches. The following sections summarise the guidelines for management of melanoma which are published by NICE, UK [47]. These guidelines were last updated in November 2019.

##### 1.1.4.1 Early (stage 0-II) melanoma management

Primary melanomas are excised with a wide-local excision (WLE) to remove the tumour and a small area of adjacent tissue (5-20mm width depending on stage). The WLE excises

any tumour cells that have escaped into the surrounding tissue, and which may remain to proliferate in the absence of the primary tumour [48]. Patients with early-stage melanoma, from stage IB, may be offered a sentinel lymph node biopsy to assess the spread of the cancer to nearby lymph nodes, and if trafficking of tumour cells in the lymph node is observed, the melanoma is confirmed as stage III. Where regional spread is confirmed or suspected, CT (computed tomography) or whole-body MRI (magnetic resonance imaging) scans are recommended to check other areas of the body for metastases.

#### 1.1.4.2 Regional (stage III) and advanced (stage IV) melanoma management

Patients with stage III melanomas have been confirmed to have lymph node involvement and have several therapeutic options available. At this stage, a key determinant of therapy choice is whether the primary melanoma has been completely removed by surgery. If surgical excision of the tumour can be achieved, the melanoma is classified as resectable. In stage III resectable melanoma, patients may be treated with adjuvant therapy.

In contrast to breast cancer, chemotherapy is used only sparingly as an adjuvant treatment for melanoma. While immunotherapies, including the administration of interferon-alpha (IFN- $\alpha$ 2b) or interleukin-2 (IL-2), have gained FDA approval for melanoma in the past owing to promising trial results [49,50], these therapies confer high probabilities of severe treatment complications [51,52]. A newer generation of immunotherapies known as checkpoint inhibitor (CPI) drugs have revolutionised the treatment of regional and advanced melanoma. These therapies aim to enhance existing immune effector mechanisms to initiate tumour cell killing [53].

Immune checkpoint molecules are naturally expressed by populations of immune cells and non-malignant tissues in both healthy individuals and cancer patients, and their

physiological functions are to establish immune tolerance and prevent autoimmunity. Immune cells may express checkpoint molecules that, when bound to their cognate receptors or ligands on healthy cells, can act as an inhibitory stimulus and prevent cytotoxicity of normal tissues from occurring. Cancer cells, being derived from autologous normal tissues, often express these inhibitory cognate receptors or ligands on their surface, so that even when a cancer neoantigen is identified by immune effector cells, they may not attack the cancer cell in the presence of such inhibitory cell-surface marker signals. CPI immunotherapies aim to neutralise these inhibitory receptors by targeting checkpoint molecules on immune or cancer cells. Currently available CPI immunotherapies are designed to target T cell-mediated effector mechanisms, and checkpoint molecules commonly expressed on T cells include the programmed cell death protein 1 (PD-1) and the cytotoxic T lymphocyte-associated antigen-4 (CTLA-4).

The first CPI drug to gain FDA approval for the treatment of melanoma was ipilimumab, an anti-CTLA4 fully human IgG1 monoclonal antibody, which has been shown to offer clinical benefit compared with a standalone cancer/melanocyte peptide vaccine in a phase 3 study of metastatic melanoma patients [54]. Pembrolizumab (humanized) [55] and nivolumab (fully human) [56] are anti-PD-1 IgG4 monoclonal antibodies that have also achieved FDA approval for the treatment of melanoma. In a phase 3 study, nivolumab was reported to offer improved overall survival compared to chemotherapy with dacarbazine in metastatic melanoma patients [57]. CPI immunotherapies such as nivolumab or pembrolizumab may be recommended for use in the adjuvant setting in stage III resectable melanoma.

Systemic targeted therapies may also be recommended for use in the adjuvant treatment setting. Approximately 40-60% of all cutaneous melanoma tumours express the proto-oncogene BRAF with a mutated V600 amino acid residue. This mutant form of BRAF

constitutively activates the MAP kinase pathway to induce cell survival and proliferation [58]. The most common BRAF mutation is V600E [59], followed by V600K [60]. Small molecule BRAF inhibitors (*e.g.*, vemurafenib and dabrafenib) have been developed and tested in the clinical setting for patients with V600-mutant BRAF, conferring a significant reduction in tumour growth, although these effects were often short lived [61]. Randomised trials comparing BRAF inhibitor therapy to chemotherapy with dacarbazine found improved overall survival with the targeted therapy [62].

Unfortunately, in most cases of BRAF inhibitor monotherapy, patients show intrinsic or acquired drug resistance due to several mechanisms including reactivation of the MAP kinase pathway, typically via concurrent driver mutations in MEK genes [63]. Therefore, targeted therapies in melanoma can be administered as a combination of BRAF and MEK inhibitors in patients with mutated BRAF melanoma [64].

In patients with unresectable stage III disease, such as when multiple in-transit metastases are identified, debulking surgery may be considered, along with oncolytic viral therapy, systemic immunotherapy, or targeted therapies. Finally, stage IV melanoma represents metastasis to distant lymph nodes and/or organs and confers a very poor prognosis. For these individuals, surgery may be used to remove these metastases, and oncolytic viral therapy, immunotherapies and/or targeted therapies administered.

### 1.1.5 The future of cancer therapy

There is an ever-increasing variety of therapeutic strategies for the treatment breast cancer, melanoma, and other cancer types. The classical therapies used over the past few decades have focused upon non-targeted agents including chemotherapy and radiotherapy which often have broadly harmful effects on healthy cells, while only exerting effects on

a fraction of the target cancer cells. Newer strategies have focused on boosting the immune system's existing detective and cytotoxic framework, instead of relying on externally administered toxic agents to directly kill cancer cells. Immunotherapeutic treatments are undoubtedly among the most promising emerging cancer treatments over the next decade and beyond. Clinically approved agents such as CPIs have shown enhanced anti-tumour efficacy when compared to chemotherapy and are currently providing therapeutic benefits to patients with advanced breast cancer and melanoma.

Nevertheless, existing CPI treatments only seek to modulate one of several immune regulatory mechanisms. This Thesis investigates additional mechanisms which in the future may have the potential to be translated into a therapeutic setting. For example, the presence of immunomodulatory cells such as regulatory B and T cells which produce immunosuppressive cytokines such as IL-10 and TGF- $\beta$  may be associated with poor clinical outcomes in melanoma [65–67]. Furthermore, in more immunogenic breast cancer subtypes such as TNBC, the presence of B cells, their recruitment, lymphoid assembly, associations with T cells, formation of tertiary lymphoid structures, and specific B cell subsets such as isotype-switched B cells and the preferential expression and clonal expansion of IgG, as opposed to IgA isotype immunoglobulin-expressing B cells within the tumour microenvironment could offer improved patient survival outcomes [68].

In addition to the promise of immunotherapy, targeted approaches exploiting the individuality of cancer phenotypes are poised to remain an important tool across the field of cancer therapy. As tumour phenotyping and classification strategies become more sophisticated, personalised medicine will provide the backbone for great strides in the treatment of all types of cancer in the future.

## **1.2 B cells and their functions in human immunity**

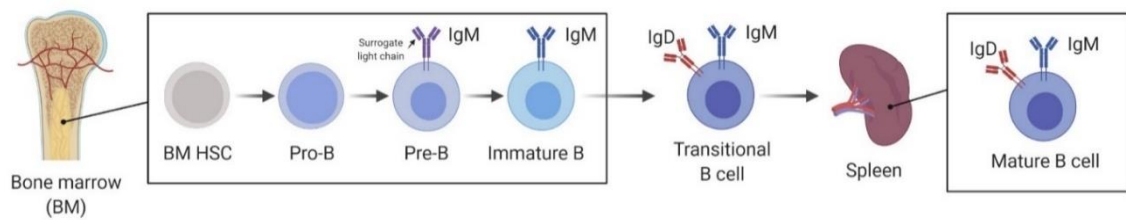
### **1.2.1 B cell development**

B cells mediate the humoral arm of the immune system's defence against pathogenic foreign bodies and cancerous cells. While B cells are most widely recognised for their immunoglobulin expression and secretion, they also act as professional antigen presenting cells and cytokine producers, thus providing several mechanisms by which they can influence local and systemic antigenic responses.

B cells arise from haemopoietic stem cells (HSCs) in the bone marrow, where their antigen receptors are developed in the form of surface immunoglobulin. In healthy individuals, a pool of pre-immune B cells each with a uniquely specific B cell receptor (BCR) circulates in the blood and lymph. Upon exposure to their cognate antigen and CD4<sup>+</sup> T cell help, signalling pathways are induced, leading to activation, differentiation and formation of memory and plasma cells. Memory B cells circulate in the body and are primed for a rapid response to subsequent challenge with the same antigen, while long-lived plasma cells provide constant levels of antibodies which are highly specific for the target antigen and can provide immunological protection [69,70].

#### **1.2.1.1 Antigen-independent and antigen-dependent B cell development**

The initial stages of the B cell development hierarchy from HSC precursors to immature B cells takes place in the absence of antigenic stimulation in a process known as antigen-independent B cell development. The major early B cell populations are illustrated in **Figure 1.3.**



**Figure 1.3 Schematic representation of the early human B cell development hierarchy.**

B cells originate from HSC precursors in the bone marrow. B cells develop from HSCs through the pro- and pre-B cell stages where the B cell receptor is formed, typically as IgM. Immature B cells leave the bone marrow as transitional cells expressing IgM and IgD, which are unresponsive to BCR stimulation. Transitional B cells home to the spleen where they finalise their early development with the formation of naïve B cells. Adapted from “B-1 and B-2 Cell Development” by BioRender.com [15].

HSCs in the bone marrow pass through early and common lymphoid progenitors to the common lymphoid-2 progenitor which is responsible for the B cell lineage. Development of this lineage depends upon the help of stromal cells, provided via IL-7 secretion, and the expression of several transcription factors in the bone marrow [71]. Additional differentiation stages within the bone marrow include the gaining of antigen specificity, heavy and light chain rearrangement and BCR formation. These processes are dependent upon enzymes including recombination activating gene 1 (RAG1) and 2 (RAG2) [72], which bind to recombination signal sequences and induce double-stranded DNA breaks, without which mature B cells cannot form [73]. There is also an important checkpoint in the bone marrow for non-functional heavy chain and pre-BCR autoreactivity [74]. B cells exit the bone marrow as transitional B cells, co-expressing IgD and IgM [70], and mark the crucial intermediate between immature B cells, and mature naïve cells capable of further antigen-dependent B cell development and differentiation [75].

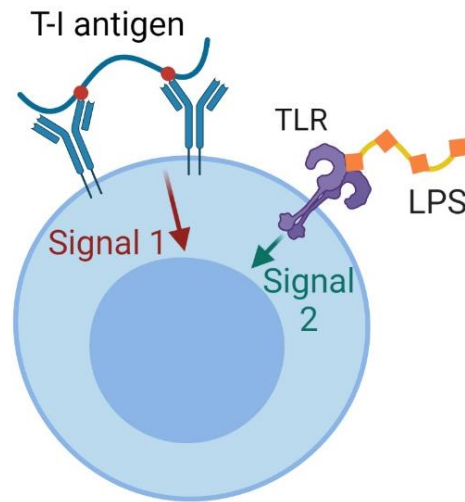
Transitional B cells are unable to respond to antigenic stimulation with T cell-dependent antigens, for example by migrating to lymph nodes for proliferation and differentiation. They fail to upregulate co-stimulatory molecule CD86 [76], and respond with anergy and

apoptosis [77], and this represents an additional checkpoint against autoreactivity. Despite this, there is evidence that immature B cells can respond to T cell-independent type-1 antigens (*e.g.*, toll-like receptor (TLR) ligands; discussed further below) in the absence of T cell help, isotype-switching or affinity maturation [78].

Transitional B cells migrate to the spleen for further development where they complete their maturation and develop into either naïve, marginal zone (MZ) or follicular B cells. MZ B cells inhabit the splenic marginal zone, while follicular B cells reside in splenic follicles and lymph nodes where T cell-dependent antigenic stimulation promotes the formation of germinal centres, and the specificity of the BCR is crucial in determining their developmental designation [79]. Much of the work to establish the B cell development hierarchy was performed in mice, wherein B cells are categorised into B-1 type cells which reside in mucosal and epithelial tissue environments and support the initial defence against pathogens, and B-2 type cells which contain both follicular and marginal zone populations [80].

In humans, splenic marginal zone and tissue-resident (B-1-like) mature B cells in intra-epithelial sites and gut-associated lymphoid tissues can respond to antigenic stimulation in the absence of CD4<sup>+</sup> T cell help. They develop into short-lived plasma cells, produce vast quantities of relatively low affinity IgM, IgA and IgG antibodies, and act as the initial defence against pathogenic infection. This response takes place via the T cell-independent pathway, illustrated in **Figure 1.4**, relies on innate-like B cells (ILBs) expressing low-specificity BCRs able to recognise conserved pathogenic motifs, and requires both BCR and TLR engagement along with co-stimulatory and cytokine signals [81].



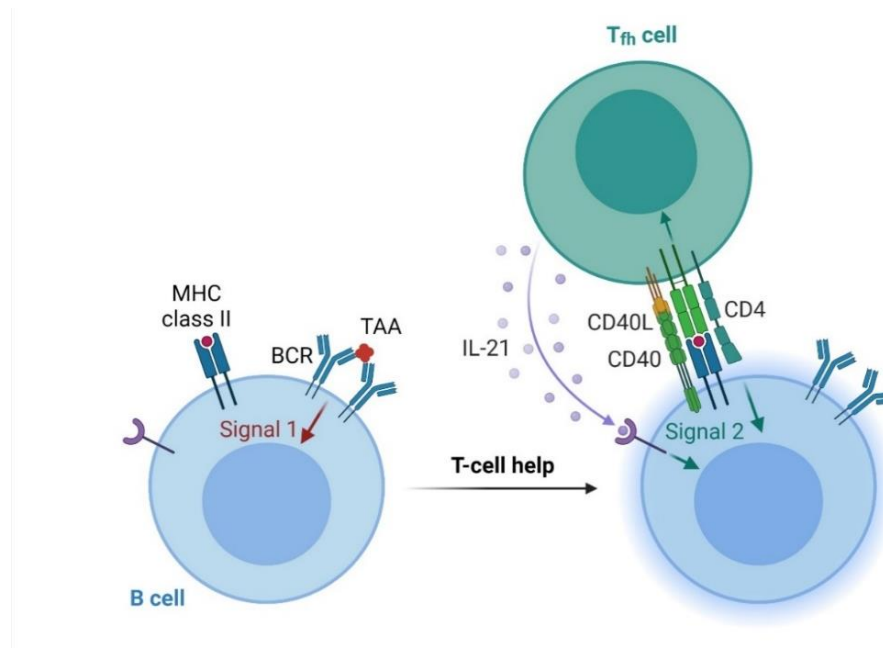


**Figure 1.4 Schematic representation of T cell-independent B cell activation in response to multivalent T-independent (T-I) antigens.**

B cells expressing broadly specific immunoglobulin cross-link conserved T-I antigens via their BCRs (signal 1). In parallel, pattern recognition receptors such as toll-like receptors (TLRs) bind to the antigen (signal 2) and initiate B cell activation in the absence of T cell help. Adapted from “Thymus-dependent Antigens Induce T-dependent B Cell Responses” by BioRender.com [15].

In contrast to ILBs, most B cells express high specificity antigen receptors encoded by diversified VDJ genes and are activated via the T cell-dependent pathway. In this pathway, antigen encounters occur within lymphoid structures such as lymph nodes, where resting naïve B cells reside in primary follicles. Antigens are transported by the lymphatic system into the cortex or paracortex of lymph nodes and are exposed to the naïve B cell pool. Upon successful antigenic recognition via their high-affinity BCR, a specific B cell will internalise the antigen-Ig complex and present the processed peptides upon major histocompatibility complex (MHC) class-II molecules on its cell surface to cognate T cells. Concurrently, the antigen will be processed by other professional antigen-presenting cells (APC) such as dendritic cells and also presented on MHC class-II to T cells. These APC will interact with cognate antigen-specific T cell receptors (TCR) on naïve T-helper cells, initiating T-helper cell activation and CD40L expression. Finally,

the pre-activated follicular T-helper cell binds its TCR to its cognate B cell MHC-peptide complex (pMHCII), initiates cytokine signaling with IL-21, and activation is achieved via the CD40/CD40L axis [82,83]. This process is illustrated in **Figure 1.5** to exemplify the recognition of a tumour-associated antigen (TAA).

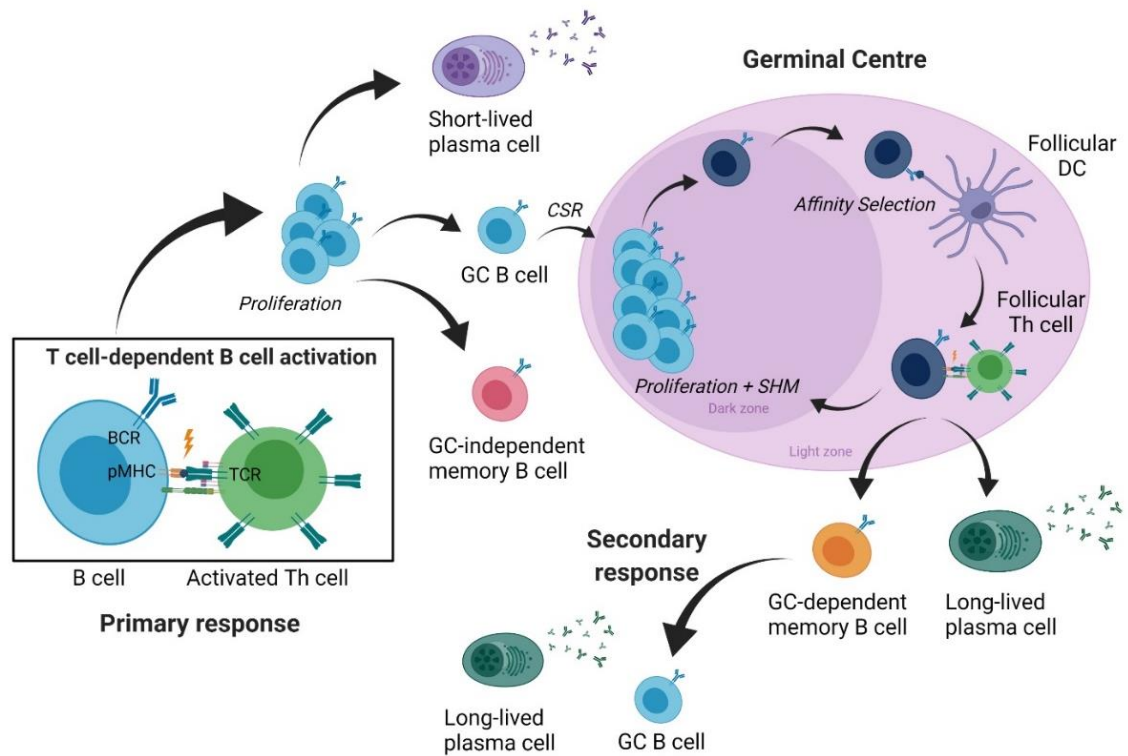


**Figure 1.5 Schematic representation of T cell-dependent B cell activation in response to tumour-associated antigens (TAA).**

Within secondary or tertiary lymphoid structures, follicular B cells bind to TAA via their antigen-specific immunoglobulin. The antigen-Ig complex is internalised (signal 1), and peptide fragments presented on MHCII molecules. Pre-activated follicular T-helper cells bind to the pMHCII complex via their specific TCR, and B cell activation is initiated via the CD40/CD40L axis (signal 2), resulting in triggering of NF $\kappa$ B and MAP-kinase pathways leading to proliferation, isotype-switching, and differentiation to memory and long-lived plasma cells. Adapted from “Thymus-dependent Antigens Induce T-dependent B Cell Responses” by BioRender.com [15].

B cells activated with T cell-dependent antigens in secondary or tertiary lymphoid structures may differentiate into either short-lived plasma cells to produce a rapid burst of low affinity antibody or enter germinal centres to later become long-lived plasma cells or memory B cells. The initial choice is dependent upon simultaneous recognition by pattern recognition receptors such as TLRs, where the presence of pathogen-associated molecular patterns (*e.g.*, CpG ligands) drives the preferential generation of short-lived

plasma cells through the downregulation of antigen processing and presentation [84,85]. While short-lived plasma cells are key players in the early stages of primary immune responses, memory B cells are critical in secondary responses, whereby under re-exposure to the same antigen, they quickly differentiate into long-lived plasma cells, or germinal centre B cells to undergo further proliferation, somatic hypermutation (SHM) and clonal selection. During primary responses, memory B cells may also arise which are independent of the germinal centre reaction. These cells are mostly IgM-expressing and lack SHM, therefore offering reduced antigen binding affinities [69]. A summary of the key stages in antigen-dependent B cell development is shown in **Figure 1.6**.



**Figure 1.6 Overview of the key stages of B cell development following T cell-dependent B cell activation.**

Within secondary or tertiary lymphoid structures, activated B cells present peptide fragments on MHCII molecules to cognate TCR expressed by an activated T-helper cell. CD40-mediated signals initiate proliferation and differentiation into short-lived plasma cells, germinal centre (GC) B cells or GC-independent memory B cells. GC B cells isotype-switch and form germinal centres, where they undergo proliferation and somatic hypermutation (SHM). B cell clones with high affinity for antigen presented by follicular dendritic cells avoid apoptosis and re-present peptides on MHCII molecules to T cells. Finally, clonally selected B cells either re-enter the dark zone or differentiate into memory B cells and long-lived plasma cells. GC-dependent memory B cells respond to antigenic restimulation by differentiating into long-lived plasma cells or GC B cells which re-enter germinal centre reactions. Created with BioRender.com [86].

Following T cell-dependent B cell activation, upregulation of activation-induced deaminase enzyme (AID) induces isotype-switching from IgD and IgM to restricted IgA, IgG or IgE expression [87]. Historically, isotype-switching was thought to take place exclusively within germinal centres (GCs). However, recent observations have identified human pre-GC B cells which are primed for class switch recombination prior to the formation of the germinal centre response [88]. Within the dark zone of germinal centres, point mutations are produced in the variable (V) regions of immunoglobulin heavy and

light chains in the process of SHM, which aids in the affinity maturation and selection of successive B cell clones in the light zone. The result is the generation of B cells expressing immunoglobulin with a high affinity for their cognate antigen, and able to initiate potent Fc-mediated effector functions against target-expressing pathogens or cancer cells.

Antigen-independent B cell development results in the generation of a pool of naïve cells primed to identify and react to a non-self-stimulus. The central tolerance of the immune system restricts reactions against self-antigens, so that when a B cell receives its cognate antigen, it represents a robust danger signal requiring immediate response. Activated B cells in germinal centres initiate clonal expansion to increase in number, affinity maturation to improve antigen recognition, and isotype-switching to express antibodies that recruit additional components of the immune system.

### 1.2.2 B cells as antibody producing cells

It is not necessary for B cells to be locally present with their surface-Ig to facilitate their effector function. B cells can greatly amplify their effect by secreting their effector immunoglobulin molecules into peripheral blood and tissues, and among the hallmarks of the B cell response to cellular pathogens is the generation of antibodies specific to pathogen-derived antigens. An example is in acute *E. coli* infection, whereby infected individuals have elevated serum IgM and IgG specific to bacterial derived lipopolysaccharides (LPS) and the R3 LPS core, compared to healthy volunteers [89].

The initial antibody response to threat is typically through low affinity IgM, secreted in response to T cell-independent antigens by B-1-like and MZ cells. These cells also secrete broadly specific spontaneous “natural antibody” in the absence of infection or immunisation, adding an additional protective layer to potential pathogenic challenge, as

well as facilitating clearance of dead cells [81]. Within germinal centres, T cell-dependent B cell activation generates rapidly dividing plasmablasts and plasma cells, with the ability to secrete highly specific and potent isotype-switched antibodies (*e.g.*, IgG1).

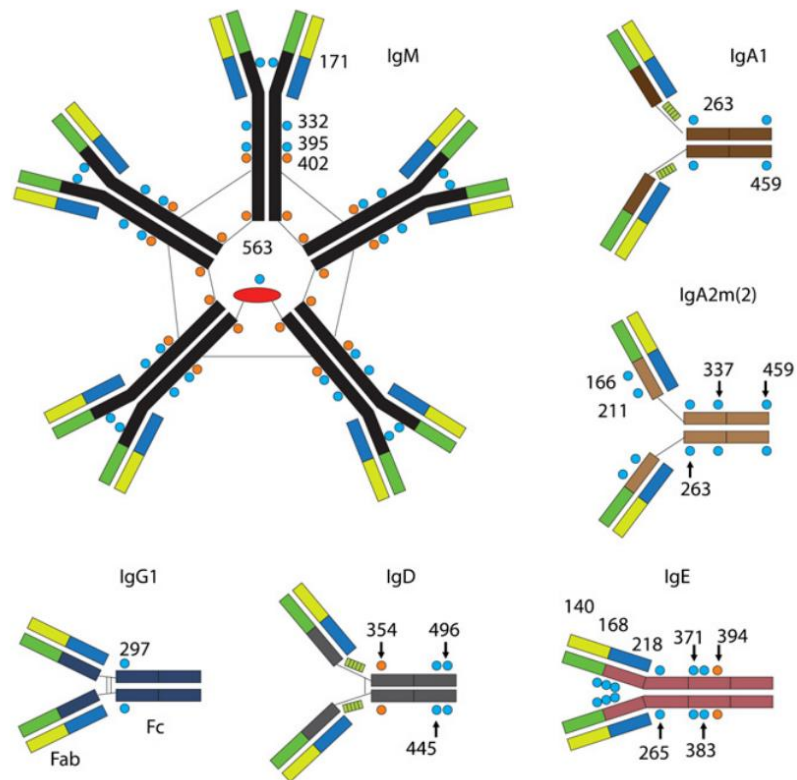
There are many parallels between the B cell defence against cellular pathogens (*e.g.*, bacteria, fungi and parasites), and the B cell defence against cancer cells. In cancer, naïve B cells recognise tumour-associated antigens which are mutated or overexpressed in cancer cells, and B cells reactive these antigens avoid deletion during autoreactivity checkpoints in the bone marrow and spleen as these antigens are absent or expressed at low levels in healthy individuals.

Overall, antibody secretion by B cells forms a crucial and dynamic immune surveillance of the periphery and tissues, neutralising foreign antigens and alerting other components of the immune system to their presence, and is the most well described property of B cells.

#### 1.2.2.1 Antibody isotype distribution

The Fc-receptor binding (Fc) portion of an antibody is denoted by the heavy chain constant regions and is responsible for cell cytotoxic and phagocytic mechanisms initiated by Fc-receptor-expressing immune effector cells including natural killer (NK) cells and macrophages. These CH regions confer the antibody isotype, and there are nine different heavy chain genes (IgD, IgM, IgG1-4, IgA1-2 and IgE) conferring nine subclasses, within five classes (or isotypes), expressed by B cells in humans. B cells usually express antibodies of a single isotype, except for IgD and IgM co-expression. The nine human antibody subclasses confer a diverse set of effector functions mediated by their distinct heavy-chain Fc-receptor binding regions with unique affinities for Fc-receptors on

immune effector cells, allowing for the initiation of a wide range of immune responses in a flexible and plastic approach to responding to different foreign antigens [90].



**Figure 1.7 Human antibody isotype structure and glycosylation sites.**

Glycosylation sites within the CH region confer binding affinities and specificities to cognate Fc-receptors on immune effector cells. Numbers refer to the amino acid position of each glycosylation site. Adapted from [91].

Of the five main antibody isotypes (IgD, IgM, IgE, IgA and IgG), IgD is rarely secreted and most often functions as the membrane bound BCR of transitional and naïve cells. IgE is associated with the pathogenicity of allergic diseases and with the protective effects of anti-parasite immune responses [91]. IgE circulates in the periphery at very low concentrations, is also tightly bound on its cognate high affinity FcεRs on circulating basophils and tissue-resident mast cells, and it carries high immune effector activatory potency. IgG isotypes confer the largest proportion (~75%) of the total immunoglobulin pool in the serum of healthy individuals [92]. IgG isotype antibody is typically secreted

by GC-dependent plasma cells and comprises four antibody subclasses (IgG1-4; numbered from highest to lowest serum concentration) with differing Fc-receptor binding affinities and effector function profiles. IgM is the second largest component [92], usually has lower affinity for its target antigen and may take on a pentameric form which can offer the chance of increased avidity for IgM-antigen immune complexes [93].

IgA is the third most common antibody isotype in healthy volunteer serum and is associated with mucosal immunity [92]. **Figure 1.7** illustrates the structural diversity of immunoglobulin isotypes and highlights the presence of glycosylation sites, a proportion of which confer binding affinities and specificities to Fc-receptors on immune effector cells.

#### 1.2.2.2 Functions of antibodies

##### 1.2.2.2.1 Neutralisation

Neutralisation is the simplest antibody mechanism as it does not rely on accessory proteins or effector immune cells. Neutralising antibodies bind to important pathogen-derived, or cancer-associated proteins and hinder their functionality. Neutralising antibodies bind to important functional motifs such as the variable loops of gp120 and the receptor site surfaces of HIV-1 [94]. Similar properties likely exist in a proportion of the tumour-specific antibodies that have been observed in melanoma patients. In support, an antibody neutralising human growth factor, a protein associated with cancer cell proliferation and progression, has been shown to suppress tumour growth *in vivo* in mouse glioblastoma models [95]. Overall, neutralising antibodies are an important player in immune responses to pathogenic and cancerous threats.



#### 1.2.2.2.2 Antibody-dependent cellular cytotoxicity and phagocytosis

Another important function, particularly for IgG antibodies, is via the Fc regions of the antibodies. Antibodies bound to multiple copies of an antigen expressed by a pathogen or of a tumour-associated antigen are cross-linked to the Fc-receptor of cytotoxic immune effector cells, such as the FcγRs expressed on NK cells [91,96]. Cross-linking induces NK cells to release perforin/granzyme which has a potent cytotoxic effect upon the target cell, and results in antibody-dependent cellular cytotoxicity (ADCC) of the target. In antibody-dependent cellular phagocytosis (ADCP), antibodies are instead cross-linked to the Fc-receptors of phagocytes (*e.g.*, monocytes, macrophages) or granulocytes (*e.g.*, neutrophils), which engulf and digest the target with proteolytic enzymes in lysosomal vesicles [97].

Both mechanisms have been shown to be crucial in the immune defence against pathogens. ADCP has been shown to aid clearance of *L. pneumophila* bacteria [98], and antibodies with enhanced ability to activate ADCC have been implicated in protection from influenza infection [99]. Both ADCC and ADCP have been shown to mediate the function of anti-tumour monoclonal antibodies in the clinic, such as trastuzumab, an anti-HER2 antibody used in breast cancer therapy [100]. Trastuzumab also exhibits direct inhibitory (neutralisation) effects upon breast cancer cells, as HER2-binding blocks HER dimerization and initiates a signalling cascade that induces CDK2 and causes cell cycle arrest. Trastuzumab therefore can engender three separate antibody effector mechanisms. ADCC, and likely ADCP, also has active functional roles in “natural” anti-tumour immune responses.

#### 1.2.2.2.3 Complement activation

The complement system consists of a pool of cascading proteins which induce antimicrobial and inflammatory responses [96]. IgM and IgG antibodies forming hexameric complexes drive the activation of complement proteins via the initial recruitment of the complement component 1q (C1q) to induce direct cytotoxicity through the membrane attack complex, phagocytosis via complement receptors on phagocytes, and chemoattractant production. While individuals with complement system deficiencies have increased susceptibility to infections [101], the impact of the complement system upon tumour progression remains controversial, and studies have indicated that the recruitment of macrophages by the activated complement system has a pro-tumour effect [102].

#### 1.2.3 B cells as antigen presenting cells

B cells are also professional antigen presenting cells, and can interact with and regulate the immune system in additional ways, such as by inducing T cell activation and contributing to tolerance mechanisms [103]. B cells bind exogenous antigen via their specific BCR, initiating BCR-peptide complex endocytosis, and the peptide is processed and presented upon MHC class-II molecules in small fragments (Section 1.2.1.1). In theory, the pMHCII molecules presented on the surface of B cells interact with the TCR of CD4<sup>+</sup> T-helper cells to induce priming and activation of the T cell in addition to the B cell. However, studies have demonstrated that prior to the interaction, T-helper cells express the costimulatory molecule CD154, indicating activation. As a result, T cell-dependent B cell activation may rely upon the pre-activation of T-helper cells by follicular

dendritic cells [104] and may not always contribute to T cell priming, although B cells do possess the ability to prime naïve T-helper cells *in vivo* [105].

In contrast, there is evidence that some protein antigens are exclusively presented by B cells as opposed to dendritic cells [106], and thus the role of B cells in direct antigen presentation appears to depend upon the type of antigen, which likely moulds specific immune responses. Resting B cells can also induce T cell tolerance via antigen presentation, and so may inhibit immune responses, which may occur in autoimmunity and allergy.

#### 1.2.4 B cells as cytokine expressors

In addition to producing antibody and presenting antigen, B cells can also shape immune responses via their cytokine expression. B cells produce a wide variety of cytokines which may help categorise B cells into regulatory and effector subsets. Regulatory B cells are characterised by a variety of immunosuppressive functions, including via expression of IL-10 or TGF- $\beta$  (discussed in detail in Sections 1.4.2.1 and 1.7). Effector B cell subsets can secrete pro-inflammatory cytokines such as IL-2, TNF- $\alpha$  and IFN- $\gamma$  [107]. TNF- $\alpha$  produced by B cells controls the development of follicular dendritic cells, formation of B cell follicles and regulation of T cell-dependent antibody responses [108].

B cells have heterogenous cytokine expression, which may depend upon the T-helper cell subset and the antigenic class initiating B cell activation. Th1 help induces the expression of IFN- $\gamma$  and IL-12 by B effector 1 (Be-1) cells and Th2 help induces the expression of IL-2, IL-4, and IL-13 by B effector 2 (Be-2) cells. IFN- $\gamma$  and IL-2-secreting B cells are found in human peripheral blood, and these cytokines have been shown to amplify effector T cell responses *in vivo* [109].

In mice, effector B cells may derive from follicular cells, as these cells, but not MZ cells, have been shown to produce IFN- $\gamma$  upon TLR stimulation [110]. Moreover, there may be specific subsets of follicular B cells that are predisposed to become effector cells expressing IFN- $\gamma$ , IL-2, IL-4, and IL-12 [111]. Cytokines play a key role in determining the effector status of B cells, and it is postulated that differentiation into either Be-1 or Be-2 cell types may proceed independently of BCR stimulation, although peptide is required to commit Th1 [112] or Th2 [113] cell help. In addition, T cell co-stimulation via CD40, and CD80 engagement on the surface of B cells may be necessary for effector commitment, and both Be-1 and Be-2 effector lineages can secrete antibodies.

In summary, B cell cytokine expression profiles are dynamic, may be influenced by external T cell-dependent and T cell-independent signals [107], and can regulate the differentiation of naïve CD4<sup>+</sup> T cells into Th1 or Th2 phenotypes through expression of polarizing cytokines such as IFN- $\gamma$  or IL-4 [109].

#### 1.2.4.1 Regulatory B cells

Regulatory B cells (Bregs) are characterised by diverse immunosuppressive functions and have been shown to have roles in murine models of tolerance [114], silencing chronic inflammation [115] and supporting tumour progression [116].

Bregs also have diverse, and controversial, origins. Bregs may derive from either follicular or MZ cells, and a murine CD1d<sup>+</sup> CD19<sup>++</sup> B cell subset has been identified which protects from inflammatory bowel disease, and strongly resembles MZ cells [115,117]. While the current view is that Bregs may be generated from multiple developmental lineages, they can be defined according to their mode of activation. Innate Bregs are derived from Innate-like B cells comprising B-1-like and MZ cells, are

activated via the innate (*e.g.*, TLR) pathway and respond to pathogen-associated signals in the absence of T cell help (discussed in Section 1.2.1.1) [118]. In contrast, adaptive Bregs are activated via the T cell-dependent pathway with BCR and CD40-mediated stimulation, while immature Bregs may be generated either via CD40 ligation [119], or via antigenic priming [120].

Although considerable progress has been made within the murine setting, there is a paucity of data delineating the function of effector and regulatory B cells in humans and their roles in the onset of different diseases. Investigations have been hindered by the lack of ubiquitous lineage markers associated with distinct human B cell cytokine expression profiles, which preclude straightforward functional studies. Moreover, heterogeneous and contradictory B cell cytokine expression profiles (*e.g.*, co-expression of IFN- $\gamma$  with IL-10 [121]), and the potential divergent cytokine-mediated responses with T cell-independent or -dependent B cell activation further conflate the difficulties of functional studies to better evaluate Bregs.

There are currently 11 subpopulations of IL-10-expressing regulatory B cells described in mice [122], which reflects the heterogeneity of these cytokine-expressing B cells. Substantial efforts have been made using a wide range of extracellular markers to identify subpopulations of human Bregs with some success, including the identification of IgG4<sup>+</sup> IL-10<sup>+</sup> Bregs [123]. However, due to the fragmentary nature of human Breg subpopulations, it remains commonplace to quantify IL-10 cytokine expression among the major B cell subsets including memory, naïve, transitional and MZ (often designated IgM<sup>+</sup> memory B cells in humans [124]). Indeed, the most promising populations of human regulatory B cells have been described broadly as properties of the CD24<sup>hi</sup> CD38<sup>hi</sup> transitional [121], CD24<sup>hi</sup> CD27<sup>+</sup> memory B cell and CD27<sup>hi</sup> CD38<sup>hi</sup> plasmablast [125] pools. Overall, the regulatory B cell pool appears to represent a distinct cell phenotype

from effector Be-1 and Be-2 cells and can modulate both innate and adaptive immune responses.

#### 1.2.4.1.1 Regulatory B cells in non-cancerous disease

Patients with autoimmune disorders have been found to have dysregulated populations of IL-10-expressing regulatory B cells. Multiple sclerosis patients have lower circulating quantities of IL-10-expressing B cells compared to healthy volunteers [126], and downregulation and functional impairment of transitional IL-10<sup>+</sup> Bregs have been observed in systemic lupus erythematosus and rheumatoid arthritis [121,127]. These observations suggest that impaired Bregs responses could play a crucial pathogenic role in autoimmune diseases and highlight the wider role of B cells in contributing to immune outcomes via their differential cytokine expression, whether through regulatory or pro-inflammatory mechanisms.

IL-10<sup>+</sup> Bregs have also been shown to be modulated in patients with chronic inflammatory conditions such as Crohn's disease and ulcerative colitis, and their collapse has been associated with disease progression [128]. Regulatory B cells may also play a role in facilitating pathogenic survival in infectious diseases. Patients with chronic HIV-1 infections possess elevated percentages of IL-10-producing Bregs, something observed from early infection stages. This may represent a mechanism of viral immune escape, instigated by the innate immune system via TLR-signalling [129]. These observations support the presence of a subset of innate Bregs which respond to commonly expressed pathogenic motifs via TLR ligands in a likely T cell-independent manner.

Transplant rejection is a common outcome for patients receiving allografts, whereby the host immune system mounts a response against the foreign tissue. This results in

considerable toxicity and eventually functional graft-rejection. Rejection is most often associated with T cell-dependent cytotoxicity, although T-helper cells facilitate the production of alloantibodies by B cells via CD40 stimulation [130]. To reduce the probability of rejection, transplantation recipients typically receive immunosuppressive drugs such as cyclosporine, a calcineurin inhibitor which prevents T cell activation and IL-2 cytokine secretion and upregulates TGF- $\beta$  expression [131]. Patients with graft rejection have been shown to possess transitional B cells with a reduced IL-10:TNF- $\alpha$ -expressing ratio, demonstrating the potential role of Bregs in contributing to graft survival. Moreover, the study demonstrates that the IL-10:TNF- $\alpha$  ratio, compared to IL-10 alone, may be more important in delineating the regulatory function of B cell subsets, as B cell subsets with the same IL-10 expression can have diverse effector functions owing to conflicting TNF- $\alpha$  expression [132]. Additional work using a mouse model of antibody-induced transplantation tolerance has shown that TGF- $\beta$ -expressing B cells induce FOXP3<sup>+</sup> Treg generation and promote graft survival [133].

Lastly, in allogeneic stem cell transplantation (allo-SCT), graft-versus host disease (GVHD) represents a major and lethal complication whereby transplant-derived immune cells attack host tissue, and allo-SCT transplants containing higher percentages of transitional-phenotype Bregs are associated with reduced incidence of chronic GVHD [134]. Collectively, these studies illustrate that regulatory B cells possess potent immunosuppressive abilities and are clinically relevant in silencing inflammation, downregulating Th1 immune responses and inhibiting T cell effector function. The role of regulatory B cells in patients with cancer, specifically melanoma, forms a major part of this Thesis, and will be discussed further in Section 1.7.

### **1.3 Systemic immunity in cancer**

The impact of tumorigenesis on patient immunity extends beyond the boundaries of the tumour microenvironment (TME). Immune responses are coordinated across tissues, and systemic immune responses may be substantially modulated in cancer patients. Therefore, to provide the most accurate and reliable interpretation of immune responses to cancer, peripheral as well as intratumoural immunity must be considered. Moreover, with the recent advent of systemic immunotherapies which have revolutionised cancer therapy, systemic immunity is now being acknowledged as an essential component of the anti-tumour immune machinery.

#### **1.3.1 Perturbations of systemic immunity in breast cancer and melanoma**

Several perturbations of peripheral immune cell subsets have been identified in breast cancer and melanoma, with considerable overlap, and **Table 1.4** summarises the list of observations to date which provide evidence for extensive remodelling of the systemic immune landscape in patients with cancer. Studies have shown that in many cancer patients, including those with breast cancer or melanoma, haematopoiesis is dysregulated, which routinely manifests as aberrations in populations of immature neutrophils and monocytes [135]. Importantly, these cells may traffic to the tumour microenvironment where they may contribute to localised immunosuppression [136], and elevated neutrophil frequencies in the blood are associated with poor prognosis across a range of cancers [137].



**Table 1.4 Peripheral immune perturbations observed in breast cancer, melanoma, or both.** List of observations to-date analysing the modulation of circulating immune cell types in patients with breast cancer or melanoma. Observations common to both cancer types are coloured blue. Adapted from [138].

Immune cell type	Change	Cancer type
Haematopoietic stem cells [135]	Increased frequency	Breast
Multipotent progenitor cells [135]	Increased frequency	Breast
Granulocyte monocyte progenitors [135]	Increased frequency	Breast
Dendritic cell precursors [139]	Decreased frequency	Breast
Immature neutrophils/ PMN MDSCs [140,141]	Increased frequency	Breast, melanoma
Immature monocytes/M-MDSCs [142]	Increased frequency	Melanoma
Dendritic cells [139,143]	Decreased frequency	Breast, melanoma
T cells [144]	Decreased TCR repertoire	Breast
Treg cells [145]	Population expansion	Breast
Treg cells [146,147]	Clonal expansion	Breast, melanoma
CD4 <sup>+</sup> and CD8 <sup>+</sup> T cells [148]	Decreased IL-2 and IFN $\gamma$ production after PMA and ionomycin stimulation	Breast
CD4 <sup>+</sup> T cells [149]	Decreased pSTAT1 and pSTAT3 signalling after IL-6 stimulation	Breast
Natural killer cells [150]	Decreased activating receptors, increased inhibitory receptors, decreased cytotoxic potential	Breast
IgG4 <sup>+</sup> B cells [151]	Increased frequency	Melanoma
CD27 <sup>+</sup> memory B cells [152]	Decreased frequency	Melanoma
PD-L1 <sup>+</sup> B cells [153]	Increased frequency	Melanoma
Proangiogenic (CD49b <sup>+</sup> CD73 <sup>+</sup> ) B cells [154]	Increased frequency	Melanoma

Downmodulation of peripheral dendritic cell frequencies has also been observed across several solid tumour types, including breast cancer and melanoma [139,143]. These findings have considerable implications for anti-tumour immune responses, as dendritic cells are critical antigen presenting cells which prime CD4<sup>+</sup> and CD8<sup>+</sup> T cells, leading to activation, differentiation, and effector responses [155,156]. This collapse in circulating

mature dendritic cells may depend upon tumour-derived granulocyte colony stimulating factor (G-CSF) [139] or VEGF [157].

Extensive perturbations in circulating T cell phenotype and function have been observed in patients with breast cancer. Decreases in TCR repertoire diversity have been detected and were associated with less favourable overall survival in metastatic disease [144]. In addition, diminished expression of IL-2 and IFN- $\gamma$  by peripheral CD4<sup>+</sup> and CD8<sup>+</sup> T cell in response to PMA/ionomycin stimulation [148], and unresponsiveness to IL-6 stimulation [149], together highlight impeded functionality of circulating T cells in breast cancer.

Immunosuppressive regulatory T cells (Tregs) have received substantial attention in recent years and have been shown to be expanded in the breast cancer periphery [145]. Circulating Tregs share phenotypic and TCR repertoires with tumour-infiltrating T lymphocytes (TIL-T), indicating that a proportion of tumour-resident Tregs derive from thymic Tregs as opposed to *in situ* induction from intratumoural CD4<sup>+</sup> T cells [147]. Tregs expressing TCRs specific for tumour neoantigens have been observed in the periphery of several solid tumours, including melanoma, indicating possible clonal expansion within the peripheral compartment, as well as the tumour [146].

Peripheral NK cells in breast cancer patients have been shown to possess dysregulated expression of activatory and inhibitory receptors, with decreased activatory NKG2D and increased inhibitory NKG2A alongside disease progression [150]. As expected from these observations, these cells are functionally impaired at killing tumour cells and degranulating *in vitro*.

While considerable attention has been paid towards the circulating T cell compartment in patients with solid tumours, including breast cancer and melanoma, observations

concerning the modulation of circulating B cell populations remains limited. An expansion in the frequency of circulating IgG4-expressing B cells [151] (discussed further in Section 1.4.1), and collapse in CD27<sup>+</sup> memory B cells [152] have been identified in melanoma patients. Evidence is also growing that regulatory B cells may have a role to play in human cancers, including melanoma, where PD-L1<sup>+</sup> [153] and proangiogenic CD49b<sup>+</sup> CD73<sup>+</sup> B cell subpopulations [154] have been shown to be expanded in patient circulation (regulatory B cells in cancer are discussed further in Section 1.7). This Thesis aims to provide novel insights into the phenotype and function of circulating, and intratumoural, B cells in breast cancer and melanoma patients and elucidate their wider role in contributing to tumour progression.

All together, these findings indicate widespread corruption of the immune macroenvironment in patients with solid tumours, including breast cancer and melanoma. The dysregulation of peripheral immune subpopulations is likely to be a key factor in driving tumour progression, and for successful immune-mediated tumour clearance, a robust peripheral immune macroenvironment is expected to be a pre-requisite.

### 1.3.2 Systemic immune predictive biomarkers in breast cancer and melanoma

Considering the key role of the systemic immune system in coordinating pro- or anti-tumour responses, and introduction of immunotherapies into clinical practice, there has been substantial interest in the identification of predictive biomarkers leveraging systemic immunity. Either protein or cellular biomarkers may be used to develop predictive biomarkers which could help to inform patient treatment decisions, and **Table 1.5** summarises the list of observations to-date which analyse the association of peripheral blood immune features and prognosis in patients with breast cancer or melanoma.

Although increased serum titres of cytokines associated with ongoing immune responses are expected to indicate more favourable prognosis, for example in response to CPI immunotherapy (IL-2 at baseline and IL-4 on treatment) in small cell lung cancer [158], elevated baseline serum IL-8 has been found to be associated with poor response to CPIs [159]. The latter observation may be explained by the finding that IL-8 attracts myeloid suppressor cells to tumours [160].

**Table 1.5 Peripheral immune predictive biomarkers in breast cancer and melanoma.**

List of observations to-date analysing the association of peripheral blood immune features and response to treatment in patients with breast cancer and melanoma. Adapted from [138,161].

Peripheral blood immune feature	Prognosis	Cancer type
More CD45RA <sup>-</sup> FOXP3 <sup>hi</sup> Treg cells at baseline [147]	Relapse after surgery	Breast
High neutrophil to lymphocyte ratio [162]	Worse response to CPIs	Melanoma
High serum IL-8 [159]	Worse response to CPIs	Melanoma
Low serum LDH [163]	Better response to CPIs	Melanoma
Higher relative eosinophil count [163]	Better response to CPIs	Melanoma
Higher relative lymphocyte count [163]	Better response to CPIs	Melanoma
Higher TCR repertoire diversity at baseline [164]	Better response to CPIs	Melanoma
Fewer M-MDSCs at baseline [165]	Prolonged overall survival after CPI (anti-CTLA4) therapy, better response to neoantigen vaccine immunotherapy	Melanoma
More Treg cells at baseline [166]	Improved response to CPIs (anti-CTLA4)	Melanoma
More CD127 <sup>lo</sup> PD1 <sup>lo</sup> CD4 <sup>+</sup> T cells after treatment [167]	Better response to CPIs (anti-CTLA4 and GM-CSF)	Melanoma
Proliferating and/or clonal expansion CD8 <sup>+</sup> T cells after treatment [168,169]	Better response to CPIs (anti-PD1 or anti-PD1 + anti-CTLA4)	Melanoma
Melanoma specific antibodies to MDA and NY-ESO-1 at baseline [170]	Better response to CPIs	Melanoma
High titres of IgG, IgG1, IgG2 and IgG3 at baseline [171]	Better response to CPIs	Melanoma
More plasmablasts after treatment [172]	Better response to CPIs	Melanoma

From a cellular perspective, higher systemic TCR repertoire diversity has been reported to predict response to CPI immunotherapy in metastatic melanoma [164]. Systemic biomarkers of myeloid cell subsets (peripheral neutrophils [162] and eosinophils [163]) at baseline, likely representing inflammatory responses to cancer, are also associated with improved response to CPIs in melanoma. As expected, reduced circulating populations of immunosuppressive M-MDSCs have been found to associate with prolonged overall survival following CPI therapy [165].

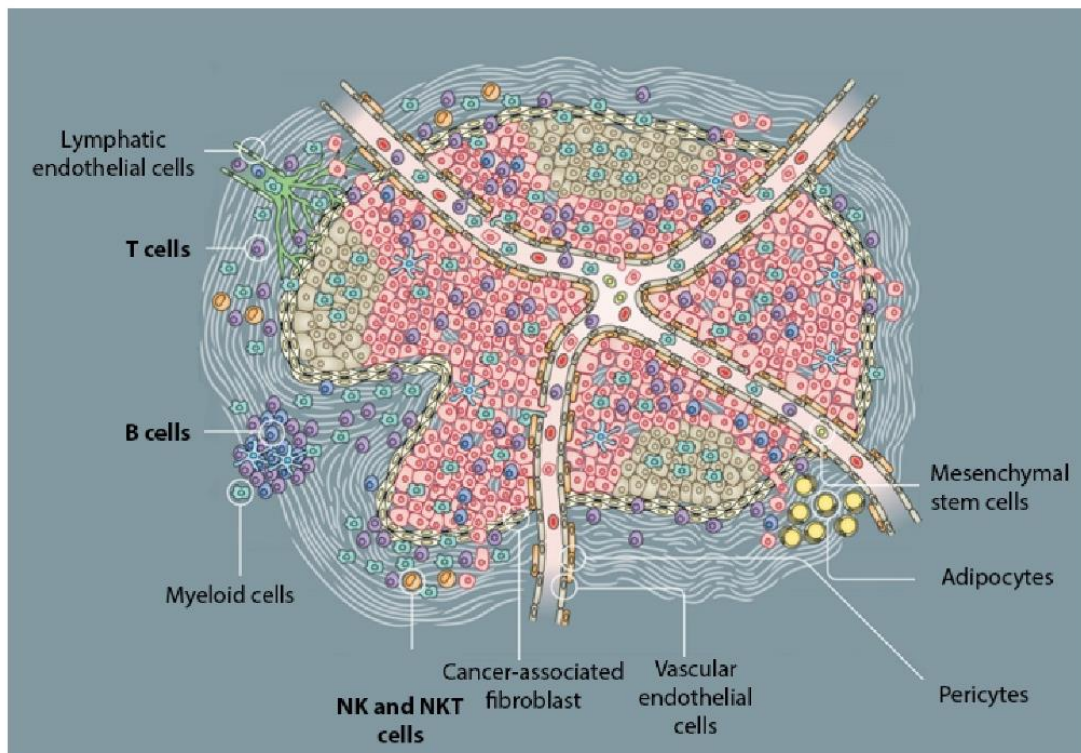
Due to the more recent entry of immunotherapy into the clinical practice of breast cancer compared to melanoma, reliable information is not yet available concerning the correlation of systemic biomarkers with immunotherapy outcomes in these individuals. However, enhanced circulating CD45RA<sup>-</sup> FOXP3<sup>hi</sup> Tregs have been shown to correlate with relapse following surgical resection [147]. In contrast, baseline peripheral Tregs may correlate with improved clinical outcomes following anti-CTLA4 immunotherapy in melanoma [166], and this observation may be explained by the constitutive expression of CTLA4 by Tregs, making them susceptible to anti-CTLA4 antibodies. In addition, multiple studies have shown that, in general, peripheral features of activated [167] and proliferating [169] T cells, including clonal expansion [168], confer improved clinical outcomes in melanoma patients receiving CPI immunotherapy.

Finally, there is evidence that baseline features of serum immunoglobulin, particularly IgG1, IgG2 and IgG3 subclasses [171] and melanoma specific antibodies [170], may be associated with improved outcome to CPI immunotherapies. In addition, elevated levels of circulating plasmablasts during treatment have been found to predict outcome to CPIs [172]. These emerging findings that peripheral B cell subsets and their secreted circulating immunoglobulin are associated with immunotherapy response highlight the importance of systemic B cell responses in contributing to clinical outcomes in cancer,

and this Thesis aims to provide new insights into the phenotype and function of circulating, and intratumoural, B cells and their secreted immunoglobulin in patients with solid tumours, including breast cancer and melanoma.

## **1.4 The tumour microenvironment**

The tumour microenvironment (TME) goes beyond a simple amalgamation of malignant cells. The TME can be thought of as a distinct complex “organ” which contains and recruits many different types of cells, malignant or otherwise. It is the interaction between malignant and non-malignant cells which generate the TME. Non-malignant cells (NMC) typically make up >50% of the cells in the tumour and are co-opted to aid in tumour progression by directing the formation of nourishing blood vessels [29].



**Figure 1.8 Landscape of the tumour microenvironment.**

In addition to malignant cells, the TME contains a vast array of non-malignant cells, including immune cells, the tumour vasculature and lymphatics, and fibroblasts and pericytes. Adapted from [173].

Communication within the diverse cellular mass is mediated by cytokines, chemokines, growth factors and inflammatory enzymes. The TME possesses molecular and immunological characteristics which bear some similarity to the processes of wound healing and inflammation, as many of these processes are activated downstream of the driver mutations in proto-oncogenes and tumour-suppressors.

The landscape of the TME is illustrated in **Figure 1.8**. In addition to malignant cells, the TME contains immune cells, the tumour vasculature and lymphatics, and fibroblasts and pericytes [173]. The immune cell infiltrates, specifically lymphocytes, are of special importance as they are considered to denote a heightened anti-tumour immune response and may correlate with anti-tumour activity and a more favourable prognosis. Tumour-infiltrating lymphocyte (TIL) subsets which may correlate with favourable patient survival outcomes include CD8<sup>+</sup> memory T cells, CD4<sup>+</sup> T-helper cells [174], B cells [175] and NK cells [176]. Tumour-infiltrating B lymphocytes (TIL-B) are sometimes found outside or inside the tumour margin, and often present inside tertiary lymphoid structures adjacent to the tumour mass, as well as in tumour-draining lymph nodes.

1.4.1 Th2-bias in the tumour microenvironment

The microenvironments of several solid tumours, including melanoma [177] and glioma [178], are often classified as holding Th2-biased cytokine expression profiles [179]. These microenvironments typically bestow pro-tumour properties such as promoting angiogenesis and inhibiting cell-mediated responses, such as those mediated by cytotoxic

T-lymphocytes (CTLs). The prototypical Th2 cytokine is interleukin-4 which, in addition to interleukin-13, can induce tumour clearance [180]. IL-10 is another Th2 cytokine with potent suppressive effects upon CTLs, and is produced by Bregs, Tregs and M2-type macrophages in the tumour microenvironment. IL-10 can also trigger a modified, otherwise named as alternative, Th2 response by inducing B cell IgG4 subclass switching in the presence of IL-4 [181]. IgG4 subclasses have been shown to be prevalent in melanoma lesions [182], and this phenomenon is discussed further in Section 1.6.1.2.

#### 1.4.2 Tertiary Lymphoid Structures













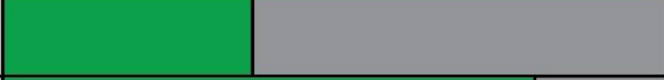


Primary lymphoid structures such as the bone marrow and thymus comprise the organs where lymphocytes form and mature. Lymphocyte activation typically occurs in secondary lymphoid structures including lymph nodes, the spleen and mucosal-associated lymphoid tissue [183]. During chronic inflammation, tertiary lymphoid structures (TLS) may transiently form, which confer sites enriched in B and T lymphocytes and dendritic cells present from disordered amalgamations to highly specialised germinal centre-like formations [184]. As tumours share many of the characteristics of chronic inflammation, it is unsurprising that TLS have been identified in a range of cancers, including in 60-90% of primary TNBCs [185], and 24% of metastatic melanoma lesions [186]. The presence of TLS has been shown to be associated with a more favourable prognosis in solid tumours [187], including in TNBC [188], melanoma [189] and non-small cell lung cancer (NSCLC) [190], and there is evidence of ongoing B cell maturation at these sites driving clonal amplification, isotype-switching and somatic hypermutation.

Recent studies have found that T cells in metastatic melanoma tumours lacking TLS have dysfunctional molecular phenotypes [189], and the presence of TLS predicts positive



response to CPI immunotherapy [189,191]. The organisation of TIL-B into TLS therefore appears to be a crucial component of anti-tumour immunity, and potential therapeutics encouraging their formation and development may gain success in the clinic.

#### 1.4.3 Anti- and pro-tumour roles of B cells in different cancers

<b>Cancer Type</b>	<b>TIL-B prognostic value (+ve/neut/-ve)</b>	<b>Studies</b>
Bladder		2
Brain		3
Breast		13
Colorectal		10
Esophageal		3
Gastric		3
Head and Neck		3
Kidney		5
Liver		9
Lung		20
Melanoma		7
Mesothelioma		2
Ovarian		8
Pancreatic		5
Squamous		3

**Figure 1.9 Summary of studies to-date analysing the prognostic significance of tumour-infiltrating B lymphocytes in patients with solid tumours.**

Horizontal bars represent the proportion of studies indicating positive (green), neutral (grey) or negative (red) prognostic value of TIL-B in each cancer type. Plasma cell and IgA-specific evaluations were excluded, and total number of studies are shown in the right-hand column. Data obtained from [192].

The precise role of B cells in being associated with anti-tumour or pro-tumour activity remains a somewhat controversial topic, and the outcome of studies investigating the prognostic significance of TIL-B in patients with solid tumours is summarised in **Figure 1.9**. Across most solid tumour types, TIL-B appear to carry an overall positive prognostic value, with the exception in brain and kidney cancers. These differences may be explained by observations of high densities of regulatory B cells in kidney renal clear cell carcinoma [193], and co-infiltration of pro-tumour macrophages [194] in brain cancers such as glioblastoma [195]. Overall, the discrepancies observed for the prognostic role of TIL-B within and across cancer subtypes likely reflects the multi-faceted role of B cells in contributing to patient clinical outcomes through antibody production, antigen presentation, and cytokine expression, which may reflect a combination of pro-tumour or anti-tumour effects likely influenced by several inflammatory signals within specific tumour microenvironments.

### **1.5 Breast tumour-infiltrating B lymphocytes**

The extent of lymphocyte infiltration into breast tumours has received considerable attention and emerged as a critical prognostic and predictive biomarker for patients [196]. TIL densities vary by molecular subtype, and TNBC/basal-like tumours typically contain the highest TIL densities, despite conferring a paradoxically poor prognosis. A “TIL working group” was established in 2014 with the aim of establishing a standardised

protocol for pathological assessment of TILs, and these guidelines are now routinely used in clinical and translational settings [197]. With the advent of CPI immunotherapy in breast cancer, and the expectation that TILs correlate with tumour immunogenicity [198], clinical algorithms are warranted which can infer curated treatment plans from TIL densities [199].

Of particular interest to this Thesis is the role of B lymphocytes and particularly mature and class-switched memory B lymphocytes in the immune response to breast tumours, and an overview of studies to date investigating the prognostic significance of breast tumour-infiltrating B lymphocytes and immunoglobulin expression is shown in **Table 1.6**, highlighting the considerable disparity of scientific reports regarding the impact of TIL-B within the breast TME. The discrepancies observed may result from differences in experimental design (*e.g.*, analysing B cell density versus percentage B cells of total TILs), or could reflect the presence of pro-tumour regulatory B cells, which in certain settings may offset anti-tumour effector mechanisms to skew the impact of B cell infiltrates in the TME towards a neutral or negative effect.

In addition, while there is uncertainty concerning the overall impact of B cells in breast cancer, the presence of CD138<sup>+</sup> plasma cells have consistently been associated with poorer survival outcomes [200], and this observation could suggest that dysregulated immune responses which strongly favour humoral over T cell-mediated immunity may hinder cytotoxic immune responses.

**Table 1.6 List of studies to-date analysing the prognostic significance of tumour-infiltrating B lymphocytes and immunoglobulin expression in breast cancer patients.**

Identification technique, B cell signature, subcohort and associated features are described. Prognostic value of TIL-B in each study is indicated in the right-hand column. Adapted from [192].

Identification technique	B cell signature	Cohort	Associated feature	Prognostic value
IHC [201]	CD20 <sup>+</sup> B cells	Primary operable invasive ductal breast cancer	N/A	Neutral
	CD138 <sup>+</sup> plasma cells		Lower expression of PR, ER & HER2	Negative
H&E morphological analysis [202]	Plasma cells	Primary operable invasive ductal breast cancer	N/A	Negative
IHC [203]	CD20 <sup>+</sup> B cells	Primary invasive breast carcinoma	Higher grade, ER <sup>-</sup> and PR <sup>-</sup> , basal phenotype	Positive
IHC [204]	CD20 <sup>+</sup> B cells	Primary operable invasive ductal breast cancer	N/A	Positive
IHC [205]	Peritumoural and stromal CD20 <sup>+</sup> /CD19 <sup>+</sup> B cells	Ductal carcinoma in situ with or without an invasive component	Higher tumour grade and size, lymph node metastases, ER <sup>-</sup> /PR <sup>-</sup> , HER2 <sup>+</sup>	Negative
	Intratumoural B cells		N/A	Neutral
	CD138 <sup>+</sup> plasma cells		N/A	Negative
IHC [206]	CD20 <sup>+</sup> B cells	Invasive breast cancer	ER <sup>-</sup> , PR <sup>-</sup> , or triple-negative	pCR: positive
IHC [207]	CD20 <sup>+</sup> B cells	Primary triple negative breast cancer	N/A	pCR: positive
IHC [208]	CD20 <sup>+</sup> cell count before chemotherapy	Stage II or III breast cancer after neoadjuvant chemotherapy	N/A	pCR: positive
RNA expression microarray [209]	B cell gene signature (predominantly IG genes)	Node negative, high proliferation subtype	N/A	Positive
		Node negative, low proliferation subtype	N/A	Neutral
RNA expression microarray of fresh frozen tissue and publicly available microarray data, RT-PCR, IHC [210]	B cell gene signature, IGKC gene expression	Node negative or positive, with or without chemotherapy	IGKC expression in mature plasma cells, equal predictive value	Positive

Identification technique	B cell signature	Cohort	Associated feature	Prognostic value
TCGA RNASeq, gene signatures [211]	B cell gene signatures, IgG gene signatures	Basal subtype	N/A	Positive
		HER2-enriched subtype	N/A	Positive
		luminal A/B subtypes		Neutral
TCGA RNASeq, gene signatures [212]	Immature B cells, memory B cells, activated B cells	Primary breast cancer	N/A	Negative
Antigen microarray [213]	<i>Ex vivo</i> IgG response of tumour infiltrating B cells to cancer associated antigens	Untreated invasive primary breast carcinomas, stage I to III at diagnosis	HER2 overexpression, lower CD8 <sup>+</sup> T cell infiltration	Negative

In summary, although the presence of tumour-infiltrating B lymphocytes, plasma cells [214] and immunoglobulin [213] may be common features of breast tumour microenvironments, there is still considerable uncertainty regarding their roles in contributing to clinical outcomes. A key aim of this Thesis is to disentangle the B cell response to breast tumours including the presence of isotype-switched B cell subsets, their location in the tumour microenvironment, and functional crosstalk with T cells. In addition, this Thesis investigates Ig isotype expression and B cell clonal expansion, including identification of immune bias towards specific isotypes. Together, these studies will provide new insights into the role of B cells in the breast TME.

## **1.6 Melanoma tumour-infiltrating B lymphocytes**

Melanoma is the most immunogenic cancer type, evidenced by systemic and local activation of immune responses, significant infiltration of immune cells, and high neoantigenic load in relation to other tumour types [215]. Moreover, lymphocyte

infiltrates are largely considered to have a positive prognostic value in patients with primary cutaneous melanoma [216]. Melanoma lesions typically contain populations of infiltrating B lymphocytes that are either dispersed within the tumour stroma, tumour islets, or organised into follicle-like aggregates [217]. A summary of published studies to date investigating the prognostic significance of melanoma tumour-infiltrating B lymphocytes and immunoglobulin expression is shown in **Table 1.7**, displaying how the presence of TIL-B has consistently been found to correlate with favourable patient survival [218,219].

Notably, studies have demonstrated a negative prognostic value for IgA-biased intratumoural immunoglobulin expression [220], and the presence of plasma cell sheets associated with IgA isotypes [221]. These findings may reflect the expected lower specificity and reduced effector function of IgA compared to IgG isotypes, which may hinder anti-tumour immunity [192]. Alternatively, emerging evidence has pointed to the existence of a regulatory loop, mediated by TGF- $\beta$ , which initiates B cell isotype-switching to IgA, alongside IL-10 and PD-L1 expression [222]. IL-10-producing regulatory B cells [121] have been shown to exhibit pro-tumour activity within inflammation-induced skin cancer mouse models, likely via the exertion of suppressive effects upon other immune cell types in the surrounding peri-tumoural space and in tertiary lymphoid structures [223].

This alternate explanation may represent a potential mechanism of immune evasion mediated by the tumour. Evaluating the presence and function of cytokine producing and regulatory B cells in melanoma patients forms a key part of this thesis.

**Table 1.7 List of studies to-date analysing the prognostic significance of tumour-infiltrating B lymphocytes and immunoglobulin expression in melanoma patients.**

Identification technique, B cell signature, subcohort and associated features are described. Prognostic value of TIL-B in each study is indicated in the right-hand column. Adapted and references (unless stated) available from [192].

Identification technique	B cell signature	Cohort	Associated feature	Prognostic value
TCGA data analysis for intratumoural IG genes [220,224]	IG expression	Primary and metastatic melanomas	N/A	Positive
	IG clonality, IGHG1 clonality		N/A	Positive
	IGHG1:IGH ratio		N/A	Positive
	IgA/IGH ratio		N/A	Negative
TCGA RNASeq [195]	B cell gene signature	Primary and metastatic melanomas	N/A	Positive
	IgG expression		N/A	Positive
TCGA RNASeq [212]	B cell gene signature	Primary and metastatic melanomas	N/A	Positive
TCGA RNASeq [225]	Plasmablast-like dominated B cell population signature with the genes CD27, CD38, and PAX5	Primary and metastatic melanomas	Expression of CD8A, number of CD8 <sup>+</sup> T cells and macrophages, inflammatory microenvironment	Positive
RNA-seq data [225]		Advanced melanoma treated with anti-PD1 antibodies		Positive
IHC [221]	Sheets of CD138 <sup>+</sup> plasma cells	Invasive primary cutaneous melanoma	IgA isotype, oligoclonality	Negative
	Sparse CD138 <sup>+</sup> plasma cell		N/A	Positive
IHC [218]	CD20 <sup>+</sup> B cells	Metastatic melanoma	N/A	Positive
	CD138 <sup>+</sup> plasma cells		N/A	Positive
IHC [219]	CD20 <sup>+</sup> B cells	Nonmetastasized cutaneous primary melanoma with a Breslow depth of >1.0 mm	N/A	Positive
TCGA data [219]	MS4A1(CD20):CD19 mRNA ratio	Primary and metastatic melanomas	N/A	Positive
TCGA data [226]	CD20 mRNA	Primary and metastatic melanomas	N/A	Positive

The presence of B cells is also emerging as an important predictive biomarker for melanoma treatment response. Recent work has shown that plasmablast-like B cells are associated with improved response and survival outcomes in patients on anti-PD-1 CPI

immunotherapy [225]. Another study identified unique functional B cell attributes in patients responding to CPI immunotherapy, including clonal expansion and the presence of switched memory B cells in the TME [191]. Paradoxically, the presence of TIL-B has been found to be associated with decreased MAPK activity, immunosuppressive (HLA-DR/IDO-1) tumour phenotypes and reduced overall survival in patients treated with the BRAF/MEK inhibitor combination therapy dabrafenib and trametinib [227]. It is possible that B cells in TIL-B rich tumours provide additional growth signals that reduce the MAPK signaling-dependency of the tumour, providing a straightforward escape mechanism following inhibition of the BRAF/MEK pathway. Together, these studies demonstrate the potential benefit of better understanding the presence and functions of B cells in the circulation and the tumour microenvironment for biomarker discovery and patient stratification in the future.

### 1.6.1 Mechanisms of the humoral immune response and expressed antibody effector functions in melanoma

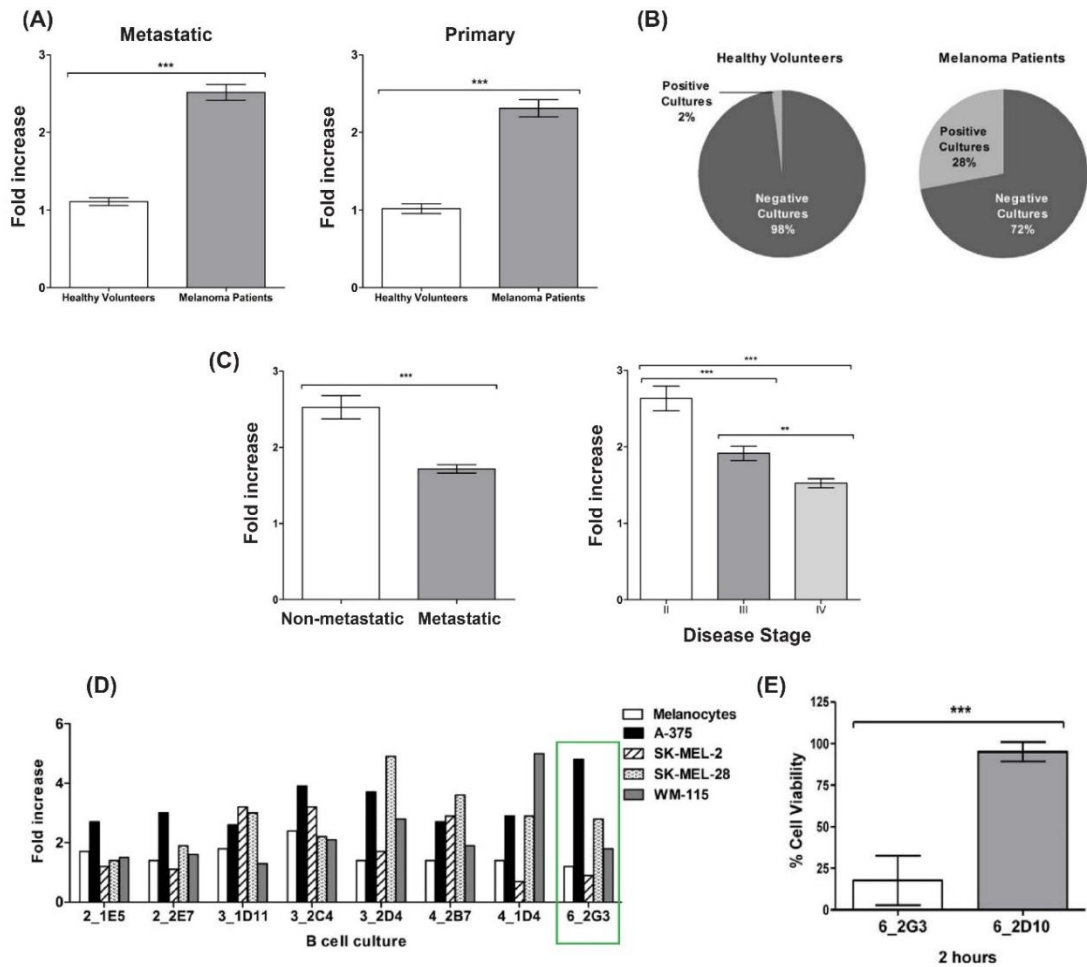
#### 1.6.1.1 Antibody expression among melanoma tumour-reactive B cells

Studies have shown that B cells in patients with melanoma are likely to recognise cancer antigens and to produce tumour-specific immunoglobulins. Antibodies to over one hundred distinct melanoma-associated antigens have been identified in patient serum, using serological identification of antigens by recombinant expression cloning (SEREX) approaches [228,229]. Recent work has reported a fluorescent bead-based technique for the identification of tumour antigen-specific B cells, which was used to derive a



monoclonal antibody from patient peripheral blood B cells which recognised a tumour-associated antigen [230].

In addition, B cells derived from melanoma patient peripheral blood have been shown to produce IgG antibodies to autoantigens *ex vivo*, detected using a cell-based ELISA technique [231]. A significantly higher frequency of B cell-derived antibodies recognising melanoma cell-associated antigens when compared to B cells from healthy volunteers has been reported (**Figure 1.10 (A)**). For example, 28% of patient-derived B cell cultures, compared to 2% of healthy volunteer cultures, produced antibodies specific to melanoma cells (**Figure 1.10 (B)**). These antibody responses appeared to decrease with disease progression, which may reflect tumour-associated immune escape mechanisms (**Figure 1.10 (C)**). In the same study, a patient-derived monoclonal antibody was shown to exhibit potent cytotoxic effects upon melanoma cells *in vitro* via ADCC (**Figure 1.10 (D-E)**), representing a potential effector mechanism mediated by secreted immunoglobulin against cancer cells [231]. These results highlight potentially active roles for circulating B cells in systemic immune responses, and potential contribution to the recognition and targeting of melanoma cells in patients.

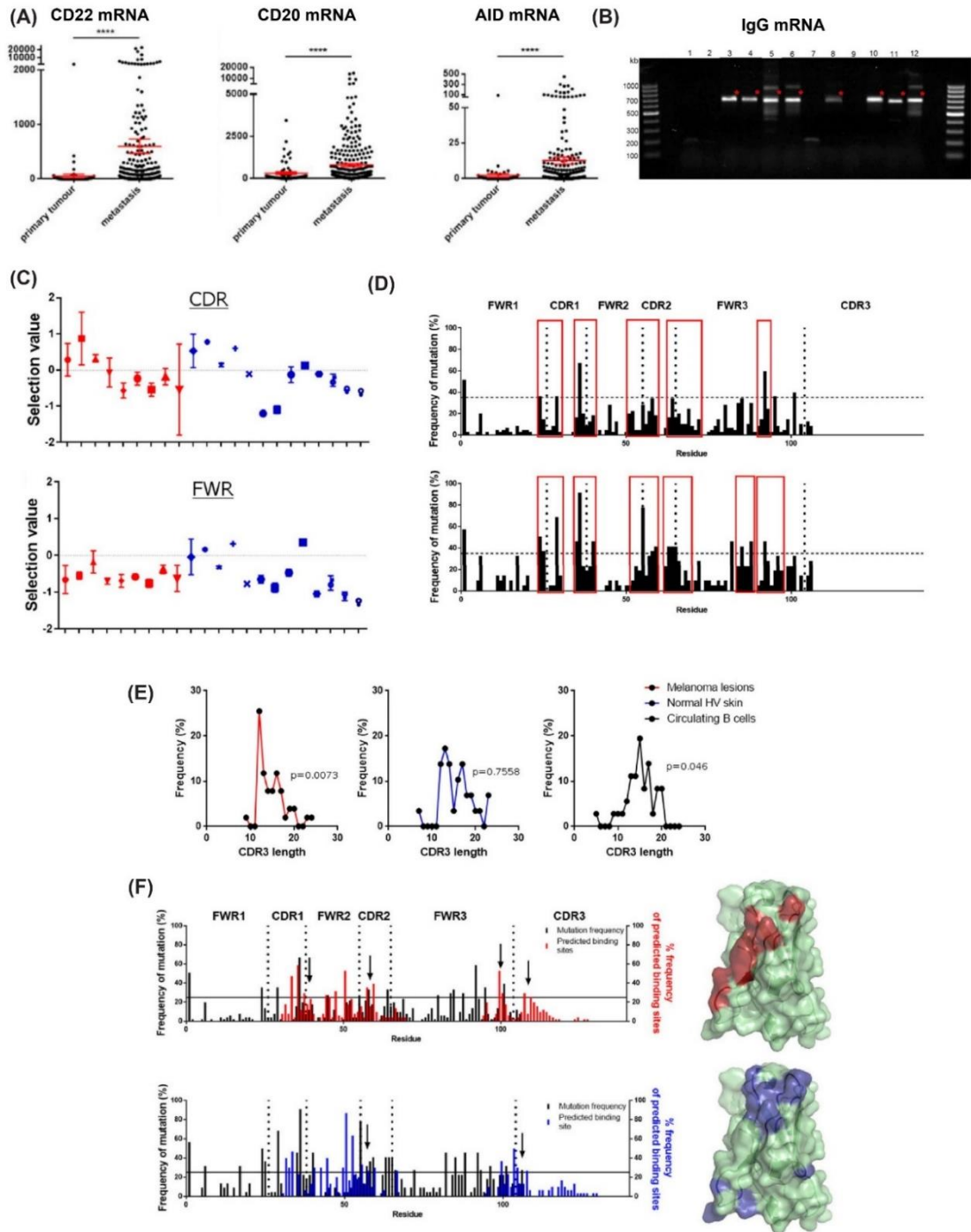


**Figure 1.10 Melanoma patient peripheral blood B cells produce IgG antibodies to autoantigens *ex vivo*.**

(A) Antibodies from *ex vivo* cultures of B cells extracted from the peripheral blood of patients diagnosed with primary and metastatic melanoma show increased reactivity to melanoma cell lines, compared to B cells from healthy volunteer blood. Antibodies were measured using a cell-based ELISA technique. (B) 28% of patient-derived B cell cultures, compared to 2% of healthy volunteer cultures, produced antibodies reactive to metastatic melanoma cells. (C) Melanoma tumour-reactive antibody declines with metastatic disease [left] and by disease stage [right]. (D) Selection of a tumour-reactive antibody culture for sub-cloning and generation of monoclonal antibody. Reactivity to four melanoma cell lines and melanocytes was evaluated, and culture 6\_2G3 was selected based upon its superior reactivity to melanoma cells relative to melanocytes. (E) A tumour-reactive monoclonal antibody (6\_2G3 clone) induced increased tumour cell cytotoxicity in a melanoma cell:monocyte co-culture, compared to a non-specific control antibody (G\_2D10 clone) from the same donor. Data published in Gilbert et al., [231].

Other studies have provided further support for the role of antibody responses in melanoma patients. Transcriptomic analyses showed the presence of B cells (CD20, CD22), mature IgG mRNA, and of the enzyme AID in melanoma lesions (**Figure 1.11 (A-B)**) [226]. Consistent with the presence of AID, the study reported evidence of clonal selection and SHM in patient tumours (**Figure 1.11 (C-D)**). A subset of melanoma-associated antibodies had shorter complementarity-determining (CDR)3 regions relative to those from circulating B cells (**Figure 1.11 (E)**), suggesting the presence of B cell clones in melanoma tumours which were different to circulating B cell clones. Despite the low frequency of B cells in human skin, distinct antibody repertoires are likely to exist between healthy skin and melanoma, as clonal amplification and homology modelling indicated divergent antigen recognition repertoires between the two tissue niches (**Figure 1.11 (F)**) [226].

Overall, the presence of tumour-reactive B cells, with IgG subclass profiles in melanoma patient blood and tumour, and evidence of SHM and clonal expansion among melanoma tumour-infiltrating B lymphocytes, support the presence of active and dynamic B cell immune responses in cutaneous melanoma. These responses may also be present in other solid tumours, including in breast cancer, the study of which forms a major part of this Thesis.



**Figure 1.11 IgG subclass switching, clonal selection and somatic hypermutation among melanoma tumour-infiltrating B lymphocytes.**

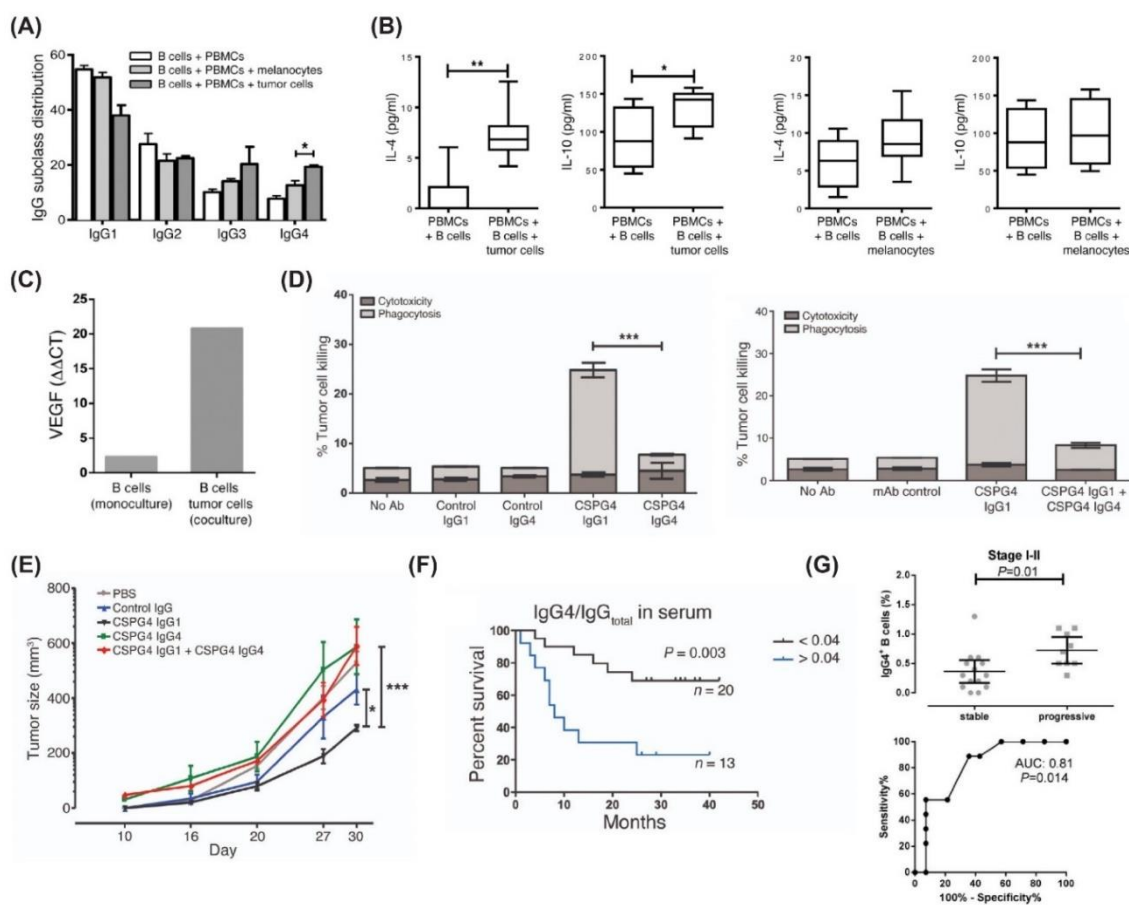
(A) mRNA transcripts conferring B cells (CD20, CD22) and AID are present in melanoma lesions and enhanced in metastatic versus primary tumours (data from The Cancer Genome Atlas (TCGA) database). (B) Mature IgG mRNA (red stars) was detected in melanoma lesions, following amplification of IgGVH regions. (C) 90% of framework region (FWR) VH sequences from melanoma samples (red), and 76% from normal skin samples (blue) were predicted to have undergone negative selection, indicative of affinity maturation and local clonal expansion. (D) Divergence from germline sequence in melanoma [top] and normal skin [bottom] IgG. Red boxes indicate mutational clusters and horizontal lines signify threshold (35%) highlighting somatic hypermutation hotspots. (E) Analysis of CDR3 length frequency in IgGs from melanoma, normal

skin, and melanoma patient peripheral blood B cells. Melanoma-associated antibodies have shorter CDR3 regions relative to those from circulating B cells. (F) Homology modelling of predicted antigenic binding regions in melanoma [top] and normal skin [bottom] IgG, highlighting divergent antigen recognition repertoires between the two niches. Data published in Saul et al., [226].

#### 1.6.1.2 IgG4 subclass switching as an immune evasion mechanism

The distribution of antibody subclasses, which confer binding affinities to immune effector cells, represent a critical component of antibody-mediated immune responses against pathogens. Early studies observed abnormalities in IgG4 serum titres in melanoma patients [232]. These observations were later confirmed [151] and have also been made in cholangiocarcinoma [233] and colorectal cancer [234], although the extent to which these trends are present in other cancer subtypes is currently unclear. In melanoma, tumour infiltrating B cells have been shown to possess skewed antibody subclass expression profiles, with a bias towards IgG4 and away from IgG1 expression, compared to patient circulating B cells [182]. In a separate study, lower proportions of IgG1 were confirmed among antibodies obtained from melanoma tumours, compared to those from circulating B cells [226].

These observations are consistent with the action of an alternative Th2 response, whereby IL-10 induces B cell IgG4 subclass switching in the presence of IL-4 [181]. In support of this, *ex vivo* co-culture of melanoma patient peripheral blood B cells with melanoma cells led to enhanced production of IgG4 (**Figure 1.12 (A)**), accompanied with upregulation of IL-4 and IL-10 expression, and this trend was not seen in co-cultures with melanocytes [182] (**Figure 1.12 (B)**). *Ex vivo* stimulated B cells were found to express VEGF, which was enhanced among B cells following co-culture with melanoma cells, and may also contribute to IgG4 polarization [182] **Figure 1.12 (C)**.



**Figure 1.12 IgG4 subclass switching as an immune evasion mechanism in patients with melanoma.**

(A) *Ex vivo* co-culture of melanoma patient peripheral blood B cells with irradiated peripheral blood mononuclear cells (PBMCs) and melanoma cells led to polarised IgG4 production, which was significantly enhanced compared to cultures involving melanocytes. (B) Significantly enhanced titres of IL-4 and IL-10 are present in PBMC + B cell + tumour co-culture supernatants compared to cultures involving melanocytes. (C) Comparative real-time PCR analysis demonstrates B cell VEGF expression is enhanced in B cell + tumour cell co-culture, compared to B cell culture alone. (D) [Left] An engineered melanoma tumour-antigen specific IgG4 antibody is ineffective at inducing effector-mediated tumour-cell killing, and [Right] inhibits tumour antigen-specific IgG1-mediated tumour-cell killing *in vitro*. (E) Co-administration of tumour-antigen specific IgG4 antibody significantly weakens IgG1-mediated tumour-growth restriction in a human xenograft mouse model. (F) Elevated serum IgG4 of total IgG is associated with significantly reduced overall survival in metastatic melanoma patients. (G) Enhanced frequencies of circulating IgG4<sup>+</sup> B cells are associated with significantly increased risk of disease progression in early (stage I-II) melanoma patients. Data published by Karagiannis et al., [182] (A-F) and [151] (G).

IgG4 antibodies are structurally distinct from IgG1, and undergo a process called Fab arm exchange which makes them unable to form stable immune complexes on the surface of effector cells. IgG4 also confers a weaker ability to bind and stimulate effector cells such

as NK cells and macrophages to initiate antibody-dependent cell-mediated cytotoxicity or phagocytosis [235,236]. An engineered melanoma-specific IgG4 antibody has been shown to be ineffective at inducing effector-mediated tumour-cell killing compared with the corresponding IgG1 isotype *in vitro* [182] (**Figure 1.12 (D, left)**). Moreover, IgG4 antibodies inhibit the cytotoxic function of anti-melanoma IgG1 isotypes (**Figure 1.12 (D, right)**) by competing for Fc-gamma receptor binding, and were shown to significantly weaken IgG1-mediated tumour-growth restriction in a human melanoma xenograft mouse model partly reconstituted with human immune effector cells [182] (**Figure 1.12 (E)**). As a potential result of these mechanisms, elevated serum levels of IgG4 (**Figure 1.12 (F)**), and IgG4-expressing B cells (**Figure 1.12 (G)**) were found in patients with melanoma. Furthermore, higher levels of serum IgG4 were associated with less favourable survival outcomes in patients with melanoma over a 4.5-year follow up interval [151].

In summary, IgG4 subclass switching may confer a form of tumour immune evasion mediated by cytokines including IL-4, IL-10 and VEGF. B cells may be an important source of these cytokines. Therefore, the contribution of B cell cytokine expression to immune responses in melanoma patients forms a critical element of this thesis.

## **1.7 Regulatory B cells in cancer**

Studies from mouse models have provided evidence for a role of immunosuppressive, or “regulatory” B cells (Bregs) in affecting tumour progression. A subset of “tumour-evoked” Bregs has been shown to facilitate the metastasis of breast cancers through the induction of Tregs via TGF- $\beta$  signaling [237]. Importantly, tumour-associated antigens such as 5-lipoxygenase metabolites and placental growth factor have been shown to

induce regulatory cytokine expression among TIL-B in murine models of breast cancer [238] and glioblastoma [239]. It is therefore possible that populations of TIL-B are driven to a TGF- $\beta^+$  and/or IL-10 $^+$  regulatory phenotype by tumour-derived antigens in the TME [240], likely in concert with cytokine signals. Bregs are expected to play negative roles in anti-tumour immunity and have been shown to inhibit the efficacy of anti-CD20 immunotherapy in lymphoma-bearing mice, owing to their inhibitory effects on antibody-mediated monocyte activation and effector function through IL-10-dependent mechanisms [241].

At present there are few studies investigating the role of regulatory B cells in affecting tumour progression in humans. One study showed that IL-21 secretion by Tregs induced granzyme-B-expressing Bregs within solid tumours of breast, cervical and ovarian cancer patients, which inhibited T-helper cell proliferation [242]. In addition, transitional Bregs are upregulated in gastric cancer patient peripheral blood and tumours, and are functionally capable of suppressing the synthesis of IFN- $\gamma^+$  and TNF- $\alpha^+$  by autologous CD4 $^+$  T-helper cells via IL-10, while TGF- $\beta$ -expressing B cells mediate the conversion of CD4 $^+$  T-helper cells to Tregs [243].

### 1.7.1 Regulatory B cells in skin inflammation and cancer

In healthy individuals, subsets of circulating B cells express the skin-homing marker cutaneous lymphocyte antigen (CLA), and populations of mature, isotype-switched IgG-expressing B cells have been detected in normal human skin tissue [226]. Moreover, skin-resident B cells have been found to accumulate and proliferate in human skin in response to cutaneous antigenic challenge [244]. In addition, IL-10-expressing regulatory B cells have been shown to suppress cutaneous inflammation, and reduce disease severity, in



models of psoriasis-like inflammation [245,246]. Together, these observations highlight the dynamic role of B cells in immunosurveillance of the skin, including studies reporting anti-inflammatory properties of skin-infiltrating B cell populations.

There is currently limited evidence for the role of regulatory B cells in human cancerous skin tissue microenvironments. A recent study identified a subset of naïve PD-L1-expressing Bregs which were upregulated in advanced melanoma and suppressed *ex vivo* IFN- $\gamma$ -mediated CD4<sup>+</sup> and CD8<sup>+</sup> T cell responses [153]. A novel tumour-infiltrating IgG4<sup>+</sup> CD49b<sup>+</sup> CD73<sup>+</sup> B cell subset expressing proangiogenic cytokines including VEGF, CYR61, ADM, FGF2, PDGFA, and MDK has also recently been identified in patients with melanoma [154].

Support for the role of IL-10-expressing regulatory B cells in malignant skin tissue has been established using mouse models. A model of squamous cell carcinoma showed that IL-10-expressing B cells contribute to tumour progression [223]. Recent evidence has also shown that IL-10-expressing murine B-1 cells can inhibit IFN- $\gamma$  and TNF- $\alpha$ -expressing CD8<sup>+</sup> T cells and contribute to melanoma growth *in vivo* [247]. To date, there have been no investigations into the modulation of IL-10-, or TGF- $\beta$ -producing regulatory B cells in human melanoma, of which forms a key element of this thesis.

## **1.8 Aims and Objectives**

Previous studies from our group and others have highlighted the presence of isotype-switched B cells in patients with melanoma, with skewed immunoglobulin expression of immunologically inert antibody isotypes such as IgG4. These insights point to a dichotomy of activation and differentiation alongside regulation of the humoral response in some cancers. Therefore, the overall aim of this Thesis is to provide further insights

into the complexity of humoral responses in immunogenic tumours such as melanoma and TNBC, which may include a balance of simultaneous immunostimulatory and immunomodulatory functions. Through the study of dysregulation in the systemic and intratumoural B cell responses to breast cancer and melanoma, the ultimate aim will be to uncover previously unappreciated contributions of less well-explored immune compartments which may lead to the unravelling of potential biomarkers and therapeutic avenues.

The specific objectives of this research project are:

- I. To investigate the role of circulating and TIL-B in breast cancer, focusing upon aggressive and immunogenic subtypes such as TNBC. Chapter 3 describes my evaluations of the presence, localisation, and functional attributes, including immunoglobulin expression, of circulating and TIL-B in breast cancer, with a focus on mature, isotype-switched and memory B cell subsets. In this work, I examine evidence for systemic perturbations of humoral immunity and skewing of immunoglobulin isotype and clonal profiles. Finally, I aim to ameliorate the current uncertainty regarding the prognostic value of breast TIL-B by mapping the relative contributions of B cell lineages and functions towards clinical outcomes.
  
- II. To investigate the prevalence and potential roles of cytokine-expressing B cells as complex and dynamic players in systemic and intratumoural immunity of patients with melanoma. Chapter 4 describes my analyses of the regulatory (IL-10<sup>+</sup> and/or TGF- $\beta$ <sup>+</sup>) and pro-inflammatory (IFN- $\gamma$ <sup>+</sup> and/or TNF- $\alpha$ <sup>+</sup>) B cell compartments in melanoma patients, and their crosstalk with and roles in influencing autologous T cell phenotype and function. I examine dysregulation

and lineage sources of cytokine-expressing B cells in the peripheral blood of patients with melanoma. I also explore melanoma tumour-infiltrating populations of regulatory and inflammatory B cells and aim to uncover previously unknown interactions with TIL-T. Lastly, I evaluate evidence supporting an immune dichotomy, whereby melanoma patient B cells may simultaneously exert polarising immunostimulatory and immunomodulatory influences upon autologous T cells and their functions.

## **Chapter 2: Materials and Methods**

### **2.1 Human tissue samples and processing**

#### **2.1.1 General reagents**

Human tissue sample processing was performed using the reagents listed in **Table 2.1** below.

**Table 2.1 Reagents used for human tissue sample processing.**

<b>Name</b>	<b>Supplier</b>	<b>Catalogue Number</b>
BD Vacutainer™ SST™ II Advance Tubes	BD Biosciences	12927696
CryoTube, free standing round bottom; 1.8 mL	Thermo Fisher Scientific	UY-03755-10
PBS, sterile	Gibco	10010-023
gentleMACS™ C Tubes	Miltenyi Biotec	130-093-237
RPMI 1640	Gibco	11875-093
Trypan Blue Solution, 0.4%	Gibco	15250-061
FBS	Gibco	10106-159
DMSO, Anhydrous	Invitrogen	D12345

#### **2.1.2 Human tissue sample collection**

Human venous blood samples were obtained from healthy volunteers (HVs) and patients with either breast cancer or melanoma. Bloods were taken either before or after occurrence of surgical resection, and patients receiving checkpoint inhibitor immunotherapy were excluded from the study. Breast and melanoma tumour specimens were also provided following excision as part of standard clinical care. Matched non-adjacent non-tumour (NANT) tissue from patients with breast cancer, and normal breast tissue from healthy individuals were obtained to serve as controls. All samples were

collected in compliance with the Human Tissue Act 2006 and with informed written consent in accordance with the Helsinki Declaration. Breast cancer patients were recruited by Breast Cancer Now, and study design was approved by the Guy's Research Ethics Committee, Guy's and St. Thomas' NHS Foundation Trust (REC No. 07/H0804/131). Melanoma patients were recruited as part of the Melanoma Immunomodulation and Immune Responses of the Skin Study: A Translational Science Research Protocol (MISST) study, and study design approved by the London Central NRES Committee and conducted at Guy's and St Thomas NHS Foundation Trust (REC No. 16/LO/0366).

### 2.1.3 Serum collection and processing

Serum was collected from HV and patients with melanoma or breast cancer. Whole blood was collected in BD Vacutainer® Serum Separator tubes and allowed to clot at room temperature (RT) for 30 minutes. The tubes were then spun at 3000rpm (1500xg) for 20 minutes at 4 degrees Celsius (°C), and serum was transferred into 200µl aliquots in cryovials and stored at -80°C. Vials were removed from storage and thawed on ice as required.

### 2.1.4 Tumour, NANT and normal tissue processing

Breast tumour, melanoma samples, NANT and normal tissue specimens were initially kept in PBS following surgical excision. Tissues were cut into small (2-4mm) segments and transferred into gentleMACS C tubes containing RPMI 1640 (2ml for <0.2g and 4ml for >0.2g specimens). Tubes were then attached upside-down onto the sleeve of a

gentleMACS dissociator. Dissociation was performed using the “m h\_tumor\_01” program. The resulting suspension was passed through a 40µm filter, washed through with 20ml RPMI 1640, and slow spun for 7 minutes at 565rpm (300xg). Where necessary, cell counts were performed using a haemocytometer with trypan blue staining (1:10 dilution in PBS). Percentage viability (mean ± SD) was determined as 36.4 ± 23.8 for breast tumour, 38.2 ± 26.2) for melanoma tumour, and 58.6 ± 32.4 for NANT and normal tissues. The cell suspensions containing tumour cells, stromal cells, and tumour infiltrating lymphocytes were used immediately in experimental work, or aliquoted into freezing solution (FBS, RPMI 1640 and DMSO at 4:4:1 ratio) and stored in 1.5ml aliquots in cryovials at -80°C in Mr. Frosty containers. Vials of frozen cells were removed from storage and thawed at RT as required.

## **2.2 Immune cell isolation**

### **2.2.1 General reagents**

Immune cell isolation was performed using the reagents using the reagents and in-house produced buffers listed in **Table 2.2** and **Table 2.3**, respectively.

**Table 2.2 Reagents used for immune cell isolation.**

<b>Name</b>	<b>Supplier</b>	<b>Catalogue Number</b>
BD Vacutainer® EDTA Blood Collection Tubes	BD Biosciences	1167106
PBS, sterile	Gibco	10010-023
FBS	Gibco	10106-159
Ficoll-Paque PLUS density gradient media	VWR	17-1440-03
SepMate™-50 (IVD) Tubes	STEMCELL Technologies	85460

Name	Supplier	Catalogue Number
Falcon 50mL Conical Centrifuge Tubes	Thermo Scientific Fisher	10788561
eBioscience™ 10X RBC Lysis Buffer (Multi-species)	Invitrogen	00-4300-54
RPMI 1640	Gibco	11875-093
DMSO, Anhydrous	Invitrogen	D12345
CryoTube, free standing round bottom; 1.8 mL	Thermo Scientific Fisher	UY-03755-10
Falcon™ Round-Bottom Polystyrene Test Tubes	Thermo Scientific Fisher	10186360
Human BD Fc Block™	BD Biosciences	564219
LIVE/DEAD™ Fixable Near-IR Dead Cell Stain Kit	Invitrogen	L10119
autoMACS Rinsing Solution	Miltenyi Biotec	130-091-222
Albumin, from bovine serum	Sigma	A3059
Sterile Cell Strainers, 40 µm	Cole-Parmer	UY-06336-63
DMEM, high glucose, pyruvate	Gibco	41966-029
Penicillin-Streptomycin (10,000 U/mL)	Gibco	15140-122
RosetteSep™ Human B Cell Enrichment Cocktail	STEMCELL Technologies	15064
RosetteSep™ Human CD4 <sup>+</sup> T Cell Enrichment Cocktail	STEMCELL Technologies	15062

**Table 2.3 In-house produced buffers used for immune cell isolation.**

Name	Composition
FACS buffer	PBS with 5% FBS
Sorting buffer	autoMACS Rinsing Solution with 0.5% bovine serum albumin (BSA)

### 2.2.2 Antibodies

Immune cell isolation was conducted using the antibodies listed below (**Table 2.4**), during positive selection using the BD FACS Aria II sorter.

**Table 2.4 Antibodies used for immune cell isolation using the BD FACS Aria II cell sorter.**

Specificity	Clone	Conjugate	Host species	Supplier	Catalogue number
CD19	HIB19	V500	Mouse	BD Biosciences	561121
CD4	A161A1	PE	Rat	BioLegend	357404
CD25	M-A251	PerCP-Cy5.5	Mouse	BioLegend	356112
CD127	A019D5	PE-Cy7	Mouse	BioLegend	351320

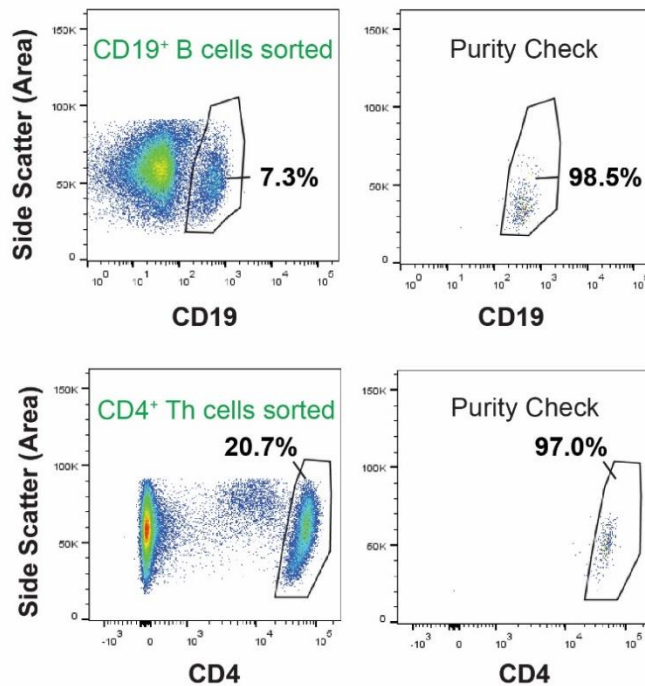
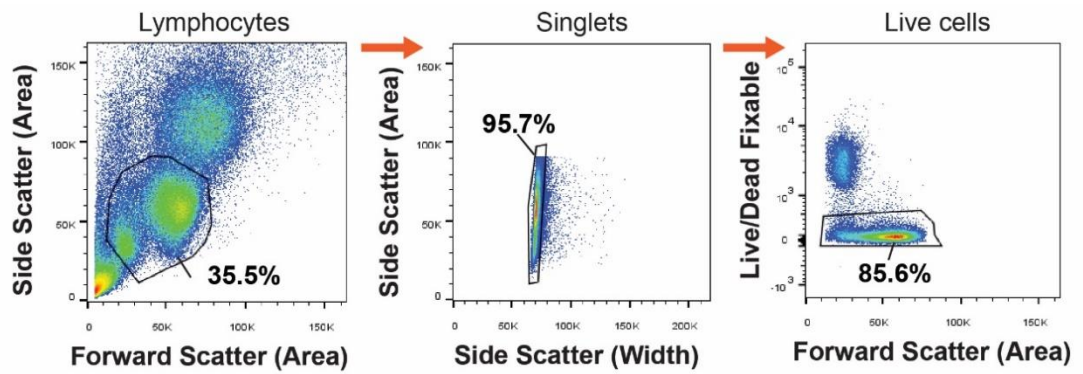
### 2.2.3 Peripheral Blood Mononuclear Cell isolation

Whole blood samples from HVs and cancer patients were collected in BD Vacutainer® EDTA tubes and kept on a roller-shaker for a maximum of 24 hours. The blood was diluted at in FACS buffer (PBS with 5% FBS) at a 1:1 ratio and layered over 15ml Ficoll-Paque PLUS density gradient media in SepMate-50 (IVD) tubes, before being spun at 2260rpm (1200xg) for 20 minutes at RT with brake. The platelet-enriched plasma cell layer was removed, and the peripheral blood mononuclear cell (PBMC) layer was transferred into a fresh 50ml Falcon tube. PBMCs were washed twice in FACS buffer at 1500rpm (720xg) for 5 minutes. Cells were then resuspended in 25ml RBC Lysis Buffer and incubated for 10 minutes at 4°C. Cells were pelleted, resuspended in 25ml FACS buffer, and pelleted again at 1500rpm. Where necessary, PBMC counts were performed as previously described (Section 2.1.4). At this point, the isolated PBMCs were either used immediately in experimental work, processed further (*e.g.*, cell sorting, or enrichment performed), or aliquoted in freezing solution and stored in 1.5ml aliquots at  $1 \times 10^6$  cells/ml in cryovials at -80°C in Mr. Frosty containers. Vials of frozen PBMCs were removed from storage and thawed at RT as required.



#### 2.2.4 Positive isolation of B and T-helper cells from HIV and melanoma patient peripheral blood

B cells and T-helper cells were isolated from HIV and melanoma patient PBMCs using positive selection with anti-CD19 and anti-CD4 antibodies (**Table 2.4**), for use in *ex vivo* co-culture experiments (Section 2.4). Selection was performed using the BD FACS Aria II cell sorter to obtain purified CD19<sup>+</sup> B and CD4<sup>+</sup> T-helper cell suspensions for downstream cytokine suppression and Treg induction assays. Isolated PBMCs (1x10<sup>8</sup> cells/ml) were transferred into individual 5ml Round Bottom Polystyrene FACS Tubes and incubated with 5µl human Fc block for 5 minutes at RT. Next, 5µl LIVE/DEAD Fixable Near-IR Dead Cell Stain (pre-diluted 1:20 in PBS) was added alongside 2.5µl each of anti-CD19-V500 and anti-CD4 PE, and cells incubated for 30 minutes at 4°C. Cells were washed twice in 2ml FACS buffer at 1500rpm (720xg) and resuspended in 500µl sorting buffer (autoMACS Rinsing Solution with 0.5% BSA), at a maximum of 6x10<sup>7</sup> cells/ml. Finally, cells were passed through a 40µm filter into fresh FACS tubes and sorted into CD19<sup>+</sup> and CD4<sup>+</sup> fractions in DMEM (10% FBS, 50U/ml Pen-Strep) media according to the gating strategy outlined in **Figure 2.1**.

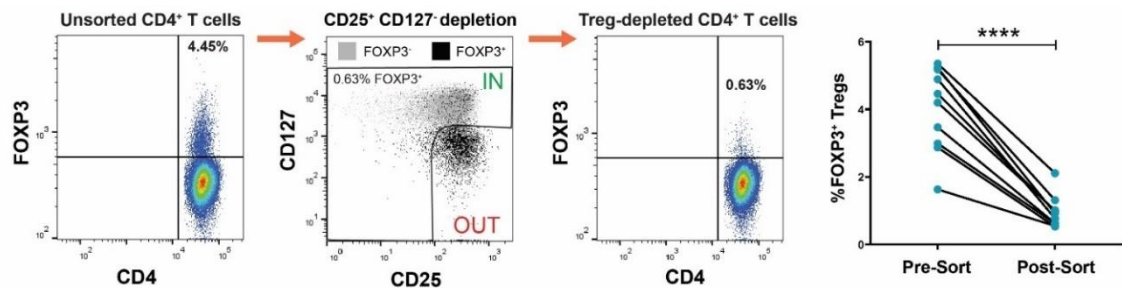


**Figure 2.1 Gating strategy and purity check for the positive isolation of CD19<sup>+</sup> B cells and CD4<sup>+</sup> T-helper cells from the peripheral blood of healthy volunteers and melanoma patients using the BD FACS Aria II cell sorter.**

Exceptionally high purities of 97.1% in CD19<sup>+</sup> and 98.9% in CD4<sup>+</sup> sorted fractions were obtained, measured as means across N = 27 samples.

For measurement of the potential *ex vivo* effect of B cells in inducing autologous Treg differentiation from CD4<sup>+</sup> T-helper cells, pre-culture exclusion of FOXP3<sup>+</sup> Treg cells was necessary, to accurately measure the quantity of induced Tregs, and eliminate the potential influence of existing Tregs upon the measured outcome. Treg depletion was achieved by employing an extra step in the sorting gating strategy, which is outlined in **Figure 2.2**. This step involved the addition of 2.5µl each of anti-CD25 PerCP-Cy5.5 and

anti-CD127 PE-Cy7 in the pre-sort antibody incubation step. In the extra step, a population demonstrably enriched in FOXP3-expressing Tregs, of CD25<sup>+</sup> CD127<sup>-</sup> extracellular phenotype, is depleted from the sample, leaving a population with minimal percentages of FOXP3<sup>+</sup> Tregs, for downstream use in the *ex vivo* Treg induction assay (Section 2.4.3.3).



**Figure 2.2 Gating strategy for the positive isolation of CD4<sup>+</sup> CD25<sup>-int</sup> CD127<sup>+</sup> non-Treg (conventional) T cells from the peripheral blood of healthy volunteers and melanoma patients using the BD FACS Aria II cell sorter.**

Unsorted CD4<sup>+</sup> T-helper cells contain a notable population of FOXP3<sup>+</sup> Tregs. FOXP3-expressing cells were removed during sorting by using a combination of CD25 and CD127 expression, to obtain a population of Treg-depleted CD4<sup>+</sup> cells for use in the *ex vivo* Treg induction assay. In this figure, cells were fixed, permeabilised and co-stained for FOXP3 to indicate the localisation of FOXP3<sup>+</sup> cells within the CD25/CD127 gate.

### 2.2.5 Isolation of purified B and T-helper cells from HV and melanoma patient peripheral blood mononuclear cells by negative selection

B and T-helper cells were also isolated from HV and melanoma patient PBMCs using a negative selection technique, for use in additional *ex vivo* co-culture experiments, comprising the measurement of B cell-mediated modulation of autologous T-helper cell proliferation. This method involved an additional 10-minute incubation step prior to Ficoll-Paque PLUS density gradient centrifugation, with 45µl of either RosetteSep Human B cell or CD4<sup>+</sup> T cell enrichment cocktails added per 1ml whole blood. The B

cell enrichment cocktail contains tetrameric antibody complexes with specificities to Glycophorin A, CD16, CD36, CD56, and CD66b, while the CD4<sup>+</sup> T cell cocktail has specificity to Glycophorin A, CD8, CD16, CD19, CD36, CD56, CD66b and TCR $\gamma\delta$ . Unwanted (complexed) cells pellet along with red blood cells, resulting in a highly purified population of either CD19<sup>+</sup> B or CD4<sup>+</sup> T-helper cells at the interface between the density medium and plasma layer.

## **2.3 B cell phenotyping using flow cytometry**

### **2.3.1 General reagents**

Flow cytometric B cell phenotyping was performed using the reagents and in-house produced buffers listed in **Table 2.5** and **Table 2.6**, respectively.

**Table 2.5 Reagents used for flow cytometric B cell phenotyping.**

<b>Name</b>	<b>Supplier</b>	<b>Catalogue Number</b>
Anti-Mouse Ig, $\kappa$ /Negative Control Compensation Beads	BD Biosciences	552843
Anti-Rat Ig $\kappa$ /Negative Control Compensation Beads	BD Biosciences	552845
DMEM, high glucose, pyruvate	Gibco	41966-029
FBS	Gibco	10106-159
Penicillin-Streptomycin (10,000 U/mL)	Gibco	15140-122
CpG oligodeoxynucleotide (ODN) 2006	Miltenyi Biotec	130-100-106
Recombinant Human CD40L (TNFSF5) (carrier-free) protein	BioLegend	591704
Corning™ Costar™ Flat Bottom Cell Culture Plates 24-well	Thermo Fisher Scientific	10377841
Cell Activation Cocktail (with Brefeldin A)	BioLegend	423304
PBS, sterile	Gibco	10010-023
LIVE/DEAD™ Fixable Near-IR Dead Cell Stain Kit	Invitrogen	L10119
Cytofix/Cytoperm Soln Kit	BD Biosciences	554714

**Table 2.6 In-house produced buffers used for flow cytometric B cell phenotyping.**

Name	Composition
FACS buffer	PBS with 5% FBS

### 2.3.2 Antibodies

Flow cytometric B cell phenotyping was conducted using the antibodies listed in **Table 2.7** below.

**Table 2.7 Antibodies used for flow cytometric B cell phenotyping.**

Antibodies targeting intracellular antigens are coloured in blue.

Specificity	Clone	Conjugate	Host species	Supplier	Catalogue number
CD45	HI30	PE-Cy7	Mouse	BioLegend	304016
CD20	2H7	FITC	Mouse	BD Biosciences	555622
CD3	344818	APC-Cy7	Mouse	BioLegend	344818
CD14	M5E2	APC-Cy7	Mouse	BioLegend	301820
CD56	HCD56	APC-Cy7	Mouse	BioLegend	318332
CD19	HIB19	V500	Mouse	BD Biosciences	561121
IgM	MHM-88	PE-Cy7	Mouse	BioLegend	314532
IgD	IA6-2	BV421	Mouse	BioLegend	348226
CD27	O323	PE, BV711	Mouse	BioLegend	302808, 302834
CD24	ML5	BUV395	Mouse	BD Biosciences	566221
CD38	HIT2	BV786	Mouse	BioLegend	303530
CD5	L17F12	AF700	Mouse	BioLegend	364026
IL-10	JES3-9D7	AF647	Rat	BioLegend	501412
TGF- $\beta$ 1	TW4-9E7	PE	Mouse	BD Biosciences	562339
TNF- $\alpha$	MAb11	AF488	Mouse	BioLegend	502915
IL-4	MP4-25D2	BV605	Rat	BioLegend	500828
IFN- $\gamma$	B27	AF700	Mouse	BioLegend	506516
TLR9	S16013D	PE	Mouse	BioLegend	394804

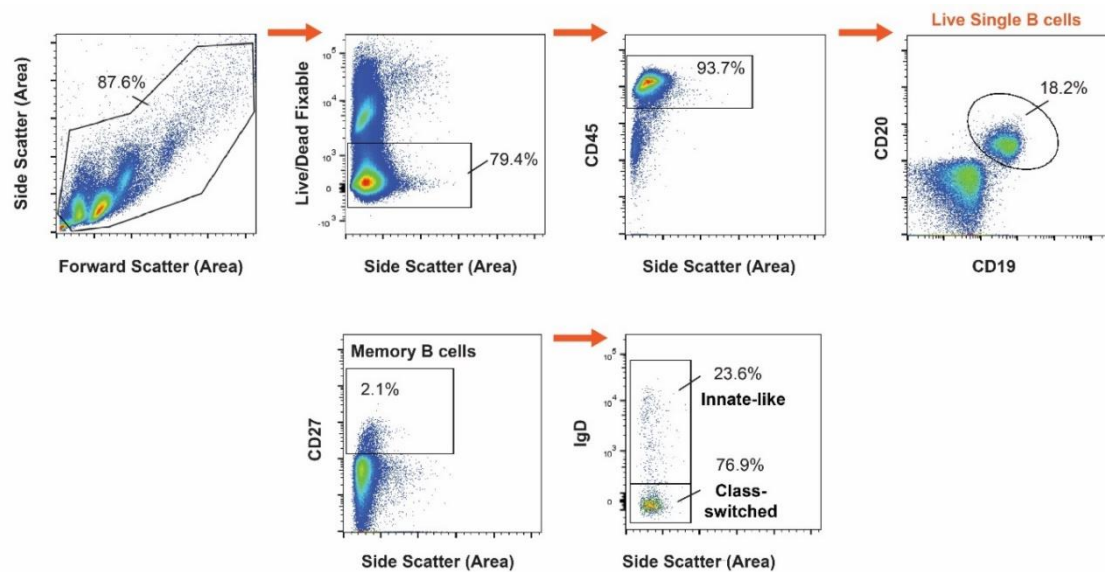
### 2.3.3 Phenotyping of memory and isotype-switched B cells from HV and breast cancer patient peripheral blood and breast tissues

Flow cytometry was used for the identification and quantification of memory and isotype-switched B cell phenotypes in HV and breast cancer peripheral blood, and breast tissue (normal breast, NANT and tumour). The panel used is displayed in **Table 2.8** and associated flow cytometry gating strategy is outlined in **Figure 2.3**.

**Table 2.8 Flow cytometry panel for detection and quantification of memory and isotype-switched B cells in healthy volunteer and breast cancer patient peripheral blood, and breast tissue.**

A description of each target is indicated in the right-hand column.

<b>Target</b>	<b>Fluorophore</b>	<b>Description</b>
Live/Dead	Near-IR (APC-Cy7)	Dead cell exclusion
CD45	PE-Cy7	Leukocyte
CD19	V500	Pan-B cell
CD20	FITC	Pan-B cell
CD27	PE	Activation/Memory
IgD	BV421	Immunoglobulin



**Figure 2.3 Gating strategy for the detection and quantification of memory and isotype-switched B cell phenotypes in HIV and breast cancer patient peripheral blood, and breast tissue.**

Representative breast cancer patient peripheral blood sample shown. Following exclusion of debris, doublets, dead cells, and non-leukocytes, B cells were identified by co-expression of the lineage markers CD19 and CD20. Memory B cells were defined by expression of CD27, and further categorised by IgD expression into innate-like (IgD<sup>+</sup>) and isotype-switched (IgD<sup>-</sup>) subsets.

Staining was performed using the following protocol. First, PBMCs and breast tissue single cells were isolated as previously described (Sections 2.1.2 and 2.2.2). Cells were washed twice in 2ml PBS at 1500rpm (720xg), resuspended in 100µl FACS buffer, and incubated with 2µl human Fc block for 5 minutes at RT. Next, 5µl LIVE/DEAD Fixable Near-IR Dead Cell Stain (pre-diluted 1:20 in PBS) was added, prior to extracellular labelling using the panel outlined in **Table 2.8**, with the following antibody volumes: 2.5µl (IgD, CD19, CD27, CD45) and 10µl (CD20). Cells were incubated for 30 minutes at 4°C, washed twice in 2ml PBS at 1500rpm, and resuspended in 150µl FACS buffer. Finally, cells were acquired on the BD FACS Canto Flow Cytometer, and analysed in FlowJo v10.4.

### 2.3.4 B cell intracellular cytokine phenotyping in HV and melanoma patient peripheral blood, and melanoma tumours

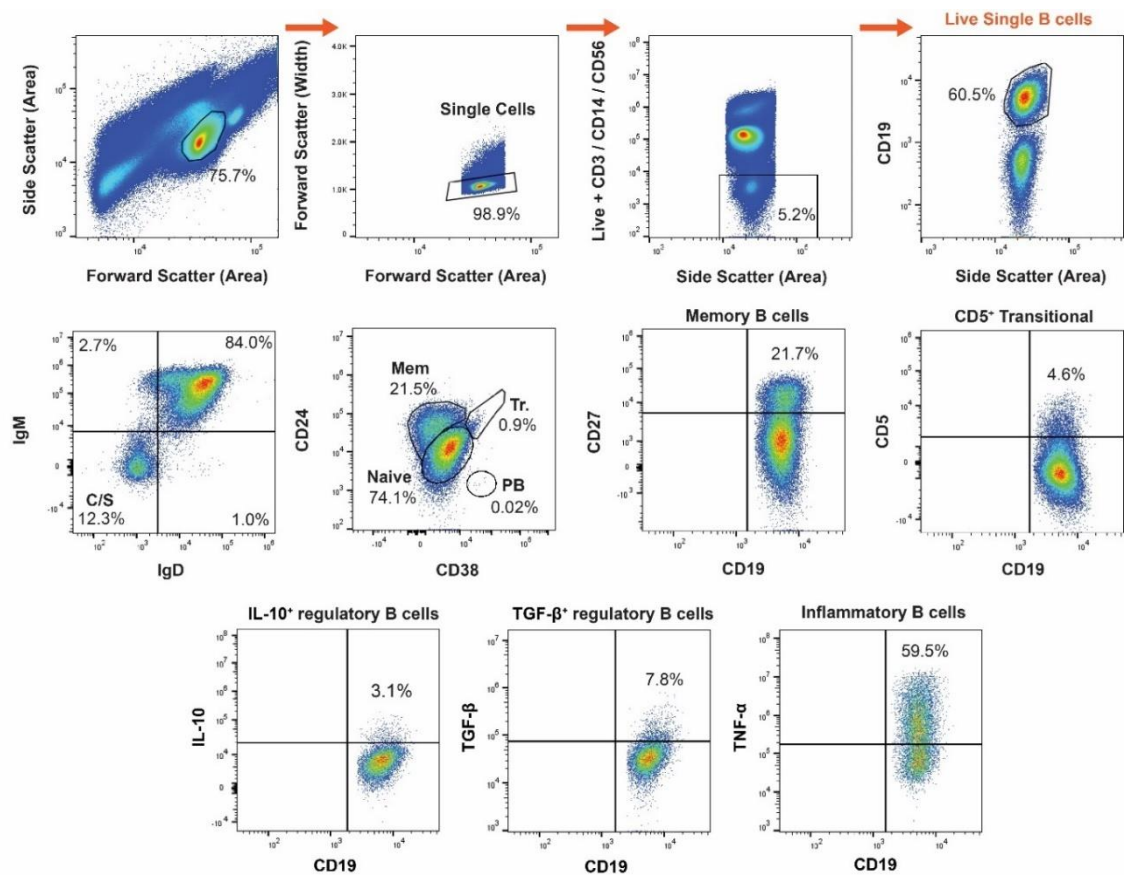
A flow cytometry-based intracellular cytokine assay was used to investigate the cytokine expression profiles among key B cell subpopulations in HV and melanoma patient peripheral blood, and melanoma tumours. Lineage markers were chosen in consultation with the current best practice for B cell lineage phenotyping outlined in the literature [248]. The 11-colour panel is shown in **Table 2.9**, and gating strategy outlined in **Figure 2.4**.

**Table 2.9 Flow cytometry panel for detection and quantification of B cell cytokine expression profiles among B cell lineage subpopulations.**

A description of each target is indicated in the right-hand column. Dump target included the following APC-Cy7 conjugated antibodies: anti-CD3, anti-CD14 and anti-CD56.

Target	Fluorophore	Description
Live/Dead + Dump	APC-Cy7	Dead + non-B cell exclusion
CD19	V500	Pan-B cell
IgM	PE-Cy7	Immunoglobulin
IgD	BV421	Immunoglobulin
CD27	BV711	Activation/Memory
CD24	BUV395	Lineage
CD38	BV786	Lineage
CD5	AF700	Transitional
IL-10	AF647	Cytokine
TGF- $\beta$ 1	PE	Cytokine
TNF- $\alpha$	AF488	Cytokine





**Figure 2.4 Gating strategy for the detection and quantification of B cell cytokine expression profiles among key B cell subpopulations in HV and melanoma patient peripheral blood, and melanoma tumours.**

Representative melanoma patient peripheral blood sample shown. Following exclusion of debris, doublets, dead cells, and non-B ( $CD3^+$ ,  $CD14^+$  and  $CD56^+$ ) cells, B cells were identified by presence of the lineage marker CD19. B cells were defined by antibody expression into non-isotype-switched ( $IgM^+ IgD^+$ ,  $IgM^+ IgD^-$ ,  $IgM^- IgD^+$ ) and isotype-switched ( $IgM^- IgD^-$ ) subsets.  $CD19^+$  B cell lineage phenotypes were also categorised according to CD24 and CD38 expression as follows: memory B cells (Bm;  $CD24^{hi} CD38^-$ ), transitional B cells (TrB;  $CD24^{hi} CD38^{hi}$ ), naïve B cells ( $CD24^{int} CD38^{int}$ ) and plasmablasts (PB;  $CD24^- CD38^{++}$ ). Memory B cell phenotypes were also detected according to expression of CD27. CD5 expression was used to confirm transitional cell phenotypes.  $IL-10^+$  and  $TGF-\beta^+$  regulatory B cells, and  $TNF-\alpha^+$  inflammatory B cells were identified following fixation, permeabilization, and staining for intracellular cytokines.

Staining was performed using the following protocol. First, PBMCs were isolated from peripheral blood, and single cells isolated from melanoma lesions as previously described (Sections 2.1.4 and 2.2.3). Cell suspensions ( $4 \times 10^6$  cells/ml) were cultured in sterile DMEM (10% Fetal Bovine Serum (FBS) and 50U/ml Pen-Strep) media containing B cell

activation stimuli, comprising either: 0.1µg/ml CpG oligodeoxynucleotide (ODN) 2006, 10µg/ml CpG ODN 2006, 1µg/ml CD40L or both 1µg/ml CD40L and 10µg/ml CpG ODN 2006. 500µl per well was added to flat-bottom 24 well plates for each condition, and the plates were incubated at 37°C with 5% CO<sub>2</sub> for 72 hours. Cell Activation Cocktail (with Brefeldin A), containing PMA and Ionomycin, was added for the final 6 hours of culture to stimulate intracellular cytokine production towards detectable levels. For each sample, an unstimulated condition containing no Cell Activation Cocktail was analysed, to set the cut-off between cytokine<sup>-</sup> and cytokine<sup>+</sup> cells.

Following culture, cells were washed twice in 2ml PBS at 1500rpm (720xg), resuspended in 100µl FACS buffer, and incubated with 2µl human Fc block for 5 minutes at RT. Next, 5µl LIVE/DEAD Fixable Near-IR Dead Cell Stain (pre-diluted 1:20 in PBS) was added, prior to extracellular labelling with the panel outlined in **Table 2.9**. Cells were incubated for 30 minutes at 4°C, with antibody volumes as follows: 2.5µl (anti-IgM, IgD, CD3, CD14, CD56, CD27) and 7.5µl (anti-CD5, CD24, CD38). The cells were washed twice in 2ml PBS at 1500rpm. Pellets were vortexed, resuspended in 250µl BD Fixation/Permeabilization solution, containing 4.2% formaldehyde, and stored for 20 minutes at 4°C. Cells were then washed twice in 2ml PBS at 1500rpm, resuspended in 1ml FACS buffer, and stored overnight at 4°C. Next, cells were spun at 1500rpm, resuspended in 1ml BD Perm/Wash Buffer, containing FBS and saponin, and incubated for 15 minutes at RT. Cells were spun again at 1500rpm and intracellular labelling performed with 15µl each of anti-IL-10-AF647, anti-TGF-β1-PE and anti-TNF-α-AF488. Anti-IL-4-BV605, anti-IFN-γ-AF700 and anti-TLR9-PE (15µl each) were also included in select experiments. Cells were incubated for 30 minutes at 4°C, washed twice in 1ml BD Perm/Wash Buffer at 1500rpm, and resuspended in 150µl FACS buffer. Finally, cells were acquired on the CytoFLEX Flow Cytometer, and analysed in FlowJo v10.4.

#### 2.3.4.1 Dimensionality reduction of B cell lineage phenotyping data using the tSNE and FlowSOM Algorithms

Dimensionality reduction analysis was used to provide a two-dimensional visualization of the major B cell lineages in melanoma patient peripheral blood, and provide an alternative exploration of IL-10, TGF- $\beta$ , and TNF- $\alpha$  cytokine expression profiles among the key B cell lineage subpopulations.

Live single CD19<sup>+</sup> B cells were gated (**Figure 2.4**), and dimensionality reduction was applied using the t-Distributed Stochastic Neighbor Embedding (tSNE) algorithm. Two-dimensional tSNE projections were generated utilizing the following parameters: CD27, IgD, IgM, CD24 and CD38. The Exact (vantage point tree) KNN and Barnes-Hut gradient algorithms with opt-SNE configuration (up to 1000 iterations) were used. Additionally, the FlowSOM algorithm was used to generate six meta-clusters per sample based upon the above five-marker panel and used to distinguish the major B cell lineage subpopulations, for visualization using the generated tSNE projections.

#### 2.3.5 B cell CyTOF phenotyping of HV and melanoma patient peripheral blood

A 29-marker B cell panel including cell surface and intracellular markers was used for CyTOF phenotyping analysis. Cells were stained with a mixture of commercially available, and in-house conjugated antibodies. The full panel is shown in **Table 2.10** and was employed for the downstream identification of IL-10 and TGF- $\beta$  expressing regulatory B cell subsets in HV and melanoma patient peripheral blood. This work was completed in collaboration with Dr. Zena Willmore, King's College London (KCL).

**Table 2.10 CyTOF phenotyping panel for identification of IL-10 and TGF- $\beta$  expressing regulatory B cell subsets in HIV and melanoma patient peripheral blood.**

Intracellular antigen targets are coloured blue.

CyTOF phenotyping panel		
CD45	CD21	IgM
CD3	Ig Lambda	CD28
CD19	IgG	CD4
CD38	CD5	CD16
CD81	CD79B	BCL-6
IgD	FasR	IL-10
CD20	CD40	Ki-67
CD8a	CD27	
CD25	CD24	
CD138	TGF- $\beta$	
HLA-DR	CD185	

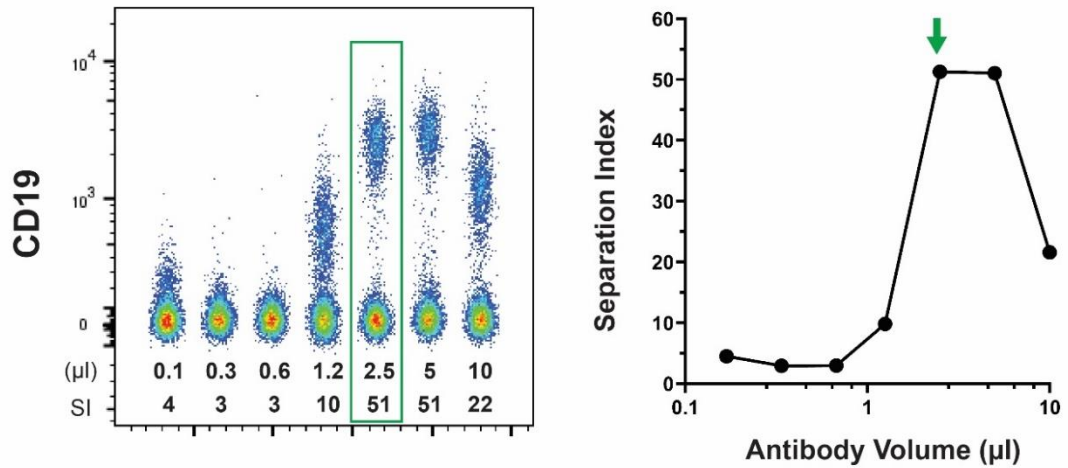
### 2.3.6 Flow cytometry panel optimisations

#### 2.3.6.1 Compensation of fluorescence spillover

Compensation was performed using BD positive/negative compensation beads for each fluorophore. Beads and single antibody stains were incubated for 30 minutes at 4°C and washed twice in 2ml PBS at 1500rpm. For each experiment, an aliquot of representative PBMCs was thawed and used for the unstained control, and separately stained with 5 $\mu$ l LIVE/DEAD Fixable Near-IR Dead Cell Stain (pre-diluted 1:20 in PBS) for the relevant single stain control.

#### 2.3.6.2 Antibody titrations

During development of the B cell phenotyping panels, antibody staining volume titrations were performed to maximise the assay signal:noise ratio in the final assays. An example titration is shown in **Figure 2.5**, for the anti-CD19 FITC conjugate.



$$\text{Separation Index} = \frac{\text{MedianPositive} - \text{MedianNegative}}{(\text{84\%Negative} - \text{MedianNegative})/0.995}$$

**Figure 2.5 Example antibody titration for optimisation of assay resolution.**

Stain volume of anti-CD19 FITC was titrated from 0.1-10µl, and separation index was calculated according to the equation illustrated. The condition with optimal separation index is 2.5µl, representing best-case signal:noise ratio for the CD19 stain.

### 2.3.6.3 Fluorescence minus one

Where appropriate, fluorescence minus one (FMO) controls, whereby cells were stained with all the panel fluorophores minus one fluorophore, were used to set the threshold between negative and positive-expressing populations for particular markers.

## **2.4 Ex vivo B cell functional studies**

### **2.4.1 General reagents**

*Ex vivo* B cell functional studies were performed using the reagents and in-house produced buffers listed in **Table 2.11** and **Table 2.12**, respectively.

**Table 2.11 Reagents used for *ex vivo* B cell functional studies.**

<b>Name</b>	<b>Supplier</b>	<b>Catalogue Number</b>
DMEM, high glucose, pyruvate	Gibco	41966-029
FBS	Gibco	10106-159
Penicillin-Streptomycin (10,000 U/mL)	Gibco	15140-122
Dynabeads Human T-Activator CD3/CD28	Gibco	11131D
Human IL-2	Peprotech	200-02-100
CpG ODN 2006	Miltenyi Biotec	130-100-106
96-Well Polystyrene Round Bottom Microwell Plates	Thermo Fisher Scientific	10418623
Cell Activation Cocktail (with Brefeldin A)	BioLegend	423304
PBS, sterile	Gibco	10010-023
LIVE/DEAD™ Fixable Near-IR Dead Cell Stain Kit	Invitrogen	L10119
Cytofix/Cytoperm Soln Kit	BD Biosciences	554714
eBioscience Foxp3 / Transcription Factor Staining Buffer Set-1 kit	Invitrogen	00-5523-00
eBioscience™ Cell Proliferation Dye eFluor™ 670	Invitrogen	65-0840-85
ExCellerate B Cell Expansion Media, Xeno-Free	Bio-Techne	CCM031
Recombinant Human IL-10 (carrier-free) protein	BioLegend	571002
Recombinant Human TNF-α (carrier-free) protein	BioLegend	570102

**Table 2.12 In-house produced buffers for *ex vivo* B cell functional studies.**

<b>Name</b>	<b>Composition</b>
FACS buffer	PBS, 5% FBS

## 2.4.2 Antibodies

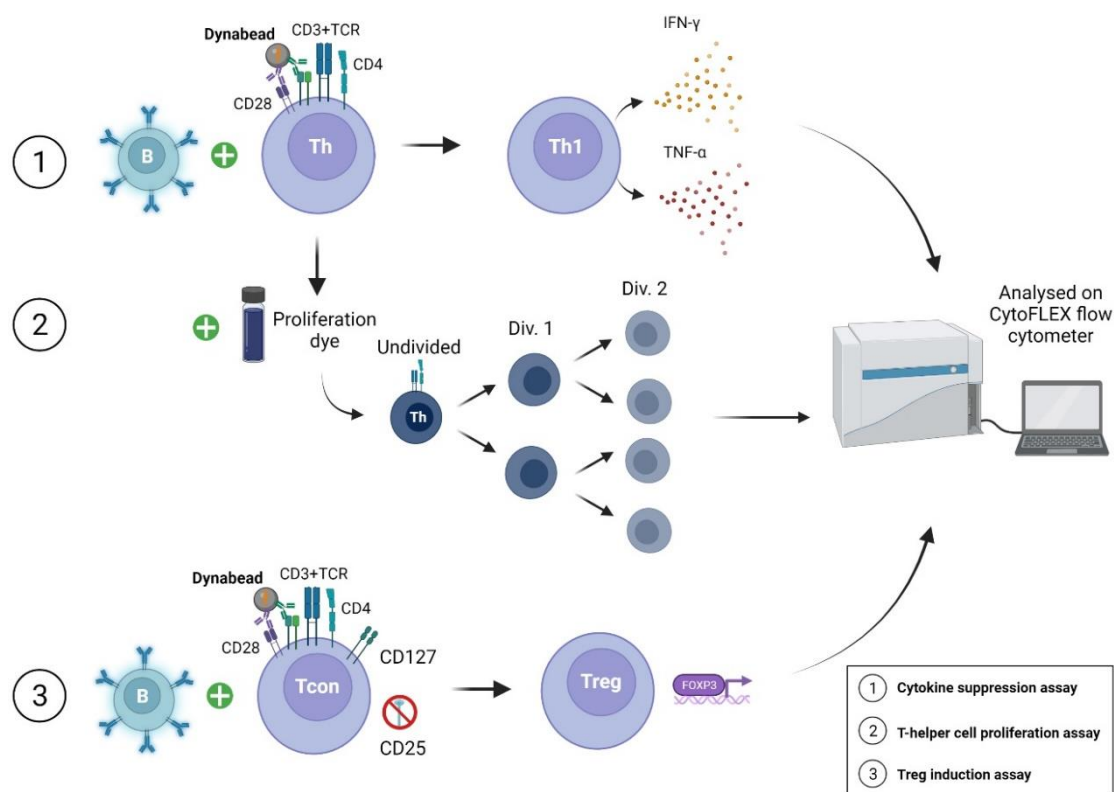
*Ex vivo* B cell functional studies were conducted using the antibodies listed in **Table 2.13** below.

**Table 2.13 Antibodies used for *ex vivo* B cell functional studies.**

Specificity	Clone	Conjugate	Host species	Supplier	Catalogue number
IFN- $\gamma$	4S.B3	APC	Mouse	BioLegend	502512
TNF- $\alpha$	MAb11	AF488	Mouse	BioLegend	502915
TGF- $\beta$	1D11	None	Mouse	Bio-Techne	MAB1835-100
FOXP3	259D	AF488	Mouse	BioLegend	320212
PD-1	5C4.B8 (nivolumab)	None	Human	Bristol Myers Squibb	N/A

## 2.4.3 *Ex vivo* B cell functional studies of melanoma patient circulating B cells

Three *ex vivo* functional assays were performed to investigate the functional modulation of T-helper cell phenotype and effector function by B cells derived from melanoma patient peripheral blood. A schematic representative of these assays is shown in **Figure 2.6**.



**Figure 2.6 Schematic representation of *ex vivo* B cell functional studies of melanoma patient circulating B cells contained within this Thesis.**

B and T-helper cells were isolated from melanoma patient blood and co-cultured with Dynabeads® Human T-Activator CD3/CD28 and recombinant IL-2. Expression of IFN- $\gamma$  and TNF- $\alpha$  was measured from T-helper cells post-culture, conferring the Th1 cell phenotype (1). T-helper cells were also stained with eBioscience Cell Proliferation Dye eFluor 670, and proliferation modelling was performed to track T-helper cell divisions in response to the presence of B cells (2). To investigate B cell-mediated Treg generation, isolated CD25<sup>-int</sup> CD127<sup>+</sup> conventional T-helper (Tcon) cells were co-cultured with B cells in the presence of Dynabeads and IL-2, and FOXP3<sup>+</sup> Treg cells were measured post-culture (3). Created with BioRender.com [86].

#### 2.4.3.1 Cytokine suppression assay

The ability of melanoma patient circulating B cells to functionally suppress autologous expression of IFN- $\gamma$  and TNF- $\alpha$  by T-helper cells was tested using an *ex vivo* cytokine suppression assay. First, CD19<sup>+</sup> B and CD4<sup>+</sup> T-helper cells were isolated from the peripheral blood of patients with melanoma using the BD FACS Aria II cell sorter, as previously described (Section 2.2.4). Purified B and T-helper cell suspensions were co-



cultured ( $1 \times 10^5$  each/well) in sterile DMEM (10% FBS, 50U/ml Pen-Strep) media containing Dynabeads® Human T-Activator CD3/CD28 ( $1 \times 10^5$  beads/well) and 10U/ml recombinant IL-2. CpG ODN 2006 (10 $\mu$ g/ml) was added to selected co-culture wells. T-helper cells ( $1 \times 10^5$ ) were also cultured alone as control. 100 $\mu$ l final volume per well was added to round-bottom 96 well plates for each condition, and the plates were incubated at 37°C with 5% CO<sub>2</sub> for 72 hours. Cell Activation Cocktail (with Brefeldin A) was added for the final 6 hours of culture. For each sample, an unstimulated condition containing no Cell Activation Cocktail was analysed, to set the cut-off between cytokine<sup>-</sup> and cytokine<sup>+</sup> cells.

Post-culture, cells were washed twice in 2ml PBS at 1500rpm (720xg), resuspended in 100 $\mu$ l FACS buffer, and incubated with 2 $\mu$ l human Fc block for 5 minutes at RT. Next, 5 $\mu$ l LIVE/DEAD Fixable Near-IR Dead Cell Stain (pre-diluted 1:20 in PBS) was added alongside 2.5 $\mu$ l anti-CD4-PE, and cells were incubated for 30 minutes at 4°C. The cells were washed twice in 2ml PBS at 1500rpm. Pellets were vortexed, resuspended in 250 $\mu$ l BD Fixation/Permeabilization solution, and stored for 20 minutes at 4°C. Fixed cells were then washed twice in 2ml PBS at 1500rpm, resuspended in 1ml FACS buffer, and stored overnight at 4°C. Next, cells were spun at 1500rpm, resuspended in 1ml BD Perm/Wash Buffer, and incubated for 15 minutes at RT. Cells were spun again at 1500rpm and intracellular labelling performed with 5 $\mu$ l each of anti-IFN- $\gamma$ -APC and anti-TNF- $\alpha$ -AF488, diluted in 40 $\mu$ l of BD Perm/Wash buffer. Cells were incubated for 30 minutes at 4°C, washed twice in 1ml BD Perm/Wash Buffer at 1500rpm, and resuspended in 150 $\mu$ l FACS buffer. Finally, cells were acquired on the CytoFLEX Flow Cytometer, and data were analysed in FlowJo v10.4.

#### 2.4.3.2 T-helper cell proliferation assay

CD19<sup>+</sup> B and CD4<sup>+</sup> T-helper cells were isolated from peripheral blood of melanoma patients using RosetteSep B and CD4<sup>+</sup> T cell enrichment cocktails as previously described (Section 2.2.5). Purified B and T-helper cell suspensions were individually stained with 0.5 $\mu$ M eBioscience Cell Proliferation Dye eFluor 670 in 1ml PBS, vortexed, and incubated for 10 minutes at 37°C. Unstained B and Th lymphocytes were also incubated alongside stained samples, to serve as negative staining control. Staining was quenched in 5ml sterile ExCellerate B Cell Media (50U/ml Pen-Strep) for 5 minutes at RT, and cells pelleted at 1500rpm (720xg). Cells were then washed three times in 5ml media at 1500rpm, and cell counts performed as previously described (Section 2.1.4).

B and T cells were co-cultured (1x10<sup>5</sup> each/well) in media containing Dynabeads® Human T-Activator CD3/CD28 (1x10<sup>5</sup> beads/well) and 10U/ml recombinant IL-2. Unstimulated control wells, without the addition of Dynabeads or recombinant IL-2, served to benchmark the non-proliferative population. 50 $\mu$ g/ml anti-PD-1 antibody (nivolumab) was added to selected co-culture wells. T-helper cells (1x10<sup>5</sup>) were also cultured alone as control, and 0.01-1 $\mu$ g/ml recombinant IL-10 or TNF- $\alpha$  was added to selected Th monoculture wells. 100 $\mu$ l final volume per well was added to round-bottom 96 well plates for each condition, and the plates were incubated at 37°C with 5% CO<sub>2</sub> for 72 hours.

Post-culture, cells were washed twice in 2ml PBS at 1500rpm, resuspended in 100 $\mu$ l FACS buffer, and incubated with 2 $\mu$ l human Fc block for 5 minutes at RT. Next, 5 $\mu$ l LIVE/DEAD Fixable Near-IR Dead Cell Stain (pre-diluted 1:20 in PBS) was added alongside 2.5 $\mu$ l anti-CD4-PE, and cells incubated for 30 minutes at 4°C. Cells were

washed twice in 2ml PBS at 1500rpm and resuspended in 150µl FACS buffer. Finally, cells were acquired on the CytoFLEX Flow Cytometer, and proliferation modelling was performed in FlowJo v10.4.

#### 2.4.3.3 Treg induction assay

The capability of melanoma patient circulating B cells to induce differentiation of Tregs from autologous T-helper cells was investigated using an *ex vivo* Treg induction assay. First, CD19<sup>+</sup> B lymphocytes and CD4<sup>+</sup> CD25<sup>-int</sup> CD127<sup>+</sup> conventional T-helper (Tcon) lymphocytes were isolated from peripheral blood of melanoma patients using the BD FACS Aria II cell sorter, as previously described (Section 2.2.4). Purified B and Tcon cell suspensions were co-cultured (1x10<sup>5</sup> each/well) in sterile DMEM (10% FBS, 50U/ml Pen-Strep) media containing Dynabeads® Human T-Activator CD3/CD28 (1x10<sup>5</sup> beads/well) and 10U/ml recombinant IL-2. A neutralizing anti-TGF-β antibody (50µg/ml) was added to selected co-culture wells. Tcon cells (1x10<sup>5</sup>) were also cultured alone as control. 100µl final volume per well was added to round-bottom 96 well plates for each condition, and the plates were incubated at 37°C with 5% CO<sub>2</sub> for 72 hours.

Post-culture, cells were washed twice in 2ml PBS at 1500rpm (720xg), resuspended in 100µl FACS buffer, and incubated with 2µl human Fc block for 5 minutes at RT. Next, 5µl LIVE/DEAD Fixable Near-IR Dead Cell Stain (pre-diluted 1:20 in PBS) was added alongside 2.5µl anti-CD4-PE, and cells incubated for 30 minutes at 4°C. The cells were washed twice in 2ml PBS at 1500rpm. Pellets were vortexed, resuspended in 1ml Foxp3 Fixation/Permeabilization solution, and vortexed again. Fixed samples were then stored overnight at 4°C. Next, cells were washed twice at 1500rpm in 2ml Permeabilization Buffer, containing saponin. Intracellular labelling was performed with 5µl anti-FOXP3-

AF488 antibody, and cells were incubated for 30 minutes at 4°C. Cells were then washed twice in 2ml Permeabilization Buffer at 1500rpm and resuspended in 150µl FACS buffer. Finally, cells were acquired on the CytoFLEX Flow Cytometer, and analysed in FlowJo v10.4.

## **2.5 Gene expression and immunoglobulin repertoire profiling**

### **2.5.1 Bulk gene expression profiling of lymphocyte and lymphoid assembly markers in breast tumours**

Gene expression levels obtained from breast tumour specimens were analysed from internal Guy's Hospital (TNBC-enriched) [249] and TCGA Breast [250] cohorts, and compared between PAM50 (Basal-like, HER2, luminal A, luminal B and normal-like) and TNBC-subtypes (basal-like 1/2, immunomodulatory, mesenchymal, mesenchymal stem-like, luminal androgen receptor) [251]. Gene expression data were generated using Affymetrix Human Exon 1.0ST arrays (E-MTAB-5270) (Guy's Hospital cohort) [249] and the RNAseq v2 platform (TCGA cohort) [252]. A B cell metagene signature was also analysed from published NanoString data of primary and metastatic breast cancers (GSE102818) [253].

#### **2.5.1.1 KM plotter prospective cohort study**

The publicly available Kaplan–Meier (KM) plotter tool, capable of correlating tumour mRNA expression and patient survival, was utilised to investigate the prognostic significance of B cells, B cell functional signatures, and lymphoid assembly markers in

breast cancer. Molecular subtypes were defined by expression of HER2, ESR1 and MKI67 (Basal: ESR1<sup>-</sup>/HER2<sup>-</sup>; luminal A: ESR1<sup>+</sup>/HER2<sup>-</sup>/MKI67 low; luminal B: ESR1<sup>+</sup>/HER2<sup>-</sup>/MKI67 high and HER2<sup>+</sup>/ESR1<sup>+</sup>; HER2<sup>+</sup>: HER2<sup>+</sup>/ESR1<sup>-</sup>) [254,255]. B cell function-associated gene sets, detailed in **Table 2.14**, were identified from the gene ontology (GO) database. A lymphoid assembly-associated gene signature was also compiled from a set of known markers [256]. Individual genes (*e.g.*, CD20 and CD3G), and compiled gene sets were analysed for prognostic significance, in terms of overall survival.

**Table 2.14 GO annotations for KM plotter prospective cohort study gene sets.**

Annotation	Genes	ID
Positive regulation of B lymphocyte activation	9	GO:0050871
Positive regulation of B lymphocyte differentiation	13	GO:0045579
Positive regulation of B lymphocyte proliferation	44	GO:0030890
Isotype switching mechanism	15	GO:0045190
Positive regulation of IgG-isotype switching	10	GO:0048304
Positive regulation of IgA-isotype switching	5	GO:0048298

#### 2.5.1.2 CIBERSORT analysis of tumour-infiltrating B lymphocyte subsets

CIBERSORT deconvolution was applied to quantify the abundance of 22 immune subsets in 177 TNBC samples, including naïve B cells, plasma cells and memory B cells [257]. Gene expression was obtained using the Affymetrix GeneChip Human Exon 1.0ST microarray (E-MTAB-5270), and TNBCs were selected based on the IHC status of HER2 and ER [249]. Only tumours for which deconvolution was considered successful ( $P < 0.05$ ) were taken forward ( $N = 116$ ). Semi-quantitative TIL classification was performed by a trained histopathologist using tissue microarrays. Each tumour was scored as following: 0 (absence of lymphocytes); 1 (minimal infiltration), 2 (mild infiltration), 3 (moderate infiltration), and 4 (marked infiltration).

Tumours with a semi-quantitative score  $\geq 3$  were considered to have high TILs. An iterative process to determine the optimal cut-off point by a minimal P-value approach was employed to identify the cut-off for each of the immune subsets used in the outcome analyses. Univariate Cox proportional hazards regression models were used to investigate the prognostic importance of immune subsets in high and low TIL infiltrated tumours. This work was completed in collaboration with Dr. Jelmar Quist, KCL.

### 2.5.2 Single-cell RNA-sequencing (scRNA-seq) analysis of breast cancer circulating and tumour-infiltrating B lymphocytes

Analyses of breast cancer circulating and tumour-infiltrating B lymphocytes were performed on a published scRNA-seq dataset (GSE114725) [258], using R package *Seurat* [259]. Dimensionality reduction was performed using Uniform Manifold Approximation and Projection (UMAP), and B cells were clustered using the Louvain algorithm [259]. Ig isotypes were detected based upon heavy chain gene expression. Differentially expressed genes identified by *Seurat* were used to perform gene set enrichment analysis (GSEA) using the *fgsea* package [260]. Gene sets were obtained from Broad Institute Molecular Signature Database using R package *msigdb*.

CellPhoneDB v2.0 was used to infer B cell-T cell interactions in the breast TME [261]. Previously annotated T cell subtypes (CD4<sup>+</sup> central memory (CM), CD4<sup>+</sup> effector memory (EM), CD4<sup>+</sup> naive, CD8<sup>+</sup> CM, CD8<sup>+</sup> EM, CD8<sup>+</sup> naive, Treg) were combined into a single annotation. The list of B and T cell IDs was used to subset the imputed dataset. A pseudocount of 2.591 (the minimal absolute normalised expression value) was added to shift the data to non-negative space for downstream analysis of cell-cell interactions. Default settings were used for the statistical analysis. False discovery rate (FDR)

correction using an FDR <0.001 threshold was applied to identify interactions between B and T cells. Predicted interactions were further manually curated to include communication pathways associated with lymphoid assembly, cytokine signalling, co-stimulation, B cell dependent T-cell activation and CTL activation. The R code used to analyse scRNA-seq data obtained from GSE114725 can be accessed from <https://codeocean.com/capsule/8562693>. This work was completed in collaboration with Mr. Roman Laddach, KCL.

### 2.5.3 Single-cell RNA-sequencing (scRNA-seq) analysis of melanoma tumour-infiltrating B lymphocytes

Analyses of melanoma circulating tumour-infiltrating B lymphocytes were performed on a published scRNA-seq dataset (GSE123139) [262], using R package *Seurat* [259]. Dimensionality reduction was performed using UMAP, and B cells were clustered using the Louvain algorithm [259].

CellPhoneDB v2.0 was used to infer interactions of TGF- $\beta^+$ /TNF- $\alpha^+$  B cells with Tcon and Treg cells in the melanoma TME [261]. Statistical analysis was performed as in Section 2.5.2. Predicted interactions were further manually annotated into communication pathways associated with cell-cell contact, inhibitory checkpoints, costimulation, pro-inflammatory mediators, lymphocyte homing, recruitment, and assembly, leukotriene synthesis, negative regulation of inflammation, and inhibition of B cell responses. This work was completed in collaboration with Mr. Roman Laddach, KCL.

#### 2.5.4 Long-read immunoglobulin repertoire analysis of breast cancer and normal breast tissues

Immunoglobulin repertoire analysis was performed from cDNA synthesised from two ER<sup>+</sup> cancers, two TNBC and a normal breast sample using the 5' RACE template switch method (Suppl. Materials and Methods). Full-length immunoglobulin cDNA was PCR-amplified with primers containing unique molecular barcodes, with each isotype (IgA, IgG, IgM) amplified separately. Purified DNA samples were sequenced using PacBio Single Molecule, Real-Time (SMRT) Sequencing platform [263]. Redundant sequences with identical molecular barcodes were removed. Ig genes and CDR3 sequences were determined using IMGT/HighV-QUEST [264]. Relatedness among sequences were estimated using BRepertoire webserver [265] “Clonotype clustering” function, by partitioning all CDR3 DNA sequences by the sample and the V gene family used, and calculating Levenshtein distances between all sequence pairs within each partition [266].

Related sequence pairs were determined as having a distance of 0.18 [265]. Hierarchical clustering was performed on this pairwise distance matrix to define clonotypes. The clones defined are therefore specific to each sample, and are independent from the isotype. Modal sequences of each clonotype were determined as representatives. This representative subset (here denoted R) was compared against all the sampled sequences (denoted S) to delineate immunoglobulin isotype and subclass distributions of clonally expanded repertoire. Specifically, the number of sequences for each Ig isotype and subclass were quantified separately in R and S sequence sets, and fold change was quantified for each isotype/subtype as:

$$\text{fold difference} = \frac{\text{Number of Ig sequences in S} - \text{Number of Ig sequences in R}}{\text{Number of Ig sequences in R}}$$



A large fold difference implies sizeable clonal expansion. This method of quantification was applied to compare isotype, subtype and VDJ gene usage combination changes following clonal expansion. Data visualization was performed using the ggplot2 package in the R Statistical Programming environment (version 3.6.2). Lastly, selection pressure analysis was performed using R package *shazam* [267]. The R code used to analyse breast tissue immunoglobulin repertoire data can be accessed at <https://codeocean.com/capsule/8594411>. This work was completed by Dr. Joseph Ng, KCL.

## **2.6 Serum antibody isotype profiling**

### **2.6.1 General reagents**

Serum antibody isotype profiling was performed using the reagents listed in **Table 2.15**.

**Table 2.15 Reagents used for serum antibody isotype profiling.**

<b>Name</b>	<b>Supplier</b>	<b>Catalogue Number</b>
Antibody Isotyping 7-Plex Human ProcartaPlex™ Panel	Invitrogen	EPX070-10818-901

### **2.6.2 7-plex antibody isotyping of HV and breast cancer patient serum**

To examine the potential modulation of serum immunoglobulin isotype profiles in breast cancer patients, a high-throughput antibody isotyping magnetic bead-based Luminex assay was performed, according to manufacturer's instructions. Titers of IgG1, IgG2, IgG3, IgG4, IgM, IgA and IgE were quantified in HV and breast cancer patient serum,

which was collected as described in Section 2.1.3, stored at -80°C, and thawed on ice prior to analysis.

### 2.6.3 AMORIS analysis of Ig isotype titres in breast cancer patient serum

Baseline serum immunoglobulin isotype titres (IgA, IgG, IgM and IgE) were evaluated in the Swedish Apolipoprotein MOrtality-related RISk (AMORIS) cohort [268]. Association of serum immunoglobulin isotype titre with probability of breast cancer-specific death was analysed. Mean follow-up time was 5.2 years patients who died of breast cancer (N = 3 89), and 8.8 years for patients who did not die of their breast cancer during follow-up (N = 3643). This work was completed by Dr. Aida Santaolalla, KCL.

## 2.7 Fluorescence immunohistochemistry

### 2.7.1 General reagents

Fluorescence immunohistochemistry evaluations were performed using the reagents and in-house produced buffers listed in **Table 2.16** and **Table 2.17**, respectively.

**Table 2.16 Reagents used for fluorescence immunohistochemistry evaluations.**

Name	Supplier	Catalogue Number
Tonsil Tissue Slides (Normal)	Bio-Techne	NBP2-30207
Xylene mixture of isomers	Sigma	214736
Ethanol, reagent grade	Sigma	362808
Tween 20 Molecular Biology Grade	VWR	437082Q
Phosphate Buffered Saline, 10X Solution	Thermo Scientific Fisher	10468543
ImmEdge Hydrophobic Barrier Pen	Bio-Techne	310018
Albumin, from bovine serum	Sigma	A3059
Normal Goat Serum	Generon	900.077

Name	Supplier	Catalogue Number
Cover Glass 20X20mm Thickness No.1.5	VWR	630-2101
ProLong Gold Antifade Mountant with DAPI-10 mL	Invitrogen	P36931
ProLong Gold Antifade Mountant-10 mL	Invitrogen	P36930
Rimmel London 60 Seconds Super Shine, 8g, Clear	Rimmel London	34778209740

**Table 2.17 In-house produced buffers used for fluorescence immunohistochemistry evaluations.**

Name	Composition
10mM Citric acid solution	2.94g tri-sodium citrate (dihydrate) and 0.5ml (0.05%) Tween 20 in 1000ml dH <sub>2</sub> O, pH 6.0
Blocking buffer	TBS-T (2.4g Tris base, 8.8g NaCl and 1ml (0.1%) Tween 20 in 1000ml dH <sub>2</sub> O, pH 7.6), containing 1% BSA and 10% normal goat serum

### 2.7.2 Antibodies

Fluorescence immunohistochemistry evaluations were conducted using the antibodies listed in **Table 2.18** below.

**Table 2.18 Antibodies used for fluorescence immunohistochemistry evaluations.**  
Secondary antibodies are coloured blue.

Specificity	Clone	Conjugate	Host species	Dilution Factor (1:X)	Supplier	Code number
CD20	L26, Polyclonal	None	Mouse, Goat	50, 200	Abcam	ab9475, ab194970
CD3	CD3-12	None	Rat	100	Abcam	ab11089
PanCK	KRT/1877 R	None	Rabbit	200	Abcam	ab234297
CD27	EPR8569	None	Rabbit	1500	Abcam	ab131254
IgD	EPR6146	None	Rabbit	3500	Abcam	ab124795
IgM	Polyclonal	None	Goat	200	Abcam	ab97201
IgG	EPR4421	None	Rabbit	1000	Abcam	ab109489
IgA	AD3	None	Mouse	100	Novus Biologicals	NB500-469

Specificity	Clone	Conjugate	Host species	Dilution Factor (1:X)	Supplier	Code number
CD138	Polyclonal	None	Goat	13	Thermo Fisher Scientific	PA547395
BCL6	EPR11410-43	None	Rabbit	1500	Abcam	ab172610
IL-10	Polyclonal	None	Rabbit	500	Abcam	ab217941
TNF- $\alpha$	TNFA/1172	None	Mouse	100	Abcam	ab220210
Mouse IgG	N/A	AF488	Goat, Donkey	200	Abcam	ab150117, ab150109
Rabbit IgG	N/A	AF594	Goat, Donkey	200	Abcam	ab150088, ab150064
Rat IgG	N/A	AF647	Goat	200	Abcam	ab150167
Goat IgG	N/A	AF647	Donkey	200	Abcam	ab150135
Rabbit IgG	N/A	AF405	Donkey	200	Abcam	ab175649
Goat IgG	N/A	AF594	Donkey	200	Abcam	ab150136
Rabbit IgG	N/A	AF647	Donkey	200	Abcam	ab150063

### 2.7.3 Fluorescence immunohistochemistry evaluation of breast TIL-B localisation and immunoglobulin isotype expression

Formalin-fixed paraffin embedded (FFPE) breast cancer and normal breast tissue sections were provided by Bart's Cancer Institute, Queen Mary University of London. Healthy volunteer tonsil tissue was also obtained from a commercial source, for positive control staining. All tissue sections were of 4 $\mu$ m thickness. Three slides were provided per patient or healthy volunteer specimen, and each slide was stained to comprise 3 antibody panels as illustrated in **Table 2.19**. Identification of tumour-infiltrating CD20<sup>+</sup> B cells and CD3<sup>+</sup> T cells in reference to PanCK-expressing tumour-islets was facilitated using Panel 1. TIL-B were further characterised by immunoglobulin (IgD, IgM, IgA, IgG), and CD27 expression across Panels 2 and 3. Staining for CD138 and BCL6 was also performed within selected experiments in collaboration with Ms. Elena Alberts, to identify tumour-infiltrating plasma and germinal centre B cells.

**Table 2.19 Fluorescence immunohistochemistry staining panels for identification of TILs, naïve B cells, and B cell immunoglobulin isotype expression within the breast TME.**

Panel	Identification	Markers
1	TIL classification	DAPI, CD20, CD3, PanCK
2	Naïve B cell identification	DAPI, CD20, IgD
3	Ig isotype expression	IgM, IgA, IgG, CD27

### 2.7.3.1 Preparation, antigen retrieval, and staining of FFPE tissues

Slides were prepared for antigen retrieval using a deparaffinization and rehydration protocol. FFPE sections were warmed to 56°C on a heated plate for 2 minutes to melt the paraffin wax. Slides then underwent a series of 5 minutes washes: 1) Xylene; 2) Xylene; 3) 100% Ethanol; 4) 95% Ethanol; 5) 70% Ethanol. Next, Slides were rinsed under running tap water for 5 minutes. Antigen retrieval was performed using a citric acid solution (10mM sodium citrate, 0.05% Tween 20, pH 6.0). Slides were incubated in a microwavable pressure cooker containing 1 litre of pre-heated acid and cooked for 150 seconds with the pressure valve activated. The cooker was then removed from the microwave and rinsed under tap water for 10 minutes, until all residual citric acid solution had been replaced. Slides were removed from the cooker and rinsed for three lots of 5 minutes in PBS with gentle (40rpm) agitation.

Next, sections were prepared for staining by being outlined with a hydrophobic wax pen. Tissues were blocked with blocking buffer (0.1% TBS-T containing 1% BSA and 10% normal goat serum) for one hour at RT in a humidifying chamber. Tissues were then incubated overnight at 4°C with primaries antibodies diluted in blocking buffer (outlined in **Table 2.18**), conferring the panels shown in **Table 2.19**.

The following day, slides were rinsed three times for 5 minutes with PBS to remove the primary antibodies. Tissues were then incubated for 1 hour at RT in the humidifying

chamber with appropriate secondary antibodies diluted in blocking buffer (outlined in **Table 2.18**). Slides were again rinsed three times for 5 minutes with PBS. Finally, excess moisture was removed from the slides using absorbent blue roll, and sections were mounted with #1.5 thickness coverslips, using ProLong™ Gold Antifade Mountant either with DAPI (Panels 1 and 2), or without DAPI (Panel 3). Slides were sealed using clear nail varnish, placed on a flat, dry surface, and left to incubate for 24 hours at 4°C. The stained tissues were visualised using the Nikon TE 2000-U inverted confocal, and Olympus VS120-S5 slide scanning microscopes.

#### 2.7.3.2 Quantitative technique for determination of TIL-B densities

For cancer specimens, the area of analysis for TIL density quantification was determined as being within the borders of the invasive lesion, guided by TIL working group guidelines [197] and a trained breast pathologist, Dr. Fangfang Liu, and discerned using PanCK and DAPI staining. Dr. Liu also provided guidance on the identification of other features of breast pathology, including DCIS, normal lobules, and tertiary lymphoid structures.

To investigate TIL-B structural formation and localisation within the TME, B lymphocytes were classified into distinct groups. TIL-B were categorised as being intratumoural or stromal, according to their location inside or outside of tumour islets respectively, defined using PanCK staining. Furthermore, the presence of B lymphocytes within TIL clusters was determined as those belonging to groups of at least thirty B lymphocytes immediately adjacent to at least thirty T lymphocytes, within 100µm of tissue.

Quantitative analysis was performed by capturing 40 randomly distributed image fields within each defined tumour section, using a Nikon TE 2000-U confocal microscope. TILs positive for relevant markers were counted manually using ImageJ software, and the cellular density of each TIL subset (per mm<sup>3</sup> tumour) was calculated using the basic formula:

Mean cells per image x 1/image area (mm<sup>2</sup>) x 1/section thickness (mm<sup>3</sup>) = cell density/mm<sup>3</sup> tumour.

B cell densities were also quantified in normal (control) breast tissue, within the area surrounding normal lobules, and using the basic formula above.

#### 2.7.4 Fluorescence immunohistochemistry evaluation of melanoma tumour-infiltrating IL-10<sup>+</sup> regulatory and TNF- $\alpha$ <sup>+</sup> inflammatory B cells

Frozen melanoma tumour sections (4 $\mu$ m thickness) were stained with fluorescently conjugated antibodies specific to human IL-10, TNF- $\alpha$ , and CD20, and DAPI counterstained, for identification of regulatory and pro-inflammatory cytokine-expressing CD20<sup>+</sup> TIL-B.

##### 2.7.4.1 Preparation and staining of frozen tissues

Unfixed cryosections were removed from storage at -80°C and thawed for 5 minutes at RT. Slides were next fixed with pro-cooled Acetone and then Ethanol for 10 minutes each. Slides were washed in PBS for 5 minutes and staining and mounting was performed as in Section 2.7.3.1. Primary and secondary antibodies used are outlined in **Table 2.18**. Stained tissues were visualised using the Olympus VS120-S5 slide scanning microscope.

## **2.8 Statistical methods**

GraphPad Prism (version 9.0) and R were used for statistical analyses of paired and unpaired datasets. All data included in this Thesis represent mean  $\pm$  standard error mean (SEM), unless otherwise stated. Correlation analyses were performed using linear regression, with correlation coefficient ( $r$ ) and Probability ( $P$ ) values reported. Analyses of differences in means between two groups were performed using the student's two-tailed T-test for normally distributed data, and Mann-Whitney U test for non-normally distributed data, where normality was tested using the Shapiro-Wilk test. Where multiple group means were compared, one-way Analysis of Variance (ANOVA) was used, with a Tukey's post-hoc comparison test. P-values were reported for all comparisons with the following associated symbols:  $P > 0.05$  (ns),  $P < 0.05$  (\*),  $P < 0.01$  (\*\*),  $P < 0.001$  (\*\*\*),  $P < 0.0001$  (\*\*\*\*).  $P < 0.05$  was considered to represent a significant difference in all statistical tests.



## **Chapter 3: B Lymphocyte Subsets, Immunoglobulin Isotype Expression, and Clonal Features in Breast Cancer**

### **3.1 Introduction**

Initiation of effective adaptive immunity may contribute to tumour growth restriction through specific antigen-directed responses. The T lymphocyte component of anti-tumour immunity has received significant attention [218]. In contrast, B lymphocytes, especially the memory and isotype-switched compartments, and their expressed antibody profiles remain only partially elucidated. Emerging findings suggest that aspects of humoral immune responses may correlate with improved clinical outcomes via B cell tumour-infiltration and expression of antibodies in lesions or in the circulation [213,217]. These could differ across tumour types, potentially offering opportunities for stratification and for guiding therapy options.

Breast cancer is one of the most frequently diagnosed malignancies, divided into biological, and differential therapy-associated subtypes based on ER, PR, and HER2 expression, with specific prognostic and predictive biomarker implications. Triple-negative breast cancers (TNBC) do not express any of these markers and demonstrate the least favourable prognosis due to both an aggressive phenotype and limited targeted therapies [269]. Although breast cancer has not traditionally been regarded as a typical immunogenic malignancy, emerging studies report the presence and potential clinical significance of tumour-infiltrating immune cells for clinical outcomes [270]. Paradoxically, despite an overall poor prognosis of patients with TNBC, immune infiltration is more pronounced compared with other breast cancer types. Consistent with

an immunogenic tumour microenvironment, some TNBC patients may benefit from anti-programmed death-ligand 1 (PD-L1) and anti-PD-1 immunotherapy with atezolizumab in combination with chemotherapy [44]. TNBCs are characterised by immunologically variable and compartmentalised tumours with structural features in the tumour-immune interphase and large variability across individuals, mandating the need for patient stratification for therapy selection [271]. The most thoroughly studied effector cells within the breast cancer setting are CD8<sup>+</sup> cytotoxic T lymphocytes and natural killer (NK) cells [272]. However, TIL-B aggregating within tertiary lymphoid structures [185] may have an antigen-educated phenotype [273] and autoantibodies are thought to trigger tumour cell clearance [274]. TIL-B might also serve as antigen-presenting cells to promote anti-tumour Th responses [275]. Therefore, it is increasingly recognised that humoral immune responses may be important contributors to breast cancer outcome, especially in more immunogenic TNBCs.

The interaction between the immune system and malignant cells therefore constitutes a major focus of current translational and clinical investigation [215]. Recent studies have provided evidence of TIL-B and tumour-reactive immunoglobulin in several solid tumours, including in breast cancer, and TIL-B have been reported to respond to B cell receptor stimulation and produce immunoglobulins *ex vivo* [191,214,276].

## **3.2 Hypothesis, objectives, and published work**

### 3.2.1 Hypothesis

Overall, the results presented within this Chapter, were generated using a range of techniques including cytofluorimetric, transcriptomic, immunofluorescence, single-cell RNA-seq and long-read immunoglobulin repertoire studies. The aim was to provide novel insights into the systemic and intratumoural B cell responses to breast cancer, focusing upon the more aggressive triple-negative breast cancers, with reference to the modulation of isotype-switched and memory B cell subsets, immunoglobulin isotype distribution, and B cell clonal expansion profiles. Attention is paid to unravelling the prognostic value of breast TIL-B, including stratification by key B cell functional signatures, with the aim of alleviating the current uncertainty surrounding the impact of B cells in the breast TME.

### 3.2.2 Objectives

The objectives of this Chapter comprise the following:

1. To assess B cell phenotypes including memory, activated, and isotype-switched subsets, in the peripheral blood and cancer lesions of patients with breast cancer.
2. To elucidate the localisation and structural formation of B cells infiltrating breast tumours, and their relationship with T cells, focusing on TNBC.
3. To investigate characteristics of immunoglobulin expression, and clonal features, of B cells infiltrating breast tumours, particularly in TNBC.

4. To evaluate the prognostic value of breast TIL-B, with stratification according to naïve, plasma or memory B cell subsets, functional profiles, and by breast cancer molecular subtype.

### 3.2.3 Published Work

This Chapter contains findings included in a peer-reviewed manuscript entitled “Tumor-Infiltrating B Lymphocyte Profiling Identifies IgG-Biased, Clonally Expanded Prognostic Phenotypes In Triple-Negative Breast Cancer” [68] which was published in 2021 in *Cancer Research*. The full manuscript, supplementary figures, and tables can be found in the **Appendix**. Analysis of serum immunoglobulin titres (**Figure 3.3**) in the AMORIS cohort was completed by Dr. Aida Santaolalla, KCL. Analysis of CD27<sup>+</sup> expression distribution and germinal centre B cell marker expression across B cell populations analysed by single-cell gene expression was conducted in collaboration with Mr. Roman Laddach, KCL, and immunohistochemistry/immunofluorescence (IHC/IF) studies (**Figure 3.4**) were done in collaboration with Ms. Elena Alberts, KCL. B cell metagene NanoString analysis (**Figure 3.5 (C)**) was conducted in collaboration with Dr Alicia Chenoweth, KCL. CIBERSORT analysis of TIL-B subsets (**Figure 3.5 (E)**) was conducted in collaboration with Dr Jelmar Quist, KCL. Single cell RNA-seq analysis of TIL-B activatory signatures (**Figure 3.8 (A-C)**), B cell-T cell interactions (**Figure 3.8 (E)**) and Ig isotype expression (**Figure 3.13 (A-D)** and **Figure 3.14**) was conducted in collaboration with Mr. Roman Laddach, KCL. Lastly, Immunoglobulin repertoire analysis of breast cancer samples (**Figure 3.16** and **Figure 3.17**) was conducted in collaboration with Dr. Joseph Ng, KCL.

### 3.3 Patient and healthy volunteer cohort characteristics

A collection of internal and external cohorts of healthy volunteer and breast cancer patient samples analysed in this Chapter are summarised in **Table 3.1**.

**Table 3.1 Summary of healthy volunteer (control) and breast cancer patient cohorts.**

<p><b>Flow cytometry data:</b> <i>KCL flow cohort</i> Peripheral blood PBMC (Fig. 1B)</p> <p><b>Breast tissue single cell extraction</b> (Fig. 1C, 1D, 1E)</p>	<p><b>Control group:</b> Healthy volunteer PBMC (N=29). Age: 50 years (+/- 12); age range: 31-81.</p> <p><b>Experimental group:</b> Breast cancer patient PBMC (N=55). Age: 55 years (+/- 13); age range: 33-83. Receptor: ER+ (N=39), ER- (N=16); HER2+ (N=13); HER2- (N=40); TNBC (N=11). Stage: 1 (N=7); 2 (N=21); 3 (N=8); 4 (N=18). Chemotherapy: none (N=10); &lt;1 year post-chemo (N=21); &gt;1 year post-chemo (N=22).</p> <p><b>Control group:</b> Normal breast (reduction surgery) (N=9). Age: 37 years (+/- 5); age range: 32-45.</p> <p><b>Experimental group:</b> Treatment naive tumor (N=17) and NANT (N=12), with matched PBMC. Age: 62 years (+/- 15); age range: 38-87. ER+ (N=11), ER- (N=6); HER2+ (N=5); HER2- (N=12); TNBC (N=3).</p>										
<p><b>IHC/IF data:</b> <i>Bart's IHC cohort</i> (Fig. 2A, 2B, 2D, 2F, 2G, 3A to 3C, 5A to 5E; Suppl. Fig. 3C, 3E, 4A, 6 and 7)</p>	<p><b>Control group:</b> Normal breast (reduction surgery/prophylactic mastectomy) (N=15). Age: 42 years (+/- 10); age range: 27-63.</p> <p><b>Experimental group:</b> Grade 3 IDC TNBC tumor (N=14 primary). Age: 64 years (+/- 10); age range: 45-86. Receptor: ER+ (N=0), ER- (N=15); HER2+ (N=0); HER2- (N=15); TNBC (N=15). Stage: 1 (N=5); 2 (N=5); 3 (N=2); 4 (N=1). Chemotherapy: none (N=13); neoadjuvant (N=1).</p>										
<p><b>Transcriptomic data:</b> <i>KCL and TCGA GEx cohorts</i> (Fig. 2A, 2B, 2E, 3D; Suppl. Fig. 4A, 4B, 4D; Suppl. Fig. 5, 8, 9)</p> <p><i>NanoString cohort</i> (GSE102818, Szekely et al.) (Fig 2C)</p>	<p><b>Control group:</b> KCL: normal breast (N=10); TCGA: non-TNBC (N=515);</p> <p><b>Experimental group:</b> KCL: TNBC (N=131); Lehmann et al. TNBC subtypes - mesenchymal, luminal androgen receptor, basal-like 1/2 and immunomodulatory (N=122); TCGA: TNBC (N=123)</p> <p><b>Control group:</b> primary tumor (N=31)</p> <p><b>Experimental group:</b> Metastatic site (N=17)</p>										
<p><b>Survival data:</b> <i>KM plotter cohort</i> (<a href="https://kmplot.com/">https://kmplot.com/</a>; Györfy et al.) (Fig. 2D, 3E, 4D, 6E; Suppl. Fig. 4C)</p>	<table border="1"> <thead> <tr> <th>Investigated groups:</th> <th>Chemotherapy:</th> </tr> </thead> <tbody> <tr> <td>Basal-like (N=241)</td> <td>N=188</td> </tr> <tr> <td>Luminal A (N=611)</td> <td>N=321</td> </tr> <tr> <td>Luminal B (N=433)</td> <td>N=246</td> </tr> <tr> <td>HER2 (N=117)</td> <td>N=98</td> </tr> </tbody> </table>	Investigated groups:	Chemotherapy:	Basal-like (N=241)	N=188	Luminal A (N=611)	N=321	Luminal B (N=433)	N=246	HER2 (N=117)	N=98
Investigated groups:	Chemotherapy:										
Basal-like (N=241)	N=188										
Luminal A (N=611)	N=321										
Luminal B (N=433)	N=246										
HER2 (N=117)	N=98										
<p><b>scRNA-seq data:</b> <i>Single cell cohort</i> (GSE114725, Azizi et al.) (Fig. 2E, 4A to 4C, 4E, 6A to 6D; Suppl. Fig. 3A, 3B, 3D, 10D)</p>	<p><b>Investigated groups:</b> Breast cancer patient peripheral blood (ER, N=2): 1,476 cells.</p> <p>Treatment naive primary tumor: B cells 1,021 cells; T cells, 11,006 cells. Age: 58 years (+/- 13); age range: 38-78. Receptor: ER+ (N=5), ER- (N=3); HER2+ (N=1); HER2- (N=7); TNBC (N=2).</p>										
<p><b>B cell repertoire data:</b> <i>KCL sequencing cohort</i> Breast tissue samples (Fig. 7A to 7E, Suppl. Fig. 10A to 10C)</p>	<p><b>Control group:</b> Normal breast (N=1): 1,771 sequences. Age: 35 years old.</p> <p><b>Experimental group:</b> Treatment naive primary tumor. Age: 47 years (+/- 14); age range: 35-61. Receptor: ER+ (N=2), ER- (N=2); HER2+ (N=0); HER2- (N=4); TNBC (N=2). Stage: 1 (N=3), 2 (N=1). 5,899 sequences.</p>										
<p><b>Luminex assay data:</b> <i>KCL Luminex cohort</i> Serum samples (Suppl. Fig. 1A, 1B)</p>	<p><b>Control group:</b> Healthy volunteer serum (N=18)</p> <p><b>Experimental group:</b> Breast cancer patient serum (ER, N=9; HER2, N=3; TNBC, N=9). Chemotherapy: No chemo (N=12), Chemo (N=9).</p>										
<p><b>AMORIS data:</b> <i>AMORIS cohort</i> (Walldius et al.) (Suppl. Fig. 2)</p>	<p><b>No breastcancer-specific death:</b> Did not die from breast cancer or still alive. Mean follow-up time: 8.8 years (N=3,643)</p> <p><b>Breast cancer-specific death:</b> Death from breast cancer. Mean follow-up time: 5.2 years (N=389)</p>										

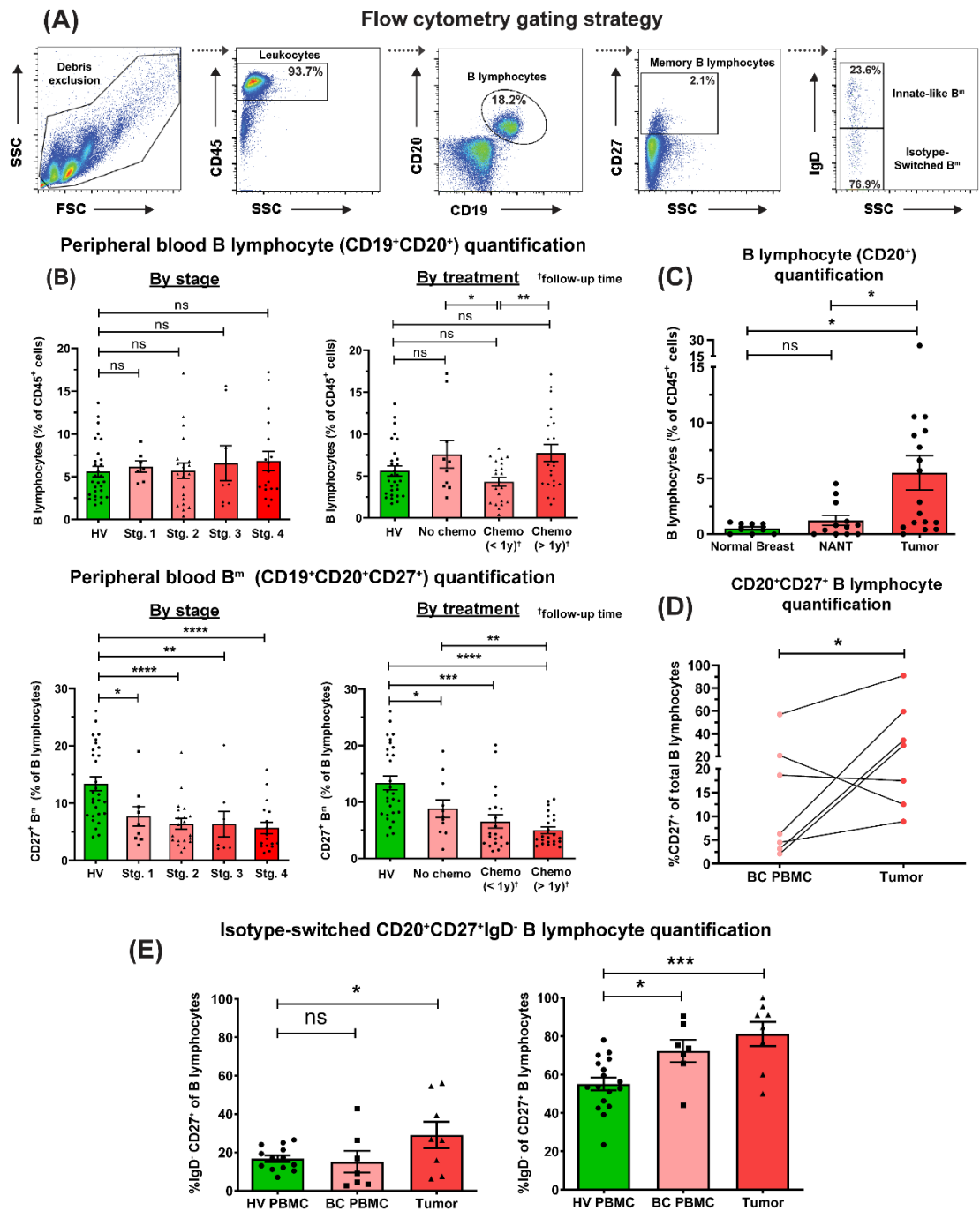
## **3.4 Results**

### **3.4.1 Collapse in circulating memory B cells contrasts with amplification of intratumoural class-switched memory B cell compartment in breast cancer**

I first investigated the differences in B cell subset distribution between HV and breast cancer patient peripheral blood, and breast tumours, using the KCL flow cohort (flow cytometry gating strategy is illustrated in **Figure 3.1 (A)**). Percentages of B cells (CD19<sup>+</sup> CD20<sup>+</sup>) and memory (CD19<sup>+</sup> CD20<sup>+</sup> CD27<sup>+</sup>) B cells (B<sup>m</sup>) in patients (N = 55) and healthy subjects (N = 48) were compared by flow cytometry. Consistent with a report in melanoma [277], peripheral B<sup>m</sup> were diminished in patients compared to healthy volunteers (**Figure 3.1 (B)**, bottom panels). This was independent of disease stage or chemotherapy treatment status. Significantly lower proportions of B cells (analysed as percentage of CD45<sup>+</sup> cells) were observed in the circulation of patients with recent chemotherapy compared to those without treatment (**Figure 3.1 (B)**, top right panel). Moreover, reduced serum immunoglobulin titres were observed in chemotherapy-treated individuals, but not in patients without treatment, compared to healthy volunteers (**Figure 3.2**, KCL Luminex cohort). In addition, baseline serum immunoglobulin isotype titres, analysed in the AMORIS cohort [272], did not predict breast cancer-specific death (**Figure 3.3**). Together, these observations suggest that while chemotherapy impairs systemic B cell profiles and limits serum IgG titres, collapse of peripheral B<sup>m</sup> is a common feature among breast cancer patients, regardless of treatment status.

I observed higher B cell proportions in tumour single-cell suspensions (N = 17), compared to NANT (N = 12) and normal breast (N = 9) tissues (**Figure 3.1 (C)**). In matched blood and tumour samples (N = 7), tumours contained higher CD20<sup>+</sup> CD27<sup>+</sup> B cell percentages

(Figure 3.1 (D)). The total population of CD27<sup>+</sup> IgD<sup>-</sup> B cells was enhanced in tumours compared to those in healthy volunteer circulation, and both peripheral and intratumoural CD20<sup>+</sup> CD27<sup>+</sup> B cell populations demonstrated a bias towards the loss of IgD expression (N = 32) (Figure 3.1 (E)).

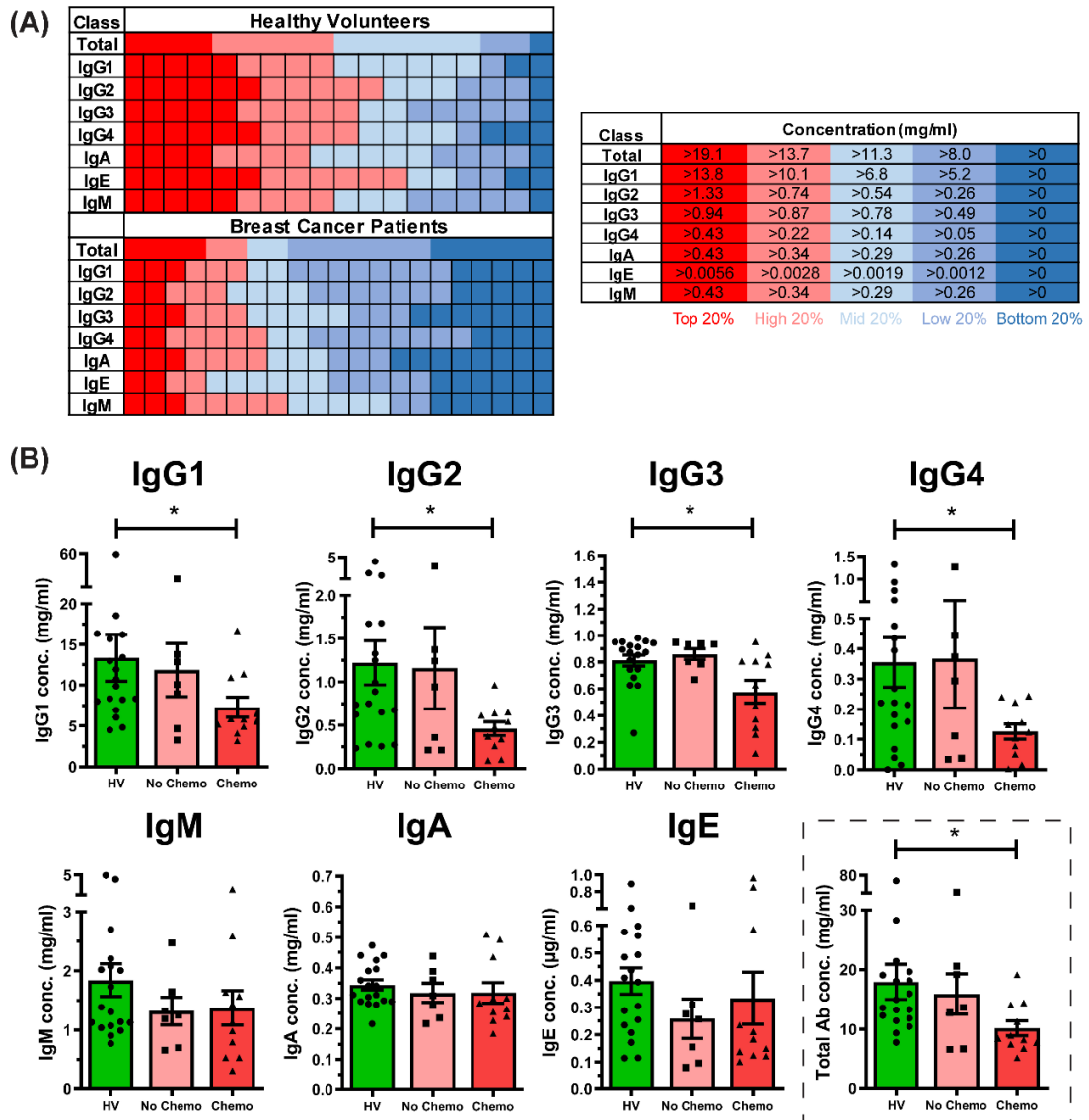


**Figure 3.1 Flow cytometric analyses reveal reduced circulating CD20<sup>+</sup>CD27<sup>+</sup> memory and amplification of breast tumour-infiltrating CD20<sup>+</sup>CD27<sup>+</sup>IgD<sup>-</sup> isotype-switched subsets among B cells.**

(A) Gating strategy for identification of B cells and memory (B<sup>m</sup>) B cells derived from PBMC (example patient PBMC shown). (B) Quantification of total circulating-B cells [top] and B<sup>m</sup> cells [bottom] as % of CD45<sup>+</sup> cells in HV (N=48) and patient (N=55) peripheral blood (KCL flow cohort; **Table 3.1** for patient information), stratified according to stage and treatment status. (C) Quantification of B cells (CD20<sup>+</sup>) from single cell suspensions of normal breast (N=9), NANT (N=12) and cancer tissue (N=17) samples. (D) Quantification of matched patient circulating- and tumour-infiltrating CD20<sup>+</sup>CD27<sup>+</sup> B cells (matched samples of 7 patients). (E) Quantification of CD20<sup>+</sup>CD27<sup>+</sup>IgD<sup>-</sup> B cells in HV (N=17), patient peripheral blood (N=7) and tumour lesions (N=8) shown out of total CD20<sup>+</sup> B cells [left] and CD20<sup>+</sup>CD27<sup>+</sup> B cells [right]. Statistical significance was determined using the Student's *t*-test.

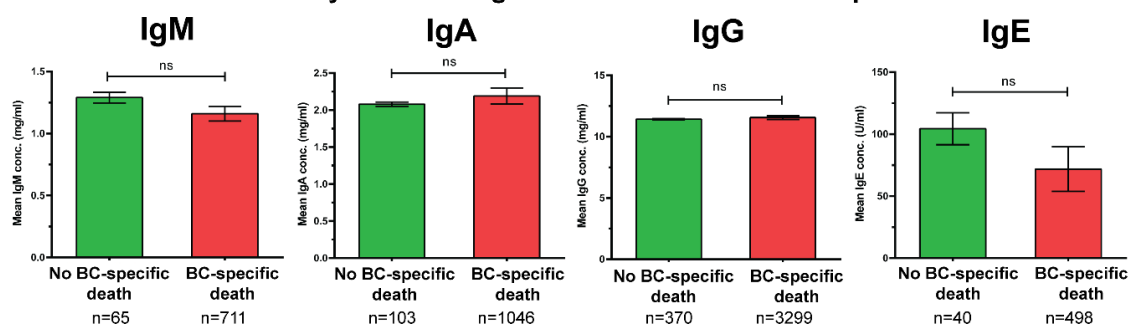


### Serum Immunoglobulin Isotyping



**Figure 3.2 Serum IgG titres are collapsed in breast cancer patients following chemotherapy.** (A) Heat map showing serum immunoglobulin isotype concentrations in healthy volunteers (N=18) and breast cancer patients (N=7 No Chemo, N=11 Chemo) (KCL Luminex cohort, **Table 3.1**) determined via Luminex 7plex assay. Concentrations were split into quintiles using pooled global concentrations of each isotype, with increasing concentrations ordered from left to right within each isotype for each subject group (coloured from blue (low) to red (high)). A significant overall reduction, particularly in IgG and IgE serum concentrations, can be visualised in the breast cancer group compared to the HV group. (B) Statistical comparison of serum immunoglobulin isotype concentrations within HV and patients with or without previous or ongoing chemotherapy treatment. Significant decreases in concentration of IgG subclasses but not of IgE, IgA or IgM isotypes are apparent in the chemotherapy treated patient cohort, resulting in a reduced total serum immunoglobulin titre.

### AMORIS analysis: serum Ig titer and likelihood of BC-specific death



	Breast cancer-specific death N = 389 n (%)	No breast cancer-specific death N = 3,643 n (%)
Mean Age (years) (SD)	62.1 (13.35)	63.4 (11.88)
Education		
Missing	32 (8.23)	143 (3.93)
Low	104 (26.74)	1,061 (29.12)
Middle	155 (39.85)	1,532 (42.05)
High	98 (25.19)	907 (24.90)
Parity		
Yes	312 (80.21)	2,847 (78.15)
No	77 (19.79)	796 (21.85)
Charlson Comorbidity Index		
0	298 (76.61)	2,827 (77.60)
1	39 (10.03)	345 (9.47)
2	30 (7.71)	320 (8.78)
3+	22 (5.66)	151 (4.14)
Mean follow-up time (years) (SD)	5.2 (4.26)	8.8 (6.27)
IgM (mg/mL)		
Mean (SD)	1.16 (0.48)	1.29 (1.15)
< 2.08 mg/mL	61 (15.68)	635 (17.43)
≥ 2.08 mg/mL	4 (1.03)	76 (2.09)
Missing	324 (83.29)	2,932 (80.48)
IgA (mg/mL)		
Mean (SD)	2.19 (1.11)	2.08 (0.96)
< 3.66 mg/mL	94 (24.16)	976 (26.79)
≥ 3.66 mg/mL	9 (2.31)	70 (1.92)
Missing	286 (73.52)	2,597 (71.29)
IgG (mg/mL)		
Mean (SD)	11.55 (3.11)	11.42 (2.92)
< 15.00 mg/mL	320 (82.26)	2,908 (79.82)
≥ 15.00 mg/mL	50 (12.85)	391 (10.73)
Missing	19 (4.88)	344 (9.44)
IgE (U/mL)		
Mean (SD)	71.83 (113.34)	104.43 (287.29)
< 100 U/mL	32 (8.23)	384 (10.54)
≥ 100 U/mL	8 (2.06)	114 (3.13)
Missing	349 (89.72)	3,145 (86.33)

	Events/Total N	Hazard Ratio <sup>1</sup> (95% CI)
IgM (mg/mL)		
< 2.08 mg/mL	61/696	1.00 (Ref)
≥ 2.08 mg/mL	4/80	0.52 (0.19-1.40)
IgA (mg/mL)		
< 3.66 mg/mL	94/1,070	1.00 (Ref)
≥ 3.66 mg/mL	9/79	1.35 (0.69-2.62)
IgG (mg/mL)		
< 15.00 mg/mL	320/3,228	1.00 (Ref)
≥ 15.00 mg/mL	50/441	1.19 (0.88-1.60)
IgE (U/mL)		
< 100 U/mL	32/416	1.00 (Ref)
≥ 100 U/mL	8/122	0.84 (0.42-1.69)

<sup>1</sup> Adjusted for age, parity, education and CCI.

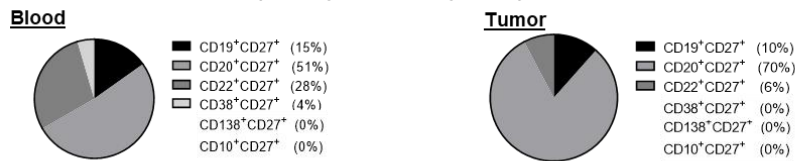
**Figure 3.3 Serum immunoglobulin isotype titres do not serve as a predictive marker for breast cancer-related mortality.**

Examination of whether serum immunoglobulin isotype titres affect the overall risk of breast cancer-specific death. Mean serum immunoglobulin isotype concentrations were compared for breast cancer patients who either died specifically from breast cancer (N=389) (mean follow-up time 5.2 years) and those patients for whom no breast cancer-specific death was recorded (N=3,643) (mean follow-up time 8.8 years) (AMORIS cohort). The distribution of Ig among the breast cancer specific death group and deaths from other causes group, was not statistically significant. The Ig categories used in the analysis were selected following the medical cut-offs established by the Central Automation Laboratory (CALAB) in Stockholm, Sweden, where the samples were analysed. Moreover, the multivariate Cox Proportional Hazards regression analysis was adjusted for age, parity, education status and Charlton Comorbidity Index (CCI). The analyses did not show any difference in survival based on the Ig isotype categories. These analyses were completed by Dr. Aida Santaolalla, KCL.

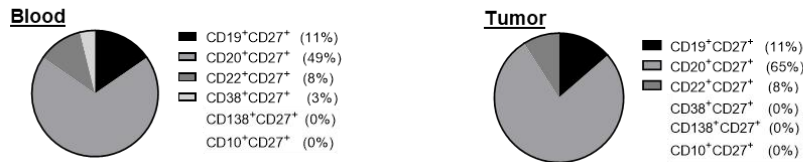
Additional quantitative single B cell gene expression analyses (Single cell cohort) also confirmed larger proportions of CD20<sup>+</sup> CD27<sup>+</sup> and CD20<sup>+</sup> CD27<sup>+</sup> IgD<sup>-</sup> B cells in tumours compared to patient blood (**Figure 3.4 (A-B)**). Furthermore, isotype-switched TIL-B populations comprise memory, GC B cells and plasma cells in non-TNBC and TNBC (IHC/IF, KCL IHC cohort and Single cell cohort) (**Figure 3.4 (A-E)**).

Overall, these findings reveal a reduced peripheral B<sup>m</sup> population in patients compared to healthy volunteers, independently of disease stage or treatment, in parallel with an enriched tumour-infiltrating isotype-switched B cell compartment in the breast TME compared to matched patient blood.

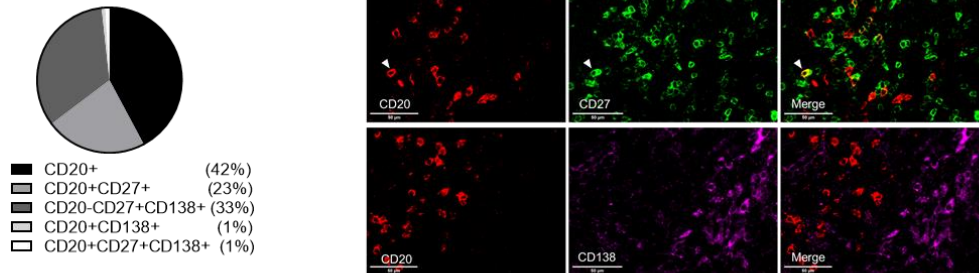
**(A) CD27<sup>+</sup> cell distribution in blood (N = 66) and tumor (N = 30)**



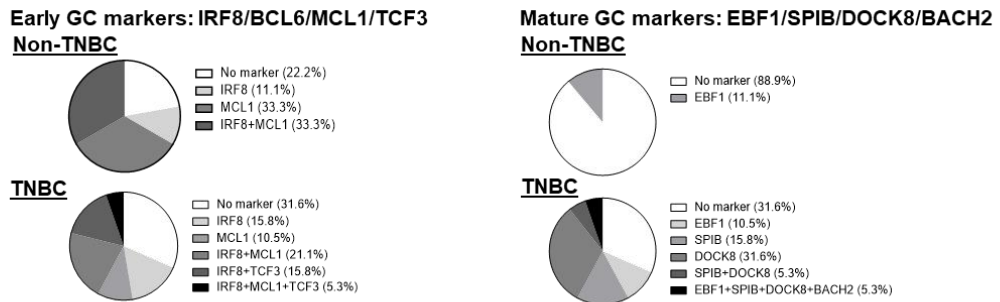
**(B) CD27<sup>+</sup>IgD<sup>-</sup> cell distribution in blood (N = 37) and tumor (N = 26)**



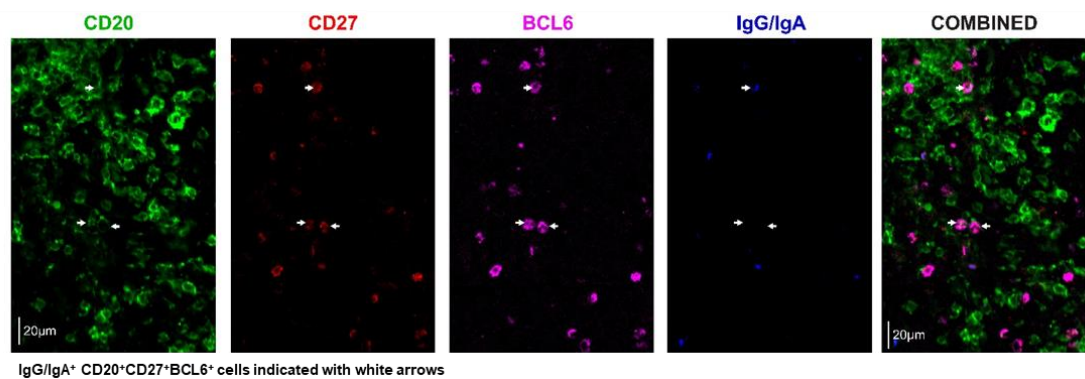
**(C) B cell population in TNBC (N = 7) by IHC/IF (% of density: cells/mm<sup>3</sup>) with representative images depicting memory B cell IHC/IF staining**



**(D) GC B cell marker expression in class-switched (IgD-IgM-) CD19/CD20/CD22<sup>+</sup>CD27<sup>+</sup> B cell in non-TNBC (N=9) and TNBC (N=19)**



**(E) Representative IHC/IF images depicting expression of GC B cell marker BCL6 among CD20<sup>+</sup>CD27<sup>+</sup> B cells within TNBC tumor**



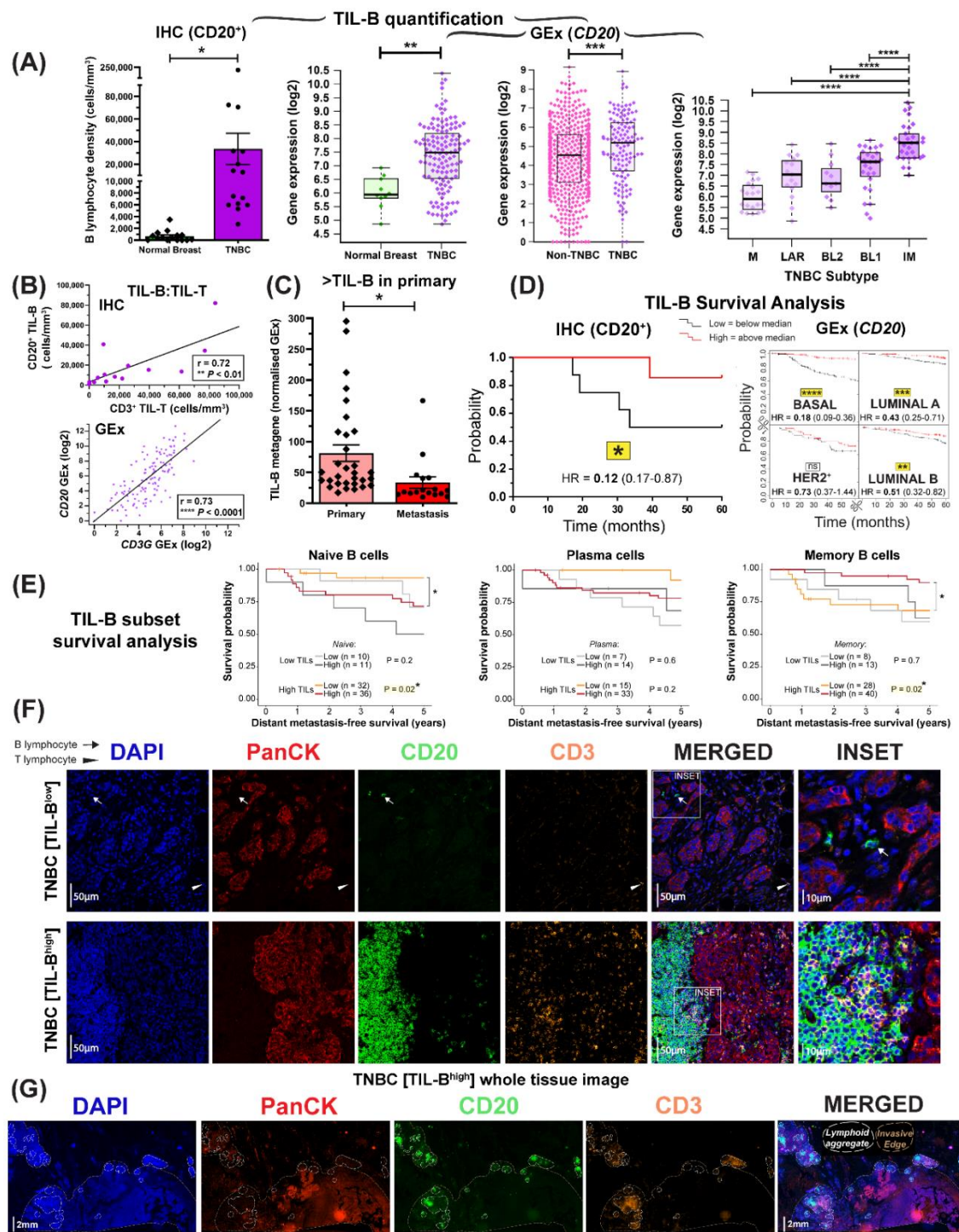
**Figure 3.4 CD27<sup>+</sup> expression distribution and GC B cell marker expression across B cell populations analysed by single-cell gene expression and IHC/IF.**

The distribution of CD27<sup>+</sup> populations was investigated by scRNA-seq. (A) CD27<sup>+</sup> cells and (B) CD27<sup>+</sup>IgD<sup>-</sup> cells in breast cancer patient blood and tumour samples (Single cell cohort). All transcript counts were of cells positive for either or both BCR complex CD79A and CD79B

markers. **(C)** Analyses for B cell subpopulations were also performed by IHC/IF in seven TNBC tumour samples (KCL IHC cohort), with representative images for IHC/IF staining. White arrows indicate memory B cells as CD20<sup>+</sup>CD27<sup>+</sup> (visible in yellow colour (merge)), while CD138<sup>+</sup> cells are mostly negative for CD20 staining. Scale bar=50µm. **(D)** Analysis of GC markers expressed by B cells using scRNA-seq. Expression of GC B cell markers in isotype-switched (IgD<sup>+</sup>IgM<sup>-</sup>) CD19<sup>+</sup>CD20<sup>+</sup>CD22<sup>+</sup>CD27<sup>+</sup> memory B cells was investigated for early (IRF8, BCL6, MCL1, TCF3) and mature (EBF1, SPIB, DOCK8, BACH2) GC markers [278] in tumour samples (Single cell cohort), consistent with initial BCR stimulation inducing GC B cells to differentiate into long-lived plasma cells and memory B cells in GCs and by subsequent antigen recall responses that may drive memory B cells to either differentiate into long-lived plasma cells or to re-enter the GC reaction [69]. **(E)** Representative immunofluorescence images of a TNBC lesion showing isotype-switched CD20<sup>+</sup>CD27<sup>+</sup> (including IgG/IgA<sup>+</sup>) B cells co-expressing the early GC marker BCL6 (White arrows). Scale bar=20µm. These experiments were completed in collaboration with Ms. Elena Alberts, KCL.

#### 3.4.2 TIL-B signatures and assembly within stromal clusters are elevated in TNBC compared with other breast cancer subtypes

I next asked whether TNBC demonstrate increased immune cell infiltration, with particular focus on the TIL-B population, compared with normal breast or other breast cancer subtypes. Quantitative IHC/IF evaluations (Bart's IHC cohort) revealed an expansion of CD20<sup>+</sup> TIL-B and CD3<sup>+</sup> TIL-T within TNBC lesions compared with normal tissues (**Figure 3.5 (A), Figure 3.6 (A)**). Confirmatory gene expression (GEx) analyses (KCL and TCGA GEx cohorts) found that the expression of B cell (*CD20* and BCR complex *CD79A*) and T cell (*CD3G*) markers were also elevated in TNBC, compared to both normal and non-TNBC tissues (**Figure 3.5 (A), Figure 3.6 (A-B)**). The combination of overall enhanced B and T cell infiltrates, representing a strong backdrop for immunological analyses, and the current unmet clinical need of TNBC patients, provided the stimulus for focusing my investigations presented in this Chapter around the TNBC subtype.



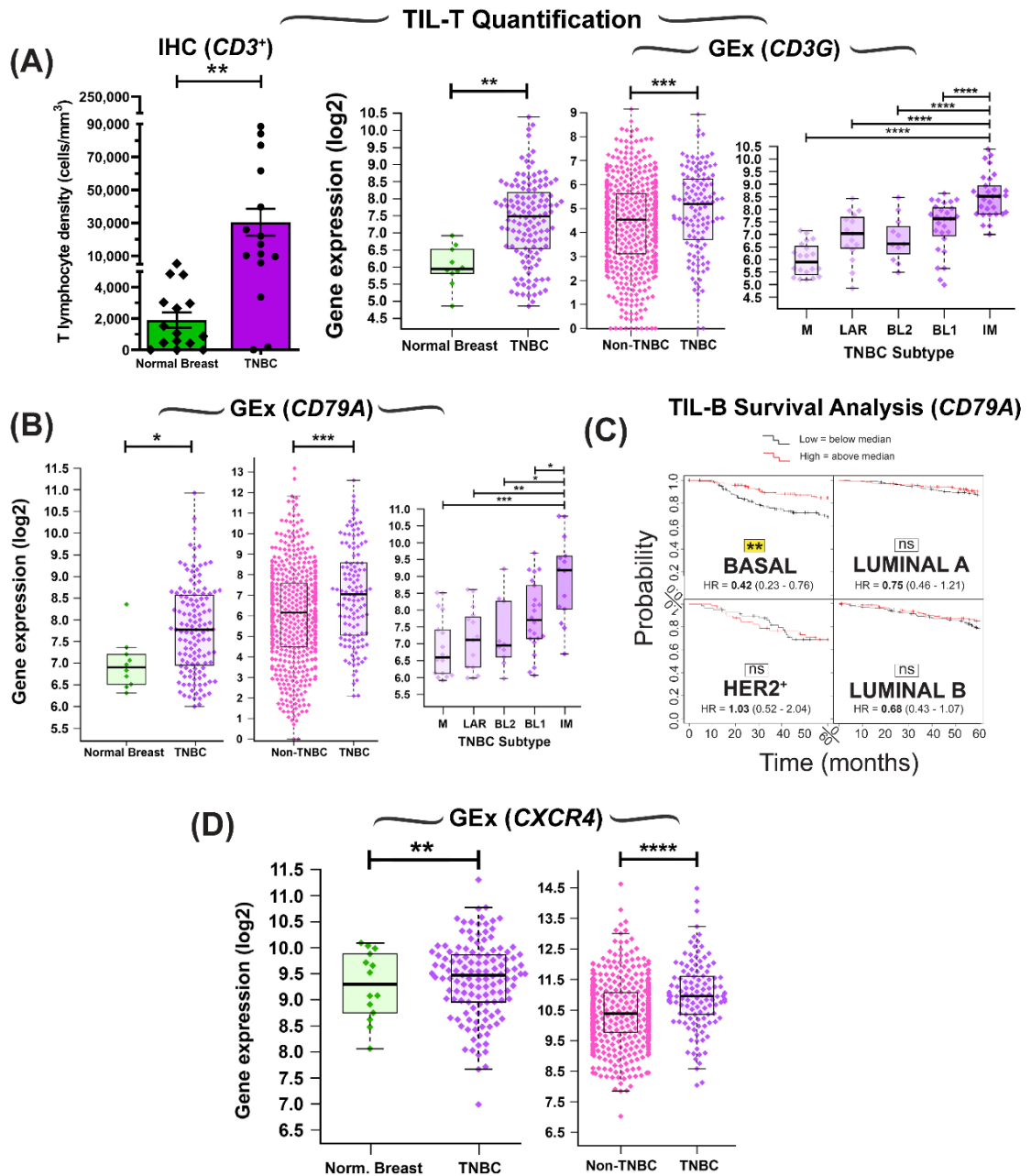
**Figure 3.5 B cell infiltration and its positive prognostic value in TNBC.**

(A) TIL-B density comparison by IHC within normal breasts and TNBC (N=15 each, Bart's IHC cohort), and by GEx (normal breast vs TNBC (N=10 vs 131, KCL GEx cohort); non-TNBC vs TNBC (N=515 vs 123, TCGA GEx cohort); TNBC subtypes (mesenchymal (M), luminal androgen receptor (LAR), basal-like 1 and 2 (BL1 and 2) and immunomodulatory (IM) (N=122, KCL GEx cohort). Mann-Whitney test was used for statistical significance (B) TNBC TIL-B

correlation with TIL-T by IHC ( $r=0.72$ , Bart's IHC cohort) and by GEx ( $r=0.73$ , KCL GEx cohort). Linear regression analysis was used to calculate correlation coefficients ( $r$ ) and  $p$ -values. **(C)** B cell metagene NanoString GEx data comparing B cells in primary tumours with metastatic sites (N=31 vs 17) (NanoString cohort). This analysis was completed in collaboration with Dr. Alicia Chenoweth, KCL. **(D)** High (above median) TIL-B densities by IHC were associated with better overall survival in TNBC (N=15) (Bart's IHC cohort), and in the basal-like subtype by high *CD20* GEx (N=241) (KM plotter cohort) (log rank test used to assess statistical significance). **(E)** Kaplan–Meier survival curves display distant metastasis-free survival (DMFS) for naïve B cells, plasma cells and memory B cells in TNBC (KCL GEx cohort) using CIBERSORT [257]. Data were divided into four groups based on B cell subset and TIL levels stratified by semi-quantitative TIL classification. Statistical significance was assessed using univariate Cox proportional hazards regression models. These analyses were performed in collaboration with Dr. Jelmar Quist, KCL. **(F)** Representative IHC/IF images (Bart's IHC cohort) depicting nucleated cells (DAPI), epithelial cells (PanCK), B cells (CD20) and T cells (CD3) within normal breast and TNBC. Scale bar=50 $\mu$ m. **(G)** Representative TNBC images highlighting numerous lymphoid aggregates (within white lines) consisting of B cells assembled adjacent to a T cell zone. Brown dash lines indicate carcinoma edge. Scale bar=2mm.

Among TNBC subtypes, gene expression markers representing B and T cells were highest in the Lehmann's immunomodulatory (IM) molecular TNBC subtype, known to be enriched in core immune signal transduction pathways and cytokine signaling (N = 122) [269] (**Figure 3.5 (A), Figure 3.6 (A-B)**). TIL-B density and *CD20* gene expression positively correlated with TIL-T density and *CD3* gene expression, respectively (**Figure 3.5 (B)**), highlighting strong association of B and T cells in the breast TME. Also, the expression of a B cell metagene signature (NanoString cohort) was significantly enhanced in primary breast cancer compared to patient-matched metastatic sites (N = 31 vs N =17), suggesting a diminished immune TME with advanced disease (**Figure 3.5 (C)**).

Both quantitative IHC/IF (N = 15) and KM-plotter survival analysis (N = 241) demonstrated that TIL-B in primary tumours were significantly associated with more favourable overall survival, most prominently in basal-like/TNBC (**Figure 3.5 (D), Figure 3.6 (C)**).



**Figure 3.6 TIL-B, TIL-T and B cell recruitment markers in TNBC.**

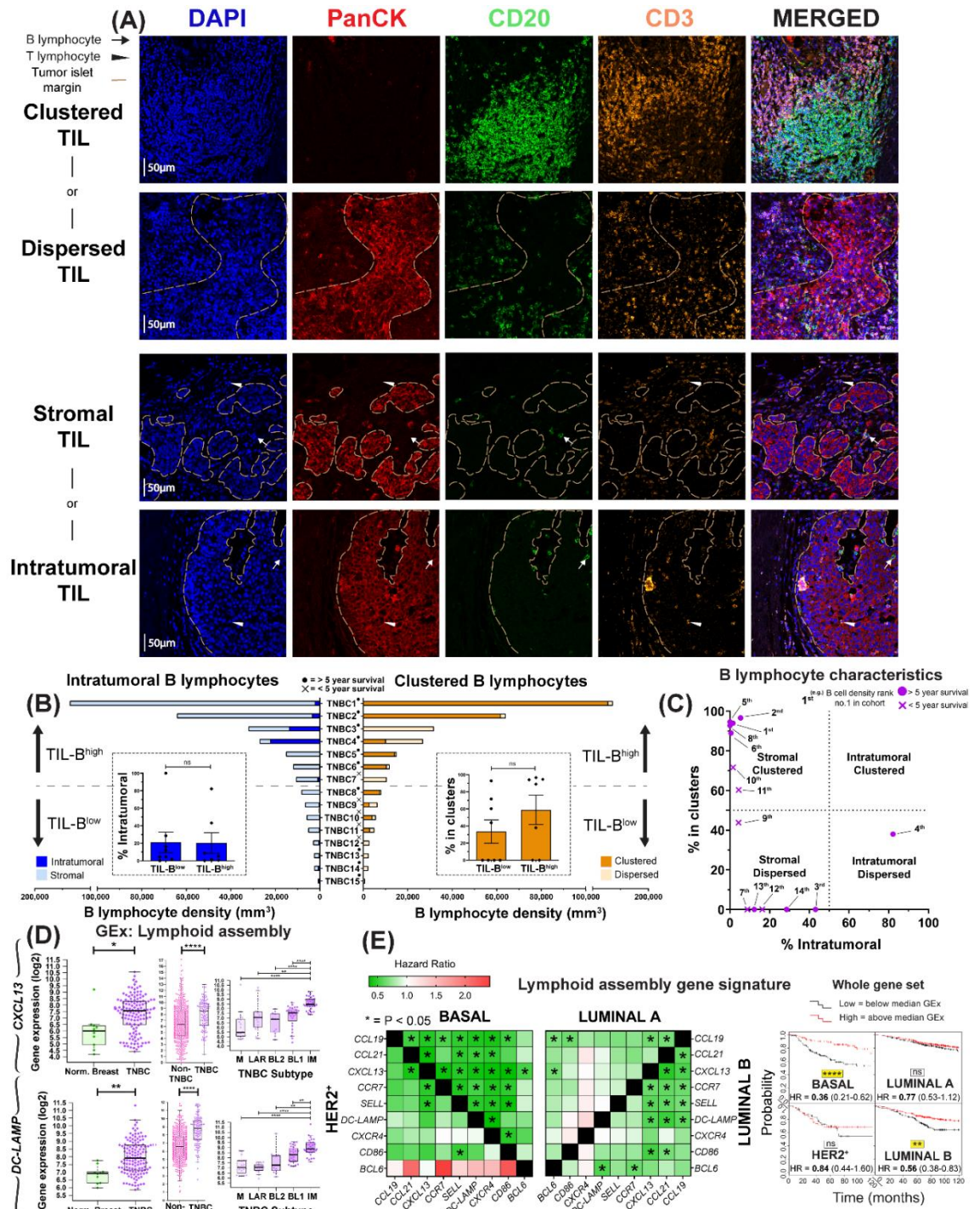
(A) Quantitative IHC analysis of  $CD3^+$  T cells within normal breast tissues and TNBC lesions (N=15 each) (Bart's IHC cohort), and by GEx: normal breast vs TNBC ([left] N=10 vs 131, KCL GEx cohort); non-TNBC vs TNBC ([middle] N=515 vs 123, TCGA GEx cohort); and TNBC subtypes ([right] N=122, KCL GEx cohort) (B) TIL-B GEx of the BCR complex  $CD79A$  marker: normal breast vs TNBC ([left] N=10 vs 131, KCL GEx cohort), non-TNBC vs TNBC ([middle] N=515 vs 123, TCGA GEx cohort) and TNBC subtypes ([right] N=122, KCL GEx cohort). (C) High TIL-B ( $CD79A$  expression) demonstrate better overall survival in basal-like subtype (N=241) (KM plotter cohort). (D) GEx data for the B cell recruitment marker gene  $CXCR4$ : normal breast vs TNBC ([left] N=10 vs 131, KCL GEx cohort); non-TNBC vs TNBC ([right] N=515 vs 123, TCGA GEx cohort).



Additional Kaplan-Meier analyses employing CIBERSORT deconvolution and utilizing data from the KCL GEx cohort [257] was used to investigate the associations between distant metastasis-free survival (DMFS) and naïve, plasma and memory B cell phenotypes in TNBC (N = 89). TIL infiltrates were classified using tissue microarrays, and in tumours with high TILs, memory B cells were associated with a more-favourable DMFS, while a negative prognostic value was shown for naïve B cells in this cohort (**Figure 3.5 (E)**). IHC/IF staining analyses (Bart's IHC cohort) confirmed the heterogeneity of TIL-T and TIL-B (**Figure 3.5 (F)**), with evidence of expansive cluster formation (demarcated in white (>30 TIL-B and >30 TIL-T aggregated), typically of a B cell assembly adjacent to a T cell zone) (**Figure 3.5 (G)**). This highlighted close B-T cell interactions within the TME.

Since B-T cell clusters were observed in a large proportion (9 of 15) of TNBCs (Bart's IHC cohort), I next evaluated TIL-B spatial and structural characteristics. TIL-B were characterised as either stromal or intratumoural, according to penetration within PanCK<sup>+</sup> tumour islets. B cells were further categorised as forming either clusters or dispersions, corresponding to the extent of aggregation along with CD3<sup>+</sup> TIL-T (**Figure 3.7 (A)**). Tumours were split by median TIL-B density into TIL-B<sup>low</sup> and TIL-B<sup>high</sup> groups. B cells typically formed within stromal clusters irrespective of overall TIL-B density (**Figure 3.7 (B)**). Five individuals featuring highly clustered TIL-Bs survived for over 5 years post-surgery (**Figure 3.7 (C)**). Consistent with the B-T cell cluster formation observed, elevated expression of B cell recruitment and lymphoid assembly marker genes (*CXCL13*, *CXCR4* and *DC-LAMP*) was found in TNBC tumours, compared to both normal breast and non-TNBC, and within the TNBC cohort the highest expression of these genes was detected in IM tumours (**Figure 3.7 (D)**, **Figure 3.6 (D)**, KCL and TCGA GEx cohorts). Increased expression of these signatures was also associated with significantly improved

overall survival, using a 10-year follow-up, in basal-like/TNBC (Figure 3.7 (E), KM plotter cohort).



### **Figure 3.7 Occurrence of B cells in stromal clusters.**

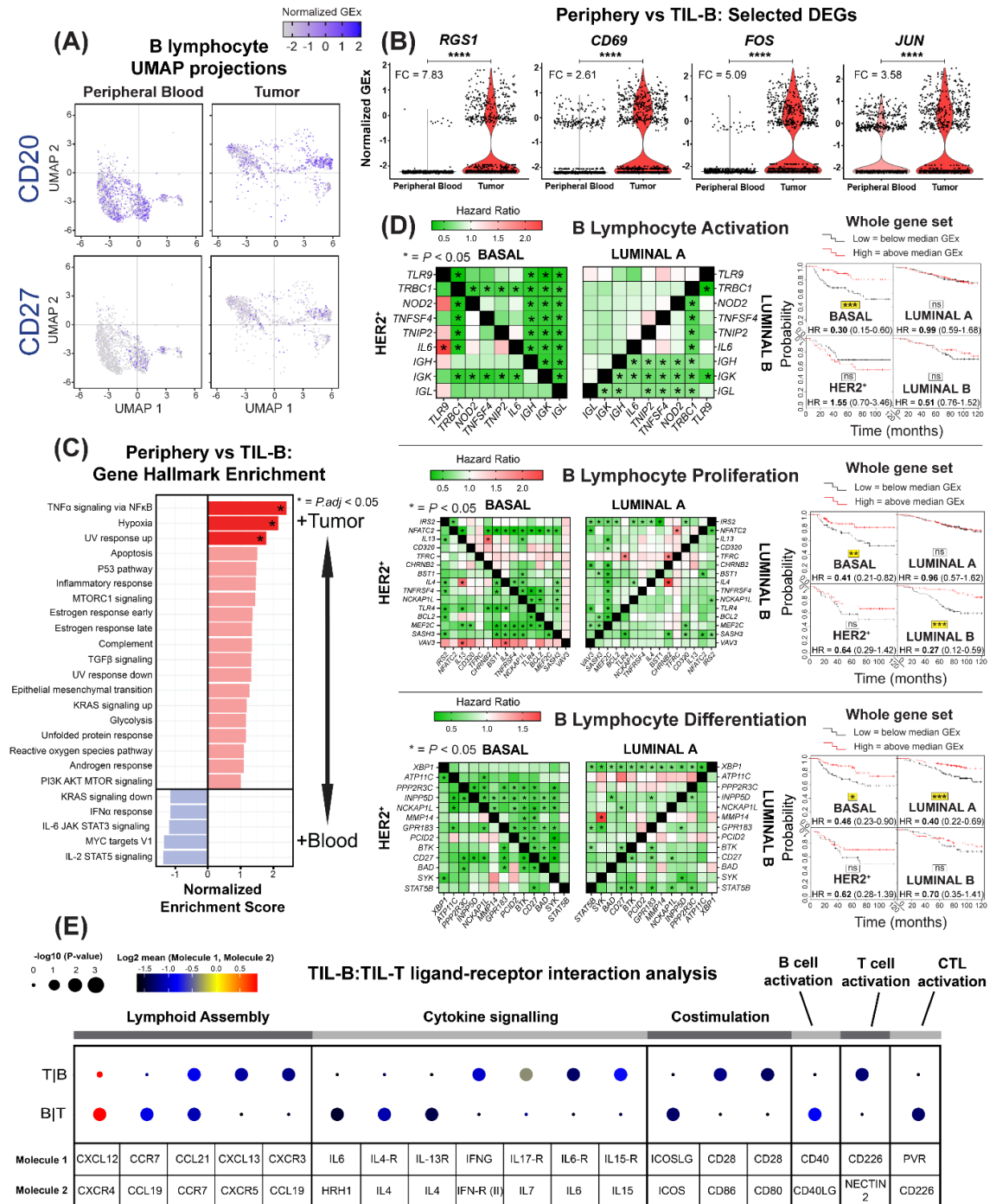
(A) Representative IHC/IF images (Bart's IHC cohort), highlighting key TIL characteristics: clustered TIL versus dispersed TIL and stromal TIL (outside tumour nests) vs intratumoural TIL (within tumour nests). Scale bar=50µm. (B) Quantitative assessment of TIL-B spatial and structural characteristics within TNBC (N=15): [left] intratumoural vs stromal; [right] clustered versus non-clustered. Patients ranked according to CD20<sup>+</sup> TIL-B density (TNBC1=highest), and overall survival data indicated. [Inset] Patients samples split at median density into high and low TIL-B groups and the % of intratumoural (left) or clustered (right) B cells were analysed. Statistical significance was determined using Student's *t*-test. (C) Characterization of TNBC TIL-B profile as stromal clustered, intratumoural clustered, stromal dispersed, or intratumoural dispersed. Overall survival data are indicated. (D) GEx data for lymphoid assembly marker genes *CXCL13* and *DC-LAMP* ([left] normal breast vs TNBC (N=10 vs 131, KCL GEx cohort); non-TNBC vs TNBC ([middle] N=515 vs 123, TCGA GEx cohort); TNBC subtypes ([right] N=122, KCL GEx cohort). (E) Survival analysis in KM Plotter of determined ER<sup>-</sup>HER2<sup>-</sup>/basal surrogate, HER2<sup>+</sup>, luminal A, luminal B subtype KM plotter surrogate subgroups (19) (KM plotter cohort). These indicate that expression of lymphoid cell assembly genes carries positive prognostic value in TNBC/basal-like and luminal B subtype ([left] Individual genes were evaluated in combination with each other gene, and [right] gene set as a whole).

Together, these findings show that TIL-B markedly infiltrate TNBC, and typically form stromal clusters along with T cells. TIL-B marker (*CD20* and *CD79A*), and GEx features conferring B cell recruitment and lymphoid assembly are enhanced in TNBC compared to non-TNBC and normal breast tissues, and associate with more favourable survival outcomes in basal-like/TNBC subtype. In addition, the observation that memory, as opposed to naïve B cell phenotypes, confer positive prognostic value in high-TIL breast tumours hints at the importance of active and dynamic humoral immunity profiles in contributing to breast cancer survival outcomes.

### 3.4.3 Breast tumour-infiltrating B lymphocytes are activated via the B Cell Receptor

Next, direct evidence for active roles of B cells in the TME was sought using a previously published RNAseq dataset (Single cell cohort). Dimensionality reduction (UMAP) was applied to single-cell B cell populations and revealed distinct CD20<sup>+</sup> and CD27<sup>+</sup> tumour-

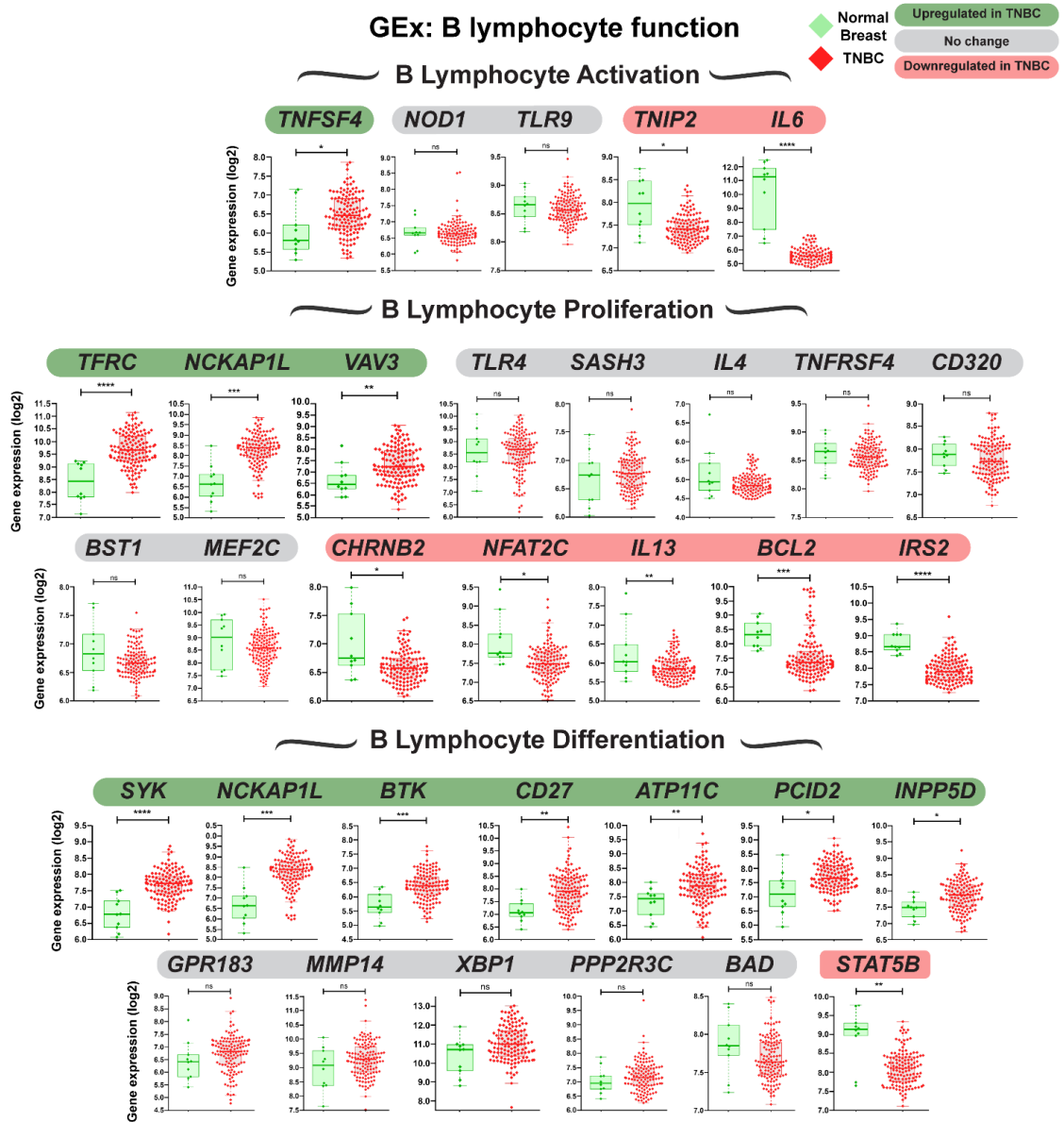
infiltrating B lymphocyte populations compared to those in the circulation (N = 1,476 circulating B cells and N = 1,021 TIL-B derived from eight patients) (**Figure 3.8 (A)**).



**Figure 3.8 scRNA-seq analysis reveals BCR-driven TIL-B activatory signatures and B cell lineage gene markers predict positive survival outcome.**

(A) UMAP visualization according to global GEx of single B cells pooled from the peripheral blood (1,476 cells) and tumours (1,021 cells) of eight patients (Single cell cohort), coloured by relative normalised gene expression levels for *CD20* and *CD27*. (B) The detection of differentially expressed genes (DEGs, on cells originally annotated by Azizi *et al.* [258] as B cells) demonstrates elevated expression of *FOS*, *JUN*, *RGS1* and *CD69*, indicated by fold change (FC) (determined using Wilcoxon Rank Sum test). (C) Gene set enrichment analysis of TIL-B relative to circulating B cells using hallmark gene sets. Red colour indicates significant upregulation of normalised enrichment scores in TIL-B. (D) Survival analysis in KM Plotter of determined ER<sup>-</sup>HER2<sup>-</sup>/basal surrogate, HER2<sup>+</sup>, luminal A, luminal B subtype KM plotter surrogate subgroups [254] (KM plotter cohort) for expression of gene signatures positively regulating key B cell properties (activation, proliferation, and differentiation). Representative genes listed for B cell proliferation (44 total in set). Signatures from all three functions carry positive prognostic value in the basal-like cancer subtype ([left] Individual genes were evaluated in combination with each other gene, and [right] gene set as a whole). (E) CellPhoneDB [261] was applied to analyse B cell-T cell interactions (Single cell cohort). After false discovery rate (FDR<0.001) correction, predicted communication pathways identified included lymphoid assembly, cytokine signaling, co-stimulation, T-cell dependent B cell activation, and CTL activation. Circle sizes indicate *p*-value while colour-coding represents the average expression level of interacting molecule 1 in cluster 1 and interacting molecule 2 in cluster 2. Analyses (A-C and E) were completed in collaboration with Mr. Roman Laddach, KCL.

Downstream differential expression gene (DEG) analysis identified several upregulated genes in TIL-B, compared to circulating B cells: *FOS* and *JUN*, molecules downstream of the BCR complex pathway [279]; *RGS1*, germinal centre B cell regulator of chemokine receptor signaling [280]; and the lymphocyte activation marker *CD69*, triggered through crosslinking of surface Ig [281] (**Figure 3.8 (B)**). Hallmark enrichment analysis [282] revealed significantly elevated expression among TIL-B for genes controlling TNF $\alpha$  signaling via NF $\kappa$ B, hypoxia and UV response pathways (**Figure 3.8 (C)**). In addition, several genes known to positively regulate B cell activation, proliferation and differentiation functions were upregulated in TNBC compared to normal breast (**Figure 3.9**, KCL and TCGA GEx cohorts). Survival analysis of these gene signatures revealed positive associations with overall survival, using a 10-year follow up, which was most pronounced in basal-like/TNBC (**Figure 3.8 (D)**, KM plotter cohort).



**Figure 3.9 Expression data of genes that positively regulate key B cell functions.** GEx data (normal breast vs TNBC (N=10 vs 131, KCL GEx cohort) of individual genes evaluated in TNBC compared to normal breast. Pathways investigated include B cell activation, proliferation, and differentiation.

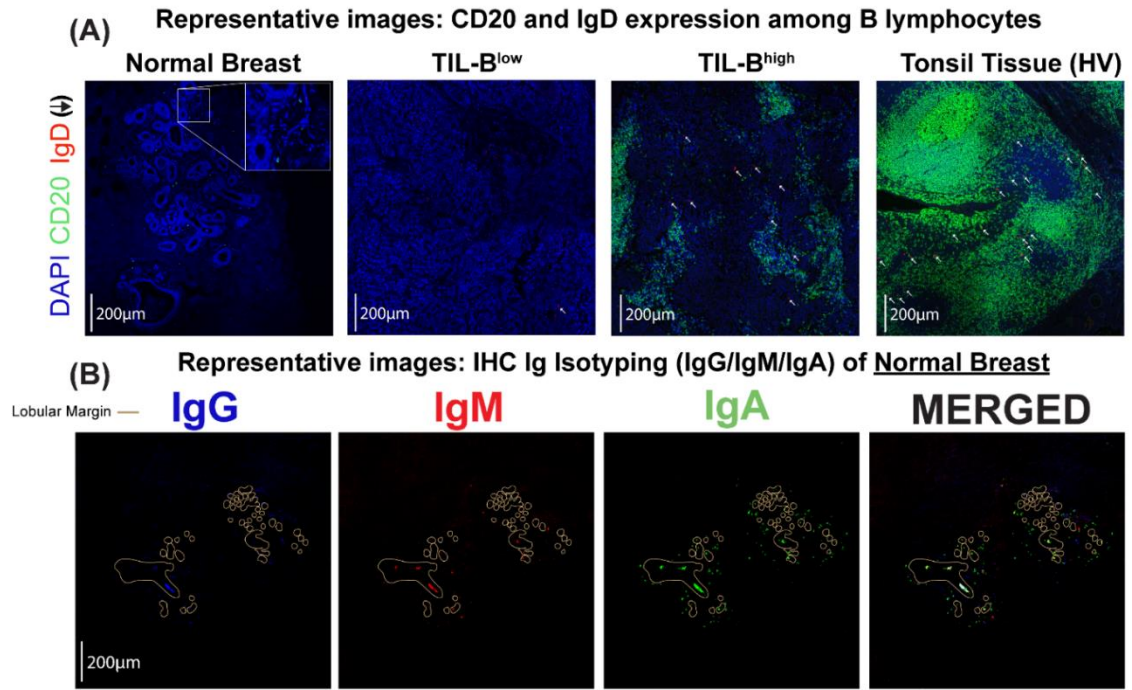
Next, B cell-T cell interactions in the tumour microenvironment (Single cell cohort) were investigated using CellPhoneDB [261]. Predicted cell communication pathways were identified which are associated with lymphoid assembly (CXCL12, CCL19, CCL21 and CXCL13), cytokine signaling (IL-4, IL-6, IL-13, IL-15, IL-17 and IFN $\gamma$ ), co-stimulation (CD28 and ICOS) and immune activation (CD40 and CD226). These findings support potential bi-directional functional crosstalk between tumour-infiltrating B and T lymphocytes (**Figure 3.8 (E)**).

Overall, these results indicate the presence of distinct B cell populations between breast cancer patient blood and tumours, and evidence of TIL-B antigen-Ig complex, BCR pathway stimulation and B cell-T cell functional crosstalk. Key functional attributes for the initiation of B cell responses are associated with improved patient outcomes, especially in TNBC.

#### 3.4.4 IgG<sup>+</sup> B cell densities are elevated in TNBC, and IgG isotype-switching predicts positive survival outcomes in TNBC

I next examined B cell densities according to Ig isotype expression in primary TNBC lesions by employing quantitative IHC/IF of IgD, IgM, IgA and IgG isotype-expressing B cells (Bart's IHC cohort) (normal breast tissue, N = 10; TNBC, N = 14). Naïve (IgD<sup>+</sup>) B cells were found at low densities in normal breast, TIL-B<sup>low</sup> and TIL-B<sup>high</sup> tumours (**Figure 3.10 (A)**). Enhanced IgG<sup>+</sup> and IgM<sup>+</sup> B cell densities were found in TIL-B<sup>high</sup> and, to a lesser extent, in TIL-B<sup>low</sup> tumours compared with normal breast (**Figure 3.11 (A-B)**). In contrast, IgA<sup>+</sup> B cell densities were consistent among tissue compartments, which overall constitutes a bias towards increased IgG<sup>+</sup>:IgA<sup>+</sup> B cell ratio within tumours

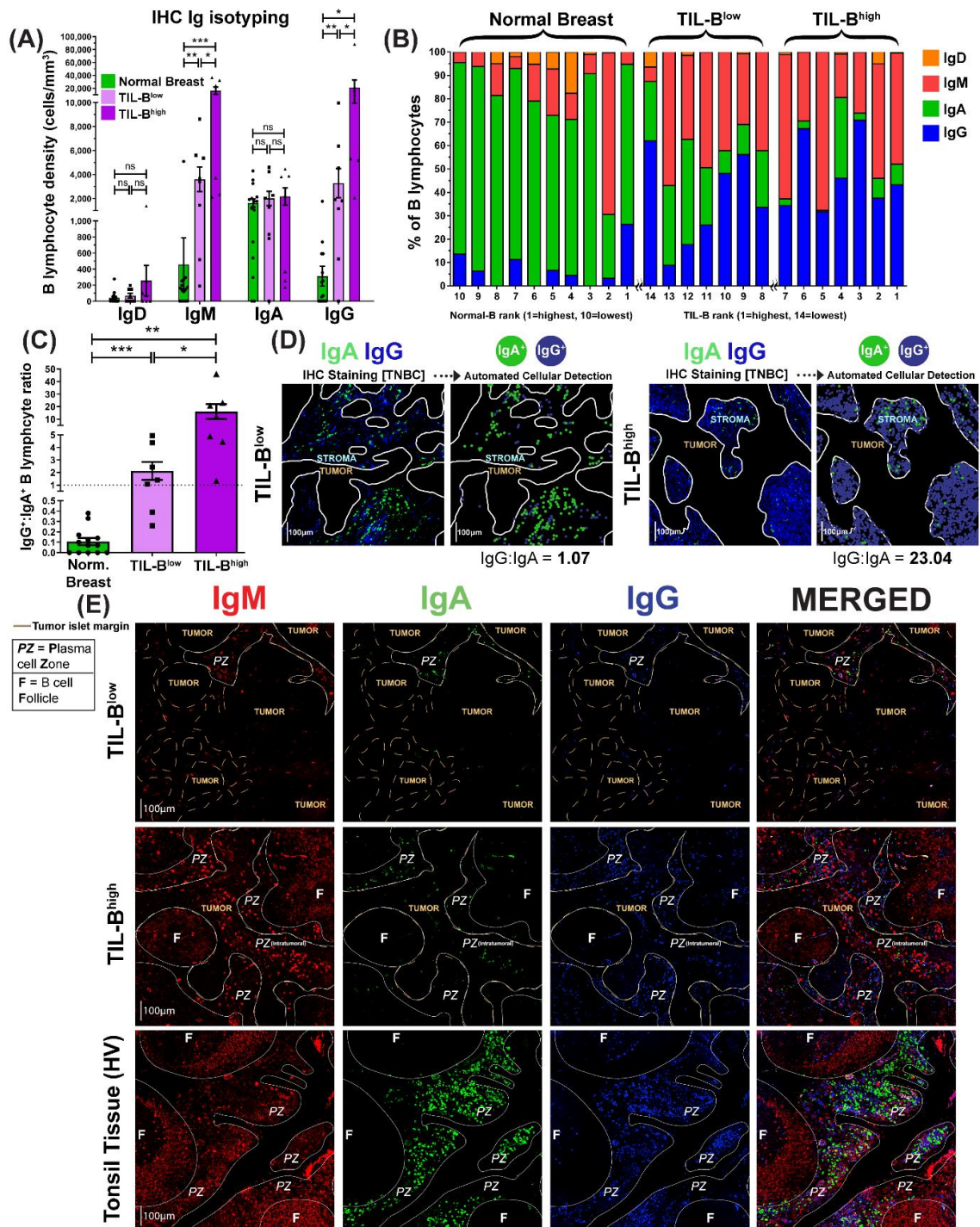
compared to normal breast, and within TIL-B<sup>high</sup> compared to TIL-B<sup>low</sup> cancers (**Figure 3.11 (C-D)**).



**Figure 3.10 IHC staining demonstrate CD20 and IgD expression in normal breast and TNBC tumours.**

(A) IF images show that naïve (IgD<sup>+</sup>, arrows) B cell distribution in TNBC TIL-B<sup>high</sup> tumours is analogous to secondary lymphoid organs (tonsil). (B) As a control, IF images illustrating Ig isotype distribution in normal breast tissue (Bart's IHC cohort). Scale bar=200µm.



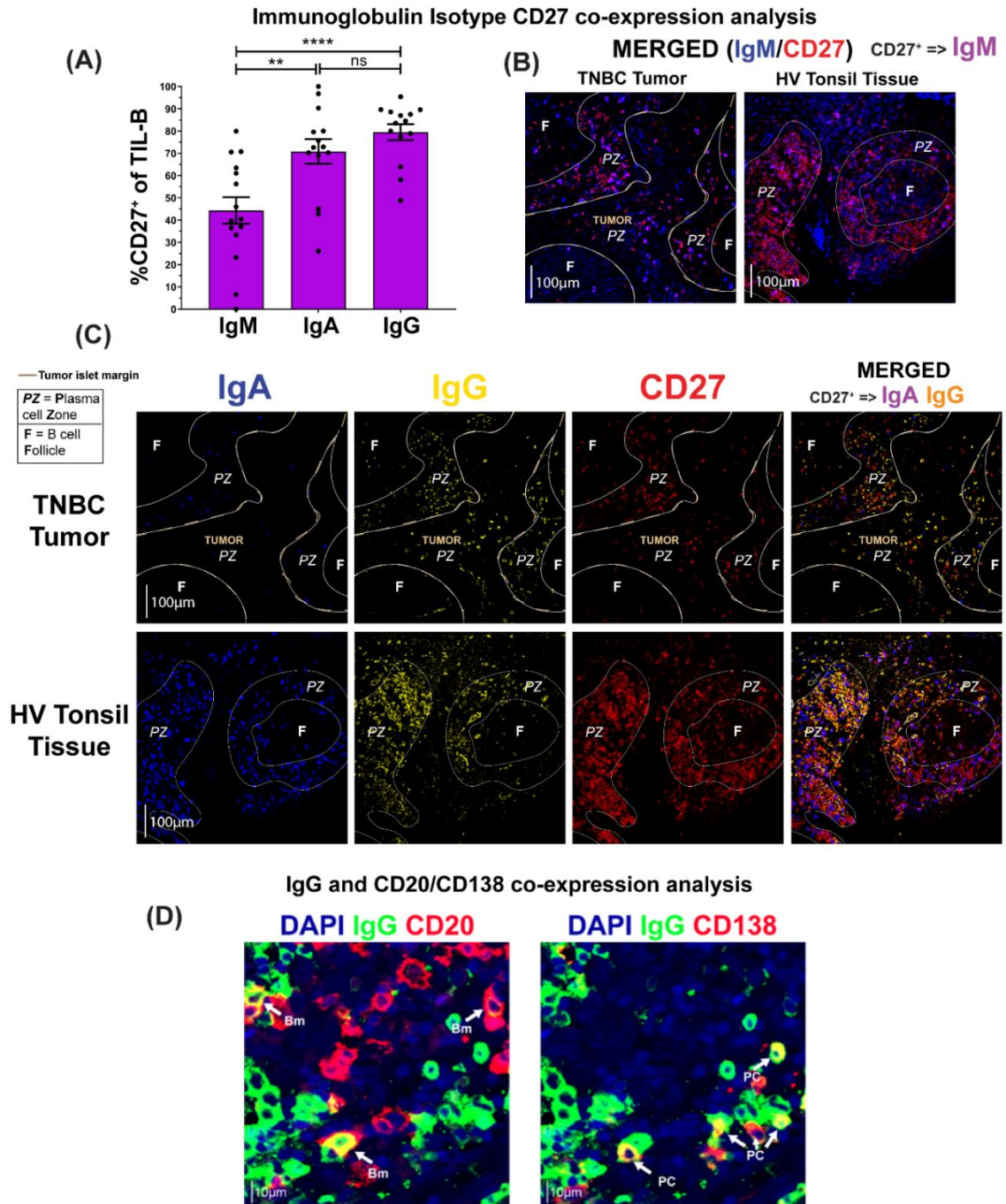


**Figure 3.11 Quantitative fluorescence IHC reveals elevated IgG<sup>+</sup>:IgA<sup>+</sup> ratio within high TIL-B tumours, implicating expansion of IgG<sup>+</sup> B cells within TNBC tumour microenvironment.**

(A) Comparison of surface immunoglobulin-expressing B cell density in normal breast and TNBC with low TIL-B density (below median CD20<sup>+</sup>) and high TIL-B density (above median CD20<sup>+</sup>). (B) Quantitative IHC analysis profiling the proportions of B cells present within the microenvironment of normal breast tissue (N=10) and TNBC (N=14) expressing each Ig isotype. (C) Enumeration of IgG<sup>+</sup>:IgA<sup>+</sup> B cell ratios. (D) [Right] Example images illustrating IgG<sup>+</sup> and IgA<sup>+</sup> B cells in a typical TIL-B low individual and a TIL-B high individual. Automated cellular

detection identifies IgA (green) and IgG (blue) B cells. Scale bar=100 $\mu$ m. **(E)** Representative images depicting typical Ig isotype expression among B cells: IgM<sup>+</sup> (red), IgA<sup>+</sup> (green), and IgG<sup>+</sup> (blue). Images from Bart's IHC cohort. Brown dash lines indicate margin of the cancer. White lines separate distinct regions of B cell compartments (PZ=plasma cell zone; F=B cell follicle). Scale bar=100 $\mu$ m. Statistical significance was determined using the Student's *t*-test.

IHC/IF showed the dominating IgA<sup>+</sup> B cell profile present in normal breast is contained within normal lobules and their periphery (**Figure 3.10 (B)**). While TIL-B<sup>low</sup> cancers lacked large B cell follicles and contained small IgM/IgA/IgG plasma cell zones, TIL-B<sup>high</sup> tumours typically contained denser IgM/IgA/IgG plasma cell zones surrounding expansive IgM<sup>+</sup> follicular B cell clusters with defined germinal centers (**Figure 3.11 (E)**). The resulting B cell assembly in these TIL-B<sup>high</sup> tumours shares some structural similarities with those in tonsil tissues. Moreover, IgG and IgA expression were accompanied with CD27 upregulation, validating the differentiated, isotype-switched status of these cells (**Figure 3.12 (A-C)**). I further confirmed that intratumoural IgG<sup>+</sup> cells comprised both CD20<sup>+</sup> as well as CD138<sup>+</sup> (plasma) cell populations, the latter being low or negative for CD20 expression (**Figure 3.12 (D)**, **Figure 3.4 (C)**).

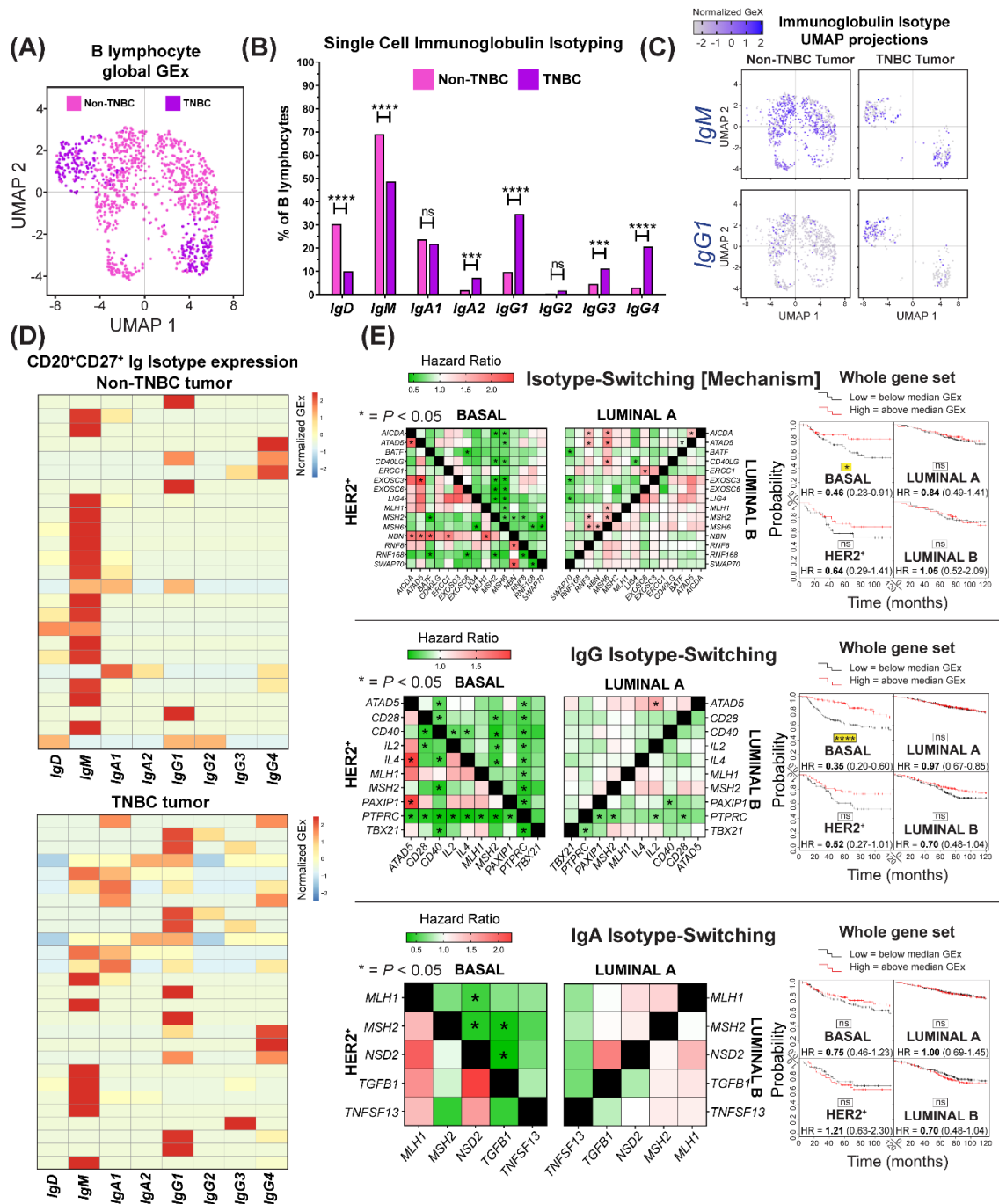


**Figure 3.12 IHC staining demonstrates CD27 expression in isotype-switched TIL-B and presence of both memory/GC B and plasma IgG<sup>+</sup> B cells in TNBC.**

**(A)** Significantly-greater CD27 co-expression among IgA<sup>+</sup> and IgG<sup>+</sup> than IgM<sup>+</sup> TIL-B in TNBC (N=15). **(B)** Example images illustrating the extent to which IgM<sup>+</sup> B cells co-express CD27 in a typical TIL-B<sup>high</sup> individual and secondary lymphoid organ (tonsil) of healthy volunteer. Scale bar=100µm. **(C)** Representative images depicting the extent to which isotype-switched IgA<sup>+</sup> (blue) and IgG<sup>+</sup> (yellow) B cells co-express CD27<sup>+</sup> (red). Brown dash lines indicate margin of tumour. White lines separate distinct regions of B cell compartments (PZ=plasma cell zone; F=B cell follicle) (Bart's IHC cohort). Scale bar=100µm. **(D)** Representative images for IgG<sup>+</sup> B cell

populations performed by IHC/IF in TNBC samples (KCL IHC cohort). White arrows indicate IgG-expressing memory/GC B cells (CD20) or plasma cells (CD138) (visible in yellow colour (merge)). Scale bar=10µm.

Since TNBCs feature high levels of IgG-expressing B cells, B immunoglobulin isotypes (Ig heavy chain) were investigated using a published scRNA-seq dataset (Single cell cohort; N = 1,021 TIL-B across eight patients). UMAP applied to single-cell B cell populations revealed distinct TIL-B populations in TNBC compared with non-TNBC samples. This analysis also revealed enhanced isotype-switching to IgG1, IgG3, IgG4 and IgA2 subclasses in TNBC (**Figure 3.13 (A-B)**). UMAP confirmed differential isotype-expressing B cell compartments in TNBC compared with non-TNBC for IgM and IgG1 based on clustering (**Figure 3.13 (C)**). Heatmaps of single CD20<sup>+</sup> CD27<sup>+</sup> B cell IgCH expression showed a propensity towards non-switched IgM transcripts in blood, in contrast to high levels of isotype-switched IgG and IgA B cells in tumour samples (**Figure 3.14**), and higher levels of isotype-switching in TNBC compared to non-TNBC tumour samples (**Figure 3.13 (D)**). These point to an active tumour-resident humoral response, different to the equivalent response in the circulation, and likely driven by inflammatory and possibly antigenic signals which may support Ig class-switch recombination in the breast cancer microenvironment, especially in TNBC.



**Figure 3.13 Single cell RNA-seq data analysis reveals favor of IgG isotypes in TNBC and isotype-switching gene markers predict positive survival outcome.**

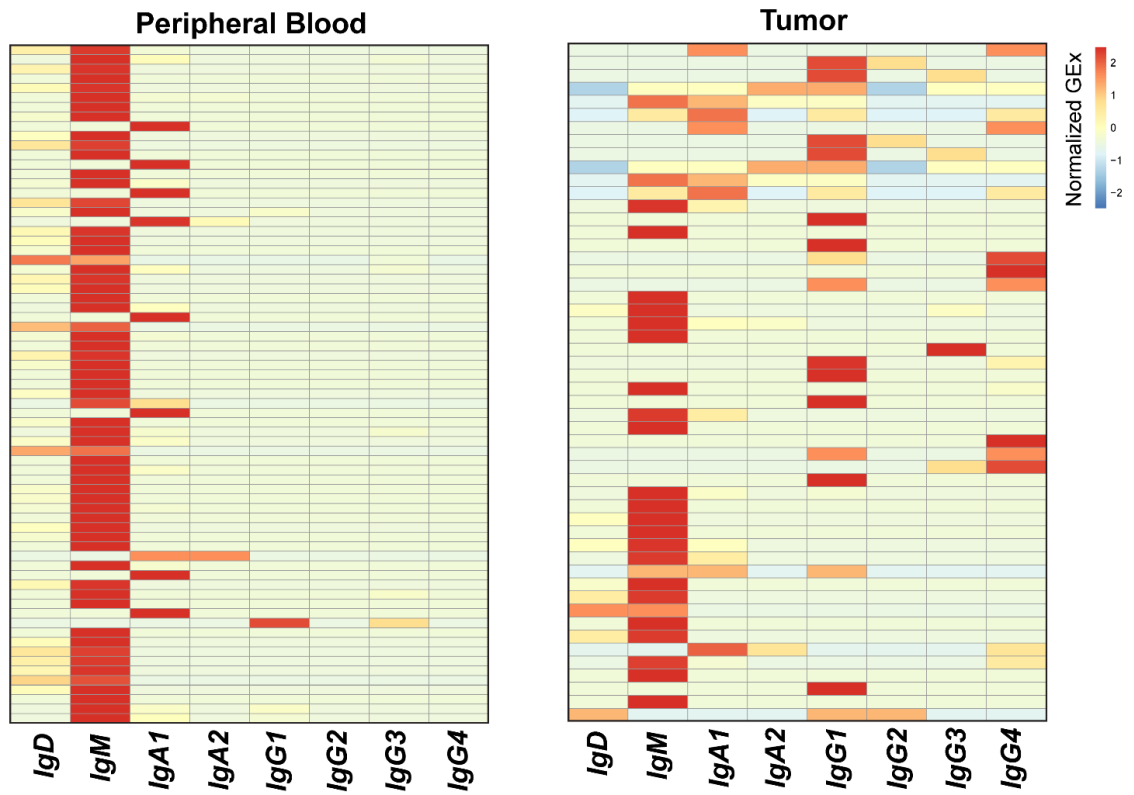
(A) UMAP visualization of B cell populations in non-TNBC vs TNBC (Single cell cohort). (B) Percentage of each Ig isotype based upon raw data of Ig heavy chain (Student's *t*-test) (C) UMAP visualization for IgM and IgG1 isotypes coloured by relative normalised gene expression levels (N=1,021 cells). (D) IgCH switch transcripts of single B cells (CD19<sup>+</sup>CD27<sup>+</sup>/CD20<sup>+</sup>CD27<sup>+</sup>/CD22<sup>+</sup>CD27<sup>+</sup> single cells) were analysed in non-TNBC and TNBC tissues and demonstrated more Ig isotype-switching events in the TNBC samples. (E) Survival analysis in KM Plotter of determined ER-HER2<sup>+</sup>/basal surrogate, HER2<sup>+</sup>, luminal A, luminal B subtype KM plotter surrogate subgroups [254] (KM plotter cohort) for expression of gene

signatures positively regulating isotype-switching (total Ig, IgG and IgA isotype-switching). Signatures from all three functions carry positive prognostic value in basal-like cancer ([left] Individual genes were evaluated in combination with each other gene, and [right] the gene set as a whole). Analyses (**A-D**) were completed in collaboration with Mr. Roman Laddach, KCL.

Survival analysis of isotype-switching gene signatures revealed a positive association with 10-year overall survival for IgG, but not for IgA, isotype-switching, most pronounced in basal-like/TNBC (**Figure 3.13 (E)**, KM plotter cohort). Moreover, as expected, several genes involved in the mechanism of and/or positively regulating isotype-switching were upregulated in TNBC compared to normal breast (**Figure 3.15**, KCL and TCGA GEx cohorts).

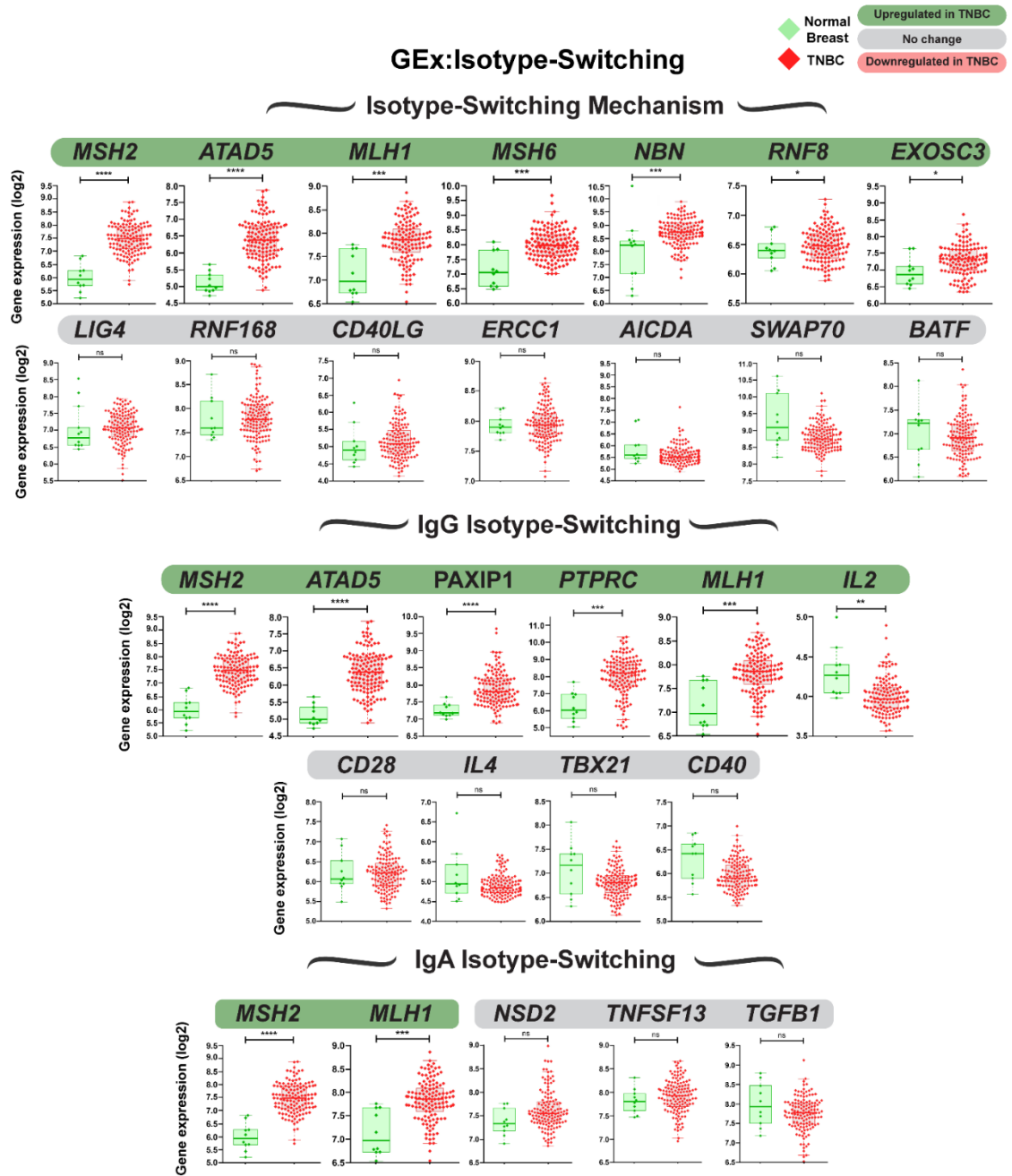
These findings indicate a shift in favour of IgG<sup>+</sup> B cells in TIL-B<sup>high</sup> TNBC and point to IgG isotype-switching as a contributor to the positive role of B cell responses to breast cancers.

CD20<sup>+</sup> CD27<sup>+</sup> Ig Isotype expression



**Figure 3.14 IgCH transcripts of CD27<sup>+</sup> B cells.**

IgCH switch transcripts of single B cells (CD19<sup>+</sup>CD27<sup>+</sup>/CD20<sup>+</sup>CD27<sup>+</sup>/CD22<sup>-</sup>CD27<sup>+</sup> single cells) were identified in patient blood (N=71) and breast cancer tissues (N=52) (Single cell cohort). This analysis was completed in collaboration with Mr. Roman Laddach, KCL.



**Figure 3.15 Expression data in TNBC of key genes known to positively regulate B cell isotype-switching.**

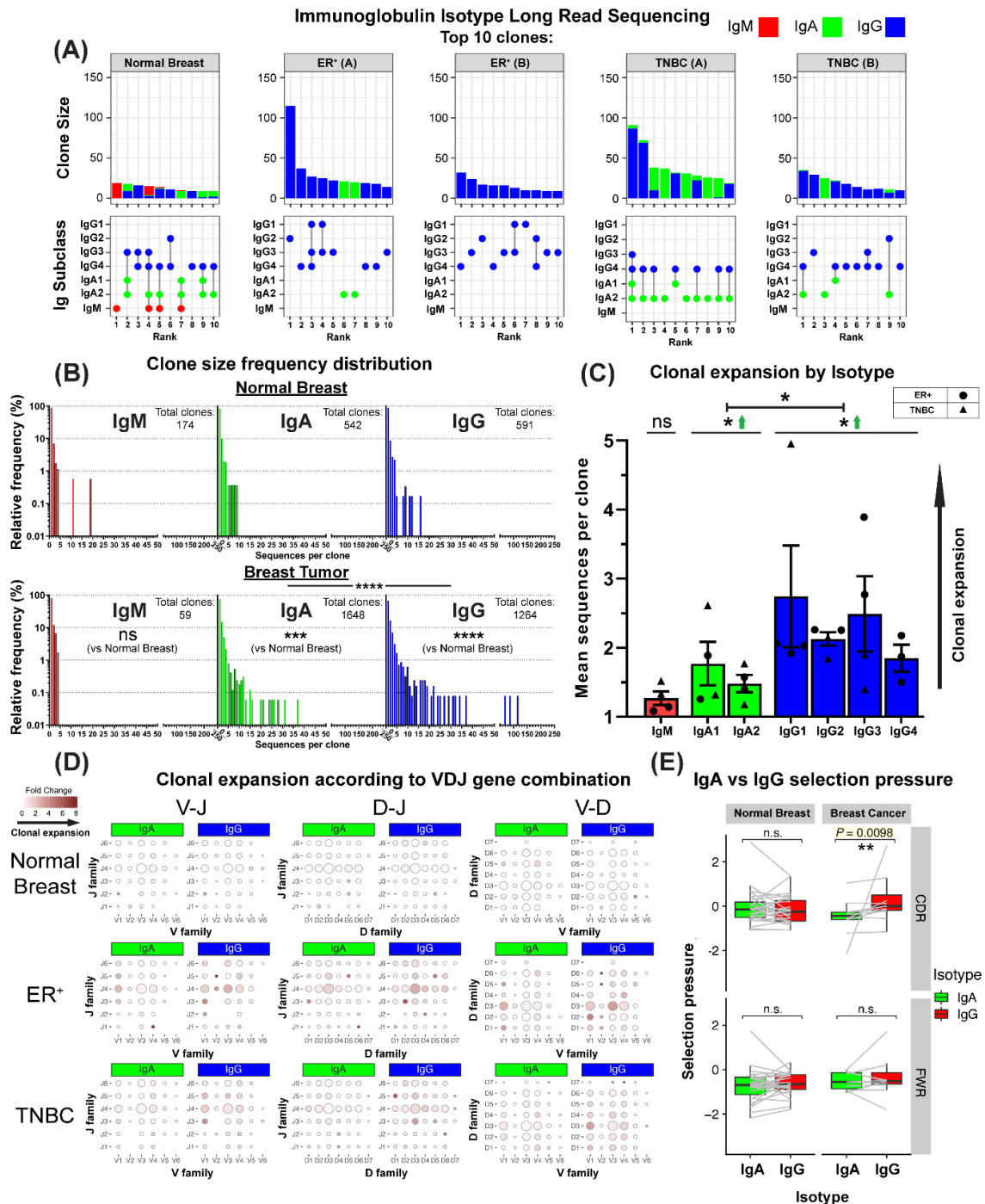
GEx data (normal breast versus TNBC (N=10 vs 131, KCL GEx cohort) of individual genes evaluated in TNBC compared to normal breast. Pathways investigated include isotype-switching mechanism and IgG/IgA isotype-switching.



### 3.4.5 IgG-biased, clonally-expanded, immunoglobulin repertoires in breast cancer

Lastly, using long-read sequencing, a dataset of Ig heavy chain repertoires (N=7,670) from two TNBCs, two ER<sup>+</sup> cancers and one normal breast tissue (KCL sequencing cohort) was generated, and sequence clustering analyses were performed to define clonotypes and compare the distributions of Ig isotypes following B cell clonal expansion. Consistently larger clonal family sizes were observed within the 10 largest clones of cancers compared to normal breast (**Figure 3.16 (A)**, top panel). B cell sequences from ER<sup>+</sup> cancers featured a heterogeneous IgG subclass expansion with few IgA clones. In contrast, TNBCs showed clones with co-existing IgG1 and IgA1 subclasses, suggested intra-clone isotype-switching (**Figure 3.16 (A)**, bottom panel). Kolmogorov-Smirnov analyses revealed that IgG and IgA clonal family frequency distributions were significantly different between carcinomas and normal breast (**Figure 3.16 (B)**). Accordingly, IgG and IgA were clonally expanded within tumours (**Figure 3.17 (A-B)**), and on average IgG<sup>+</sup> B cells belonged to larger clonal families than IgA<sup>+</sup> cells (**Figure 3.16 (C)**). These analyses point to an inherent bias towards the preferential clonal expansion of IgG isotypes within breast cancers. When variable region gene usage was compared, specific V(D)J genes were identified whose combined usage was overrepresented in clonally expanded IgG and IgA sequences in tumours. Specific combinatorial gene usages appeared to expand in TNBC but not ER<sup>+</sup> lesions, and vice versa, suggestive of clonally restricted, likely antigen-focused, immunoglobulin repertoires (**Figure 3.16 (D)**, **Figure 3.17 (C)**). Furthermore, immunoglobulin light chain repertoire transcripts from single CD20<sup>+</sup> CD27<sup>+</sup> B cells from two matched blood and tumour samples (Single cell cohort, **Figure 3.17 (D)**) showed similarities in kappa and

lambda chain V genes (IGKV, IGLV) and J genes (IGKJ, IGLJ), pointing to potential common clonal origins.



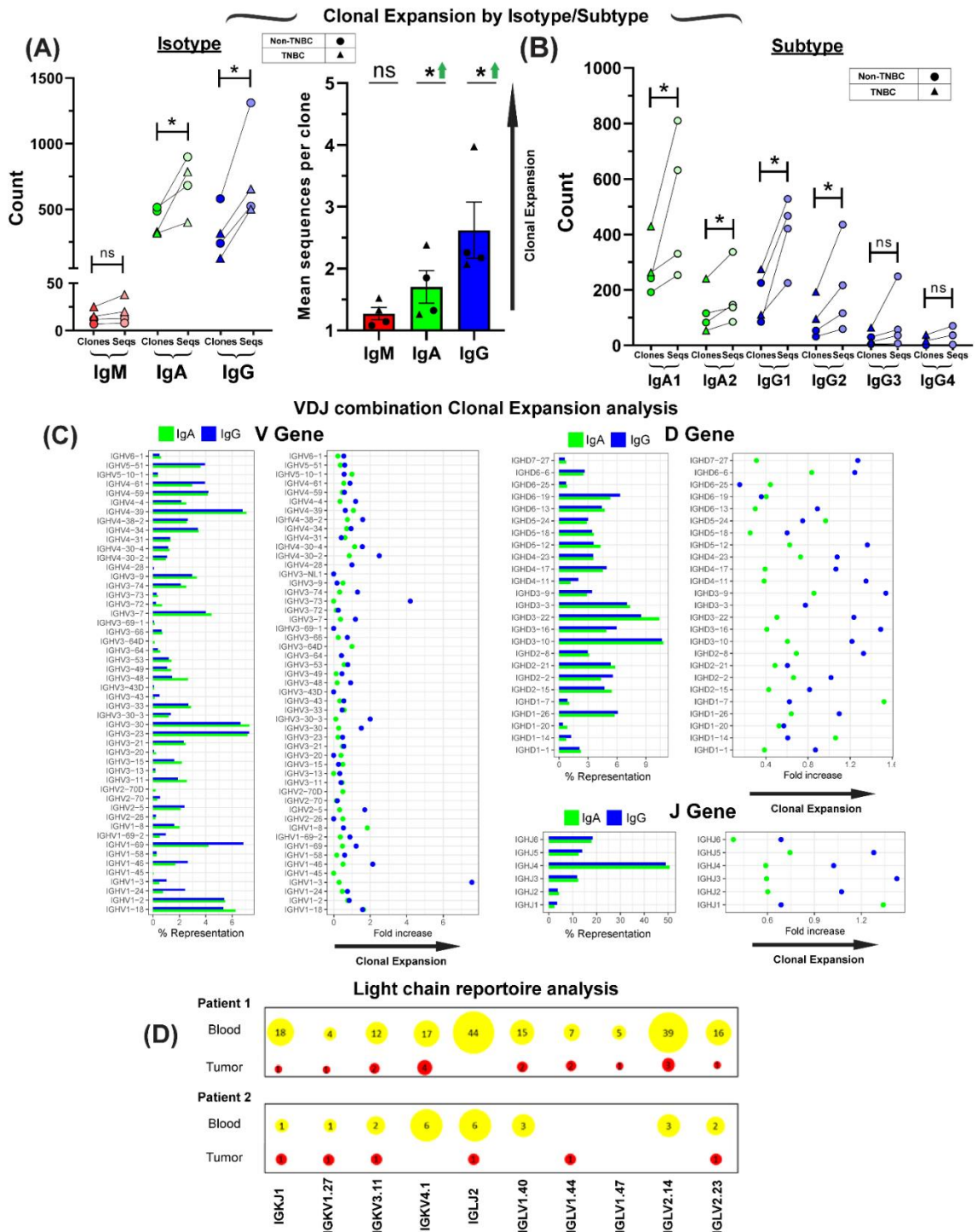
**Figure 3.16 B cell repertoire analyses of immunoglobulin isotype-switching and clonal expansion in breast cancers.**

(A) 7,670 immunoglobulin heavy chain sequences were analysed (KCL sequencing cohort). Top 10 clones determined by B cell repertoire long read data analyses. Clonotypes were estimated via clustering CDR3 sequences. [Top] Bars depict sizes of clones and their breakdown by isotypes.

[Bottom] Isotypes present in each clone are indicated by dots. Vertical lines signify co-occurrence of isotypes in the same clone. **(B)** Clone size frequency distribution of IgM/IgA/IgG sequences in normal breast (1,771 sequences) and breast cancer (5,899 sequences). Kolmogorov-Smirnov analysis highlights significant differences in clone size frequency distributions. **(C)** Mean sequences per clone of IgM/IgA/IgG isotypes. IgG and to a lesser extent, IgA isotypes are clonally expanded, while on average IgG isotypes have significantly larger clone sizes than IgA. **(D)** Comparisons of IgA and IgG variable usage of V-J, D-J and V-D genes extracted from normal breast, ER<sup>+</sup> cancer and TNBC. For each gene usage combination, dot size is proportional to the frequency prior to clonal expansion. Dot colours correspond to fold change in the number of sequences following clonal expansion, indicating the preference of B cells with that specific VDJ combination to be clonally expanded. **(E)** Selection pressure in clonally related IgA and IgG. Clonally related sequences are represented as paired observations (grey lines), and selection pressure is considered separately for the Complementarity-Determining Regions (CDR) and Framework Regions (FWR). Sequences are grouped into normal breast and breast cancer (containing two TNBC and two ER<sup>+</sup> samples). Paired Wilcoxon tests were conducted, and *p*-values were corrected (Benjamini-Hochberg) for multiple comparisons. These experiments were completed in collaboration with Dr. Joseph Ng, KCL.

Furthermore, a stronger positive selection pressure in the CDRs of IgG, compared to their clonally related IgA in tumour samples, was observed, while such a relationship was absent in the FWR, and in BCRs from normal breast. **(Figure 3.16 (E))**. This hints at different aspects of B cell responses where IgA expression may act as an early response, and IgG<sup>+</sup> B cells may confer higher affinity antigen-driven responses.

Large clonal families, isotype-switching within clonally expanded TIL-B, and a bias for IgG subclasses accumulating mutations on specific variable region gene combinations, together suggest a mature humoral immune response driven towards specific antigenic stimuli in breast cancer. Further understanding of these features may reveal therapeutic targets, prognostic biomarkers, and patient subpopulations upon whom to focus therapies enhancing adaptive immune responses.



**Figure 3.17 Immunoglobulin repertoire analysis of breast cancer samples.**

Clonal expansion separated by Ig isotypes and subtypes (KCL sequencing cohort). Total count of Ig sequences for (A) each isotype or (B) subtype per sample. [Right panel in (A)] Mean number of sequences for each Ig subtype per clonal family. A larger number indicates greater clonal expansion. (C) Usage of V, D, and J genes in IgA and IgG sequences. The left panels depict the percentage of sequences utilising each V/D/J gene. The right panels indicate the fold change obtained by comparing the total sequence set with the representative subset. A large fold change

thus indicates greater clonal expansion for sequences carrying that particular V/D/J gene. **(D)** The B cell repertoires in matched blood and tumour samples (Single cell cohort) from each of two patients with breast cancer show similarities in the kappa and lambda chain V genes (IGKV, IGLV) and J genes (IGKJ, IGLJ) between a patient's blood and tumour-associated CD20<sup>+</sup>CD27<sup>+</sup> B cells. Yellow circles represent light chain repertoires in blood; red circles represent the light chain repertoire in tumours. Numbers in circles indicate the raw transcript count of each gene. These experiments were completed in collaboration with Dr. Joseph Ng, KCL.

### **3.5 Discussion and future directions**

Clinical outcomes in cancer patients may be influenced by the initiation of effective anti-tumoural adaptive T cell responses, but these are likely to be significantly more effective when launched in combination with humoral immunity, including induction of isotype-switched B cells and secretion of antibodies. The results contained within this Chapter presented data from flow cytometric, IHC/IF, bulk GEx, scRNA-seq and long-read immunoglobulin sequencing analyses to investigate activated, memory and isotype-switched B cells in breast cancers, including the more-aggressive and more-immunogenic TNBC subtypes.

Consistent with previous reports [283,284], my results highlight how the TIL-B compartment in the tumour stroma is typically organised into clusters of lymphocytes including class-switched memory, GC B cells, and plasma cells. Enhanced isotype-switched B cells, with an IgG-isotype bias may be part of the humoral clonal expansion mechanism, especially pronounced in TIL-B<sup>high</sup> TNBC. The accompanied narrow mature immunoglobulin variable region repertoires and enhanced BCR signaling in TIL-B strongly signify antigen-driven responses. This dynamic humoral immune profile is especially associated with immunogenic TNBC and indicative of more favourable patient outcomes.

I found a depleted memory CD19<sup>+</sup>CD20<sup>+</sup>CD27<sup>+</sup> B cell repertoire in patients' peripheral blood regardless of stage or treatment history for their carcinoma. Moreover, this effect appears to be exacerbated in breast cancer patients who have undergone chemotherapy, possibly owing to the depletion of B cells during treatment, which may irreversibly diminish long-lived memory populations. Accordingly, patients receiving chemotherapy have lower total serum immunoglobulin titres, indicative of a depleted circulating antibody-secreting B cell population. In contrast, flow cytometric analyses revealed an upregulated CD20<sup>+</sup>CD27<sup>+</sup>IgD<sup>-</sup> B cell compartment among TIL-B. In agreement, single-cell transcriptomic analyses point to a bias towards non-switched IgM transcripts in blood memory CD20<sup>+</sup>CD27<sup>+</sup> B cells and higher levels of isotype-switched IgG and IgA CD20<sup>+</sup>CD27<sup>+</sup> B cells in tumour samples. Consistent with an immunogenic signature in TNBCs, higher levels of isotype-switching were seen in single CD20<sup>+</sup> CD27<sup>+</sup> B cell transcripts in TNBC samples compared to non-TNBC tumours. These may be driven by a combination of antigen exposure and inflammation in the breast cancer microenvironment which promotes Ig class-switch recombination.

The TIL-B population is largely assembled in clusters (defined in my investigations as >30 TIL-B and >30 TIL-T aggregated) and positively associates with overall survival. Whilst evident across breast cancer types, transcriptomic analysis suggests that TIL-B infiltration is more pronounced in TNBC compared to non-TNBC. TNBC, especially the IM molecular subtype, featured elevated expression of B cell recruitment and lymphoid cell assembly (*CXCL13*, *CXCR4*, *DC-LAMP*) genes, compared to normal breast. Enhanced local expression of CXCL13 in arthritic synovial fluids can draw circulating B cells to inflammation sites [285], and B cells may traffic from the blood towards lymphoid tissues via CXCR4 stimulation [286]. The evident expression of these signals within the TME may recruit B cells, including B<sup>m</sup>, from the periphery to cancer lesions. Consistent

with this, reduced circulating and enhanced intratumoural CD20<sup>+</sup> CD27<sup>+</sup> B cell compartments were seen in patients. Such chemoattractant signals may also promote local B cell assembly into B-T clusters, in line with my observations of close proximity and strong correlation between tumour-infiltrating B and T lymphocytes. Whilst the B-T clusters I describe are not entirely equivalent to TLSs identified in routine histology [287], within these clusters, B-T lymphocytic crosstalk can lead to B cell activation, immunoglobulin isotype-switching and local clonal expansion [283,288].

Alongside immunohistochemical evidence of spatial B-T association, an active and functional B cell compartment is also indicated by BCR signaling and isotype-switching. Analyses of scRNA-seq data demonstrated that breast TIL-B are phenotypically distinct to those in blood, featuring upregulated BCR complex pathway molecules *FOS* and *JUN*, germinal center chemokine regulator *RGS1*, lymphocyte activation marker *CD69* and TNF $\alpha$  signaling via NF $\kappa$ B. These implicate active BCR engagement by immune complexes. In concordance, Ig repertoire analyses revealed IgG-skewed clonal family expansion with clonally restricted immunoglobulin variable regions. Significantly larger IgG and to a lesser extent IgA, clones with narrow variable region repertoires were found in cancers compared to normal breast, indicative of antigen-focused clonal expansion. Together, these suggest a dynamic expanded IgG-biased humoral response focused towards a small repertoire of antigenic stimuli in the TME, the greater understanding of which has the potential to inform therapeutic and biomarker strategies in patients.

Several studies reported that breast TIL-B carry positive prognostic value [197,270], while others found no significant effect [207], or even poorer survival with CD138<sup>+</sup> plasma cell infiltrates [200]. However, the extent to which B cell phenotype and function may correlate with prognosis has not been addressed. In TNBC patients, positive prognostic associations of memory, but not of naïve or plasma, B cell infiltration was

observed in high-TIL tumours. This may point to positive contributions of memory B cells as part of the humoral response in immunogenic breast cancers and especially in TNBC. In concordance, my findings indicate that genes which positively regulate B cell functions, particularly those involved in activation, proliferation, differentiation and isotype-switching, and especially genes associated with isotype-switching to IgG, may carry positive prognostic value. Further investigations taking into account patient heterogeneity and the influence of gene expression across related pathways may help to extend and confirm these findings.

Furthermore, evidence of a bi-directional functional crosstalk between B and T cells, reveals expression of gene pairs associated with lymphoid assembly, co-stimulation, cytokine-cytokine receptor interactions, cytotoxic T cell activation and T cell-dependent B cell activation. These predicted interactions between B and T cells may have functional relevance in driving B cell stimulation and maturation. Positive associations with prognosis may stem from the observed crosstalk between B and T cells within TLS [289], where antigen presentation and antibody affinity maturation may occur. B cell-mediated T-helper cell activation may contribute to immunotherapy response in TNBC with high mutation burden [290] and local antigen presentation could amplify tumour antigen-specific immune responses [275]. The findings presented in this Chapter also provide support for the involvement of TIL-B in tumour immune surveillance through secretion of cytokines such as  $TNF\alpha$ , which may promote differentiation of Th1 cells and polarize immune effector cells towards classically activated phenotypes [107]. Tumour-associated B cells may therefore receive, trigger and respond to significant T cell-mediated innate and antigenic signals including BCR-immune complex formation and co-stimulation. These may induce Ig class-switch recombination and affinity maturation, especially in TNBC.



My results highlighted an IgG-dominated clonally expanded B cell response in those breast cancers which were highly infiltrated by immune cells, and positive associations between IgG isotype regulator signatures and patient outcome, especially in TNBC. The immunoglobulin isotypes produced in the TME may be critical for containing tumour growth. Antibodies can directly block cancer cell signalling, and if expressed of the IgG isotype, and specifically IgG1, they engender immune-mediated clearance of cancer cells via complement activation and engagement of Fc receptor-expressing monocytes, macrophages and NK cells [291]. In cancer lesions we observed a higher mutation load in the CDRs of IgG compared to their clonally related IgA, absent in the FWR, and in BCRs from normal breast. This stronger positive selection pressure on IgG<sup>+</sup> B cells may represent different aspects of humoral immunity, likely arising from a common B cell precursor, with IgA<sup>+</sup> and IgG<sup>+</sup> B cells driven to generate highly specific but divergent BCRs. My work carries significant implications regarding the effectiveness of anti-tumour B cell responses within highly-infiltrated cancers, where a higher IgG<sup>+</sup>:IgA<sup>+</sup> ratio among the expansive B cell infiltrate could engender potent anti-tumour responses through the increased relative proportion of IgG isotypes, featuring increased capacity to trigger antibody-dependent cellular cytotoxicity by NK cells and antibody-dependent cellular phagocytosis by macrophages. Future therapeutic interventions may facilitate or take advantage of IgG<sup>+</sup> memory and plasma cell infiltrates, and thus influence the balance in favour of immune-activatory immunoglobulin isotypes in tumours.

Collectively, my findings indicate a highly activated B cell compartment is present in breast cancers. Intratumoural B cells are spatially associated with T cells within large stromal clusters, isotype-switch, expand into large clonal families featuring a bias towards IgG subclasses, and carry specific variable region gene combinations with narrow repertoires, all suggesting targeted humoral responses to specific antigenic stimuli.

Clonally restricted IgG expressing B cells may include *in situ* generated germinal centre and activated memory B cells and terminally differentiated plasma cells. Together, these may contribute to humoral immune responses in breast cancer, likely more prominent in TNBC. These expansive and clonally skewed immunoglobulin repertoires, and in particular those switched to IgG isotypes, may be associated with more-favourable patient survival. Although found across breast cancer types, these dynamic B cell traits are highly prominent in TNBC. Despite the poor prognosis and aggressive nature of TNBC in many, this analysis implicates considerable biological and associated prognostic heterogeneity that extends to the TME. Expansive and active B cell breast cancer infiltrates, in a proportion of individuals, provide a degree of anti-tumour activity that may, in combination with other arms of the immune response, confer a survival benefit and may be exploited with immunotherapies to aid in tumour clearance. Elucidating the microenvironmental conditions required to initiate, sustain and enhance these beneficial anti-tumour responses may be key to developing novel treatments.

## **Chapter 4: Phenotype and Functional Significance of Regulatory and Inflammatory B Lymphocytes In Melanoma**

### **4.1 Introduction**

Melanoma is considered to be a highly immunogenic malignancy, capable of activating potent tumour-specific adaptive immune responses [215]. In support, partial or complete regression of lesions, and spontaneous remissions, have been noted among melanoma patients [292,293]. The improvements to clinical outcomes in subsets of patients following checkpoint inhibitor immunotherapy further underscore the immunogenic nature of the disease. Studies into the immune response to melanoma, including the understudied B cell component, could provide opportunities for the identification of immunomodulatory mechanisms which may promote tumour growth, and provide insights for the potential development of novel immunotherapies.

B cells have been historically renowned as positive regulators of immune responses and can do this through several mechanisms. These include differentiation into antibody-secreting plasmablasts and plasma cells and acting as professional antigen presenting cells to contribute to the priming and activation of CD4<sup>+</sup> and CD8<sup>+</sup> T cells, which may promote the clearance of pathogens or malignant cells. In contrast, there is also evidence for the role of B cells in negative regulation of immune responses. Original work published in the 1980s identified roles for B cells in contributing to immune suppression, involving feedback with suppressive T cells, although the presence of a suppressive factor proved elusive [294]. In the early 2000s, based on studies in mouse models, consensus was achieved that B cells can engage in regulating functions to protect from autoimmunity

via the production of IL-10 [295–297], a cytokine with potent anti-inflammatory properties [298].

The role of IL-10 in healthy individuals is to maintain tissue homeostasis and prevent excessive inflammation which could lead to tissue damage, and IL-10 dysregulation may confer increased risk of inflammatory diseases. Within the human setting, IL-10-expressing Bregs have been shown to be dysregulated in patients with multiple sclerosis [126], systemic lupus erythematosus [121], and rheumatoid arthritis [127]. There is preliminary evidence that IL-10-expressing Bregs may be upregulated in patients with solid tumours, such as gastric cancer [243], and observations from mouse models indicate that IL-10<sup>+</sup> Bregs could contribute to tumour progression [116].

Besides IL-10-expressing B cells, additional subsets of regulatory B cells have been identified in humans. A recent study found evidence for naïve PD-L1-expressing B cells which are upregulated in patients with advanced melanoma and which function by curtailing T cell responses *ex vivo* [153]. Another study identified a novel IgG4<sup>+</sup> CD49b<sup>+</sup> CD73<sup>+</sup> B cell subset in the peripheral blood and tumours of melanoma patients, which expressed pro-angiogenic and inflammatory mediators including VEGF, CYR61, ADM, FGF2, PDGFA, and MDK, and promoted endothelial cell tube formation *in vitro* [154]. Outside of melanoma, B cells expressing TGF- $\beta$  have been shown to facilitate the conversion of CD4<sup>+</sup> T-helper cells to Tregs in patients with gastric cancer [243]. Overall, the systemic and intratumoural regulatory B cell landscape in cancer patients is not yet thoroughly explored, likely complex and dynamic, and may differ among tumour types, representing multiple immunomodulatory properties, B cell lineages and phenotypes.

Although the presence of B cells expressing regulatory cytokines and inhibitory ligands is beginning to be established in human cancers, the role of inflammatory B cells

expressing pro-inflammatory mediators, including TNF- $\alpha$ , remains even more poorly understood. A recent study has reported that B cells from melanoma patient peripheral blood express TNF- $\alpha$  and/or IL-6, which were shown to independently associate with reduced responsiveness to CPI immunotherapy [299]. Moreover, the presence of TNF- $\alpha$  transcripts from single B cells extracted from melanoma metastases was also found to be associated with CPI immunotherapy failure [299]. Sustained inflammation is a hallmark of cancer [300], and although TNF- $\alpha$  can induce apoptosis of tumour cells, prolonged exposure may induce survival factors including anti-apoptotic proteins, proangiogenic mediators, and metastatic markers [301], which may explain the association of TNF- $\alpha$ -expressing B cells with reduced response to CPI immunotherapy.

## **4.2 Hypothesis and objectives**

### **4.2.1 Hypothesis**

Overall, there is preliminary evidence for the presence and dynamic role of B cells as cytokine producers in patients with cancer, including their role as important sources of cytokines within the tumour microenvironment. Prior to the work reported in this Thesis, there had been no investigations into the phenotype and function of IL-10-, or TGF- $\beta$ -producing regulatory B cells, and limited investigations into IFN- $\gamma$ -, or TNF- $\alpha$ -expressing inflammatory B cells in human melanoma.

In this Chapter the aim was to investigate cytokine-expressing (IL-10, TGF- $\beta$ , IFN- $\gamma$ , and TNF- $\alpha$ -expressing) B cells, their potential roles in modulating autologous CD4<sup>+</sup> helper T cell phenotype and function (including TNF- $\alpha$ , IFN- $\gamma$  and FOXP3 expression), and their

wider significance within the context of the immune response to melanoma. Cytokine expressing B cells from patients with melanoma were studied using a range of techniques including intracellular cytokine assays, CyTOF phenotyping, scRNA-seq, IHC/IF, bulk gene expression, and *ex vivo* co-culture analyses.

#### 4.2.2 Objectives

The objectives of this Chapter are:

1. To identify perturbations in B cell cytokine expression (focusing upon IL-10<sup>+</sup>, TGF-β<sup>+</sup>, IFN-γ<sup>+</sup>, and TNF-α<sup>+</sup> subsets) among melanoma patient compared to healthy volunteer peripheral blood circulating B cells.
2. To unravel the lineage phenotype of melanoma patient circulating B cells expressing regulatory IL-10 and TGF-β, and pro-inflammatory TNF-α.
3. To characterize cytokine expression among B cells infiltrating the melanoma tumour microenvironment, including identification of B cell lineage phenotypes.
4. To assess the functional crosstalk between melanoma tumour-infiltrating TGF-β<sup>+</sup>/TNF-α<sup>+</sup> B cells with Tcon and Treg cells, including identification of inhibitory checkpoint interactions.
5. To evaluate the potential of B cells derived from melanoma patient peripheral blood to:
  - a) Suppress autologous Th1 (IFN-γ and TNF-α) cytokine expression, with or without the presence of innate pathway stimulation (CpG ODN 2006).
  - b) Modulate the proliferation of autologous T-helper cells, including with conditions of immune checkpoint blockade (nivolumab).

c) Induce a FOXP3<sup>+</sup> Treg phenotype from CD25<sup>-/int</sup> CD127<sup>+</sup> Tcon cells, with or without neutralisation of TGF-β.

6. To assess the association of melanoma patient circulating naïve TGF-β<sup>+</sup> PD-L1<sup>+</sup> B cells with overall survival outcomes.

### **4.3 Patient and healthy volunteer cohort characteristics**

A summary of characteristics for healthy volunteer and melanoma patient samples analysed in this Chapter are summarised in **Table 4.1**.

**Table 4.1 Summary of healthy volunteer (control) and melanoma patient cohorts.**

Variable	Healthy volunteers					
	CyTOF	ICA	CSA	CPA		
<b>n</b>	13	19	7	5		
<b>Age, years (mean +/- SD)</b>	60.7 ± 17.3	50.4 ± 15.5	56.4 ± 14.4	44.8 ± 16.0		
Range	28-88	24-74	38-74	24-70		
<b>Sex (%)</b>						
Male	3 (23.1)	10 (52.6)	4 (57.1)	1 (20.0)		
Female	10 (76.9)	9 (47.4)	3 (42.9)	4 (80.0)		
Variable	Melanoma patients					
	CyTOF	ICA (blood)	ICA (tumour)	CSA	CPA	TIA
<b>n</b>	30	19	16	5	10	12
<b>Age, years (mean +/- SD)</b>	74.4 ± 8.5	55.6 ± 17.1	70.2 ± 16.0	53.2 ± 20.4	61.2 ± 18.5	56.3 ± 11.6
Range	57-88	25-83	35-93	25-76	38-94	33-75
<b>Sex (%)</b>						
Male	16 (53.3)	10 (52.6)	10 (62.5)	2 (40.0)	4 (40.0)	5 (41.7)
Female	14 (46.7)	9 (47.4)	6 (37.5)	3 (60.0)	6 (60.0)	7 (58.3)
<b>Stage (%)</b>						
I	0 (0.0)	0 (0.0)	1 (6.3)	0 (0.0)	0 (0.0)	0 (0.0)
II	2 (6.7)	4 (21.0)	3 (18.7)	0 (0.0)	1 (10.0)	1 (8.3)
III	16 (53.3)	14 (73.7)	11 (68.7)	5 (100.0)	9 (90.0)	10 (83.4)
IV	12 (40.0)	1 (5.3)	1 (6.3)	0 (0.0)	0 (0.0)	1 (8.3)
<b>Substage (%)</b>						
IA	0 (0.0)	0 (0.0)	0 (0.0)	0 (0.0)	0 (0.0)	0 (0.0)
IB	0 (0.0)	0 (0.0)	1 (6.25)	0 (0.0)	0 (0.0)	0 (0.0)
IIA	0 (0.0)	1 (5.3)	0 (0.0)	0 (0.0)	0 (0.0)	0 (0.0)
IIB	1 (3.3)	2 (10.5)	1 (6.25)	0 (0.0)	1 (10.0)	0 (0.0)
IIC	1 (3.3)	1 (5.3)	2 (12.5)	0 (0.0)	0 (0.0)	1 (8.3)
IIIA	2 (6.7)	8 (42.1)	2 (12.5)	3 (60.0)	7 (70.0)	3 (25.0)
IIIB	3 (10.0)	1 (5.3)	5 (31.25)	0 (0.0)	0 (0.0)	4 (33.3)
IIIC	10 (33.3)	5 (26.3)	4 (25.0)	2 (40.0)	2 (20.0)	3 (25.0)
IIID	1 (3.3)	0 (0.0)	0 (0.0)	0 (0.0)	0 (0.0)	0 (0.0)
IV	12 (40.0)	1 (5.3)	1 (6.25)	0 (0.0)	0 (0.0)	1 (8.3)

ICA = Intracellular cytokine assay, CSA = Cytokine suppression assay, CPA = Cellular proliferation assay, TIA = Treg induction assay

## **4.4 Results**

### **4.4.1 Enrichment in TGF- $\beta$ -expressing naïve B cells and IL-10-expressing plasmablasts contrasts with diminished IFN- $\gamma$ and TNF- $\alpha$ <sup>+</sup> inflammatory B cells in melanoma patient peripheral blood**

I first performed CyTOF phenotyping of healthy volunteer and melanoma patient peripheral blood B cells. I employed the FlowSOM algorithm to generate twenty B cell meta-clusters based upon the expression of a panel of 19 markers within the CyTOF cohort (**Figure 4.1 (A)**). Subsequent analysis of these B cell meta-clusters identified enrichment in regulatory B cell populations. Specifically, the analysis showed enrichment in the percentages of IL-10-expressing CD19<sup>-</sup> CD38<sup>hi</sup> IgD<sup>-</sup> CD27<sup>+</sup> Ki67<sup>+</sup> plasmablasts (cluster 19), and TGF- $\beta$ -expressing CD19<sup>+</sup> CD38<sup>int</sup> IgD<sup>+</sup> CD27<sup>-</sup> PD-L1<sup>+</sup> naïve Bregs (cluster 12) in melanoma patient (N = 30) compared to age and sex matched healthy volunteer (N = 13) peripheral blood (**Figure 4.1 (B)**). A subset of three patients showing elevated proportions of IL-10-expressing plasmablasts (>6% of total B cells) were identified as males with stage IV disease. No clear features were observed for patients with highly polarised TGF- $\beta$ -expressing naïve Bregs (>6% of total B cells). Further investigations with larger cohorts are required to determine whether disease stage may correlate with dysregulation among circulating Breg populations.

I then applied dimensionality reduction using the UMAP algorithm to melanoma patient CyTOF phenotyping data, which highlighted wide IL-10 and narrow TGF- $\beta$  expression among circulating B cells, demonstrating differential distributions of each cytokine in the B cell compartment (**Figure 4.1 (C)**).

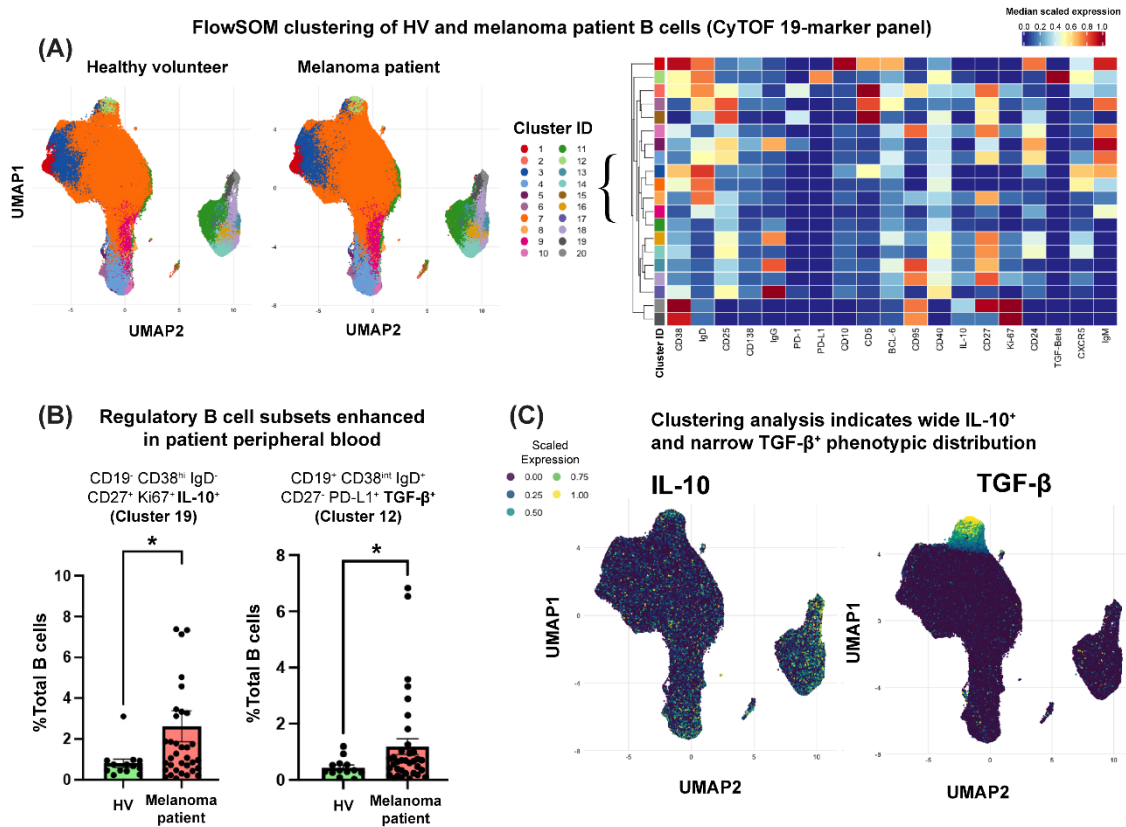


To explore the expression of several cytokines in the whole B cell compartment in the blood, an intracellular cytokine assay was developed, and multiple methods of B cell activation were tested for the induction and intracellular detection of IL-10<sup>+</sup>, IL-4<sup>+</sup>, IFN- $\gamma$  and TNF- $\alpha$ <sup>+</sup> B cells (gating strategy for identifying total CD19<sup>+</sup> B cells is shown in **Figure 4.2**; data for cytokine expression are presented in **Figure 4.3 (A-F)**). TGF- $\beta$ -expressing B cells were detected in human blood samples without *ex vivo* cellular activation.

The proportions of circulating IL-10<sup>+</sup>, IL-4<sup>+</sup>, IFN- $\gamma$ , TNF- $\alpha$ <sup>+</sup>, and TGF- $\beta$ <sup>+</sup> B cells out of the total CD19<sup>+</sup> B cell population were compared between a cohort of patients with melanoma and age and sex-matched healthy volunteers (human volunteer characteristics are detailed in **Table 4.1**) (**Figure 4.3 (A-F)**). No significant differences were found in the total percentages of circulating IL-10-expressing Bregs, or IL-4<sup>+</sup> B cells out of total CD19<sup>+</sup> B cells, between melanoma patients and matched healthy volunteers (**Figure 4.3 (A-B)**). Although only small proportions of B cells express IFN- $\gamma$  in response to activation, I observed significantly decreased percentages in circulating IFN- $\gamma$ <sup>+</sup> inflammatory B cells in melanoma patients compared to matched healthy volunteers, using innate pathway stimulation (0.1 $\mu$ g/ml CpG ODN 2006) (**Figure 4.3 (C)**). A substantial proportion of patient and HV circulating B cells responded to innate pathway activation with strongly polarised expression of TNF- $\alpha$ , however, I observed a collapse in the total percentage of circulating TNF- $\alpha$ -expressing B cells in melanoma patients compared to matched healthy volunteers (**Figure 4.3 (D)**), which was evident across all modes of B cell activation. Furthermore, I found no significant difference in the total percentages of circulating TGF- $\beta$ -expressing Bregs out of total CD19<sup>+</sup> B cells, between melanoma patients and healthy volunteers, although I noted a trend towards a higher proportion of TGF- $\beta$ -expressing B cells in the patients (seven samples) compared to the

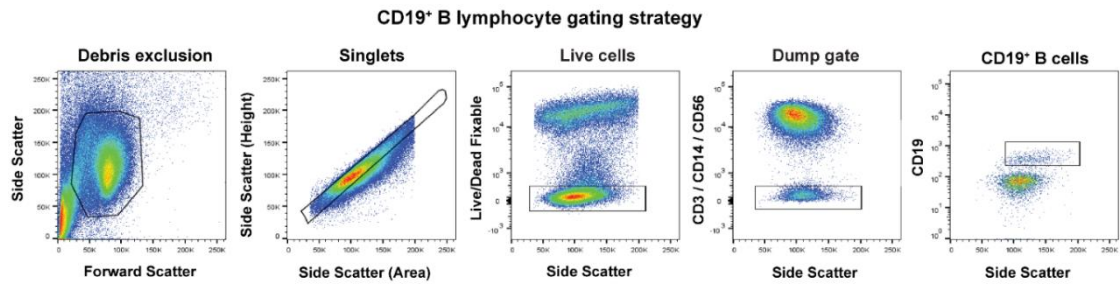
healthy volunteers (three samples) I examined (**Figure 4.3 (E)**). Interestingly, the ratio of IFN- $\gamma^+$ :IL-4 $^+$  B cells, a pro-inflammatory measure which can represent the balance between Th1 (IFN- $\gamma^+$ ) and Th2 (IL-4 $^+$ ) phenotypes, was significantly decreased in melanoma patients compared to a matched healthy volunteer cohort (**Figure 4.3 (F)**).

Collectively, these data suggest a level of dysregulation among melanoma patient circulating B cells, through an expansion in subpopulations of IL-10 $^+$  and TGF- $\beta^+$  Bregs, and a reduced IFN- $\gamma^+$  and TNF- $\alpha^+$  pro-inflammatory B cell compartment in the total B cell population in the blood of patients with melanoma.



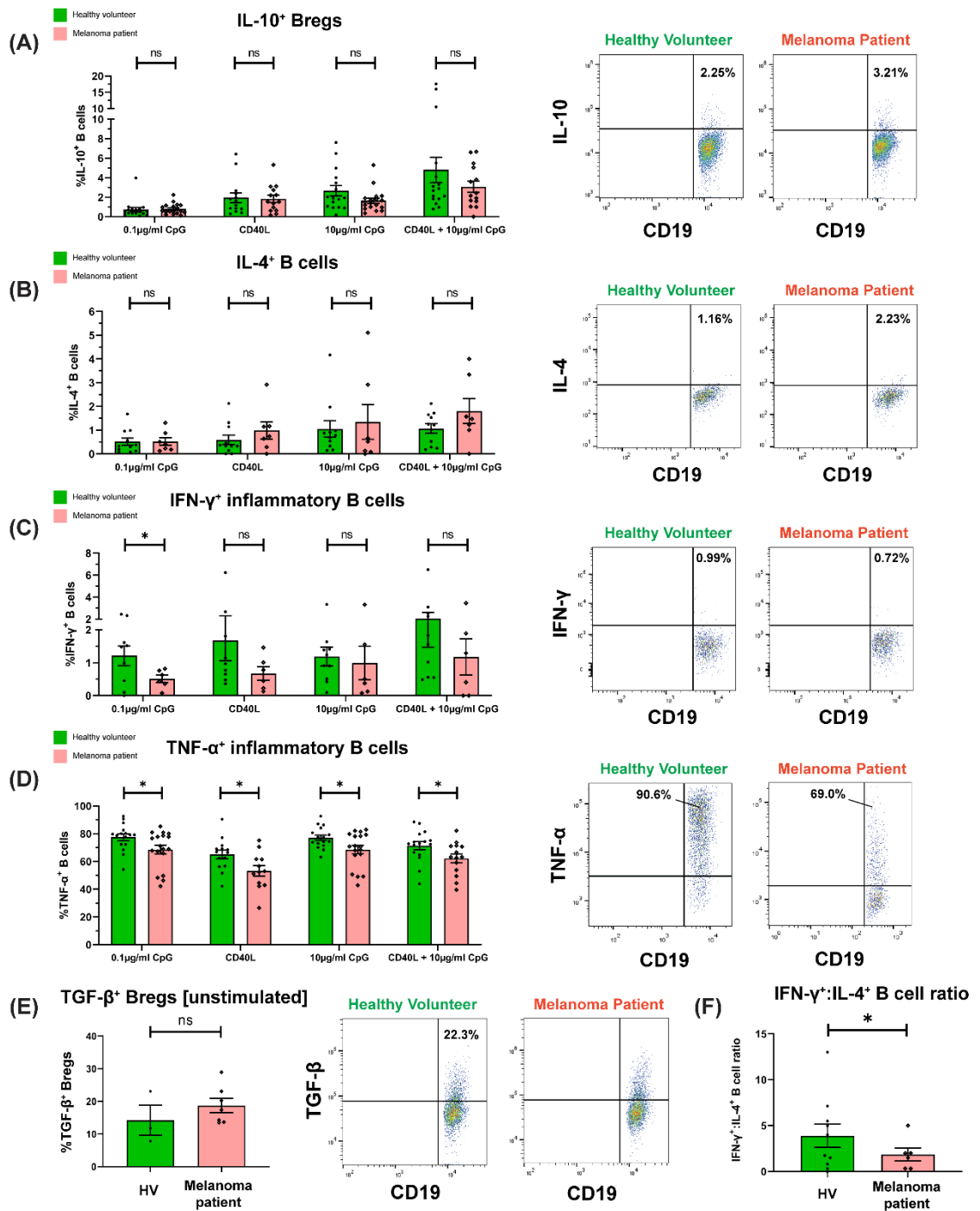
**Figure 4.1 TGF-β-expressing naïve B cells and IL-10-expressing plasmablasts are enriched in melanoma patient peripheral blood compared to healthy volunteer peripheral blood.**

(A) The FlowSOM algorithm was used to generate twenty meta-clusters from HV and melanoma patient pooled B cells based upon the expression of a panel of 19 markers within the CyTOF cohort (left). Heatmaps illustrate marker expression within each cluster (blue = low; red = high) (right). (B) CyTOF phenotyping of B cell subsets identified enrichment in regulatory B cell populations of [Left] CD19<sup>+</sup> CD38<sup>hi</sup> IgD<sup>-</sup> CD27<sup>+</sup> Ki67<sup>-</sup> IL-10<sup>+</sup> plasmablasts (cluster 19) and [Right] CD19<sup>+</sup> CD38<sup>int</sup> IgD<sup>+</sup> CD27<sup>-</sup> PD-L1<sup>+</sup> TGF-β<sup>+</sup> naïve B cells (cluster 12) in melanoma patient (N = 30) compared to matched healthy volunteer (N = 13) peripheral blood samples. (C) UMAP clustering analysis demonstrates scattered IL-10<sup>+</sup> expressing populations across B cell subsets and narrow TGF-β<sup>+</sup> phenotypic population distribution. Cells clustered according to extracellular marker expression (CyTOF 19-marker panel) and coloured from purple (0.00) to yellow (1.00) corresponding to scaled expression of each cytokine. These analyses were completed in collaboration with Dr. Zena Willmore, KCL.



**Figure 4.2** Flow cytometric gating strategy for the identification of CD19<sup>+</sup> B cells from peripheral blood mononuclear cells following ex vivo culture.

Quantification of circulating IL-10<sup>+</sup>, IL-4<sup>+</sup>, IFN- $\gamma$ <sup>+</sup>, TNF- $\alpha$ <sup>+</sup>, and TGF- $\beta$ <sup>+</sup> B cells in HVs and melanoma patients



**Figure 4.3** Flow cytometric evaluations of IL-10, IL-4, IFN- $\gamma$ , TNF- $\alpha$ , and TGF- $\beta$  expressing B cells in melanoma patient and compared to healthy volunteer peripheral blood.

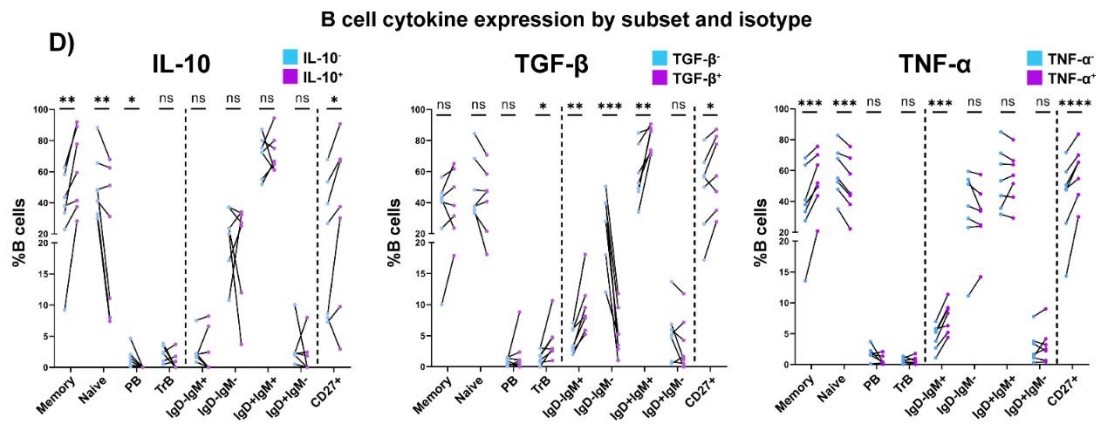
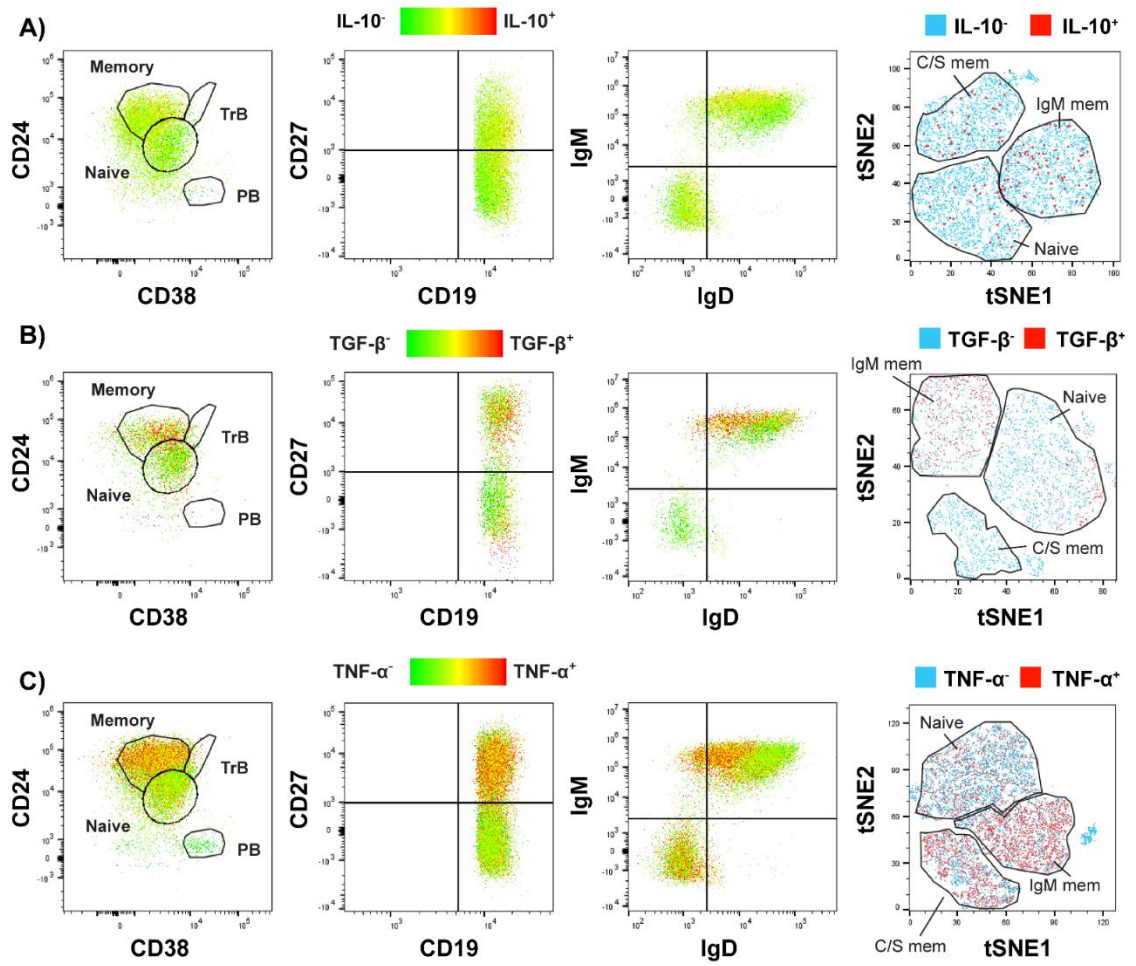
Healthy volunteer and melanoma patient peripheral blood mononuclear cells were incubated for 72 hours, with a cytokine stimulation cocktail added for the final 6 hours. For each part (A-E): [Left] Comparison of total % of cytokine-expressing B cells in a cohort of melanoma patients and matched healthy volunteers in presence (IL-10<sup>+</sup>, IL-4<sup>+</sup>, IFN- $\gamma$ <sup>+</sup>, TNF- $\alpha$ <sup>+</sup> B cells) or absence (TGF- $\beta$ <sup>+</sup> B cells) of B cell activation stimuli (0.1 μg/ml CpG, CD40L, 10 μg/ml CpG, or CD40L + 10 μg/ml CpG). [Right] Flow cytometry plots show gating of CD19<sup>+</sup> B cells by cytokine expression from a representative healthy volunteer and melanoma patient. Condition depicted

represents optimal condition for induction (CD40L + 10 $\mu$ g/ml CpG for IL-10, IL-4 and IFN- $\gamma$ , 0.1 $\mu$ g/ml CpG for TNF- $\alpha$ ,) or unstimulated condition (TGF- $\beta$ ). N numbers (healthy volunteers / melanoma patients) are as follows: IL-10 (N = 17 / 18), IL-4 (N = 12 / 7), IFN- $\gamma$  (N = 10 / 6), TNF- $\alpha$  (N = 18 / 17), and TGF- $\beta$  (N = 3 / 7). TNF- $\alpha$ <sup>+</sup> inflammatory B cells are decreased in melanoma patient compared to healthy volunteer peripheral blood across all activation conditions, while no significant differences were observed for IL-10, TGF- $\beta$ , IL-4, IFN- $\gamma$ -expressing B cells. **(F)** Ratio of IFN- $\gamma$ <sup>+</sup>:IL-4<sup>+</sup> B cells in a cohort of melanoma patients (N = 6) and matched healthy volunteers (N = 10) following B cell activation by innate stimuli (0.1 $\mu$ g/ml CpG).

#### 4.4.2 Cytokine expression among the whole melanoma patient circulating B cell compartment is preferentially associated with CD27<sup>+</sup> memory subsets

I next sought to identify the phenotype of melanoma patient circulating regulatory IL-10 and TGF- $\beta$ , and pro-inflammatory TNF- $\alpha$  expressing B cells in the total CD19<sup>+</sup> B cell compartment. Expression of all three cytokines was found to be associated with CD27 expression (**Figure 4.4 (A-D)**), a key marker of the memory B cell lineage [302]. In support, both IL-10<sup>+</sup> and TNF- $\alpha$ <sup>+</sup> B cells were significantly enriched in a separately defined CD24<sup>hi</sup> CD38<sup>-</sup> memory phenotype [248], compared to IL-10<sup>-</sup> and TNF- $\alpha$ <sup>-</sup> B cells. Neither IL-10 nor TNF- $\alpha$ -expressing B cells were found to be associated with enrichment in IgD or IgM expression, and tSNE dimensionality reduction analysis, alongside flowSOM clustering of B cells according to CD27, IgD, IgM, CD24 and CD38 expression (**Figure 4.5**), highlighted their presence within both class-switched memory and IgM memory lineage subsets. Consistent with CyTOF phenotyping (**Figure 4.1 (B)**), TGF- $\beta$ <sup>+</sup> Bregs showed a narrow phenotypic distribution, typically co-expressing IgD, IgM and CD27, suggesting a non-class-switched memory lineage, although naïve TGF- $\beta$ <sup>+</sup> Bregs were also observed.

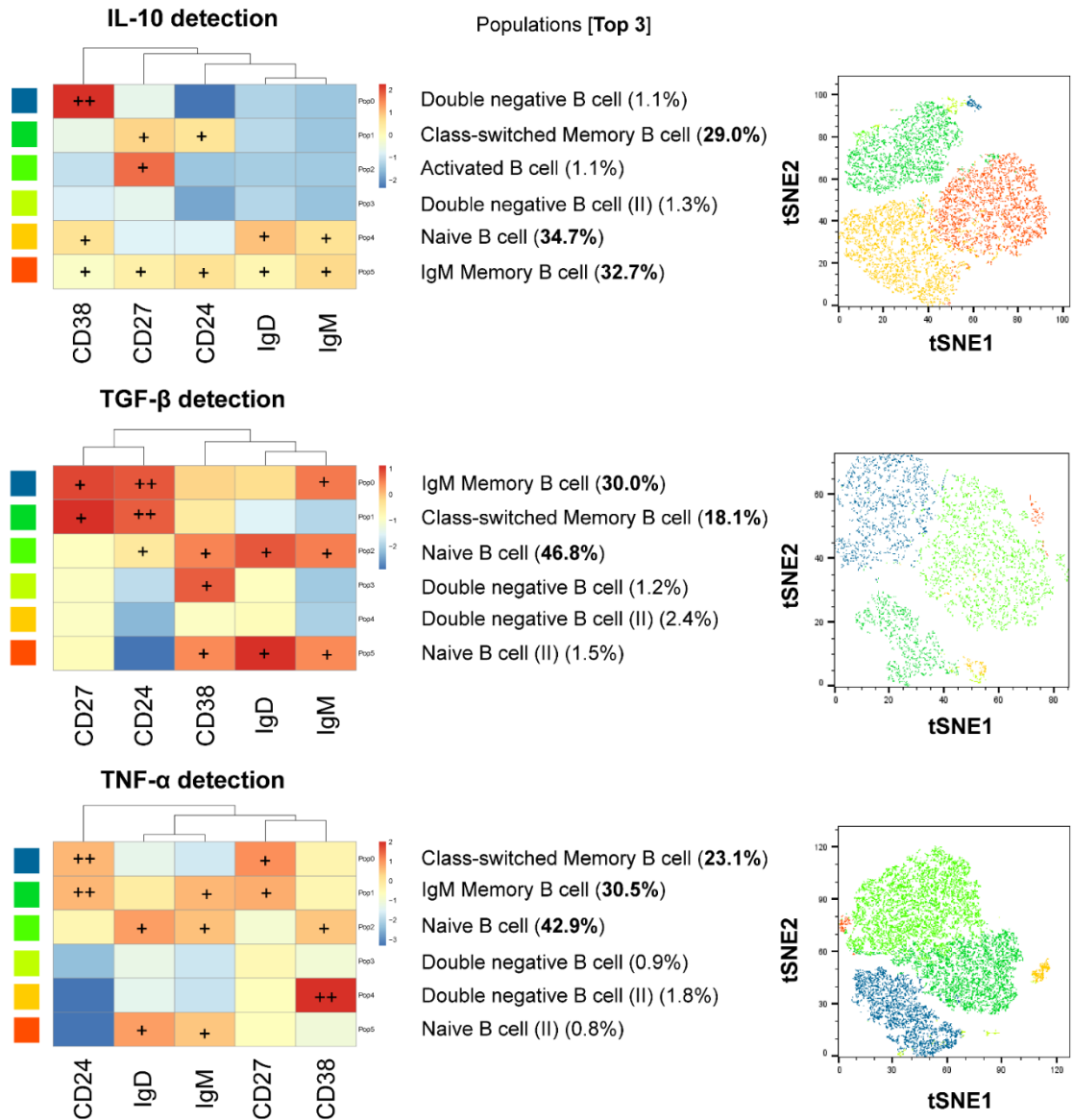
These findings reveal that melanoma patient circulating CD27<sup>+</sup> memory B cells may express both regulatory and pro-inflammatory cytokines, and TGF- $\beta$  is associated with non-class-switched memory B cells.



**Figure 4.4 Lineage analysis of B cells expressing each of IL-10, TGF- $\beta$  and TNF- $\alpha$  cytokines show wide phenotypic distribution, with preference towards a CD27<sup>+</sup> memory phenotype and with TGF- $\beta$ <sup>+</sup> cells routinely non-isotype-switched.**

Live single CD19<sup>+</sup> B cells from melanoma patient blood were gated prior to IL-10<sup>+</sup>, TGF- $\beta$ <sup>+</sup> and TNF- $\alpha$ <sup>+</sup> B cell lineage analyses. [Left] Flow cytometry plots highlighting identification of: CD24<sup>hi</sup> CD38<sup>+</sup> memory B cells, CD24<sup>hi</sup> CD38<sup>hi</sup> transitional B cells (TrB), CD24<sup>int</sup> CD38<sup>int</sup> naïve B cells and CD24<sup>+</sup> CD38<sup>++</sup> plasmablasts (PB), CD27 expression, and B cell immunoglobulin isotype distribution in peripheral blood of a representative patient. Cells are coloured according to IL-10 (A), TGF- $\beta$  (B) and TNF- $\alpha$  (C) cytokine expression (green = low; red = high). [Right] tSNE projections cluster B cells according to CD27, IgD, IgM, CD24 and CD38 expression. The top three largest populations by flowSOM clustering are naïve, IgM memory and isotype-switched (C/S) memory B cells. Cells are coloured according to IL-10 (A), TGF- $\beta$  (B) and TNF- $\alpha$  (C) cytokine expression (blue = negative; red = positive). (D) Lineage analysis of B cells by IL-10 [left], TGF- $\beta$  [middle] and TNF- $\alpha$  [right] cytokine expression (N = 7). Percentage of cytokine-expressing B cells showing particular B cell lineage phenotypes are compared to baseline phenotype (shown by cytokine<sup>-</sup> cells) to identify phenotypic preference. IL-10, TGF- $\beta$  and TNF- $\alpha$ -expressing B cell subsets were more likely to express the memory B cell marker CD27 significantly above the baseline phenotype. TGF- $\beta$ -expressing B cells additionally were more likely to be associated with IgD and IgM expression significantly above baseline, denoting that TGF- $\beta$  is associated with memory B cells of a non-isotype-switched phenotype.





**Figure 4.5 Dimensionality reduction using the tSNE and FlowSOM Algorithms for lineage analysis of B cells expressing each of IL-10, TGF-β and TNF-α.**

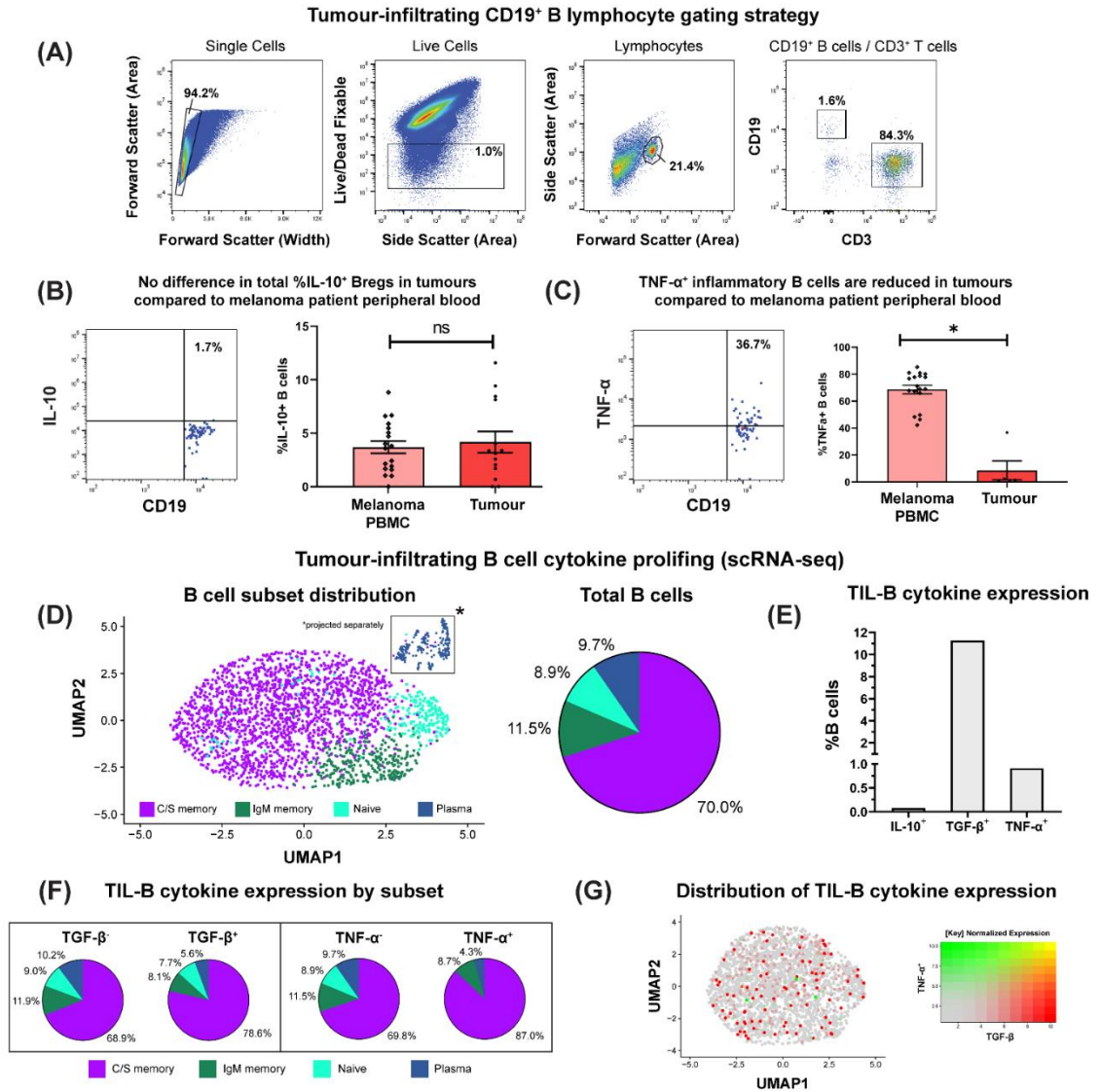
Melanoma patient peripheral blood mononuclear cell suspensions were incubated for 72 hours, with a cytokine stimulation cocktail added for the final 6 hours. B cells were activated with CD40L + 10μg/ml CpG (ODN 2006) for the detection of IL-10<sup>+</sup> Bregs and 0.1μg/ml CpG for the detection of TNF-α<sup>+</sup> inflammatory B cells. TGF-β was detected in B cells in the absence of ex vivo activation. Live single CD19<sup>+</sup> B cells were gated and used for dimensionality reduction. [Left] The FlowSOM algorithm was used to generate six meta-clusters per sample based upon the expression of CD27, IgD, IgM, CD24 and CD38. Heatmaps illustrate marker expression within each cluster (blue = low; red = high). Each cluster is annotated according to the B cell lineage phenotype and the largest three lineage populations are highlighted in bold. [Right] tSNE projections mapping B cells according to the five marker-panel. FlowSOM clusters are indicated by colour-coding. Plus (+) symbols indicate degree of expression, where “+” = low or intermediate and “++” = high expression.

#### 4.4.3 TGF- $\beta$ -expressing Bregs infiltrate melanoma patient tumours, while TNF- $\alpha$ -expressing B cells are proportionally lower in the tumour-infiltrating B lymphocyte populations compared to the circulation

I next sought to investigate the cytokine expression profiles of melanoma TIL-B, and I therefore evaluated melanoma tumour specimens by flow cytometric analyses, single cell RNA-seq analyses of publicly available datasets and immunohistochemistry. Firstly, I performed intracellular cytokine phenotyping of TIL-B within single cell suspensions obtained from melanoma tumours. While no significant difference was observed in the percentage of IL-10-expressing Bregs, the percentage of TNF- $\alpha$ -expressing (CD19<sup>+</sup>) B cells were significantly reduced in melanoma tumours compared to B cells in the patient circulation (**Figure 4.6 (A-C)**).

Single cell RNA-seq analysis of pooled TIL-B from 9 melanoma lesion samples was performed from a publicly available dataset (GSE123139) [262]. Analysis of B cells in these tumours identified 2529 B cells and showed that a proportion of tumour infiltrating B cells (11.3%) were TGF- $\beta$ <sup>+</sup> Bregs, while populations of IL-10<sup>+</sup> (0.1%) and TNF- $\alpha$ <sup>+</sup> (0.9%) TIL-B were less frequently detected (**Figure 4.6 (D-E)**). Immunohistochemistry using fluorescently labelled antibodies supported the limited presence of TNF- $\alpha$ <sup>+</sup> CD20<sup>+</sup> TIL-B, although IL-10<sup>+</sup> CD20<sup>+</sup> Bregs were identified (**Figure 4.7**).

Both tumour-infiltrating TGF- $\beta$ <sup>+</sup> (78.6%) and TNF- $\alpha$ <sup>+</sup> (87.0%) B cells were predominantly of the class-switched memory phenotype (**Figure 4.6 (F)**), supporting the notion that memory B cells may be a key source of cytokine expression in melanoma patients (as observed in blood, see **Figures 4.4-4.5**). Minimal TGF- $\beta$  and TNF- $\alpha$  co-expression was observed among TIL-B (**Figure 4.6 (G)**).

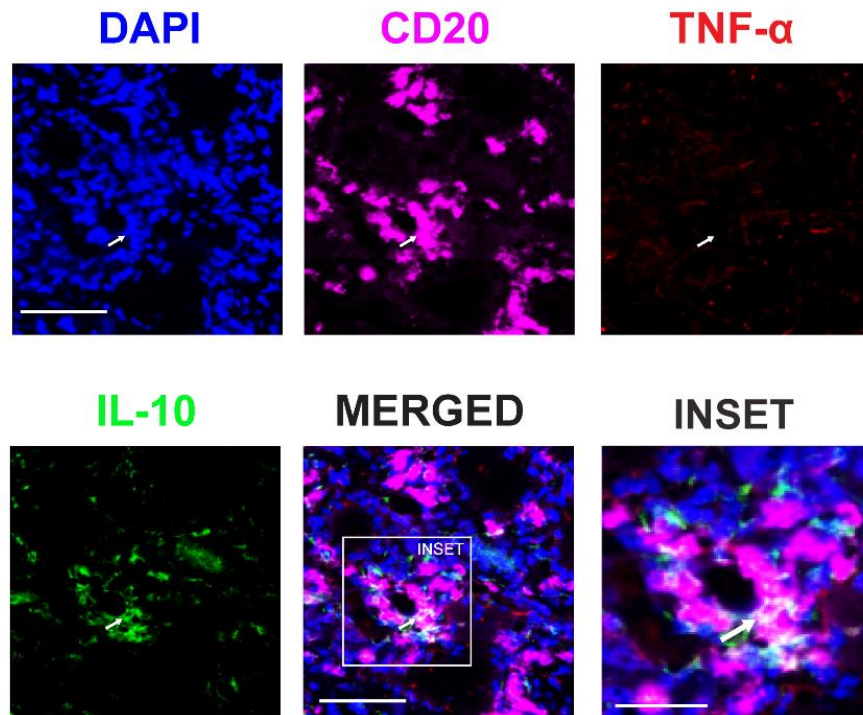


**Figure 4.6** TNF- $\alpha$ -expressing inflammatory B cell subsets are collapsed, while TGF- $\beta$ -expressing subsets are favored in melanoma lesions.

**(A)** Flow cytometry gating strategy for the identification of CD19<sup>+</sup> B cells from melanoma lesion single cell suspensions. **(B)** [Left] Flow cytometry plots show gating of CD19<sup>+</sup> IL-10<sup>+</sup> B cells from a representative tumour single cell suspension. [Right] No significant difference in the % of total IL-10<sup>+</sup> Bregs is observed between melanoma patient peripheral blood (N = 18) and tumour tissue (N = 14). **(C)** [Left] Flow cytometry plots show gating of CD19<sup>+</sup> TNF- $\alpha$ <sup>+</sup> B cells from a representative tumour single cell suspension. [Right] The proportion of TNF- $\alpha$ <sup>+</sup> inflammatory B cells out of total B cells is significantly lower in tumour lesions (N = 5) compared to melanoma patient peripheral blood (N = 18). **(D)** [Left] UMAP visualization defined by global GEx of single melanoma TIL-B pooled from N = 9 patients (2529 cells), highlighting distribution of major B cell subsets (C/S memory, IgM memory, naïve and plasma cells). [Right] Pie chart illustrates the proportions of major B cell subsets among melanoma TIL-B. **(E)** Proportions of melanoma TIL-B expressing IL-10, TGF- $\beta$  and TNF- $\alpha$ . **(F)** Lineage analysis of melanoma TIL-B by cytokine expression. Pie charts compare lineage phenotypes of B cells expressing each of TGF- $\beta$  [left panel], and TNF- $\alpha$  [right panels], to baseline phenotype (denoted as cytokine<sup>-</sup> cells) to identify phenotypic preference. TGF- $\beta$  and TNF- $\alpha$ -expressing TIL-B show a preference towards class-switched memory phenotype. **(G)** UMAP visualization of melanoma TIL-B, coloured by relative

normalised gene expression levels for TGF- $\beta$  and TNF- $\alpha$ . Analyses (D-G) were completed in collaboration with Mr. Roman Laddach, KCL.

### Limited presence of TNF- $\alpha$ <sup>+</sup> inflammatory B cells in tumours

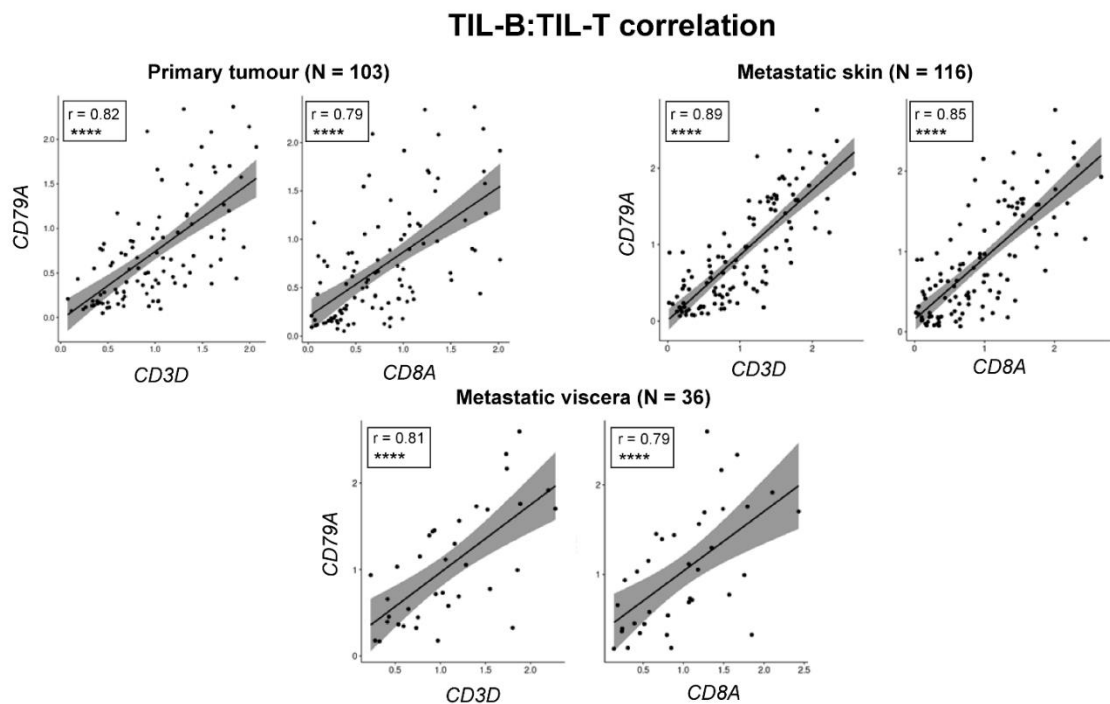


**Figure 4.7 Immunofluorescence studies of melanoma lesions revealed limited presence of TNF- $\alpha$ -expressing, but detectable IL-10-expressing B cells within the metastatic melanoma tumour microenvironment.**

Example immunofluorescence images demonstrate presence of CD20<sup>+</sup> IL-10<sup>+</sup> Bregs (white arrows) within a melanoma tumour section, while no CD20<sup>+</sup> TNF- $\alpha$ <sup>+</sup> cells were observed. DAPI; blue, CD20; purple, TNF- $\alpha$ <sup>+</sup>; red, IL-10; green. Scale bar = 100 $\mu$ m (panel images) and 50 $\mu$ m (inset image).

#### 4.4.4 Evidence for associations and crosstalk between B cells and Bregs with T cells in the tumour microenvironment

I next wished to understand whether B cells, including Breg populations, may engage with functional crosstalk with the cellular arm of adaptive immune response in melanomas. Firstly, I analysed bulk RNAseq gene expression data (TCGA cohort) for melanoma samples across primary, metastatic skin, and visceral metastases, and conducted a Spearman's rank correlation test to calculate correlation coefficients ( $r$ ) and p-values. TIL-B ( $CD79A$ ) gene expression was found to positively correlate with tumour-infiltrating T lymphocytes ( $CD3$ ), and cytotoxic T lymphocyte ( $CD8A^+$ ) gene expression (**Figure 4.8**), in both primary, skin and visceral metastases. This suggested that B and T cells may communicate, and I then specifically wished to evaluate the interaction of cytokine expressing B cells with T cells, including with conventional (Tcon) and regulatory (Treg) populations.

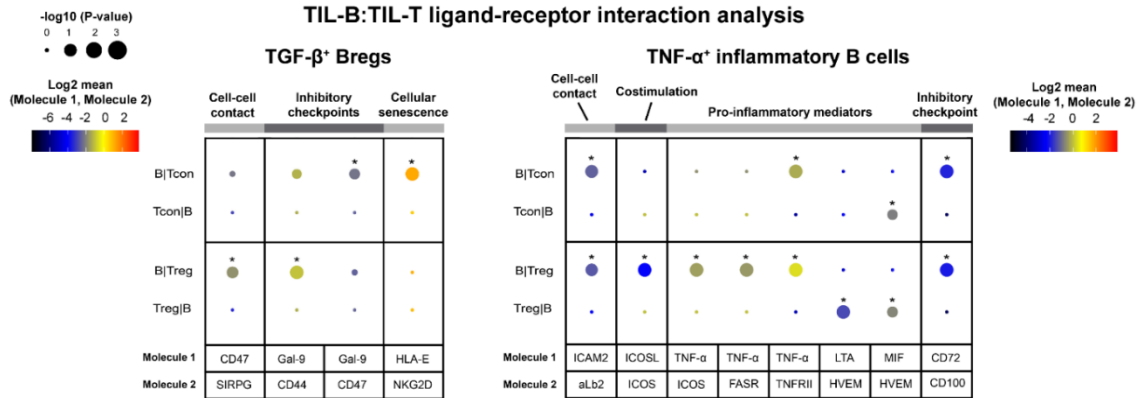


**Figure 4.8 Correlation of B and T cell densities in the tumour microenvironment in melanoma.**

Tumour-infiltrating B lymphocytes (CD79A<sup>+</sup>) positively correlate with tumour-infiltrating T lymphocytes (CD3D<sup>+</sup>), and cytotoxic T lymphocytes (CD8A<sup>+</sup>), analysed by bulk RNAseq gene expression (TCGA cohort) across cancer settings (primary, metastatic skin, and metastatic viscera). Spearman's rank correlation test was used to calculate correlation coefficients (r) and p-values (\*\*\*\* = P < 0.0001). These analyses were completed in collaboration with Mr. Roman Laddach, KCL.

Using CellPhoneDB from the single cell RNA-seq dataset [262], in which TIL-B populations from 9 melanoma lesion samples were identified, I searched for evidence of potential crosstalk between B and T cells in the tumour microenvironment. Distinct predicted B cell:T cell communication pathways were identified for tumour-infiltrating B lymphocytes stratified by their cytokine expression [261]. While cell-cell contact, and inhibitory checkpoint interactions with conventional T cells and Treg cells were predicted for both TGF- $\beta$ <sup>+</sup> and TNF- $\alpha$ <sup>+</sup> B cells, the underlying ligand-receptor pairs differed (**Figure 4.9**).

Cell-cell contact was supported by CD47:SIRP- $\gamma$  for TGF- $\beta$ <sup>+</sup> B cells with Tregs [303], and ICAM2:aLb2 for TNF- $\alpha$ <sup>+</sup> B cells engaged with Tcon and Treg populations [304]. In addition, TGF- $\beta$ <sup>+</sup> B cells expressed the immune checkpoint receptor Galectin-9 [305], which was predicted to bind CD44 on Tregs, and CD47 on Tcon cells. Importantly, the interaction of Galectin-9 and CD44 has been previously shown to promote FOXP3 expression and enhance the function and stability induced Tregs (iTregs) in mouse models, alongside complex formation with TGF- $\beta$  receptor I [306]. TGF- $\beta$ <sup>+</sup> B cells also expressed HLA-E, a non-classical HLA molecule which is upregulated in senescent cells [307,308], and my analysis indicated predicted interaction of HLA-E with NKG2D, expressed by Tcon cells. NKG2D is highly expressed on CD8<sup>+</sup> T cells, and interaction of NKG2D with its ligands is implicated in the surveillance and elimination of senescent cells [307,309].



**Figure 4.9 CellPhoneDB analysis of TGF-β<sup>+</sup> [left] and TNF-α<sup>+</sup> [right] B cell:T cell predicted communication pathways in the tumour microenvironment.**

T cells were divided into conventional (Tcon) and regulatory (Treg) subsets. After false discovery rate (FDR<0.001) correction, predicted interactions for both B cell subsets include cell-cell contact and inhibitory checkpoints, while TNF-α<sup>+</sup> B cells may also engage in co-stimulation and TNF-α signaling via ICOS, FasR and TNFR2. Circle sizes indicate p-value and colour-coding represents the average expression level of interacting molecule 1 in cluster 1 and interacting molecule 2 in cluster 2. These analyses were completed in collaboration with Mr. Roman Laddach, KCL.

As expected, TNF-α<sup>+</sup> B cells were predicted to engage in signaling with T cells via pro-inflammatory mediators, including TNF-α, lymphotoxin-α (LT-α), and macrophage migration inhibitory factor (MIF). My analysis indicated that TNF-α expressed by B cells may interact with TNFR2 of both Treg and Tcon cells, and TNF-α could also signal via FasR and ICOS expressed by Tregs. In addition, TNF-α<sup>+</sup> B cells expressed the costimulatory ICOS ligand, which was predicted to interact with its receptor ICOS expressed by Tregs, and in this context may promote the generation, proliferation, survival and suppressive ability of Tregs [310,311]. Lastly, TNF-α<sup>+</sup> B cells expressed CD72, a negative checkpoint regulator of B cell responsiveness [312,313], which was predicted to interact with CD100 expressed by both Tcon and Treg cells (**Figure 4.9**).

Collectively, these observations highlight multiple immunoregulatory interactions between tumour-infiltrating TGF-β<sup>+</sup> and TNF-α<sup>+</sup> B cells, with T cells in the TME. TGF-

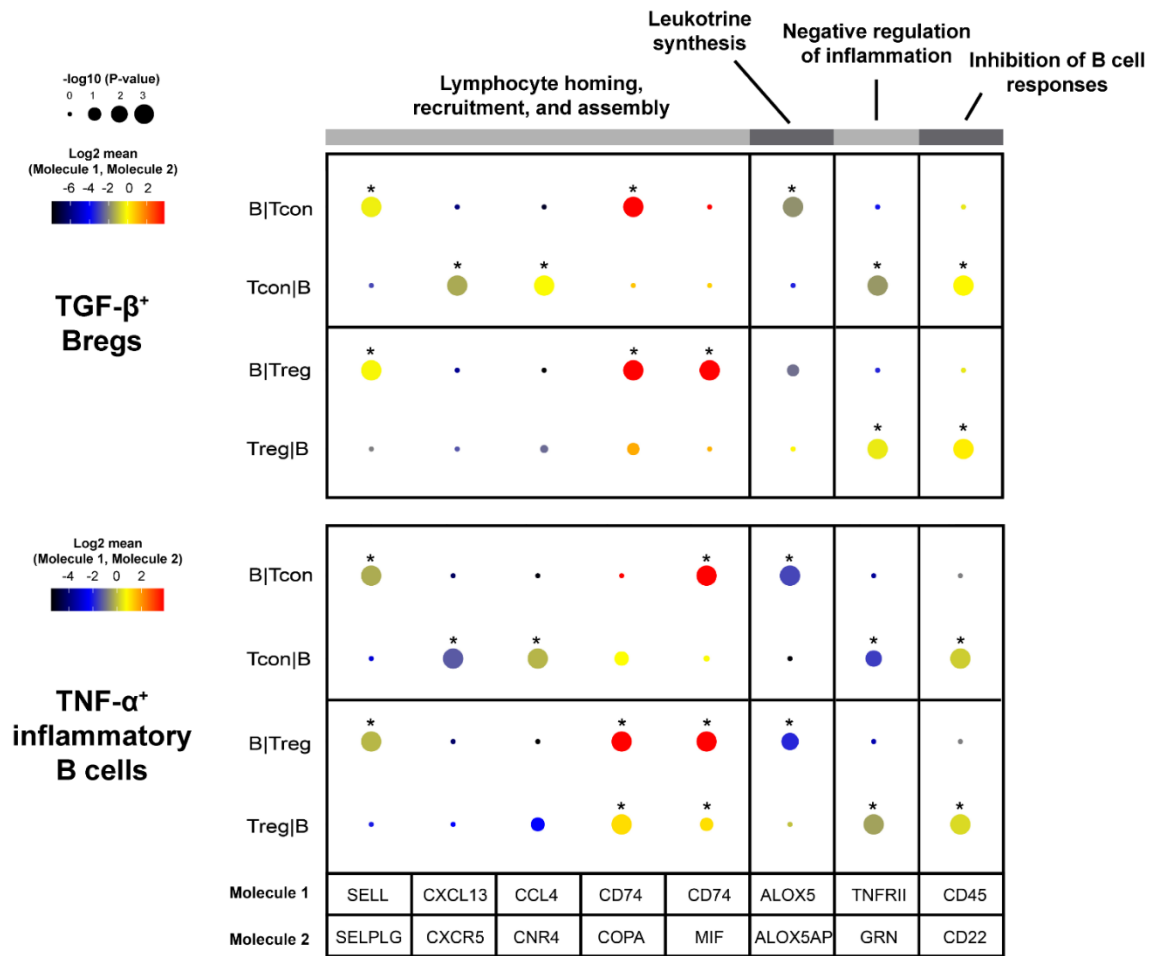
$\beta^+$  B cells have senescent properties and may support the differentiation and maintenance of Tregs in melanoma tumours through expression of Galectin-9, while  $\text{TNF-}\alpha^+$  B cells may engage in extensive crosstalk with Tregs, including via ICOS,  $\text{TNF-}\alpha$ ,  $\text{LT-}\alpha$  and MIF signaling, which could support the suppressive activity of Tregs in the melanoma TME.

CellPhoneDB analyses also identified shared communication pathways, with common ligand-receptor pairs, which were present in B cell:T cell interactions involving either  $\text{TGF-}\beta^+$  or  $\text{TNF-}\alpha^+$  B cells (**Figure 4.10**). These shared interactions included molecules associated with lymphocyte homing, recruitment, and assembly (SELL, CXCL13, CCL4 and CD74), leukotriene synthesis (ALOX5), negative regulation of inflammation (GRN) and inhibition of B cell responses (CD22).

In summary, the melanoma tumour microenvironment appears to contain substantial proportions of B cells which are polarised to express regulatory cytokines, including  $\text{TGF-}\beta$ , and may engage in immunosuppressive crosstalk with T cells in the TME via Galectin-9 signaling. Reduced proportions of  $\text{TNF-}\alpha^+$  B cells are present in tumours compared to matched blood, and the infiltrating  $\text{TNF-}\alpha^+$  cells may engage in extensive crosstalk with Tregs, which could support the suppressive activity of Tregs in the melanoma TME.



## TIL-B:TIL-T ligand-receptor interaction analysis



**Figure 4.10 TGF- $\beta$  and TNF- $\alpha$ -expressing B cells may engage in functional crosstalk with Tcon and Treg cells in the TME.**

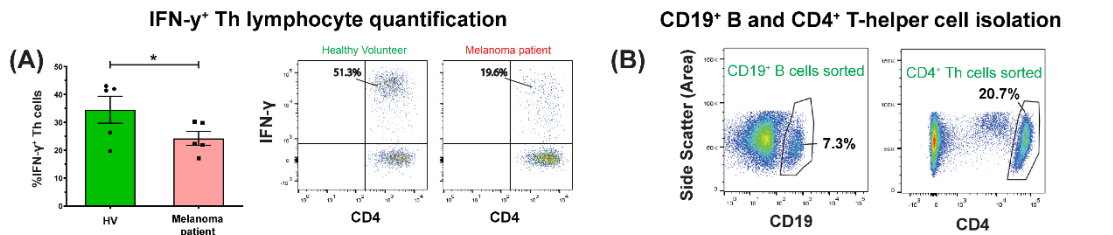
CellPhoneDB analysis of shared pathways for predicted TGF- $\beta$ <sup>+</sup> [left] and TNF- $\alpha$ <sup>+</sup> [right] B cell:T cell communication in the tumour microenvironment. T cells were divided into conventional (Tcon) and regulatory (Treg) subsets. After false discovery rate (FDR<0.001) correction, shared predicted interactions for both B cell subsets include lymphoid homing, recruitment, and assembly, leukotriene synthesis, negative regulation of inflammation, and inhibition of B cell responses. Circle sizes indicate p-value and colour-coding represents the average expression level of interacting molecule 1 in cluster 1 and interacting molecule 2 in cluster 2. These analyses were completed in collaboration with Mr. Roman Laddach, KCL.

#### 4.4.5 Melanoma patient peripheral blood-derived B cells support the proliferation of autologous T-helper cells in *ex vivo* co-culture, but do not regulate Th1 cytokine expression

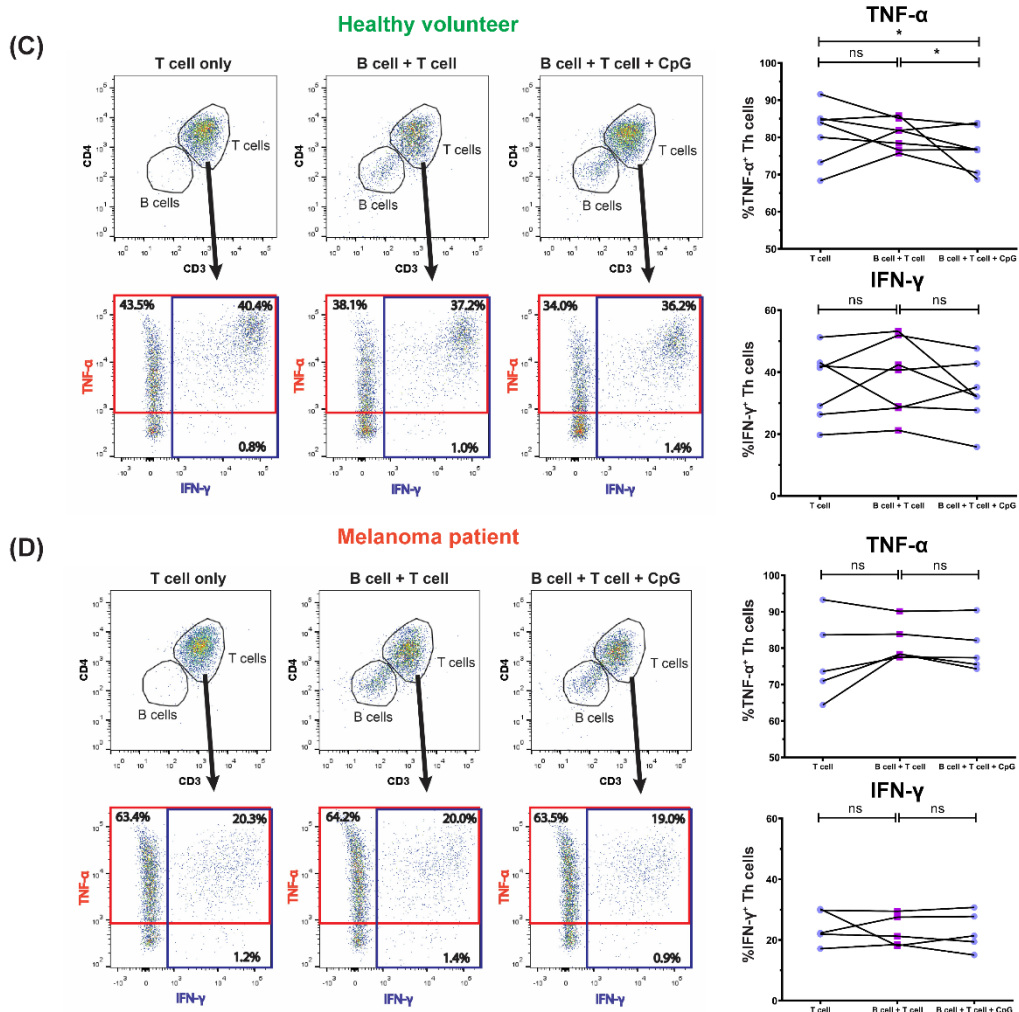
I lastly investigated the influence of melanoma patient peripheral blood-derived B cells upon autologous T cell phenotype and effector function. For this I conducted *ex vivo* B and T-helper cell co-culture studies.

I found that circulating IFN- $\gamma$ -expressing CD4<sup>+</sup> T-helper cells were significantly decreased in melanoma patient peripheral blood compared to blood from healthy volunteers (**Figure 4.11 (A)**), in agreement with previous reports [153]. This finding is also consistent with my observation of reduced TNF- $\alpha$ <sup>+</sup> inflammatory B cells in patient blood and tumours (see **Figure 4.3** and **Figure 4.6**). In autologous 1:1 co-cultures, healthy volunteer-derived B cells suppressed TNF- $\alpha$ -expression by CD4<sup>+</sup> T-helper cells in the presence of CpG (**Figure 4.11 (B-C)**). In contrast, melanoma patient-derived B cells did not suppress either IFN- $\gamma$  or TNF- $\alpha$ -expression by CD4<sup>+</sup> T-helper cells (**Figure 4.11 (D)**).

Both healthy volunteer and melanoma patient-derived B cells significantly enhanced the percentage of proliferating T-helper cells (**Figure 4.12 (A-B)**). In patients, this pro-proliferative effect was further enhanced by PD-1/PD-L1 checkpoint blockade, although only through increases in the percentage of proliferating T-helper cells, and not through the proliferation index (**Figure 4.12 (B)**). Finally, while recombinant TNF- $\alpha$  did not significantly modulate T-helper cell proliferation, as expected, recombinant IL-10 was found to inhibit proliferation [314] (**Figure 4.12 (C)**).



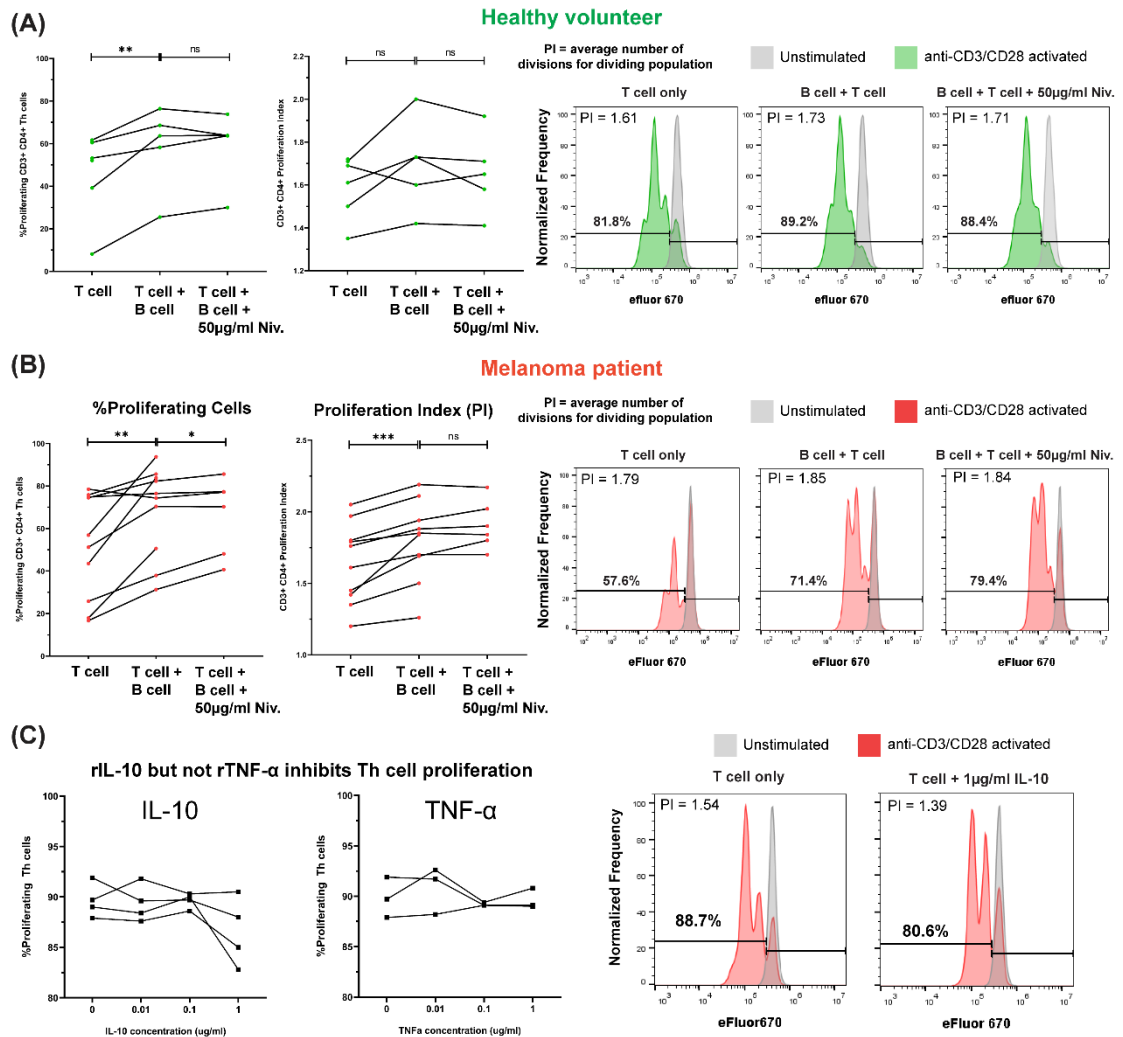
Healthy volunteer, but not melanoma patient peripheral blood B cells suppress Th1 cytokine expression *ex vivo*



**Figure 4.11 B cells derived from melanoma patient peripheral blood do not suppress Th1 (IFN- $\gamma$  and TNF- $\alpha$ ) cytokine expression.**

(A) Proportion of IFN- $\gamma$ <sup>+</sup> T cells are significantly reduced in melanoma patients (N = 5) compared to healthy volunteers (N = 5). (B) Cell-sorting strategy for the isolation of CD19<sup>+</sup> B and CD4<sup>+</sup> T-helper cells from PBMC. (C) [Left] Flow cytometry plots indicate the percentage of T cells expressing IFN- $\gamma$  and/or TNF- $\alpha$  from T-helper cells in “T cell only”, “B cell + T cell” and “B cell + T cell + CpG (ODN 2006)” culture conditions for a representative HV. [Right] Peripheral blood B cells isolated from 7 HVs suppressed TNF- $\alpha$  expression by autologous CD4<sup>+</sup> T-helper cells following *ex vivo* co-culture with CpG. (D) [Left] Flow cytometry plots indicate the percentage of T cells expressing IFN- $\gamma$  and/or TNF- $\alpha$  from T-helper cells for a representative melanoma patient. [Right] Peripheral blood B cells isolated from 5 melanoma patients did not suppress IFN- $\gamma$  and TNF- $\alpha$  expression by autologous CD4<sup>+</sup> T-helper cells following *ex vivo* co-culture.

**Melanoma patient peripheral blood B cells enhance proliferation of activated CD4<sup>+</sup> Th cells *ex vivo*, which is further amplified by PD-1 blockade**



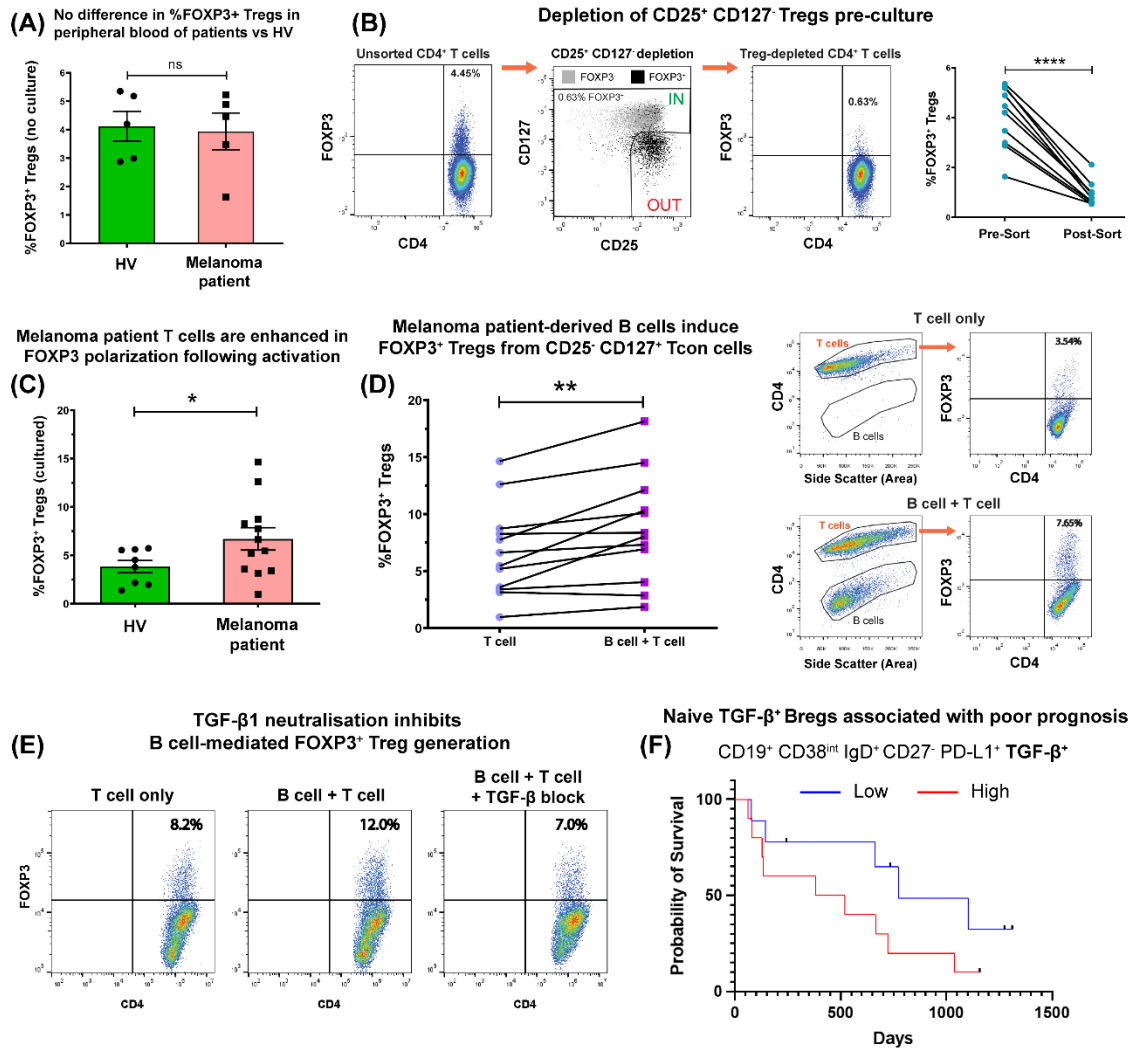
**Figure 4.12 B cells derived from melanoma patient peripheral blood enhance the proliferation of autologous T-helper cells *ex vivo*.**

(A) B cells isolated from healthy volunteer peripheral (N = 5) blood enhance proliferation of autologous CD4<sup>+</sup> T-helper cells. [Left] The addition of B cells into *ex vivo* T cell cultures enhanced the percentage of proliferating T-helper cells. Addition of 50µg/ml of the anti-PD-1 antibody nivolumab did not influence the percentage of proliferating T-helper cells in co-culture. [Right] Flow cytometry dot plots show generational peaks and indicate total percentage of proliferating T-helper cells in “T cell only”, “B cell + T cell” and “B cell + T cell + 50µg/ml nivolumab” conditions for a representative healthy volunteer. (B) B cells isolated from melanoma patient peripheral (N = 10) blood enhance proliferation of autologous CD4<sup>+</sup> T-helper cells. [Left] The addition of B cells into *ex vivo* T cell cultures enhanced both the percentage of proliferating T-helper cells, and the proliferation index (average number of divisions for dividing population). Addition of 50µg/ml nivolumab further boosts the percentage of proliferating T-helper cells in co-culture. [Right] Flow cytometry dot plots indicate total percentage of proliferating T-helper cells in culture conditions for a representative patient. (C) Recombinant IL-10 (1µg/ml) can significantly inhibit the proliferation of melanoma patient peripheral blood-derived CD4<sup>+</sup> T cells (N = 4) following anti-CD3/CD28 activation + IL-2, while recombinant TNF-α (0.01-1µg/ml) has no significant effect (N = 3). [Right] Flow cytometry plots show generational peaks and indicate the total percentage of proliferating T-helper cells in “T cell only” vs “T cell + 1µg/ml IL-10” for a representative patient.

#### 4.4.6 Melanoma patient peripheral blood-derived B cells induce TGF- $\beta$ -mediated differentiation of autologous FOXP3<sup>+</sup> Tregs from conventional T cells in *ex vivo* co-culture, and naïve TGF- $\beta$ <sup>+</sup> Bregs associate with unfavourable survival outcomes

In order to further examine the regulatory influence of melanoma patient peripheral blood-derived B cells, I utilised an additional B:T-helper cell *ex vivo* co-culture assay analyzing the modulation of FOXP3<sup>+</sup> CD4<sup>+</sup> regulatory T cells (Tregs). Initially, I observed no significant differences in the total percentages of FOXP3<sup>+</sup> Tregs between melanoma patient and healthy volunteer peripheral blood (**Figure 4.13 (A)**). For the co-culture study, I purified populations of non-Treg (conventional) T cells by removing the CD25<sup>+</sup> CD127<sup>-</sup> Treg subset enriched in FOXP3 expression (**Figure 4.13 (B)**). Following anti-CD3/CD28 activation, I observed a significantly increased percentage of FOXP3<sup>+</sup> Tregs in melanoma patient compared to healthy volunteer peripheral blood (**Figure 4.13 (C)**). This suggested that a patient-specific subpopulation of T-helper cells may respond to activation by differentiating into a Treg phenotype. *Ex vivo* B:T cell co-cultures demonstrated that melanoma patient B cells significantly induced FOXP3<sup>+</sup> Treg differentiation from the autologous purified CD25<sup>-int</sup> CD127<sup>+</sup> conventional T-helper cells (**Figure 4.13 (D)**). This suppressive effect was nullified when TGF- $\beta$ 1 was neutralised in cell cultures (**Figure 4.13 (E)**), suggesting a link between TGF- $\beta$  expression and induction of Tregs. Finally, Kaplan-Meier survival analysis of our melanoma patient cohort indicated that the presence of circulating TGF- $\beta$ -expressing CD19<sup>+</sup> CD38<sup>int</sup> IgD<sup>+</sup> CD27<sup>-</sup> PD-L1<sup>+</sup> naïve Bregs is associated with less favourable overall survival (**Figure 4.13 (F)**).

Together, these findings highlight that melanoma patient B cells can induce autologous Treg differentiation from conventional T cells through the expression of TGF- $\beta$ , and elevated circulating naïve TGF- $\beta^+$  B cells may indicate unfavourable survival outcomes.



**Figure 4.13 B cells derived from melanoma patient peripheral blood induce a FOXP3<sup>+</sup> Treg phenotype from CD25<sup>-int</sup> CD127<sup>+</sup> conventional T cells.**

(A) No significant difference in %FOXP3<sup>+</sup> Tregs is observed between unstimulated healthy volunteer (N = 5) and melanoma patient peripheral blood (N = 5) T cells. (B) [Left] Cell-sorting strategy for the depletion of CD25<sup>+</sup> CD127<sup>-</sup> Tregs from peripheral blood CD4<sup>+</sup> T cells. [Right] FOXP3-expressing Tregs are successfully depleted following cell sorting (N = 10). (C) The % of FOXP3<sup>+</sup> Tregs are elevated in melanoma patients (N = 12) compared to healthy volunteers (N = 8), following anti-CD3/CD28 stimulation. (D) B cells isolated from melanoma patient peripheral blood (N = 12) induce FOXP3<sup>+</sup> Tregs from CD4<sup>+</sup> CD25<sup>-int</sup> CD127<sup>+</sup> cells following *ex vivo* co-culture. Flow cytometry plots indicate % of FOXP3-expressing T-helper cells in “T cell only” vs “B cell + T cell” conditions for a representative patient. (E) Representative flow cytometry plots showing that antibody-mediated neutralization of TGF- $\beta$  alleviates B cell-facilitated induction of FOXP3<sup>+</sup> Tregs from CD4<sup>+</sup> CD25<sup>-int</sup> CD127<sup>+</sup> Tcon cells. (F) The presence of peripheral blood CD19<sup>+</sup> CD38<sup>int</sup> IgD<sup>+</sup> CD27<sup>-</sup> PD-L1<sup>+</sup> TGF- $\beta$ <sup>+</sup> naive Bregs is associated with decreased probability of overall survival. Patients split by %TGF- $\beta$ <sup>+</sup> naive Bregs into low (below median) and high (above median) groups. The survival analyses were completed in collaboration with Dr. Zena Willmore, KCL.

## **4.5 Discussion and future directions**

Alongside antigen presentation and immunoglobulin expression, B cells may participate in systemic and local immune responses to malignant cells via the secretion of cytokines. The results presented in this Chapter include data from intracellular cytokine and CyTOF phenotyping, transcriptomic analysis, immunofluorescence staining, and *ex vivo* co-culture analyses to investigate the phenotype and potential functional significance of cytokine-expressing B cells in patients with melanoma, including regulatory (IL-10 and/or TGF- $\beta$ -expressing) and pro-inflammatory (IFN- $\gamma$  and/or TNF- $\alpha$ -expressing) subsets.

Circulating B cells from healthy individuals and melanoma patients responded to innate pathway activation by the TLR9 agonist CpG ODN 2006 with strongly polarised expression of TNF- $\alpha$ , while B cells expressing IL-10 in response to activation were rarer in the CD19<sup>+</sup> B cell population. Furthermore, the population of IL-10<sup>+</sup> Bregs is expected to contain both innate and adaptive Bregs, as the combination of innate pathway activation with CpG ODN 2006, and adaptive pathway activation with CD40L induced a higher proportion of IL-10<sup>+</sup> Bregs, compared to each activation condition alone. A population of TGF- $\beta$ -expressing Bregs was also detected independently of B cell activation condition. This suggests that spontaneous expression of TGF- $\beta$  may occur among circulating B cell subsets.

Although the total percentages of circulating IL-10-expressing Bregs, out of the CD19<sup>+</sup> B cell population, were not significantly different, a subset of IL-10-expressing CD19<sup>-</sup> CD38<sup>hi</sup> IgD<sup>-</sup> CD27<sup>+</sup> Ki67<sup>+</sup> Bregs was found to be enriched in melanoma patient compared to age and sex-matched healthy volunteer peripheral blood. These cells likely represent



plasmablasts since the CD38<sup>hi</sup> IgD<sup>-</sup> CD27<sup>+</sup> Ki67<sup>+</sup> signature is a widely accepted plasmablast phenotype [248], and in concordance, previous studies have reported human plasmablasts to be enriched in IL-10 expression [125].

A moderate but as yet non-significant increase was seen in the overall melanoma patient circulating TGF- $\beta$ <sup>+</sup> Bregs compartment compared to those from matched healthy volunteers, studied by intracellular cytokine assay analyses. The number of samples studied in this cohort (3 healthy volunteers and 7 patients) was small. However, by interrogating samples from 30 patients with melanoma and 13 healthy volunteers by CyTOF using a panel of 25 B cell markers, my results revealed that a subset of TGF- $\beta$ -expressing CD19<sup>+</sup> CD38<sup>int</sup> IgD<sup>+</sup> CD27<sup>-</sup> PD-L1<sup>+</sup> Bregs (with the CD38<sup>int</sup> IgD<sup>+</sup> CD27<sup>-</sup> signature being a well-accepted naïve B cell phenotype [248]) were significantly enriched in the circulation of melanoma patients compared to healthy volunteers. A previous study by Wu et al. has shown that PD-L1-expressing naïve Bregs are upregulated in the circulation of patients with advanced melanoma [153], although the PD-L1<sup>+</sup> Bregs were not found to be enriched in TGF- $\beta$ -expression in that study. The cohorts evaluated within this Chapter have been age and sex-matched, and the B cell populations were studied using a larger set of B cell markers by CyTOF; together these may offer a clearer insight into different subpopulations of B cells than would otherwise be possible using a small marker panel. Therefore, the data presented in this Chapter suggest that the PD-L1<sup>+</sup> TGF- $\beta$ <sup>+</sup> Bregs may represent a distinct circulating B cell subset, which is enhanced in patients with melanoma. Taken together with my observations of enriched circulating IL-10<sup>+</sup> plasmablasts, my findings point towards dysregulation of the humoral response in favour of regulatory B cell subsets, which are associated with specific B cell lineages in the circulation of patients with melanoma.

Aside from the observed dysregulation in Breg subsets, intracellular cytokine phenotyping data also identified a collapse in the percentages of circulating IFN- $\gamma$  and TNF- $\alpha$ -expressing B cells in the whole CD19<sup>+</sup> B cell compartment in melanoma patients compared to matched healthy volunteers. Interestingly, a study published in 2021 [299] noted a fall in melanoma patient circulating TNF- $\alpha$ -expressing B cells with advancing disease, from stage I/II to stage III. With significant collapse compared to healthy states, my analyses indicate that a diminished circulating pro-inflammatory B cell compartment, comprising IFN- $\gamma$ <sup>+</sup> and TNF- $\alpha$ <sup>+</sup> cells, may be a feature of dysregulated humoral immune responses in melanoma. It is not clear however whether this feature is present across multiple disease stages. The cohort interrogated in my study includes large proportions (>75%) of late stage (III and IV) patients (**Table 4.1**), and therefore it is possible that this dysregulated B cell feature may be conspicuous in patients with more advanced disease. It is also noteworthy that the cohort interrogated in my study has been selected to include individuals who had not received checkpoint inhibitor immunotherapy. Therefore, the presence of B cells is not influenced by therapeutic activation of the immune response.

The association of human B cell cytokine polarisation with cell surface markers and lineage phenotypes is a controversial topic, with no consensus on ubiquitous extracellular markers, and phenotypic descriptions of regulatory and inflammatory B cell subsets in the circulation of melanoma patients have not yet been established. In my analyses, B cells expressing each of IL-10, TGF- $\beta$  and/or TNF- $\alpha$  cytokines were identified across multiple B cell lineages, although cytokine expressing B cells consistently showed a tendency towards a memory phenotype, with TGF- $\beta$ <sup>+</sup> cells enriched within the IgM memory B cell population. These observations add to the consensus that both regulatory and pro-inflammatory cytokines may be expressed by human B cells deriving from

multiple developmental lineages, and identify the circulating memory B cell pool as an important source of these cytokines in patients with melanoma.

Our group and others have reported that B cells infiltrate melanoma lesions and may undergo antigen-driven responses including clonal expansion, isotype-switching, and somatic hypermutation [226]. However, the role of B cells as cytokine-expressors within the melanoma tumour microenvironment has not been sufficiently elucidated. Intracellular cytokine phenotyping identified a collapse in tumour-infiltrating TNF- $\alpha$ -expressing B cells compared to those in patient circulation, and immunofluorescence and transcriptomic analysis supported the limited presence of TNF- $\alpha$ -expressing B cells within melanoma tumours. In contrast to the limited proportion of TNF- $\alpha$ <sup>+</sup> (0.9%) and IL-10<sup>+</sup> (0.1%) TIL-B, a substantial proportion of TGF- $\beta$ <sup>+</sup> TIL-B (11.3%) were identified in melanoma tumours using scRNAseq.

Functional exhaustion of tumour-specific CD8<sup>+</sup> T cells has been observed in melanoma metastases [315], and exhaustion may be associated with reduced IL-2, TNF- $\alpha$  and eventually IFN- $\gamma$  expression [316]. In the present study, the observed impairment of TNF- $\alpha$  expression among melanoma TIL-B may reflect a state of B cell exhaustion [36][36], and the small proportion of B cells which maintained TNF- $\alpha$  expression in the tumour were found to engage in inhibitory checkpoint interactions (comprising CD72 [312,313] and CD22 [318] signaling) with T cells.

In my CellPhoneDB analyses, I identified predicted interactions between tumour-infiltrating TNF- $\alpha$ <sup>+</sup> B cells and Tregs, including via pro-inflammatory mediators TNF- $\alpha$ , LT- $\alpha$ , and MIF. TNF- $\alpha$  signaling may place via multiple receptors including TNFR1, ICOS and FasR. Recent work has found that TNFR1 is the main TNF-receptor expressed by lymphocytes in tumour-draining lymph nodes [319], and the interaction between

membrane-bound TNF- $\alpha$  and TNFRII can promote lymphocyte activation and proliferation [320]. Although there is some uncertainty regarding the impact of TNF- $\alpha$  signaling on Treg function and FOXP3 expression [321], mounting evidence suggests that TNF- $\alpha$  can drive the phenotypic stability and suppressive activity of Tregs [322,323]. Moreover, TNF- $\alpha$ <sup>+</sup> B cells were predicted to engage in ICOS:ICOSL interaction with Tregs, which constitutes a known activating costimulatory immune checkpoint, and in this context is expected to promote the generation, proliferation, survival and suppressive ability of Tregs [310,311].

CellPhoneDB analysis demonstrated that tumour-infiltrating TGF- $\beta$ <sup>+</sup> B cells expressed the immune checkpoint receptor Galectin-9 [305], which was predicted to engage with CD44 expressed by Tregs. Evidence from mouse models [306] suggest that this interaction may act synergistically with TGF- $\beta$  to support the differentiation and maintenance of Tregs. These TGF- $\beta$ <sup>+</sup> B cells also expressed HLA-E, a non-classical HLA molecule associated with senescent cells [307,308], which was predicted to interact with NKG2D, expressed by Tcon cells. This interaction has been implicated in the surveillance and elimination of senescent cells [307,309] and these observations therefore point towards a senescent phenotype among intratumoural TGF- $\beta$ <sup>+</sup> B cells, which may facilitate CD8<sup>+</sup> cytotoxic T cell targeting in the TME.

Before the work presented in this Thesis, the extent to which B cells isolated from melanoma patient peripheral blood can modulate autologous T cell phenotype and effector function had been incompletely explored. In the *ex vivo* cytokine suppression assay in the present study, melanoma patient-derived B cells did not suppress either IFN- $\gamma$  or TNF- $\alpha$ -expression from CD4<sup>+</sup> T-helper cells, including in co-cultures where cells were incubated with the innate pathway activator CpG ODN 2006. On the other hand, patient B cells significantly enhanced both the proliferation index and percentage of

proliferating T-helper cells in the *ex vivo* co-culture. Taken together, my observations that patient-derived B cells allow autologous T-helper cells to produce pro-inflammatory cytokines and proliferate *ex vivo* may point to the possibility that the role of IL-10<sup>+</sup> Bregs within my *ex vivo* co-cultures was limited. Instead, these findings may highlight that patient B cells are capable of playing an overall supportive role upon T cells, and that the observed pro-proliferative effect of patient B cells on autologous T-helper cells in co-cultures may be due to the potential expression of B cell-derived growth factors. Future studies are required to elucidate the mediators involved in these pro-proliferative effects, which may include known T cell growth factors such as IL-2 [324], IL-7 [325], or IL-15 [326].

Furthermore, PD-1/PD-L1 checkpoint blockade resulted in increases in the percentage of proliferating T-helper cells within the *ex vivo* B-T cell co-cultures. This provides some support that, in addition to the previously published *ex vivo* suppression of IFN- $\gamma$ -mediated CD4<sup>+</sup> and CD8<sup>+</sup> T cell responses [153], melanoma patient circulating PD-L1<sup>+</sup> B cells may also inhibit the proliferation of activated autologous CD4<sup>+</sup> T-helper cells via the PD-1/PD-L1 axis, and more widely that B-T cell interactions may be further promoted by checkpoint blocking agents. B cell signatures including serum IgG have been found to predict outcome to anti-PD-1 CPIs nivolumab and pembrolizumab [171] in patients with metastatic melanoma, and the potential neutralization of the suppressive abilities of PD-L1-expressing B cells may provide an explanation of these findings. As such, future studies are needed to establish the association of baseline circulating PD-L1<sup>+</sup> B cells with CPI response in cohorts of metastatic melanoma patients.

While studies in mouse models have suggested that a subset of “tumour-evoked” Bregs can facilitate the metastasis of breast cancers through the induction of Tregs, the significance of melanoma patient B cells in contributing to *ex vivo* Treg generation had

not been investigated. Utilising *ex vivo* co-cultures of melanoma patient circulating B cells and autologous Tcon cells depleted of Tregs, I observed that B cells significantly induced FOXP3<sup>+</sup> CD4<sup>+</sup> Tregs in a TGF- $\beta$ 1-dependent manner. These findings may explain the observed less favourable survival outcomes in patients with elevated circulating naïve TGF- $\beta$ <sup>+</sup> Bregs, since the presence of Tregs has been consistently associated with poor prognosis in melanoma [327].

In summary, the results presented in this Chapter provide evidence for an active and dynamic role of B cells as cytokine producers in the circulation and in tumour lesions of patients with melanoma. The cytokine-expressing B cell compartment both in the circulation and in melanoma lesions may be dysregulated, favouring IL-10<sup>+</sup> plasmablast and TGF- $\beta$ <sup>+</sup> naïve Bregs, while also downregulating IFN- $\gamma$ <sup>+</sup> and TNF- $\alpha$ <sup>+</sup> B cells. I also found evidence that the circulating memory B cell pool is an important and diverse source of cytokine expression in patients with melanoma, and future studies may focus on the plasmablast and memory B cell pools as rich sources of cytokine-expressing B cells. The TME appears to contain considerable populations of TGF- $\beta$ <sup>+</sup> Bregs, while TNF- $\alpha$  and IL-10-expressing cells are scarcer. Both TGF- $\beta$ <sup>+</sup> and TNF- $\alpha$ <sup>+</sup> TIL-B were predicted to engage in inhibitory checkpoint interactions and crosstalk with Tregs. Furthermore, my *ex vivo* co-culture analyses indicate potential roles for melanoma patient circulating B cells as enhancers of autologous T-helper cell proliferation, while PD-L1<sup>+</sup> Bregs may interfere with these effects, and circulating and tumour-infiltrating TGF- $\beta$ <sup>+</sup> Bregs may be responsible for inducing autologous FOXP3<sup>+</sup> Tregs. Taken together, my analyses point towards a dichotomy in B cell responses to melanoma, which may confer a combination of immunostimulatory or immunomodulatory influences, the balance of which may depend upon B cell phenotypes, other immune cell subsets present, as well as microenvironmental conditions including the local cytokine milieu.

Lastly, the presence of systemic and tumour-infiltrating TGF- $\beta$ <sup>+</sup> Bregs, which can functionally induce FOXP3<sup>+</sup> Tregs, may contribute to tumour progression in melanoma and offer potential avenues for therapeutic intervention. In this study, I found that elevated levels of circulating naïve TGF- $\beta$ <sup>+</sup> Bregs were associated with worse overall survival. This represents a preliminary observation, which could be confounded by additional variables including the distribution of treatment and staging effects. Future investigations using larger cohorts and considering expression of additional cytokines and inhibitory ligands by B cells, including evaluating regulatory versus pro-inflammatory B cell signatures more widely, are required to elucidate the significance of TGF- $\beta$ , and other cytokine-expressing B cells in general, in contributing to clinical outcomes in melanoma.

## **Chapter 5: Discussion and Future Directions**

### **5.1 Introduction**

Unravelling of immunomodulatory mechanisms such as immune checkpoints have led to remarkable translational breakthroughs in the last decade. The emergence and clinical success of cancer immunotherapies underscores the potential benefits that may arise from improving our understanding of immune responses to tumours. Checkpoint inhibitors target T cell effector mechanisms, and the contributions of T cells towards tumour immunosurveillance are well established and have historically received extensive attention. In contrast, the potential importance and contribution of the other arm of adaptive immunity, comprising B cell responses, within both the circulating and tumour-infiltrating compartments, in engendering or hindering anti-tumour immune responses has received much less attention. Although not being considered for functions in directly killing cancer cells, B cells may play several roles within the immune response to cancers due to their ability to produce antibodies, present antigen, and express cytokines (discussed in Sections 1.2.2-1.2.4). Within the tumour microenvironment, these functions may be significantly influenced by crosstalk with malignant cells and other immune cell subsets, and these interactions may promote B cells to confer either anti-tumour or pro-tumour effector functions, and often perhaps not one but a spectrum of these.

This Thesis is focused upon unravelling this emerging dichotomy of B cell immune responses to solid tumours, with specific focus on B cell populations in immunogenic tumours such as melanoma and subsets of breast cancer.



In breast cancer, focusing upon highly aggressive triple-negative subtypes (Chapter 3), which are paradoxically also known to evoke an notable immune response, I have presented: a) a shift in cellular responses, including modulation in activation, isotype-switching, and memory phenotypes, among circulating and tumour-infiltrating B lymphocytes; b) insights into the localisation of B cells in the tumour microenvironment, including association and crosstalk with T cells; c) monitoring of immunoglobulin isotype expression in the circulation and among tumour-infiltrating B lymphocytes, including isotype-biases and clonal features therein; d) multifaceted analyses of the prognostic value of TIL-B, including stratification by lineage phenotype, and functional attributes.

In evaluating the humoral response to melanoma, with focus upon the role of cytokine-expressing B cell subsets (Chapter 4), I have presented: a) profiling of cytokine-expressing B cell subsets in patient circulation, focusing upon dysregulation among regulatory (IL-10<sup>+</sup> or TGF-β<sup>+</sup>), and inflammatory (IFN-γ<sup>+</sup> or TNF-α<sup>+</sup>) B cell subsets; b) lineage phenotyping of IL-10, TGF-β, and TNF-α-expressing B cells; c) distribution of tumour-infiltrating cytokine-expressing B cells, their lineage phenotypes, and crosstalk with Tcon and Treg cells; d) *ex vivo* functional evaluations of patient-derived B cells, including evaluation of their ability to modify autologous T-helper cell proliferation, influence Th1 cytokine expression, and induce FOXP3<sup>+</sup> Tregs from Tcon cells.

## **5.2 The role of circulating and tumour-infiltrating B lymphocytes in breast cancer**

Prior investigations have reported evidence for active and dynamic humoral immune profiles in patients with cancer. For example, the presence of tumour-reactive B cells [328], alongside evidence for prognostic significance [211] and TIL-B functional profiles,

including via immunoglobulin expression [213], have been previously demonstrated in patients with breast cancer. Although B cells are now established as notable players in the immune response in breast cancer, information regarding the role of mature memory and isotype-switched B cells, and wider B cell functional profiles, is still lacking.

Considering these observations, I sought to investigate the presence, localisation, antibody expression and functional roles of circulating and tumour-infiltrating B lymphocytes in the humoral response to breast cancer, with a focus on mature, isotype-switched and memory B cell subsets. My aim was to provide fresh insights into the potential phenotypic skewing of differentiated circulating and tumour-infiltrating B lymphocytes populations, and to identify the importance of their expressed immunoglobulin isotypes.

#### 5.2.1 Evidence for systemic perturbations of humoral immunity and for active roles of B cells in breast cancer

It is widely acknowledged that immune responses to solid tumours, including breast cancers, do not occur only within the tumour margins, but extend into the periphery. Moreover, tumour cells may instigate widespread remodelling of the immune system among cancer patients. Indeed, several perturbations in peripheral immune cell subsets have been described in breast cancer (Chapter 1, **Table 1.4**). These observations include increased frequencies of peripheral blood haematopoietic stem cell precursors, immature myeloid cells, and regulatory T cells. Yet, perturbations among B cell subsets have not been well described. Using a large cohort of N = 55 breast cancer patients and N = 48 healthy volunteers, my flow cytometry evaluations identified decreased proportions of peripheral CD27<sup>+</sup> memory B cells out of total circulating B cells in patients compared to

healthy states (Chapter 3, **Figure 3.1**). I also observed a decline in the proportions of B cells and serum immunoglobulin in patients who had received chemotherapy treatment within one year of sample collection, compared with treatment naïve individuals and healthy volunteers (Chapter 3, **Figure 3.1-3.2**). These findings indicated that chemotherapy may impair systemic B cell profiles. Importantly, I found a decline in memory B cells in treatment naïve patients compared to healthy subjects, which suggests that impaired memory B cell responses in the circulation may be a more general feature of the immune landscape in breast cancer patients rather than only a consequence of treatment. A collapse in circulating memory B cells has been previously reported in patients with advanced melanoma [152], and may be associated with lack of differentiation or proliferative signals to activate humoral immunity as part of the disease course. Alternatively, loss of memory B cell subsets may be due to sequestering to tumour lesions or sentinel lymph nodes. Future studies may investigate the origin of the decline in circulating memory B cells in breast cancer patients.

B cells are known to infiltrate and accumulate within solid tumours, including those of the breast [214]. However, little is known about the variations of B cell infiltration among breast cancer subtypes. Through bulk RNAseq evaluations, I found that the expression of B cell (CD20 and BCR complex CD79A) markers were elevated in TNBC, compared to both normal and non-TNBC tissues (Chapter 3, **Figure 3.5 – 3.6**). Among TNBC subtypes, B cell-associated gene expression was highest in the Lehmann's immunomodulatory molecular TNBC subtype, known to be enriched in core immune signal transduction pathways and cytokine signaling (Chapter 3, **Figure 3.5 – 3.6**). Overall, the immunogenic nature of TNBC, and current unmet clinical need of TNBC patients, provided the stimulus to focus my investigations presented in Chapter 3 around the TNBC subtype.

After establishing that B cells infiltrate breast tumours, and markedly in TNBCs, I sought to ascertain whether B cells possessed active and dynamic roles within the context of the breast tumour microenvironment. My flow cytometry evaluations identified a proportional amplification of circulating and breast tumour-infiltrating isotype-switched (IgD<sup>-</sup>) B cells within the CD27<sup>+</sup> compartment, compared to those in healthy volunteer blood (Chapter 3, **Figure 3.1**). In addition, single cell RNAseq analysis of matched patient blood and tumour samples revealed that B cell subsets were distinct to those from the patient blood.

My fluorescence immunohistochemical evaluations confirmed that B cells strikingly infiltrate TNBC, and typically form stromal clusters along with T cells, even in tumours which feature low immune cell infiltration (Chapter 3, **Figure 3.5-3.7**). In line with B-T cell cluster formation, I found elevated expression of B cell recruitment and lymphoid assembly marker genes (CXCL13, CXCR4 and DC-LAMP) in TNBC tumours, compared to both normal breast and non-TNBC (Chapter 3, **Figure 3.6 – 3.7**). Within the TNBC cohort the highest expression of these genes was detected in the immunomodulatory subtype (Chapter 3, **Figure 3.7**). Furthermore, single cell RNAseq analysis and immunohistochemical evaluations pointed to expression of markers associated with germinal centre B cells within tumours, further supporting the likelihood of lymphoid assembly in breast cancer. In addition, my CellPhoneDB analysis predicted extensive bi-directional functional crosstalk between tumour-infiltrating B and T lymphocytes (Chapter 3, **Figure 3.8**). Evidence is accumulating that the organisation of immune infiltrates into tertiary lymphoid structures may confer positive prognostic value in breast cancer [288,329], and this is supported by my finding that expression of a lymphoid assembly gene signature in basal-like/TNBC tumours was associated with improved overall survival (Chapter 3, **Figure 3.7**). Collectively, my findings support the notion that

B and T cell interactions are a key feature in breast tumours and may possess a critical role in engendering successful adaptive anti-tumour immune responses.

Moreover, I observed upregulation in the tumour, compared to normal breast, of several genes known to positively regulate B cell activation, proliferation, and differentiation (Chapter 3, **Figure 3.9**). BCR-driven activatory signatures were enhanced within the TIL-B compartment compared to circulating B cells, including enrichment in gene hallmarks associated with TNF- $\alpha$  signaling via NF $\kappa$ B, which suggested that B cells in tumours receive stimulation and likely antigenic signals via the BCR (Chapter 3, **Figure 3.8**). It is likely that TIL-B receive a combination of innate and adaptive signals within the TME, and these signals may support isotype-switching and differentiation into memory or plasma cell phenotypes.

Together, my observations establish B cells as active players as opposed to being bystanders in the tumour microenvironment, possessing differentiated and isotype-switched phenotypes, clustering and engaging in crosstalk with T cells, and likely responding to environmental stimuli within breast cancer lesions.

### 5.2.2 IgG-biased and clonally skewed profiles in the anti-tumour immune response in breast cancer

The distribution of antibody subclasses, which confer binding affinities to immune effector cells, embodies a crucial component of antibody-mediated B cell responses. This has been underscored by the observation that enhanced frequencies of circulating IgG4<sup>+</sup> B cells, engendering a more limited antibody-mediated effector repertoire, are associated with significantly increased risk of disease progression in early (stage I-II) melanoma patients [151]. In breast cancer, *ex vivo* stimulation of TIL-B has been reported to induce

expression of IgA and IgG antibodies with specificity to cancer autoantigens [213]. In addition, increases in IgG1, IgG2, IgG3 and IgM have been observed in breast tumours, compared to normal breast tissue supernatants [214]. However, the immunoglobulin isotype distribution, at the single B cell level, and their relationship with TIL-B densities, has not been previously investigated.

For this purpose, I performed fluorescence immunohistochemistry staining of 15 normal breast and 15 TNBC tissues, and I quantified the densities of IgD, IgM, IgA, and IgG-expressing B cells (Chapter 3, **Figure 3.10-3.11**) in relation to CD20<sup>+</sup> TIL-B infiltration. I observed elevated IgG<sup>+</sup> and IgM<sup>+</sup> B cells in TIL-B<sup>high</sup>, and to a lesser extent, TIL-B<sup>low</sup> tumours compared with normal breast tissue, while the IgA-expressing B cell compartment was consistent across tissues (Chapter 3, **Figure 3.11**). In support of the upregulation of isotype-switched B cells in breast tumours, my single cell RNAseq analysis identified enhanced levels of isotype-switched IgG and IgA-expressing CD27<sup>+</sup> B cells in tumour samples compared to those in the circulation (Chapter 3, **Figure 3.14**). This trend was especially pronounced in TNBC, and all four IgG isotypes were upregulated in TNBC compared with non-TNBC (Chapter 3, **Figure 3.13**). Together, these observations highlight biases towards isotype-switching among TIL-B, which may be especially pronounced in TNBC. Future studies may wish to investigate the extent to which these features arise from *in situ* differentiation and isotype-switching, or from preferential homing of isotype-switched B cells originating from the circulating B cell compartment.

Following on from my observation that IgG-expressing B cells are expanded in breast tumours, I performed long-read sequencing analyses to probe the B cell immunoglobulin repertoire for signatures of isotype-switching and clonal expansion (Chapter 3, **Figure**

**3.16-3.17).** I found that both IgG and IgA isotype immunoglobulins were clonally expanded within breast tumours and identified a bias towards the expansion of IgG isotypes, which on average belonged to larger clonal families than IgA, with the largest IgG clonal families containing upwards of 100 members (Chapter 3, **Figure 3.16**). These analyses therefore point towards an inherent bias towards the preferential clonal expansion of IgG isotypes within breast cancers, which has not previously been reported. In addition, my analyses of breast tumour samples revealed a stronger selection pressure among the CDRs of IgG, compared to clonally related IgA isotypes (Chapter 3, **Figure 3.16**), suggesting that IgG-expressing B cells may confer higher affinity antigen-driven responses, in contrast to IgA which may act as part of an earlier response.

Taking into account my fluorescence immunohistochemical evaluations of *in situ* immunoglobulin-expressing TIL-B with my single cell RNAseq and long-read sequencing analyses, I have established robust evidence for active mature humoral responses in breast cancers. These responses may be driven, and likely focused towards, specific antigen stimuli. This notion is supported by previous observations that TIL-B produce cancer antigen-reactive IgA and IgG antibodies [213]. Importantly, these mature antibody responses possess several features which suggest favouring towards expression of IgG immunoglobulins. It is possible that this reflects the balance of cytokine-mediated signals, such as those favouring IL-4 as opposed to TGF- $\beta$  [330]. Future studies are required to unravel the microenvironmental conditions that may lead to these IgG-biased humoral profiles in breast cancer

### 5.2.3 B cells and their functional profiles as prognostic biomarkers in breast cancer

The breast tumour-infiltrating lymphocyte compartment, comprising T cells, NK cells, and B cells, has received substantial attention in recent years and culminated in the establishment of a “TIL working group” [197], which prompted a standardised protocol for pathological TIL assessment. These guidelines are now routinely used in clinical and translational settings, and breast TILs are widely acknowledged as powerful prognostic and predictive biomarkers [196]. Our understanding of the role of the TIL-B sub-compartment in breast cancer patient outcomes has been more controversial, and there has been substantial disagreement, with TIL-B signatures being independently associated with negative [205], neutral [201], and positive [203] prognostic values across studies (Chapter 1, **Table 1.6**).

One of the key aims of the work presented in this Thesis (Chapter 3) was to ameliorate the current uncertainty concerning the prognostic value of breast TIL-B, and provide a deeper understanding of the relative contributions of B cell lineages and functions in contributing to clinical outcomes. I instigated a multibranch prognostic methodology, employing immunohistochemical analyses (Bart’s IHC cohort) and transcriptomic approaches to independently confirm the positive prognostic value of CD20<sup>+</sup> and CD79A TIL-B in basal-like/TNBC (Chapter 3, **Figure 3.5**). Using CIBERSORT deconvolution, and utilising gene expression datasets, I was able to perform survival analysis based on B cells stratified by their lineage phenotype (naïve, plasma and memory). This revealed that, in tumours with high TILs, memory B cells, in contrast to naïve B cells, were associated with improved distant metastasis-free survival (Chapter 3, **Figure 3.5**). Lastly, through analysing breast tumours for expression of gene signatures associated with the positive regulation of key B cell properties (activation, proliferation, and differentiation) using the



KM-plotter tool, I found that signatures from all three functions carry positive prognostic value in tumours of the basal-like/TNBC subtype (Chapter 3, **Figure 3.8**).

Collectively, my findings, summarised in **Table 5.1**, have established breast TIL-B as robust prognostic biomarkers. These features may be most evident in basal-like/TNBC, which is supported by previous investigations [211], but may also present in tumours with generally favourable prognosis such as LuminalA molecular subtypes, in which elements of the humoral immune response may be a further sign of anti-tumour responses and contribute to better outcomes (Chapter 3, **Figure 3.5**). In Section 5.2.1, I discussed my finding that basal-like/TNBC tumours typically contain expansive B cell infiltrates, despite conferring a paradoxically poor prognosis. The observation that TIL-B are strong prognostic biomarkers in basal-like/TNBC patients supports the notion that B cells can still contribute to anti-tumour immunity in the face of intrinsically aggressive tumours, and these traits may confer responsiveness to immunotherapeutic approaches such as checkpoint inhibitors which are beginning to find clinical utility in these subsets of patients.

**Table 5.1 Summary of the prognostic significance of breast tumour-infiltrating B lymphocyte signatures, as analysed in this Thesis.**

Identification technique, B cell signature, and cohort(s) are described. Prognostic value of TIL-B in each study is indicated in the right-hand column.

Identification technique	B cell signature	Cohort(s)	Prognostic value
IHC	CD20 <sup>+</sup> B cells (associated feature - enhanced IgG and IgM expressing B cells)	TNBC	Positive
TCGA RNAseq	CD20 <sup>+</sup> B cells	Basal-like/TNBC, Luminal A, Luminal B	Positive
		HER2 <sup>+</sup>	Neutral
	CD79A <sup>+</sup> B cells	Basal-like/TNBC	Positive
		LuminalA, HER2 <sup>+</sup> , Luminal B	Neutral
TCGA RNAseq (CIBERSORT)	Naïve, plasma, and memory B cells	TNBC with low TILs	Neutral

Identification technique	B cell signature	Cohort(s)	Prognostic value
	Naïve B cells	TNBC with high TILs	Negative
	Plasma cells	TNBC with high TILs	Neutral
	Memory B cells	TNBC with high TILs	Positive
TCGA RNAseq	B cell activation	Basal-like/TNBC	Positive
		LuminalA, HER2 <sup>+</sup> and LuminalB	Neutral
	B cell proliferation	Basal-like/TNBC, Luminal B	Positive
		LuminalA, HER2 <sup>+</sup>	Neutral
	B cell differentiation	Basal-like/TNBC, Luminal A	Positive
		HER2 <sup>+</sup> and Luminal B	Neutral
	Isotype-switching	Basal-like/TNBC	Positive
		LuminalA, HER2 <sup>+</sup> and LuminalB	Neutral
IgG isotype-switching	Basal-like/TNBC	Positive	
	LuminalA, HER2 <sup>+</sup> and LuminalB	Neutral	
IgA isotype-switching	All subtypes	Neutral	

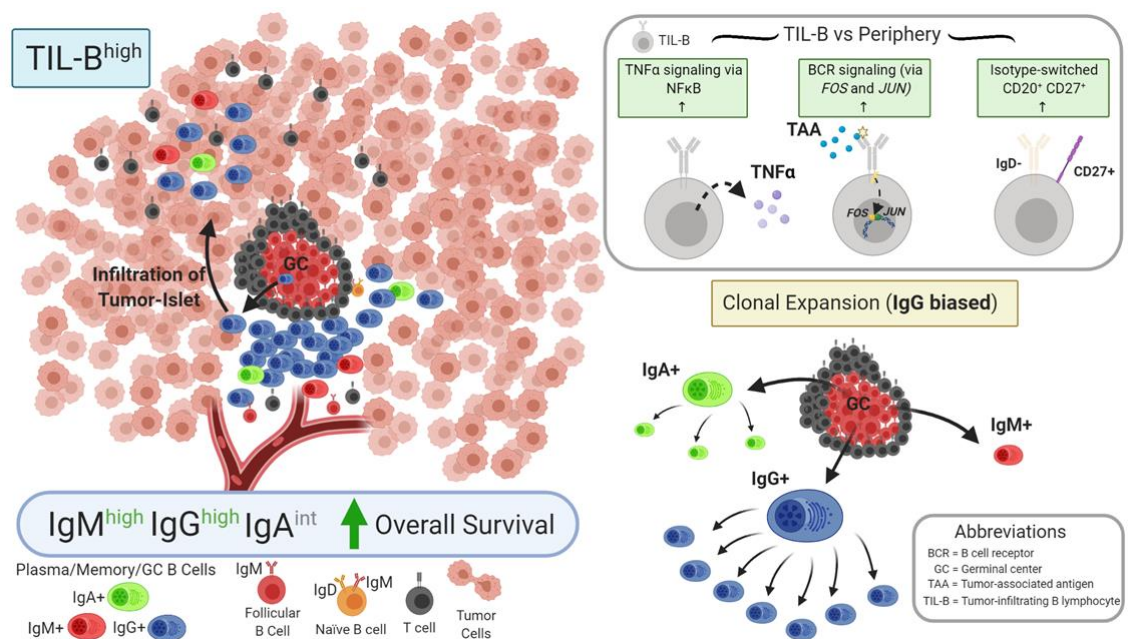
Finally, my B cell signature survival analysis (**Table 5.1**) identified a positive association with overall survival for IgG, but not for IgA, isotype-switching signatures within breast tumours, which was especially pronounced in basal-like/TNBC (Chapter 3, **Figure 3.13**). Considering this information, and the observed increased IgG<sup>+</sup>:IgA<sup>+</sup> B cell ratio within TIL-B<sup>high</sup> compared to TIL-B<sup>low</sup> cancers, it is possible that not only isotype-switching but importantly the isotype of the isotype-switched antibodies may be an important determinant of the quality of the humoral immune response and of the clinical outcome. Further work is recommended to study the tumour-infiltrating IgG<sup>+</sup>:IgA<sup>+</sup> B cell ratio as a potential novel prognostic B cell biomarker.

My investigations summarised in Section 5.2.1 established B cells as active players in the immune response to breast cancer, and my analyses here confirm that these traits, including those associated with memory B cell phenotypes, isotype-switching, and B cell functional signatures, are associated with positive prognostic value, particularly in aggressive TNBCs. Taking this information into account, potential therapeutic strategies that seek to induce or support these attributes may hold merit in the clinical setting. One

potential candidate may take the form of CD40-agonist therapy, given perhaps in combination with other anti-tumour therapies, such as checkpoint immunotherapies or anti-cancer antibodies. While *in vivo* studies have indicated that B cell-based immunotherapies, such as CD40-activated B cell cancer vaccines [331], may be well tolerated and associated with little toxicity [332], imminent clinical trials are awaited to determine their place in the arena of cancer immunotherapy.

#### 5.2.4. Graphical summary

A graphical summary of my key findings concerning the role of circulating and tumour-infiltrating B lymphocytes in breast cancer is illustrated in **Figure 5.1**.



**Figure 5.1 Breast tumour-infiltrating B lymphocytes carry an expanding IgG isotype profile in TNBC, which associates with favourable clinical outcomes.**

Created with BioRender.com [86].

My research presented in Chapter 3 identified distinct cellular phenotypes among the TIL-B compared to the circulating B cell compartment, including isotype-switched CD20<sup>+</sup> CD27<sup>+</sup> phenotypes and evidence of TNF- $\alpha$  signaling via NF $\kappa$ B downstream of the BCR. I observed upregulated expression of genes such as *FOS* and *JUN*, which are found downstream of BCR complex pathway; the germinal centre B cell regulator of chemokine receptor signaling *RGS1*, the lymphocyte activation marker *CD69*, triggered through crosslinking of surface Ig and enhanced expression of genes controlling TNF $\alpha$  signaling, among TIL-B in comparison with circulating B cells. Through immunofluorescence staining of TNBC tissue sections, I established that TIL-B<sup>high</sup> tumours contain enhanced IgM and IgG-expressing B cells and are associated with improved overall survival outcomes. Moreover, within tumours, I found enhanced expression of genes associated with lymphocyte recruitment and lymphoid assembly, and I showed that TIL-B frequently form stromal clusters with T cells, where they may engage in bidirectional functional crosstalk. Lastly, I determined that clonal expansion was biased toward IgG, showing expansive clonal families with specific variable region gene combinations and narrow repertoires. Also, stronger positive selection pressure was present in the complementarity determining regions of IgG compared with their clonally related IgA in tumour samples. Overall, I found isotype-switched B cell lineage traits to be conspicuous in TNBC, associated with improved clinical outcomes, and conferred IgG-biased, clonally expanded, and likely antigen-driven humoral responses.

### **5.3 Cytokine-expressing B cells as complex and dynamic players in systemic and intratumoural immunity of patients with melanoma**

The roles of B cells in human skin immunosurveillance have received growing attention in recent years [333], with research demonstrating that populations of mature, isotype-switched B cells reside in healthy skin tissue [226], and that B cells may accumulate and proliferate in the skin in response to cutaneous antigenic challenge [244]. Evidence has also been gathered for skin tumour-resident mature B cell and antibody compartments, which may generally confer positive prognostic value in melanoma patients [183] (summarised in Chapter 1, **Table 1.7**). Previous investigations by our laboratory and other groups have pointed to skewed isotype expression by B cells in melanoma, away from the prevalent IgG1, favouring B cells expressing isotypes such as IgA and IgG4. These features may confer a form of tumour immune evasion mediated by cytokines including IL-4, IL-10, TGF- $\beta$  and VEGF, possibly combined with a corresponding reduction or impairment of pro-inflammatory cytokines such as IFN- $\gamma$  which would support isotype-switching to IgG1. B cells may be a source of these cytokines and may thus also act in a paracrine manner to influence T cell phenotype and functions. However, despite evidence suggesting that cytokine-expressing B cell subsets can support immune modulation and tumour progression in murine models, via the secretion of IL-10, the role of circulating and intratumoural cytokine-expressing B cells in patients with melanoma has received insufficient attention [116].

I therefore sought to investigate the phenotype and function of regulatory B cells (including IL-10-, or TGF- $\beta$ -producing subsets), and pro-inflammatory B cells (including IFN- $\gamma$  and TNF- $\alpha$ -expressing subsets) in human melanoma. My aim was to provide novel

phenotypic and functional insights into the previously understudied regulatory and inflammatory B cell populations in melanoma patients.

### 5.3.1 Dysregulation and lineage sources of cytokine-expressing B cells in the peripheral blood of melanoma patients

Multiple investigations into the role of B cells as cytokine expressors have been undertaken in animal models. Such studies have been successful in describing murine effector B cell subsets comprising IFN- $\gamma$ -expressing B effector 1 (Be-1) [112] and IL-4-expressing B effector 2 (Be-2) [113] cells, the designation of which appears to depend upon T-helper cell subsets and antigenic classes initiating B cell activation. Murine effector B cell subsets can also produce TNF- $\alpha$  [107] and can therefore contribute to local pro-inflammatory responses. Regulatory B cells have also been extensively described in mice [116,117,297], and have been typically defined by expression of the cytokine synthesis inhibitory factor IL-10, which can exert potent anti-inflammatory and immunosuppressive functions. In general, regulatory B cell subsets are characterised by diverse immunosuppressive functions and therefore also include TGF- $\beta$  [133] or PD-L1-expressing [334] B cell subsets.

Within the human setting, studies examining the roles of cytokine-expressing B cells have been less forthcoming. This may stem from the theoretical and technical challenges in performing robust and meaningful analyses of cytokine-expressing human B cell subsets. There is generally a lack of consensus on ubiquitous extracellular markers which precludes easy identification of distinct cytokine-expressing B cell subsets. Furthermore, the heterogeneity of activation methods (*e.g.*, innate versus adaptive pathway stimulation) are substantial barriers to ascertain reliable investigations of B cell cytokine expression

profiles, and these methods have been markedly inconsistent across studies. In my studies, the results of which are displayed in Chapter 4, I attempted to overcome some of these barriers, and to provide a robust and reliable analysis of the cytokine-expressing B cell landscape. I studied B cells using large marker panels and in matched patient and healthy volunteer cohorts. In addition, I utilised both innate and adaptive stimuli to evaluate the circulating total B cell population for cytokine expression in *ex vivo* cultures. Considering the lack of established extracellular marker panels which are associated with B cell cytokine expression, I firstly utilised a 25-marker CyTOF panel, with the aim of delivering a detailed insight into the phenotype of immunosuppressive cytokine-expressing B cells. Through analysing peripheral blood B cells among a cohort of melanoma patients and matched healthy volunteers, I found evidence of enrichment in the percentages of two regulatory B cell populations in patient circulation: IL-10-expressing CD19<sup>-</sup> CD38<sup>hi</sup> IgD<sup>-</sup> CD27<sup>+</sup> Ki67<sup>+</sup> plasmablasts, and TGF- $\beta$ -expressing CD19<sup>+</sup> CD38<sup>int</sup> IgD<sup>+</sup> CD27<sup>-</sup> PD-L1<sup>+</sup> naïve Bregs (Chapter 4, **Figure 4.1**).

Furthermore, to provide a broader understanding of the potential dysregulation among cytokine-expressing B cells in patients with melanoma, I employed an intracellular cytokine assay to quantify the percentages of IL-10<sup>+</sup>, TGF- $\beta$ <sup>+</sup>, IL-4<sup>+</sup>, IFN- $\gamma$ <sup>+</sup> and TNF- $\alpha$ <sup>+</sup> populations among total circulating B cells by interrogating an additional cohort of melanoma patients and matched healthy volunteers. Culture conditions used to profile human B cell cytokine expression in previously published investigations have been markedly heterogeneous and have included innate pathway stimulation alone [243] (usually via TLR9 ligands such as CpG ODN 2006), adaptive pathway stimulation via CD40-signaling [121], and a combination of the two approaches [132]. I therefore opted to test a range of activation conditions from the published literature to provide a

comprehensive analysis of cytokine-expressing B cells in their response to innate and adaptive pathway stimulation, which are both expected to take place *in vivo*.

My intracellular cytokine assay analyses demonstrated significantly lower proportions of circulating IFN- $\gamma^+$  and TNF- $\alpha^+$  inflammatory B cells in the patient compared to healthy volunteer circulation. In support of the upregulation of TGF- $\beta$ -expressing B cell subsets detected by CyTOF, I found a trend towards increased total TGF- $\beta^+$  Bregs among melanoma patient compared to healthy volunteer B cells (Chapter 4, **Figure 4.3**), although among a limited cohort of ten individuals. Collectively, my analyses suggest an overall dysregulated cytokine-expressing B cell compartment in melanoma patient circulation, which appears to favour the induction of regulatory B cell subpopulations, alongside a collapse in pro-inflammatory (IFN- $\gamma^+$  and TNF- $\alpha^+$ ) B cells.

Recently published work found that decreased proportions of circulating TNF- $\alpha^+$  inflammatory B cells correlated with response to checkpoint blockade in a cohort of melanoma patients [299]. This finding highlights the complex role of known pro-inflammatory cytokines such as TNF- $\alpha$  in their contributions to anti-tumour immunity. For example, TNF- $\alpha$  expression has been shown to mediate tumour cell apoptosis and promote immune cell proliferation and survival [335]. In contrast, sustained inflammation is a hallmark of cancer [300], and it is possible that the associated chronic exposure to TNF- $\alpha$  and its network of ligands and receptors can stimulate survival factors such as anti-apoptotic proteins, proangiogenic mediators, and metastatic markers [301]. Overall, the mechanistic origin and prognostic implications of the observed collapse in pro-inflammatory (IFN- $\gamma^+$  and TNF- $\alpha^+$ ) circulating B cell phenotypes among melanoma patients presented in this Thesis necessitate elucidation in further studies.



One of the key aims of the work presented in Chapter 4 was to gain an insight the localisation of cytokine expression among B cell lineage subpopulations in the melanoma patient circulating B cell compartment, for which phenotypic descriptions of regulatory and inflammatory B cell subsets have not yet been determined. Early studies suggested that human memory B cells may produce pro-inflammatory cytokines such as lymphotoxin and TNF- $\alpha$ , while naïve cells may confer a more suppressive and tolerogenic profile involving IL-10-expression [127]. However, in our cohort, my analyses point to the identification of IL-10<sup>+</sup> Bregs within diverse B cell lineages, including the CD24<sup>hi</sup> CD38<sup>-</sup> memory B cell, CD24<sup>hi</sup> CD38<sup>hi</sup> transitional B cell, and CD24<sup>int</sup> CD38<sup>int</sup> naïve B cell lineages [248] (Chapter 4, **Figure 4.4**). This instead suggests that immunosuppressive Bregs may develop from multiple developmental lineages.

My evaluation of intracellular cytokine expression categorised by B cell lineage, revealed that melanoma patient B cells expressing each of IL-10, TGF- $\beta$  and TNF- $\alpha$  cytokines were present across B cell lineages, although with a marked preference towards a CD27<sup>+</sup> memory phenotype, while TGF- $\beta$ <sup>+</sup> B cells were mostly non-isotype-switched (Chapter 4, **Figure 4.4**). Although my results do not preclude the presence of elusive extracellular markers which may faithfully associate with B cell cytokine expression profiles, it may be appropriate to consider B cell cytokine expression as an inducible and dynamic trait which is present throughout diverse B cell lineages.

To my knowledge, I have provided the first report of the circulating memory B cell pool as an important source of both regulatory and pro-inflammatory cytokines in patients with melanoma. These observations may encourage future studies to focus upon the plasmablast and memory B cell pools as rich sources of cytokine-expressing B cells.

### 5.3.2 An immune dichotomy: Immunostimulatory and immunomodulatory influences of B cells in melanoma

Following my observations of systemic dysregulation among cytokine-expressing B cells in patients with melanoma, I sought to investigate cytokine expression profiles (regulatory IL-10 and TGF- $\beta$ , and pro-inflammatory TNF- $\alpha$ ) within the TIL-B compartment.

I found diminished proportions of TNF- $\alpha$  expressed B cells in patient tumours compared to patient peripheral blood (which were already lower than those found in the circulation of healthy volunteers) using intracellular cytokine phenotyping (Chapter 4, **Figure 4.6**). In concordance, I observed only minor populations of TNF- $\alpha$ <sup>+</sup> B cells within a pooled single cell RNA-seq cohort (Chapter 4, **Figure 4.6**) and I detected a limited presence of TNF- $\alpha$ <sup>+</sup> CD20<sup>+</sup> TIL-B when I analysed human melanoma lesion samples by immunofluorescence staining (Chapter 4, **Figure 4.7**). These findings suggest that pro-inflammatory TNF- $\alpha$ <sup>+</sup> expressing B cells are not only reduced in the circulation but are also sparse in melanoma lesions and may denote regulation of the humoral immune compartment in melanoma.

On the other hand, this Thesis reports that TGF- $\beta$ -expressing Breg populations are prominent in the blood of patients with melanoma, and scRNA-seq data in tumour lesions demonstrated the presence of a significant population of TGF- $\beta$ <sup>+</sup> B cells in the tumour microenvironment. TGF- $\beta$  expression by B cells may support an immunosuppressive environment and could engage in signaling with T cells. In concordance, *ex vivo* co-cultures of melanoma patient-derived B cells with autologous Tcon cells depleted of Tregs resulted in TGF- $\beta$ -mediated induction of FOXP3<sup>+</sup> Tregs (Chapter 4, **Figure 4.13**).

Using CellPhoneDB analyses from the pooled scRNA-seq data, I identified distinct predicted B cell:T cell communication pathways for TIL-B stratified by their cytokine expression. TGF- $\beta^+$  B cells expressed the immune checkpoint receptor Galectin-9, which may signal with Tregs via CD44 (Chapter 4, **Figure 4.9**). Moreover, this interaction has been previously described to act synergistically with TGF- $\beta$  signaling, to promote FOXP3 expression, and to enhance the function and stability induced Tregs [306]. Overall, evidence presented in this Thesis points to TGF- $\beta$  regulatory Breg populations as potential players in functionally supporting the generation and function of Tregs. These observations represent previously undescribed findings, as the significance of melanoma patient B cells in contributing to *ex vivo* Treg generation had not been investigated before. My CellPhoneDB analyses also identified predicted interactions between tumour-infiltrating TNF- $\alpha^+$  B cells and Tregs, including via pro-inflammatory mediators TNF- $\alpha$ , LT- $\alpha$ , and MIF, and the ICOS/ICOSL axis (Chapter 4, **Figure 4.9**), which may also drive the phenotypic stability and suppressive activity of Tregs [322,323]. Together with my observations of predicted TGF- $\beta^+$  B cell / Treg crosstalk, these findings reveal previously undescribed interactions between cytokine-expressing B cell subsets and Tregs. Additional studies are required to further elucidate the significance of signaling between TGF- $\beta^+$ /TNF- $\alpha^+$  B cells and Tregs, and their potential roles in supporting tumour progression through enhancements of Treg function and stability.

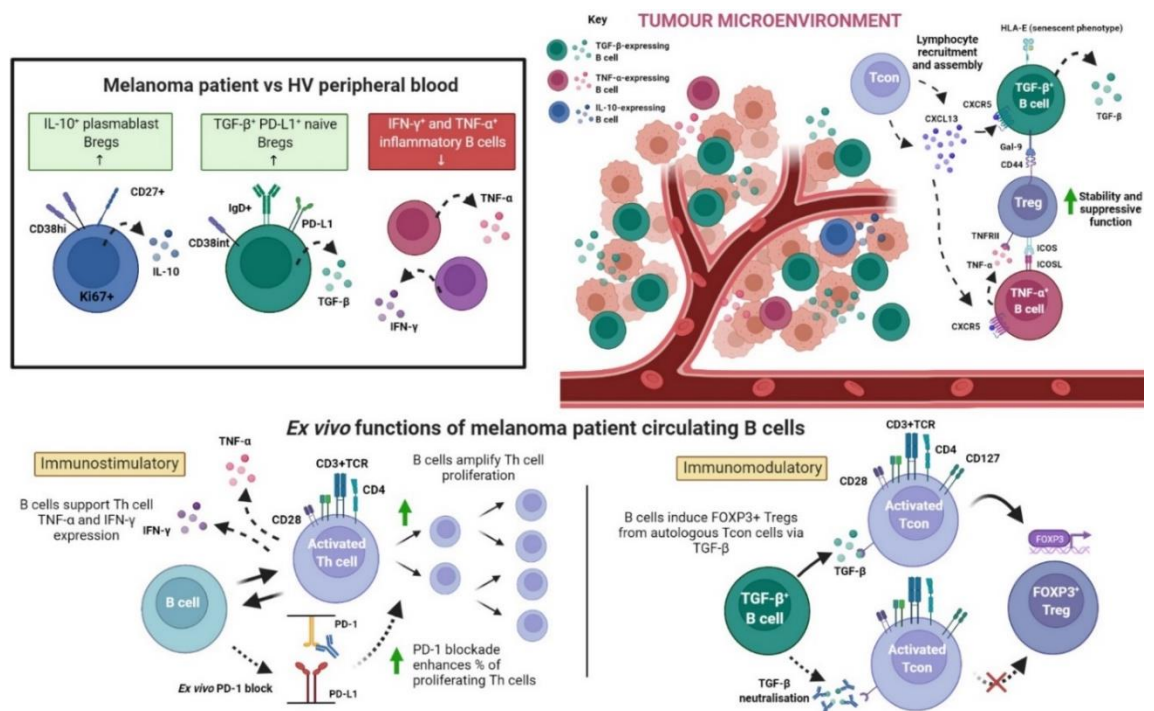
On the other hand, in this Thesis I have presented evidence that B cells, including those extracted from patients with melanoma, may have a positive influence on T cells. Strikingly, I found that patient-derived B cells promoted the *ex vivo* proliferation of autologous T-helper cells (Chapter 4, **Figure 4.12**), while allowing autologous T-helper cells to produce pro-inflammatory cytokines (IFN- $\gamma$  and TNF- $\alpha$ ) (Chapter 4, **Figure 4.11**). These observations suggest that, despite the observed declines in pro-inflammatory

cytokine expression (Chapter 4, **Figure 4.3**), patient circulating B cells maintain their immunostimulatory capacities *ex vivo*. Interestingly, anti-PD-1 treatment further enhanced B cell-associated proliferative signalling on T cells (Chapter 4, **Figure 4.12**).

Together these findings highlight the wider immune dichotomy in the roles of B cell responses in melanoma, whereby the overall contributions of B cells towards tumour surveillance may hinge upon a balance between immunostimulatory and immunomodulatory capabilities. Further investigations into the factors influencing this balance are warranted, and therapies that may compel B cell responses towards pro-inflammatory and immunostimulatory responses may offer new options for treatment success in the clinic.

### 5.3.3 Graphical summary

A graphical summary of my key findings concerning the role of cytokine-expressing B cells as complex and dynamic players in systemic and intratumoural immunity of melanoma patients is illustrated in **Figure 5.2**.



**Figure 5.2** Cytokine-expressing B cells in melanoma are dysregulated in melanoma patient circulation, may engage in crosstalk with Tregs in the TME, and engender immunostimulatory and immunomodulatory influences ex vivo.

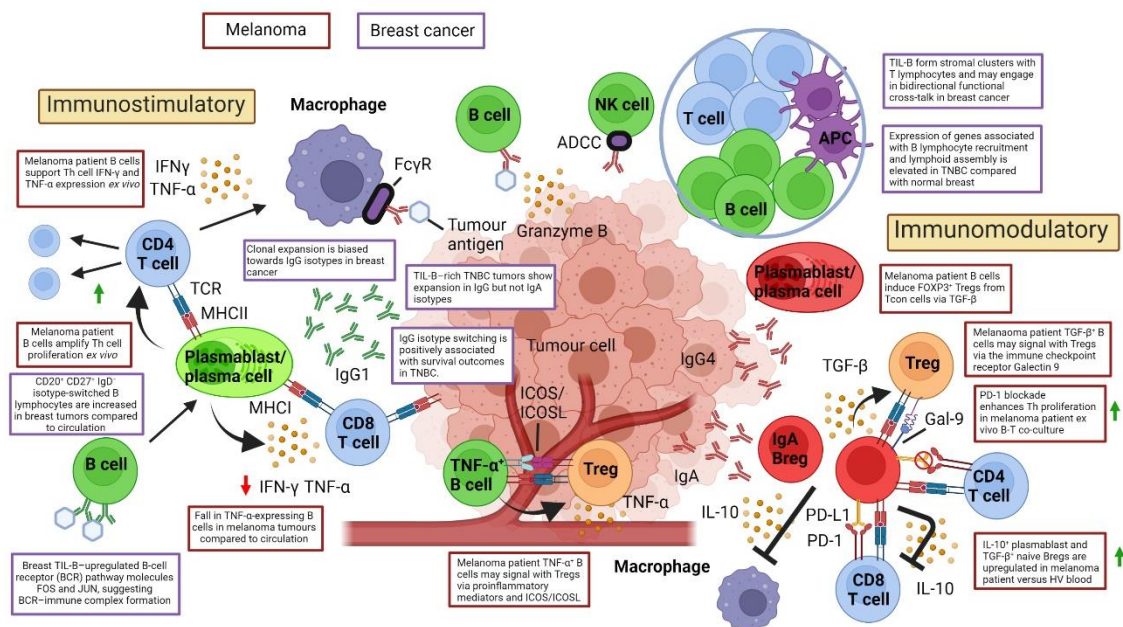
Created with BioRender.com [86].

My research presented in Chapter 4 identified dysregulation among cytokine-expressing B cells in melanoma patient circulating B cell compartment which favoured regulatory phenotypes. I found enriched circulating populations of IL-10-expressing CD19<sup>-</sup> CD38<sup>hi</sup> IgD<sup>-</sup> CD27<sup>+</sup> Ki67<sup>+</sup> plasmablasts, and TGF- $\beta$ -expressing CD19<sup>+</sup> CD38<sup>int</sup> IgD<sup>+</sup> CD27<sup>-</sup> PD-L1<sup>+</sup> naïve Bregs, simultaneous to reduced pro-inflammatory IFN- $\gamma$ <sup>+</sup> and TNF- $\alpha$ <sup>+</sup> B cells in melanoma patients compared to matched healthy volunteers. Melanoma patient

circulating B cells expressing each of IL-10, TGF- $\beta$  and/or TNF- $\alpha$  cytokines were identified across multiple B cell lineages, although cytokine expressing B cells showed a tendency towards a CD27<sup>+</sup> memory phenotype, analysed in *ex vivo* cultures. Within melanoma lesions, TNF- $\alpha$ -expressing B cells were sparse and proportionally reduced compared to those present in the patient circulation, whereas substantial populations of intratumoural TGF- $\beta$ <sup>+</sup> B cells were detected. TGF- $\beta$ <sup>+</sup> B cells featured a HLA-E<sup>+</sup> senescent phenotype and may support the differentiation and maintenance of Tregs in melanoma tumours through expression of Galectin-9. On the other hand, the less well represented tumour-associated TNF- $\alpha$ <sup>+</sup> B cells were predicted to engage in crosstalk with Tregs, including via the ICOS/ICOSL axis and TNF- $\alpha$  signaling, which could support the suppressive activity of Tregs in the melanoma TME. Expression of CXCL13 by Tcon cells may participate in the recruitment of both TGF- $\beta$ <sup>+</sup> and TNF- $\alpha$ <sup>+</sup> B cells. Lastly, *ex vivo* B:T cell co-cultures demonstrated that patient-derived B cells promoted the proliferation of autologous T-helper cells, which could be further enhanced with anti-PD-1 treatment, and also permitted autologous T-helper cells to produce pro-inflammatory cytokines (IFN- $\gamma$  and TNF- $\alpha$ ). In contrast, melanoma patient B cells significantly induced *ex vivo* FOXP3<sup>+</sup> Treg generation from autologous purified CD25<sup>-int</sup> CD127<sup>+</sup> conventional T-helper cells via TGF- $\beta$ . Overall, I established that cytokine-expressing B cells are dysregulated in the circulation of melanoma patients, may infiltrate tumours and engage in crosstalk with and promote Tregs in the TME, while still being able to participate in immunostimulatory T cell functions *ex vivo*.

## 5.4 Concluding remarks

In conclusion, the emphasis of this Thesis has been to unravel the nature of humoral immune responses to breast cancer and melanoma, including to identify novel features and biases among circulating and tumour-infiltrating B lymphocyte populations, as well as to elucidate their roles and functional significance, and to place these findings within the wider context of the adaptive immune response. A graphical summary depicting the key findings contained within this Thesis is illustrated in **Figure 5.3**.



**Figure 5.3** Graphical summary of the key findings contained within this Thesis, highlighting the contrasting immunostimulatory and immunomodulatory roles of B cells within the context of the immune response to solid tumours.

Adapted from [161] and created with BioRender.com [86].

In breast cancer, I have shown that tumour-infiltrating B cells assemble in clusters, and undergo B cell receptor-driven activation, proliferation, and isotype-switching. Moreover, I found that clonally expanded, IgG isotype-biased humoral immunity associates with favourable prognosis, primarily in triple-negative breast cancers.

In melanoma, I focused my attention upon the role of B cells as cytokine expressing cells, which in the context of the humoral response to solid tumours has received little attention to date. I found that circulating cytokine-expressing B cells are dysregulated in melanoma patient blood, with a preference towards regulatory and away from pro-inflammatory subsets. Moreover, TIL-B with TGF- $\beta$  and TNF- $\alpha$ -expressing profiles may engage in crosstalk with Tregs and support their phenotypic stability and function. Lastly, I have highlighted the contrasting immunostimulatory and immunomodulatory functions of melanoma patient B cells, whereby they may enhance autologous T-helper cell proliferation *ex vivo*, which is further enhanced during PD-L1 blockade, but they can also induce *ex vivo* FOXP3<sup>+</sup> Tregs from Tcon cells.

There may be many similarities within the B cell responses to breast cancer, melanoma, and other solid tumours. In my study in patients with breast cancer, I report a collapse of the circulating memory B cells in patients compared with healthy subjects. A similar finding has been shown in patients with melanoma [152] and confirmed in extended studies in our laboratory (Dr Silvia Crescioli, Dr Zena Willmore, personal communication and manuscripts in preparation). This impaired memory B cell compartment could be a result of reduced pro-inflammatory and differentiation signals which would normally be required to activate and retain systemic humoral immunity and may be a feature of malignant diseases. Further work would be required to determine whether this phenomenon is found in other tumour types.

More broadly, I observed perturbations of circulating B cell subsets in both melanoma and breast cancer. Aside from reduced memory B cell subsets in breast cancer, I observed enhanced regulatory B cell populations in melanoma, together supporting the notion that remodelling of the wider immune landscape may be a feature of these solid tumours. There is some evidence that dysregulation, including biases towards regulatory B cell



phenotypes, among cytokine-expressing B cells may be a common feature of patients with solid tumours. For instance, a previous study has identified an upregulated IL-10-expressing Breg compartment in the peripheral blood and tumours of patients with gastric cancer [243].

Another interesting parallel may be the skewing of immunoglobulin expression towards IgG isotypes which I have observed among TIL-B in breast cancer. For example, in single-cell RNAseq evaluations, I found enhanced IgG1, IgG2, IgG3 and IgG4 expression by memory B cells in breast cancer lesions. The features I have identified bear some parallels with previously published observations in melanoma, whereby TIL-B were reported to express isotype-switched antibodies such as IgG, and a bias away from IgG1 and towards IgG4 isotypes has also been reported in the melanoma TME [182]. Previous work has identified similar features including favoured expression of IgG4<sup>+</sup> B cells in solid tumours such as colon cancer [234] and cholangiocarcinoma [336,337]. Together, these observations may signify that B cells can receive a combination of stimulation signals in the tumour microenvironment, which may promote not only isotype-switching but also favour expression of antibodies across the IgG isotypes including the less often represented IgG4.

Finally, my observations of the contrasting immunostimulatory and immunomodulatory roles of B cells in their response to solid tumours provide the backbone for further studies investigating the underlying factors which may determine the balance of these polarising features. Biases towards immunostimulatory or immunomodulatory activity in the TME may ultimately determine the course of tumour progression and may even predict response to therapy. Therapeutic interventions which could unleash the immunostimulatory power of B cells whilst suppressing their immunomodulatory functions may be considered to improve outcomes. For example, my studies have shown

that the function of melanoma patient circulating B cells as promoters of T cell proliferation may be further enhanced by the addition of an anti-PD-1 antibody. Overall, it may be possible to combine B cell-activating therapies with existing checkpoint immunotherapies, to boost the pro-inflammatory functions of B cells. Such combinations may offer a more complete immunotherapeutic strategy that would account for a currently less-well appreciated player in the immune response to solid tumours.

# Appendix

## Full manuscript of (Harris et al. 2021)

Published OnlineFirst June 15, 2021; DOI: 10.1158/0008-5472.CAN-20-3773

CANCER RESEARCH | TUMOR BIOLOGY AND IMMUNOLOGY

### Tumor-Infiltrating B Lymphocyte Profiling Identifies IgG-Biased, Clonally Expanded Prognostic Phenotypes in Triple-Negative Breast Cancer



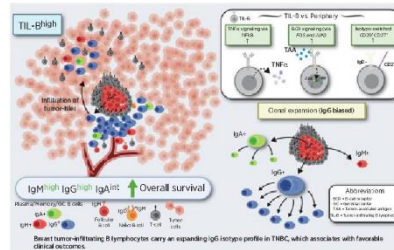
Robert J. Harris<sup>1,2,3</sup>, Anthony Cheung<sup>1,2,4</sup>, Joseph C.F. Ng<sup>5</sup>, Roman Laddach<sup>1,2,6</sup>, Alicia M. Chenoweth<sup>1,2,4</sup>, Silvia Crescioli<sup>1,2</sup>, Matthew Fittall<sup>1,2,4</sup>, Diana Dominguez-Rodriguez<sup>1,2</sup>, James Roberts<sup>1,2,6</sup>, Dina Levi<sup>4</sup>, Fangfang Liu<sup>4</sup>, Elena Alberts<sup>1,2,4</sup>, Jelmar Quist<sup>4</sup>, Aida Santaolalla<sup>7,8</sup>, Sarah E. Pinder<sup>9,10</sup>, Cheryl Gillett<sup>9,10</sup>, Niklas Hammar<sup>7</sup>, Sheeba Irshad<sup>9</sup>, Mieke Van Hemelrijck<sup>7,8</sup>, Deborah K. Dunn-Walters<sup>11</sup>, Franca Fraternali<sup>5</sup>, James F. Spicer<sup>9</sup>, Katie E. Lacy<sup>1,2</sup>, Sophia Tsoka<sup>6</sup>, Anita Grigoriadis<sup>4</sup>, Andrew N.J. Tutt<sup>4,12</sup>, and Sophia N. Karagiannis<sup>1,2,4</sup>

#### ABSTRACT

In breast cancer, humoral immune responses may contribute to clinical outcomes, especially in more immunogenic subtypes. Here, we investigated B lymphocyte subsets, immunoglobulin expression, and clonal features in breast tumors, focusing on aggressive triple-negative breast cancers (TNBC). In samples from patients with TNBC and healthy volunteers, circulating and tumor-infiltrating B lymphocytes (TIL-B) were evaluated. CD20<sup>+</sup>CD27<sup>+</sup>IgD<sup>-</sup> isotype-switched B lymphocytes were increased in tumors, compared with matched blood. TIL-B frequently formed stromal clusters with T lymphocytes and engaged in bidirectional functional cross-talk, consistent with gene signatures associated with lymphoid assembly, costimulation, cytokine-cytokine receptor interactions, cytotoxic T-cell activation, and T-cell-dependent B-cell activation. TIL-B-upregulated B-cell receptor (BCR) pathway molecules POS and JUN, germinal center chemokine regulator RGS1, activation marker CD69, and TNF $\alpha$  signal transduction via NF $\kappa$ B, suggesting BCR-immune complex formation. Expression of genes associated with B lymphocyte recruitment and lymphoid assembly, including CXCL13, CXCR4, and DC-LAMP, was elevated in TNBC compared with other subtypes and normal breast. TIL-B-rich tumors showed expansion of IgG but not IgA isotypes, and IgG isotype switching positively associated with survival outcomes in TNBC. Clonal expansion was biased toward IgG, showing expansive clonal families with specific variable region gene combinations and narrow repertoires. Stronger positive selection pressure was present in the

complementarity determining regions of IgG compared with their clonally related IgA in tumor samples. Overall, class-switched B lymphocyte lineage traits were conspicuous in TNBC, associated with improved clinical outcomes, and conferred IgG-biased, clonally expanded, and likely antigen-driven humoral responses.

**Significance:** Tumor-infiltrating B lymphocytes assemble in clusters, undergoing B-cell receptor-driven activation, proliferation, and isotype switching. Clonally expanded, IgG isotype-biased humoral immunity associates with favorable prognosis primarily in triple-negative breast cancers.



<sup>1</sup>St. John's Institute of Dermatology, School of Basic and Medical Biosciences, King's College London, London, United Kingdom. <sup>2</sup>NHR Biomedical Research Center at Guy's and St. Thomas' Hospitals and King's College London, Guy's Hospital, King's College London, London, United Kingdom. <sup>3</sup>King's Health Partners Cancer Research UK Cancer Center, King's College London, London, United Kingdom. <sup>4</sup>Breast Cancer Now Research Unit, School of Cancer and Pharmaceutical Sciences, King's College London, Guy's Cancer Center, London, United Kingdom. <sup>5</sup>Randall Center for Cell and Molecular Biophysics, King's College London, London, United Kingdom. <sup>6</sup>Department of Informatics, Faculty of Natural and Mathematical Sciences, King's College London, London, United Kingdom. <sup>7</sup>Unit of Epidemiology, Institute of Environmental Medicine, Karolinska Institutet, Stockholm, Sweden. <sup>8</sup>School of Cancer and Pharmaceutical Studies, Translational Oncology and Urology Research (TOUR), King's College London, London, United Kingdom. <sup>9</sup>School of Cancer and Pharmaceutical Sciences, King's College London, Comprehensive Cancer Center, Guy's Hospital, London, United Kingdom. <sup>10</sup>King's Health Partners Cancer Biobank, King's College London, London, United Kingdom. <sup>11</sup>Faculty of Health and Medical Sciences, University of Surrey, Guildford, United Kingdom. <sup>12</sup>Breast Cancer

Now Toby Robins Research Center, Institute of Cancer Research, London, United Kingdom.

**Note:** Supplementary data for this article are available at Cancer Research Online (<http://cancerres.aacrjournals.org/>).

R.J. Harris and A. Cheung contributed equally as co-authors of this article.

**Corresponding Author:** Sophia N. Karagiannis, St. John's Institute of Dermatology, School of Basic and Medical Biosciences, King's College London, Guy's Hospital, Tower Wing, 9th Floor, London, SE1 9RT, UK. Phone: 44-207-188-6355; E-mail: [sophia.karagiannis@kcl.ac.uk](mailto:sophia.karagiannis@kcl.ac.uk)

Cancer Res 2021;81:4290-304

doi: 10.1158/0008-5472.CAN-20-3773

This open access article is distributed under Creative Commons Attribution-NonCommercial-NoDerivatives License 4.0 International (CC BY-NC-ND).

©2021 The Authors; Published by the American Association for Cancer Research

## Introduction

Initiation of effective adaptive immunity may contribute to tumor growth restriction through specific antigen-directed responses. The T lymphocyte component of antitumor immunity has received significant attention (1). In contrast, B lymphocytes, especially the memory and isotype-switched B lymphocyte compartments, and their expressed antibody profiles remain only partially elucidated. Emerging findings suggest that aspects of humoral immune responses may correlate with improved clinical outcomes via B lymphocyte tumor-infiltration and expression of antibodies in lesions or in the circulation (2, 3). These could differ across tumor types, potentially offering opportunities for stratification and for guiding therapy options.

Breast cancer is one of the most frequently diagnosed malignancies, divided into biological, and differential therapy-associated subtypes based on estrogen receptor (ER), progesterone receptor (PR), and HER2 expression, with specific prognostic and predictive biomarker implications. Triple-negative breast cancers (TNBC) do not express any of these markers and demonstrate the least-favorable prognosis due to both an aggressive phenotype and limited targeted therapies (4). Although breast cancer has not traditionally been regarded as a typical immunogenic malignancy, emerging studies report the presence and potential clinical significance of tumor-infiltrating immune cells for clinical outcomes (5). Paradoxically, despite an overall poor prognosis of patients with TNBC, immune infiltration is more pronounced compared with other breast cancer types. Consistent with an immunogenic tumor microenvironment (TME), some patients with TNBC may benefit from anti-programmed death-ligand 1 (PD-L1) and anti-PD-1 immunotherapy with atezolizumab in combination with chemotherapy (6). TNBCs are characterized by immunologically variable and compartmentalized tumors with structural features in the tumor-immune interphase and large variability across individuals, mandating the need for patient stratification for therapy selection (7). The most thoroughly studied effector cells within the breast cancer setting are CD8<sup>+</sup> cytotoxic T lymphocytes and natural killer (NK) cells (8). However, tumor-infiltrating B lymphocytes (TIL-B) aggregating within tertiary lymphoid structures (TLS; ref. 9) may have an antigen-educated phenotype (10) and autoantibodies are thought to trigger tumor cell clearance (11). TIL-Bs might also serve as antigen-presenting cells to promote antitumor Th responses (12). Therefore, it is increasingly recognized that humoral immune responses may be important contributors to breast cancer outcome, especially in more immunogenic TNBCs.

The interaction between the immune system and malignant cells, therefore, constitutes a major focus of current translational and clinical investigation (13). Recent studies have provided evidence of TIL-Bs and tumor-reactive immunoglobulin (Ig) in several solid tumors, including in breast cancer, and TIL-Bs have been reported to respond to B-cell receptor stimulation and produce Igs *ex vivo* (14–16).

Here, in peripheral blood and cancer lesions of patients with breast cancer, specifically in individuals with TNBC, we performed flow cytometric, transcriptomic, immunofluorescence, single-cell RNA-sequencing (scRNA-seq), and long-read Ig repertoire studies to evaluate isotype-switched and memory B lymphocyte subsets, Ig isotype distribution, and clonal expansion profiles.

## Materials and Methods

### Clinical sample collection and cohort descriptions

A collection of internal and external cohorts of healthy volunteer (HV) and patient samples, including the unique accession numbers,

are summarized in Supplementary Table S1 and Supplementary Materials and Methods. All internal King's College London (KCL) samples were collected with informed written consent, in accordance with the Helsinki Declaration [study design was approved by the Guy's Research Ethics Committee (REC No. 07/H0804/131), Guy's and St. Thomas' NHS Foundation Trust]. Peripheral blood mononuclear cells were isolated using Ficoll–Paque PLUS density gradient centrifugation, and single cells from breast tissues were isolated as described previously in Supplementary Materials and Methods.

### Gene expression profiling of lymphocyte and lymphoid assembly markers

Gene expression (GEX) levels were analyzed from internal Guy's Hospital and The Cancer Genome Atlas (TCGA) Breast cohorts (KCL and TCGA GEX cohorts), and compared between PAM50 (basal-like, HER2, luminal A, luminal B, and normal-like) and TNBC subtypes (basal-like 1/2, immunomodulatory, mesenchymal, mesenchymal stem-like, and luminal androgen receptor) according to classification described previously in Brasó-Maristany and colleagues (17). A B lymphocyte metagene signature was analyzed from published Nano-String data of primary and metastatic breast cancers (GSE102818; ref. 18). Kaplan–Meier (KM) plotter tool was used to generate survival plots (19). CIBERSORT was applied to evaluate naïve B, plasma, and memory B cells identified among 22 immune subsets in the KCL GEX cohort (20). Univariate Cox proportional hazards regression models were used to investigate the prognostic importance of these immune subsets in high and low TIL-infiltrated tumors (semiquantitative TIL classification was performed by a trained histopathologist using tissue microarrays; Supplementary Materials and Methods). B lymphocyte function-associated gene sets were identified from gene ontology (GO) database (Supplementary Materials and Methods). A lymphoid assembly-associated gene signature was compiled from a set of known markers (21).

### scRNA-seq analysis

Analyses were performed on a published scRNA-seq dataset (GSE114725; ref. 22; single-cell cohort) using R package *Seurat* (23). Dimensionality reduction was performed using Uniform Manifold Approximation and Projection (UMAP) and cells were clustered using the Louvain algorithm (23). Ig isotypes were detected based upon heavy-chain gene expression. Differentially expressed genes identified by *Seurat* were used to perform gene set enrichment analysis (GSEA) using the *fgsea* package. Gene sets were obtained from Broad Institute Molecular Signature Database using R package *msigdb* (24). CellPhoneDB v2.0 was used to analyze B-cell–T-cell interactions (25).

### Immunohistochemical/immunofluorescence evaluations of TIL-B distribution and surface Ig expression

Three sections per tissue sample were stained with fluorescently labeled antibodies conferring three panels: TIL classification (DAPI/CD20/CD3/PanCK), naïve B lymphocyte identification (DAPI/CD20/IgD), and Ig isotype expression (DAPI/CD27/IgG/IgA/IgM). Antibodies used are detailed in Supplementary Table S2. TIL-B structural features were evaluated (Supplementary Materials and Methods) following TIL working group guidelines (26), guided by trained pathologists. Olympus VS120-S5 and Nikon TE 2000-U microscopes were used for imaging.

### Long-read Ig repertoire analysis

Ig repertoire analysis was performed from cDNA synthesized from breast tissues with the 5' RACE template switch method

Harris et al.

(Supplementary Materials and Methods). Full-length Ig cDNAs were PCR-amplified with primers containing unique molecular barcodes. Purified DNA samples were sequenced using PacBio Single Molecule, Real-Time (SMRT) Sequencing platform (27). Redundant sequences with identical molecular barcodes were removed. Ig genes and complementarity determining region (CDR) 3 sequences were determined using IMG1/HighV-QUEST (28). Relatedness among sequences were estimated using BRepertoire webserver (29) "Clonotype clustering" function, after partitioning all CDR3 DNA sequences by the sample and the V gene family used (30). Selection pressure analysis was performed using R package *shazam* (31).

#### Data availability

The R code used to analyze scRNA-seq data from GSE114725 (22) can be accessed from <https://codeocean.com/capsule/7488142>. The R code to analyze BCR Repertoire data collected from breast tissues can be accessed at <https://codeocean.com/capsule/4153741>.

#### Statistical analyses

GraphPad Prism and R were used for statistical analyses of paired and unpaired datasets. Data are presented as mean  $\pm$  SEM. *P* values reported as \*, *P* < 0.05; \*\*, *P* < 0.01; \*\*\*, *P* < 0.001; \*\*\*\*, *P* < 0.0001 and all tests were two-sided.

Further details can be found in Supplementary Materials and Methods.

## Results

### Collapse in circulating memory B lymphocytes contrasts with amplification of intratumoral class-switched memory B lymphocyte compartment

We compared B lymphocyte subsets between breast cancer patient blood and tumors (KCL flow cohort; see Supplementary Table S1 for information of all cohorts used). We quantified percentages of B lymphocytes (CD19<sup>+</sup>CD20<sup>+</sup>) and memory (CD19<sup>+</sup>CD20<sup>+</sup>CD27<sup>+</sup>) B lymphocytes (B<sup>m</sup>) in patients (*N* = 55) and healthy subjects (*N* = 48) by flow cytometry (Fig. 1A and B). Consistent with a report in melanoma (32), we identified a fall in peripheral B<sup>m</sup> in patients compared with HVs. This was independent of disease stage or chemotherapy treatment status. We observed significantly lower proportions of B lymphocytes (of CD45<sup>+</sup> cells) in the circulation of patients with recent chemotherapy compared with those without treatment (Fig. 1B), alongside reduced serum Ig titers in chemotherapy-treated individuals (Supplementary Fig. S1A and S1B, KCL Luminex cohort). Baseline serum Ig isotype titers in patients were not predictive of breast cancer-specific death [Supplementary Fig. S2, Apolipoprotein Mortality Risk (AMORIS) cohort; ref. 33].

In contrast, using tumor single-cell suspensions (*N* = 17), we identified a higher B lymphocyte infiltration compared with non-adjacent, nontumor (NANT; *N* = 12) and normal breast (*N* = 9) tissues (Fig. 1C). In matched blood and tumor samples (*N* = 7), tumors contained higher CD20<sup>+</sup>CD27<sup>+</sup> B-cell proportions (Fig. 1D). Both peripheral and intratumoral CD20<sup>+</sup>CD27<sup>+</sup> B-cell populations showed a bias toward the loss of IgD expression (*N* = 32; Fig. 1E). Additional quantitative single B lymphocyte gene expression analyses (single-cell cohort) also confirmed larger proportions of CD20<sup>+</sup>CD27<sup>+</sup> and CD20<sup>+</sup>CD27<sup>+</sup>IgD<sup>-</sup> B lymphocytes in tumors compared with blood (Supplementary Fig. S3A and S3B). Furthermore, isotype-switched TIL-B populations comprise

memory, germinal center (GC) B cells and plasma cells in non-TNBC and TNBC [immunohistochemical/immunofluorescence (IHC/IF), KCL IHC cohort and Single cell cohort; Supplementary Fig. S3A–S3E].

These findings reveal a reduced peripheral B<sup>m</sup> population in patients compared with HVs, independently of disease stage or treatment, in parallel with an enriched tumor-infiltrating class-switched B-cell compartment in the TME compared with matched patient blood.

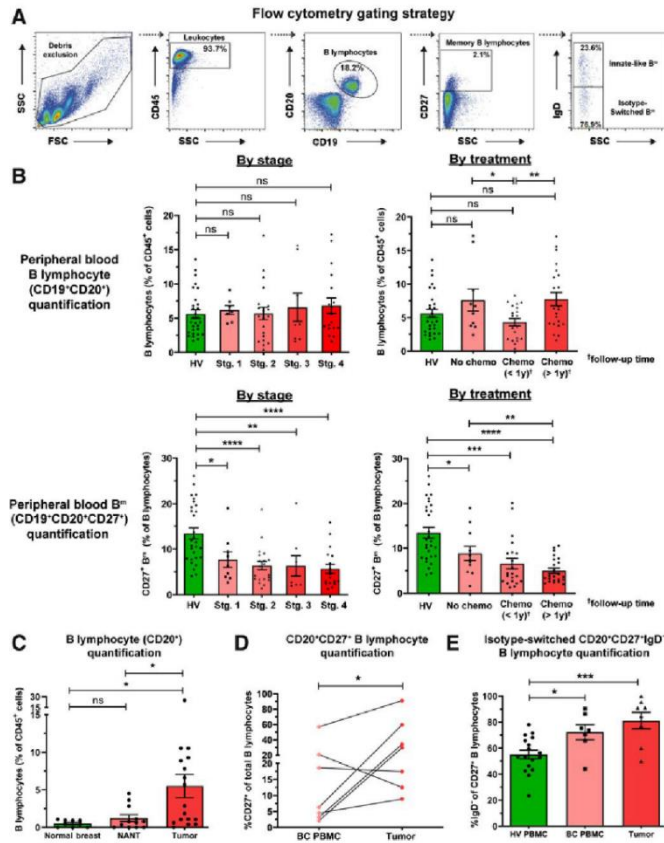
### Elevated TIL-B signatures and assembly within stromal clusters in TNBC

We asked whether TNBC demonstrate increased immune cell infiltration, particularly concentrating on the B-cell population, compared with normal breast or other breast cancer types. Quantitative IHC/IF evaluations (Bart's IHC cohort) and GEX analyses (KCL and TCGA GEX cohorts) revealed an expansion of CD20<sup>+</sup> TIL-B within TNBC lesions compared with normal tissues (Fig. 2A), and compared with non-TNBC carcinomas, expression of B lymphocyte (*CD20* and BCR complex *CD79A*) and T lymphocyte (*CD3D* and *CD3G*) markers were elevated in TNBC. Within different TNBC subtypes, these markers were elevated especially in the Lehmann's immunomodulatory (IM) molecular TNBC subtype, known to be enriched in core immune signal transduction pathways and cytokine signaling (*N* = 122; Fig. 2A; Supplementary Fig. S4A and S4B; ref. 34). TIL-B density and *CD20* gene expression positively correlated with tumor-infiltrating T lymphocyte (TIL-T) density and *CD3* gene expression, respectively (Fig. 2B). The expression of a B lymphocyte metagene signature (NanoString cohort) was significantly higher in primary cancers compared with patient-matched metastatic sites (*N* = 31 vs. 17), suggesting a diminished immune TME with advanced disease (Fig. 2C).

Both quantitative IHC/IF (*N* = 15) and KM-plotter survival analysis (*N* = 241) demonstrated that TIL-B in primary tumors were significantly associated with more favorable overall survival, most prominently in basal-like/TNBC (Fig. 2D; Supplementary Fig. S4C). Additional KM analyses using CIBERSORT (from KCL GEX cohort, see Supplementary Materials and Methods; ref. 20) investigated the associations between distant metastasis-free survival (DMFS) and naïve, plasma, and memory B-cell phenotypes in TNBC (*N* = 89). In tumors with high TIL infiltrates (classified by using tissue microarrays), memory B cells were associated with a more-favorable DMFS, whereas a negative prognostic value was shown for naïve B cells in this cohort (Fig. 2E). IHC/IF staining analyses (Bart's IHC cohort) confirmed the heterogeneity of TIL-T and TIL-B (Fig. 2F), with evidence of expansive cluster formation [demarcated in white (>30 TIL-B and >30 TIL-T aggregated), typically of a B lymphocyte assembly adjacent to a T lymphocyte zone; Fig. 2G]. This highlighted close B–T lymphocyte interactions within the TME.

Because we found B–T lymphocyte clusters in a large proportion (9 of 15) of TNBCs (Bart's IHC cohort), we next evaluated TIL-B spatial and structural characteristics. We characterized TIL-B as either stromal or intratumoral, according to penetration within PanCK<sup>+</sup> tumor islets. Cells were further categorized as forming either clusters or dispersions, according to the extent of aggregation along with CD3<sup>+</sup> TIL-T (Fig. 3A). Tumors were split into TIL-B<sup>high</sup> and TIL-B<sup>low</sup> groups, as defined by median TIL-B density. B lymphocytes typically formed within stromal clusters irrespective of overall TIL-B density (Fig. 3B). Five individuals featuring highly clustered TIL-B characteristics showed a >5 year survival post-surgery (Fig. 3C). Consistent

Expanded Tumor-Infiltrating IgG<sup>+</sup> B Cells in TNBC



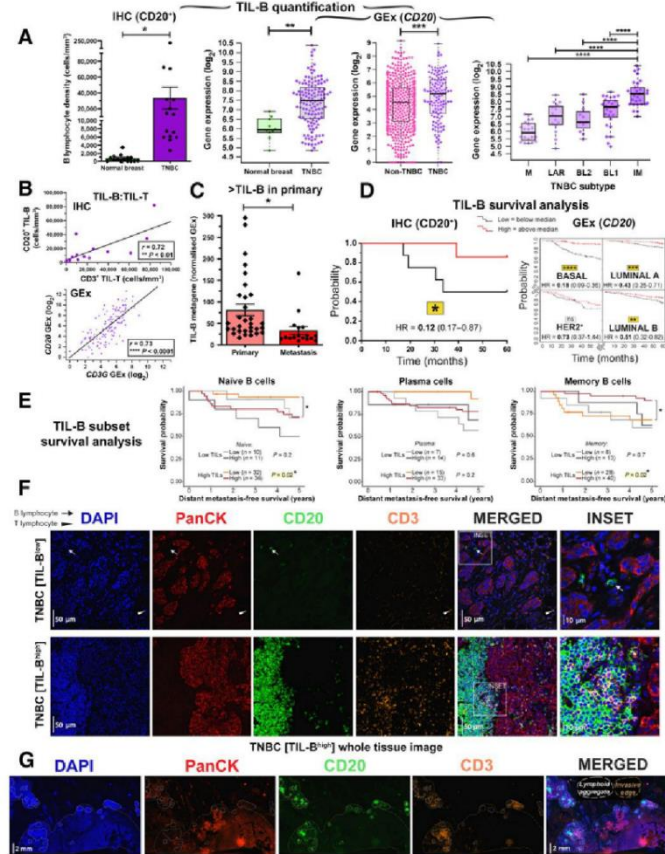
**Figure 1.** Flow cytometric analyses reveal reduced circulating CD20<sup>+</sup>CD27<sup>+</sup> memory and amplification of tumor-infiltrating CD20<sup>+</sup>CD27<sup>-</sup>IgD<sup>+</sup> class-switched subsets among B lymphocytes. **A**, Gating strategy for identification of B lymphocytes and memory (B<sup>m</sup>) lymphocytes derived from peripheral blood mononuclear cell (example patient peripheral blood mononuclear cell shown). **B**, Quantification of total circulating B cells (top) and B<sup>m</sup> cells (bottom) as percentage of CD45<sup>+</sup> cells in HV (N = 48) and patient (N = 55) peripheral blood (KCL flow cohort; Supplementary Table S1 for patient information), stratified according to stage and treatment status. **C**, Quantification of B lymphocytes (CD20<sup>+</sup>) from single cell suspensions of normal breast (N = 9), NANT (N = 12), and cancer tissue (N = 17) samples. **D**, Quantification of matched patient circulating- and tumor-infiltrating CD20<sup>+</sup>CD27<sup>-</sup> B cells (matched samples of 7 patients). **E**, Quantification of CD20<sup>+</sup>CD27<sup>-</sup>IgD<sup>+</sup> B cells in HV (N = 17), patient peripheral blood (N = 7), and cancers (N = 8) of total CD20<sup>+</sup>CD27<sup>-</sup> B cells. Statistical significance was determined using the Student *t* test. ns, nonsignificant; \*, *P* < 0.05; \*\*, *P* < 0.01; \*\*\*, *P* < 0.001; \*\*\*\*, *P* < 0.0001.

with the B-T lymphocyte cluster formation observed, we found elevated expression of B lymphocyte recruitment and lymphoid assembly marker genes (*CXCL13*, *CXCR4*, and *DC-LAMP*) in TNBC compared with both non-TNBC and normal breast, and within the TNBC cohort the highest expression of these genes was detected in IM tumors (Fig. 3D; Supplementary Fig. S4D, KCL and TCGA GEX

cohorts). Higher expression of these signatures were also associated with significantly improved odds of overall survival (10-year follow-up) in basal-like/TNBC (Fig. 3E, KM plotter cohort).

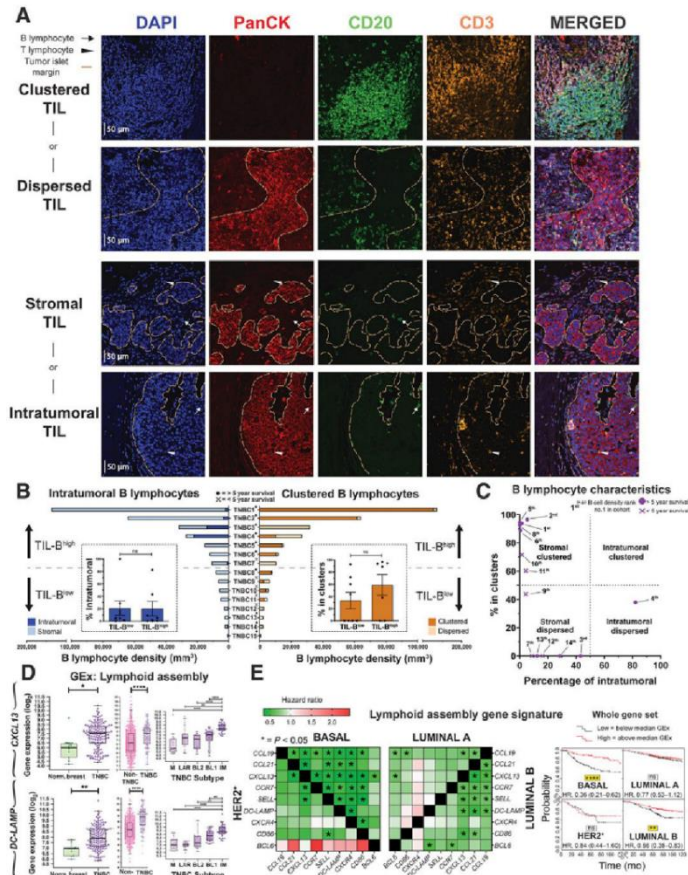
Therefore, substantial TIL-B densities in TNBC typically form clusters along with T lymphocytes. TIL-B marker (*CD20* and *CD79A*) and GEX features conferring B lymphocyte recruitment and lymphoid

Harris et al.



**Figure 2.** B lymphocyte infiltration and its positive prognostic value in TNBC. **A**, TIL-B quantification by IHC within normal breasts and TNBC ( $N = 15$  each, Bart's IHC cohort), and by GEX (normal breast vs. TNBC ( $N = 10$  vs. 131, KCL GEX cohort); non-TNBC vs. TNBC ( $N = 515$  vs. 123, TCGA GEX cohort); TNBC subtypes [mesenchymal (M), luminal androgen receptor (LAR), basal-like 1 and 2 (BL1 and 2), and immunomodulatory (IM);  $N = 122$ , KCL GEX cohort]. The Mann-Whitney test was used for statistical significance. **B**, TNBC TIL-B correlation with TIL-T by IHC ( $r = 0.72$ , Bart's IHC cohort) and by GEX ( $r = 0.73$ , KCL GEX cohort). Linear regression analysis was used to calculate correlation coefficients ( $r$ ) and  $P$  values. **C**, B lymphocyte metagene NanoString GEX data comparing B lymphocytes in primary tumors with metastatic sites ( $N = 31$  vs. 17; NanoString cohort). **D**, High (above median) TIL-B densities by IHC were associated with better overall survival in primary tumors with metastatic sites ( $N = 31$  vs. 17; NanoString cohort). **E**, Kaplan-Meier survival curves display DMFS for naive B cells, plasma cells, and memory B cells in TNBC (KCL GEX cohort) using CIBERSORT (20). Data were divided into four groups based on B lymphocyte subset and TIL levels stratified by semiquantitative TIL classification. Statistical significance was assessed using univariate Cox proportional hazards regression models. **F**, Representative IHC/IF images (Bart's IHC cohort) depicting nucleated cells (DAPI), epithelial cells (PanCK), B lymphocytes (CD20), and T lymphocytes (CD3) within TNBC TIL-B<sup>low</sup> and TIL-B<sup>high</sup> lesions. Scale bar, 50  $\mu$ m. **G**, Representative TNBC (TIL-B<sup>high</sup>) images highlighting numerous lymphoid aggregates (within white dash lines) consisting of B lymphocytes assembled adjacent to a T lymphocyte zone. Brown dash lines indicate carcinoma edge. Scale bar, 2 mm. \*,  $P < 0.05$ ; \*\*,  $P < 0.01$ ; \*\*\*,  $P < 0.001$ ; \*\*\*\*,  $P < 0.0001$ .

Expanded Tumor-Infiltrating IgG<sup>+</sup> B Cells in TNBC



**Figure 3.** Occurrence of B lymphocytes in stromal clusters. **A**, Representative IHC/F images (Bart's IHC cohort) highlighting key TIL characteristics: clustered TIL versus dispersed TIL and stromal TIL (outside tumor nests) versus intratumoral TIL (within tumor nests). Scale bar, 50  $\mu$ m. **B**, Quantitative assessment of TIL-B spatial and structural characteristics within TNBC ( $N = 15$ ; left) intratumoral versus stromal; clustered versus dispersed (right). Patients ranked according to CD20<sup>+</sup> TIL-B density (TNBC1 = highest), and overall survival data are indicated. Inset, patient samples split at median density into high and low TIL-B groups and the percentage of intratumoral (left) or clustered (right) B lymphocytes were analyzed. Statistical significance was determined using the Student  $t$  test. **C**, Characterization of TNBC TIL-B profile as stromal clustered, intratumoral clustered, stromal dispersed, or intratumoral dispersed. Overall survival data are indicated. **D**, GEX data for lymphoid assembly marker genes *CXCL13* and *DC-LAMP*; normal breast versus TNBC ( $N = 10$  vs. 131, KCL GEX cohort; left); non-TNBC vs. TNBC ( $N = 515$  vs. 123, TCGA GEX cohort; middle); TNBC subtypes ( $N = 122$ , KCL GEX cohort; right). **E**, Survival analysis in KM Plotter of determined ER-HER2<sup>+</sup>/basal surrogate, HER2<sup>+</sup>, luminal A, and luminal B subtype KM plotter surrogate subgroups (KM plotter cohort; ref. 19). These indicate that expression of lymphoid cell assembly genes carries positive prognostic value in TNBC/basal-like and luminal B subtypes. Individual genes were evaluated in combination with each other gene (left) and gene set as a whole (right). ns, nonsignificant; \*,  $P < 0.05$ ; \*\*,  $P < 0.01$ ; \*\*\*\*,  $P < 0.0001$ .



Harris et al.

assembly were elevated compared with non-TNBC and normal breast tissues, and associated with more favorable survival in basal-like/TNBC subtype.

#### TIL-Bs are activated via the B-cell receptor

We sought direct evidence of active roles for B lymphocytes in the TME, using a previously published dataset (single-cell cohort). We applied dimensionality reduction (UMAP) to single-cell B lymphocyte populations and revealed distinct CD20<sup>+</sup> and CD27<sup>+</sup> TIL-B populations compared with those in the circulation (blood ( $N = 1,476$  B cells) and tumors ( $N = 1,021$  B cells) of eight patients; Fig. 4A). Downstream differential expression gene (DEG) analysis identified several upregulated genes in TIL-B: *FOS* and *JUN*, molecules downstream of the BCR complex pathway (35); *RGS1*, germinal center B lymphocyte regulator of chemokine receptor signaling (36); and the lymphocyte activation marker *CD69*, triggered through cross-linking of surface Ig (Fig. 4B; ref. 37). Hallmark enrichment analysis (38) revealed significantly enhanced expression among TIL-B for genes controlling TNF $\alpha$  signaling via NF $\kappa$ B, hypoxia, and UV response pathways, in comparison with circulating B lymphocytes (Fig. 4C). Several genes, known to positively regulate B lymphocyte activation, proliferation, and differentiation functions were upregulated in TNBC compared with normal breast (Supplementary Fig. S5, KCL and TCGA GEx cohorts). Survival analysis of these gene signatures revealed positive associations with overall survival (10-year follow up), most pronounced in basal-like/TNBC (Fig. 4D, KM plotter cohort). We next evaluated B-cell-T-cell interactions in the TME (single-cell cohort) using CellPhoneDB (25). We identified cell communication pathways associated with lymphoid assembly (CXCL12, CCL19, CCL21, and CXCL13), cytokine signaling (IL4, IL6, IL13, IL15, IL17, and IFN $\gamma$ ), costimulation (CD28 and ICOS) and immune activation (CD40 and CD226). These findings support a bidirectional functional cross-talk between tumor-infiltrating B and T lymphocytes (Fig. 4E).

These findings indicate the presence of distinct B lymphocyte populations between patient blood and cancers and evidence of TIL-B antigen-Ig complexing, BCR pathway stimulation, and evidence of B-cell-T-cell cross-talk. Key functional attributes for the initiation of B lymphocyte responses are associated with improved patient outcomes, especially in TNBC.

#### IgG<sup>+</sup> B lymphocyte densities are elevated in tumors, and IgG isotype switching predicts positive survival outcomes in TNBC

We studied B lymphocyte densities according to Ig isotype expression in primary breast cancers by quantitative IHC/IF evaluations of IgD, IgM, IgA, and IgG isotype-expressing B lymphocytes [Bart's IHC cohort; normal breast tissue ( $N = 10$ ), TNBC ( $N = 14$ )]. Naïve (IgD<sup>+</sup>) B lymphocytes were found at low densities in normal breast, TIL-B<sup>low</sup> and TIL-B<sup>high</sup> tumors (Supplementary Fig. S6A). Higher IgG<sup>+</sup> and IgM<sup>+</sup> B lymphocyte densities were found in TIL-B<sup>high</sup> and, to a lesser extent, in TIL-B<sup>low</sup> cancers compared with normal breast (Fig. 5A and B). In contrast, IgA<sup>+</sup> B lymphocyte densities were consistent among tissue compartments, highlighting an overall bias toward increased IgG<sup>+</sup>:IgA<sup>+</sup> B lymphocyte ratio within cancers compared with normal breast, and within TIL-B<sup>high</sup> compared with TIL-B<sup>low</sup> cancers (Fig. 5C and D).

IHC/IF showed the dominating IgA<sup>+</sup> B lymphocyte profile present in normal breast is contained within normal lobules and their periphery (Supplementary Fig. S6B). Although TIL-B<sup>low</sup> cancers lacked large B lymphocyte follicles and contained small IgM/IgA/IgG plasma cell zones, TIL-B<sup>high</sup> cancers typically contained denser IgM/IgA/IgG

plasma cell zones surrounding expansive IgM<sup>+</sup> follicular B lymphocyte clusters with defined germinal centers (Fig. 5E). The resulting B lymphocyte assembly in these TIL-B<sup>high</sup> tumors shares some structural similarities with those in tonsil tissues. IgG and IgA expression were accompanied with CD27 upregulation, validating the differentiated, isotype-switched status of these cells (Supplementary Fig. S7A–S7C). We further confirmed that intratumoral IgG<sup>+</sup> cells comprised both CD20<sup>+</sup> as well as CD138<sup>+</sup> (plasma) cell populations, the latter being low or negative for CD20 expression (Supplementary Figs. S7D and S3C).

Because TNBCs feature high levels of IgG-expressing B lymphocytes, we studied Ig isotypes (Ig heavy chain) using a published scRNA-seq dataset (single-cell cohort;  $N = 1,021$  TIL-B across eight patients). UMAP applied to single-cell B lymphocyte populations revealed distinct TIL-B populations in TNBC compared with non-TNBC samples. This analysis also revealed enhanced isotype-switching to IgG1, IgG3, IgG4 and IgA2 subclasses in TNBC (Fig. 6A and B). UMAP confirmed differential isotype-expressing B lymphocyte compartments in TNBC compared with non-TNBC for IgM and IgG1 based on clustering (Fig. 6C). Heatmaps of single CD20<sup>+</sup>CD27<sup>+</sup> B lymphocyte IgCH expression showed a propensity toward non-switched IgM transcripts in blood in contrast with high levels of isotype-switched IgG and IgA B lymphocytes in tumor samples (Supplementary Fig. S8), and higher levels of isotype-switching in TNBC compared with non-TNBC tumor samples (Fig. 6D). These support an active tumor-resident humoral response, different to the equivalent response in the circulation, and likely driven by inflammatory and possibly antigenic signals that may support Ig class-switch recombination in the breast cancer microenvironment, especially in TNBC.

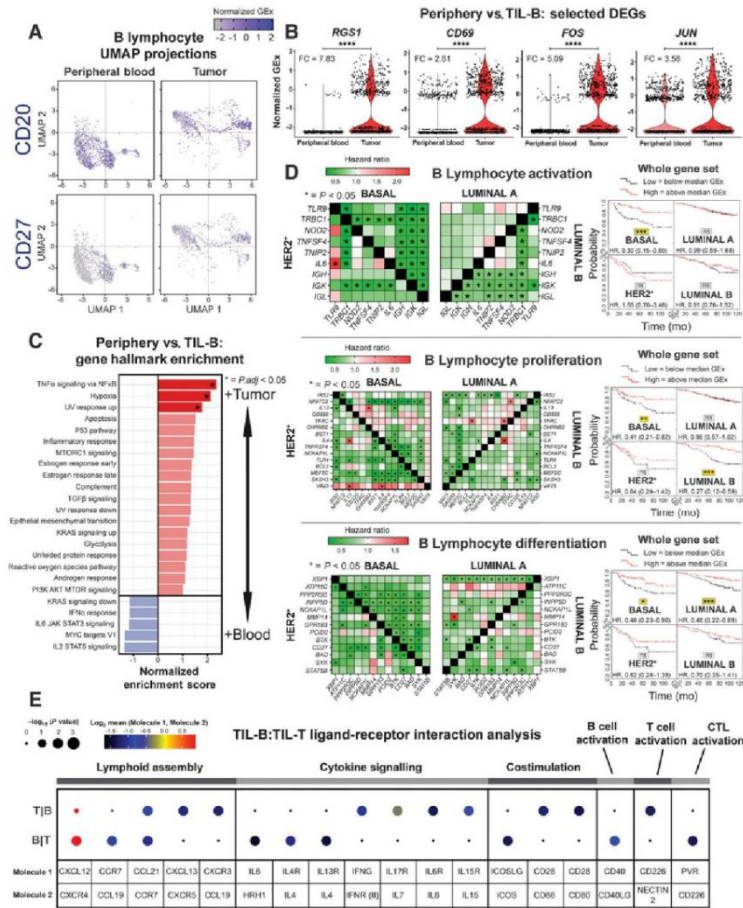
Survival analysis of isotype-switching gene signatures revealed a positive association with 10-year overall survival for IgG, but not for IgA, isotype switching, most pronounced in basal-like/TNBC (Fig. 6E, KM plotter cohort). Moreover, as expected, several genes involved in the mechanism of and/or positively regulating isotype switching were upregulated in TNBC compared with normal breast (Supplementary Fig. S9, KCL and TCGA GEx cohorts).

These findings indicate a shift in favor of IgG<sup>+</sup> B lymphocytes in TIL-B<sup>high</sup> TNBC and point to IgG isotype switching as a contributor to the overall positive role of B lymphocyte responses to breast cancers.

#### IgG-biased, clonally expanded, and Ig repertoires in breast cancer

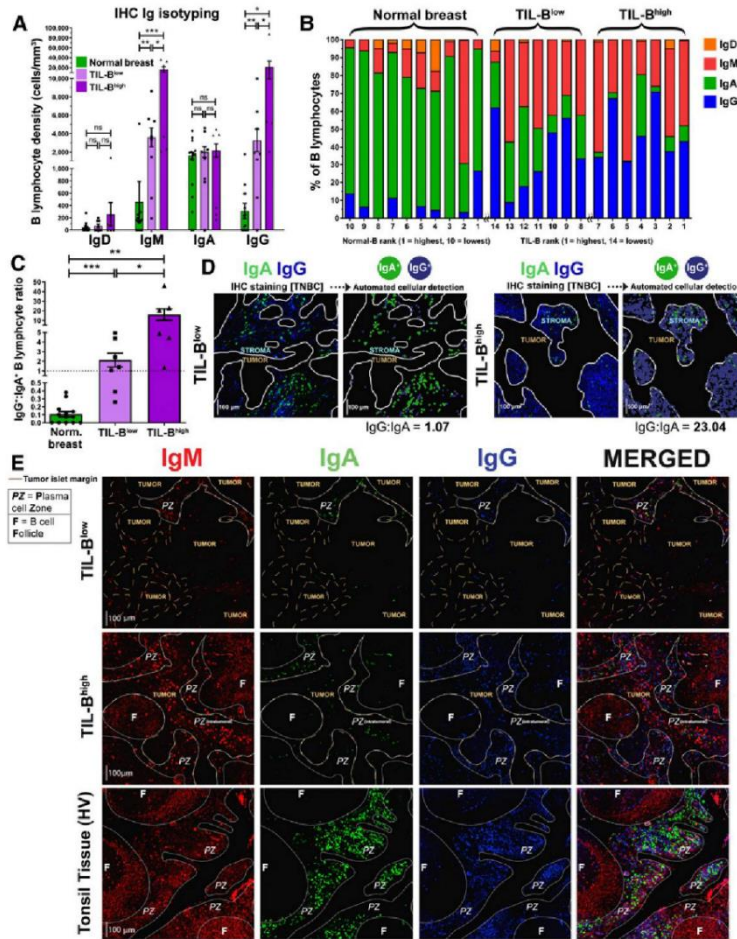
Using long-read sequencing, we next generated a dataset of Ig heavy-chain repertoires ( $N = 7,670$ ) from two TNBCs, two ER<sup>+</sup> cancers, and one normal breast tissue (KCL sequencing cohort) and performed sequence clustering analyses to define clonotypes and compare the distributions of Ig isotypes following B lymphocyte clonal expansion. We observed consistently larger clonal family sizes within the 10 largest clones of cancers compared with normal breast (Fig. 7A, top). B lymphocyte sequences from ER<sup>+</sup> cancers featured a heterogeneous IgG subclass expansion with few IgA clones. In contrast, TNBCs showed clones with coexisting IgG1 and IgA1 subclasses, suggested intraclone isotype switching (Fig. 7A, bottom). Kolmogorov-Smirnov analyses revealed that IgG and IgA clonal family frequency distributions were significantly different between carcinomas and normal breast (Fig. 7B). Accordingly, IgG and IgA were clonally expanded within cancers (Supplementary Fig. S10A and S10B), and on average IgG<sup>+</sup> B lymphocytes belonged to larger clonal families than IgA<sup>+</sup> cells (Fig. 7C). These data point to an inherent bias toward the preferential clonal expansion of IgG isotypes within

Expanded Tumor-Infiltrating IgG<sup>+</sup> B Cells in TNBC



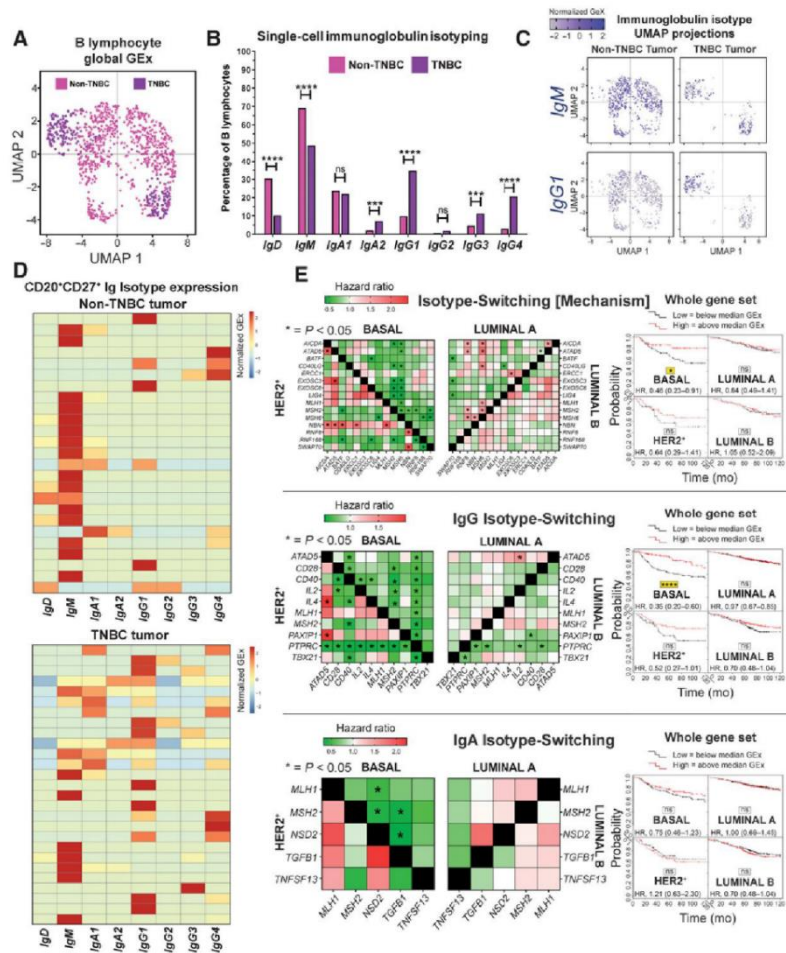
**Figure 4.** scRNA-seq analysis reveals BCR-driven TIL-B activatory signatures, and B lymphocyte functional trait gene markers predict positive survival outcome. **A**, UMAP visualization according to global GEX of single B lymphocytes pooled from the peripheral blood (1,476 cells) and tumors (1,021 cells) of eight patients (single-cell cohort), colored by relative normalized gene expression levels for *CD20* and *CD27*. **B**, The detection of differentially expressed genes (DEG; on cells originally annotated by Azizi and colleagues (22) as B cells) demonstrates elevated expression of *FOS*, *JUN*, *RGS1*, and *CD69*, indicated by fold change (FC, determined using Wilcoxon rank sum test). **C**, Gene set enrichment analysis of TIL-B relative to circulating B lymphocytes using hallmark gene sets. Red, positive normalized enrichment scores (hallmark expression enhanced in TIL-B). **D**, Survival analysis in KM Plotter of determined ER<sup>+</sup>HER2<sup>-</sup>/basal surrogate, HER2<sup>-</sup>, luminal A, and luminal B subtype KM plotter surrogate subgroups (KM plotter cohort; ref. 19) for expression of gene signatures positively regulating key B lymphocyte properties (activation, proliferation, and differentiation). Representative genes listed for B lymphocyte proliferation (44 total in set). Signatures from all three functions carry positive prognostic value in the basal-like cancer subtype. Individual genes were evaluated in combination with each other gene (left) and gene set as a whole (right). **E**, CellPhoneDB (25) was applied to analyze B-cell-T-cell interactions (single-cell cohort). After FDR (FDR < 0.001) correction, communication pathways identified included lymphoid assembly, cytokine signaling, costimulation, T-cell-dependent B-cell activation, and cytotoxic T lymphocyte (CTL) activation. Circle sizes indicate *P* value, whereas color-coding represents the average expression level of interacting molecule 1 in cluster 1 and interacting molecule 2 in cluster 2. \*\*\*\*, *P* < 0.0001.

Harris et al.



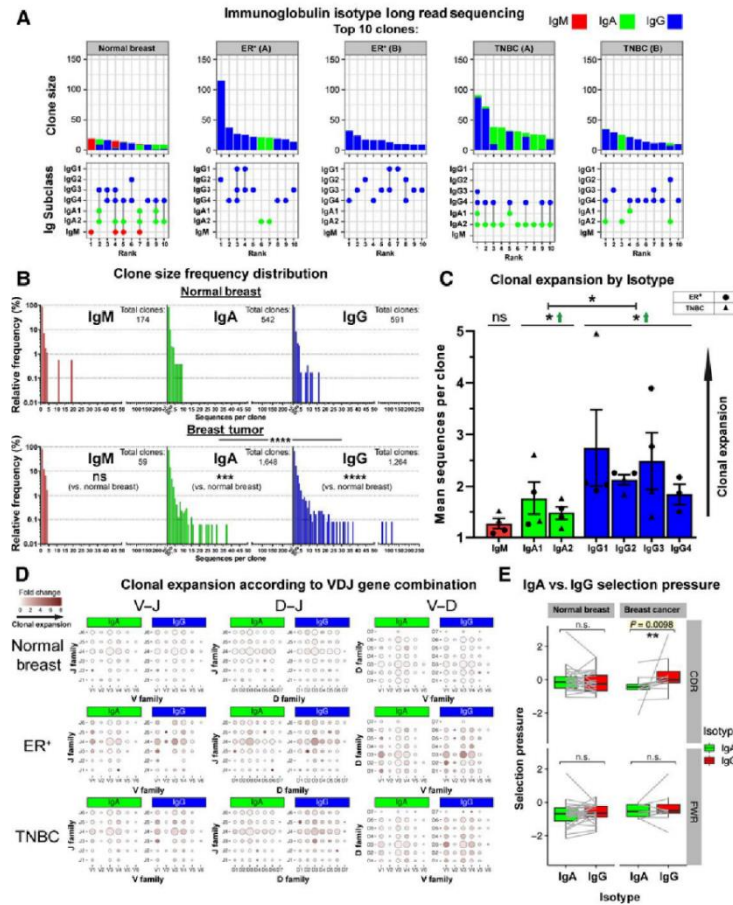
**Figure 5.** Quantitative fluorescence IHC reveals elevated IgG<sup>+</sup>IgA<sup>+</sup> ratio within high TIL-B tumors, implicating expansion of IgG<sup>+</sup> B lymphocytes within TNBC tumor microenvironment. **A**, Comparison of surface immunoglobulin-expressing B lymphocyte density in normal breast and TNBC with low TIL-B density (below median CD20<sup>+</sup>) and high TIL-B density (above median CD20<sup>+</sup>). **B**, Quantitative IHC analysis profiling the proportions of B lymphocytes present within the microenvironment of normal breast tissue (N = 10) and TNBC (N = 14) expressing each Ig isotype. **C**, Enumeration of IgG<sup>+</sup>IgA<sup>+</sup> B lymphocyte ratios. **D**, Right, example images illustrating IgG<sup>+</sup> and IgA<sup>+</sup> B lymphocytes in a typical TIL-B low individual and a TIL-B high individual. Automated cellular detection identifies IgA (green) and IgG (blue) B lymphocytes. Scale bar, 100  $\mu$ m. **E**, Representative images depicting typical Ig isotype expression among B lymphocytes: IgM<sup>+</sup> (red), IgA<sup>+</sup> (green), and IgG<sup>+</sup> (blue). Images from Bart's IHC cohort. Brown dash lines indicate margin of the cancer. White lines separate distinct regions of B lymphocyte compartments (PZ, plasma cell zone; F, B lymphocyte follicle). Scale bar, 100  $\mu$ m. Statistical significance was determined using the Student t-test. ns, nonsignificant; \*,  $P < 0.05$ ; \*\*,  $P < 0.01$ ; \*\*\*,  $P < 0.001$ .

Expanded Tumor-Infiltrating IgG<sup>+</sup> B Cells in TNBC



**Figure 6.** Single-cell RNA-seq data analysis reveals favor of IgG isotypes in TNBC, while isotype-switching gene markers predict positive survival outcome. **A**, UMAP visualization of B lymphocyte populations in non-TNBC versus TNBC (single-cell cohort). **B**, Percentage of each Ig isotype based upon raw data of Ig heavy-chain (Student *t* test). **C**, UMAP visualization for IgM and IgG1 isotypes colored by relative normalized gene expression levels ( $N = 1,021$  cells). **D**, IgCH switch transcripts of single B lymphocytes (CD19<sup>+</sup>CD27<sup>+</sup>/CD20<sup>+</sup>CD27<sup>+</sup>/CD22<sup>+</sup>CD27<sup>+</sup> single cells) were analyzed in non-TNBC and TNBC tissues and demonstrated more Ig isotype-switching events in the TNBC samples. **E**, Survival analysis in KM Plotter of determined ER<sup>+</sup> HER2<sup>+</sup>/basal surrogate, HER2<sup>+</sup>, luminal A, and luminal B subtype KM plotter surrogate subgroups (KM plotter cohort; ref. 19) for expression of gene signatures conferring isotype switching and those positively regulating isotype switching (IgG and IgA isotype switching). Signatures from all three functions carry positive prognostic value in basal-like cancer. Individual genes were evaluated in combination with each other gene (left) and the gene set as a whole (right). ns, nonsignificant; \*\*\*,  $P < 0.001$ ; \*\*\*\*,  $P < 0.0001$ .

Harris et al.



**Figure 7.** B lymphocyte repertoire analyses of immunoglobulin isotype switching and clonal expansion in breast cancers. **A**, A total of 7,670 immunoglobulin heavy-chain sequences were analyzed (KCL sequencing cohort). Top 10 clones determined by B lymphocyte repertoire long read data analyses. Clonotypes were estimated via clustering CDR3 sequences. Top bars depict sizes of clones and their breakdown by isotypes. Bottom, isotypes present in each clone are indicated by dots. Vertical lines signify co-occurrence of isotypes in the same clone. **B**, Clone size frequency distribution of IgM/IgA/IgG sequences in normal breast (1,771 sequences) and breast cancer (5,899 sequences). Kolmogorov-Smirnov analysis highlights significant differences in clone size frequency distributions. **C**, Mean sequences per clone of IgM/IgA/IgG isotypes. IgG and, to a lesser extent, IgA isotypes are clonally expanded, whereas on average, IgG isotypes have significantly larger clone sizes than IgA. **D**, Comparisons of IgA and IgG variable usage of V-J, D-J, and V-D genes extracted from normal breast, ER<sup>+</sup> cancer, and TNBC. For each gene usage combination, dot size is proportional to the frequency before clonal expansion. Dot colors correspond to fold change in the number of sequences following clonal expansion, indicating the preference of B lymphocytes with that specific VDJ combination to be clonally expanded. **E**, Selection pressure in clonally related IgA and IgG. Clonally related sequences are represented as paired observations (gray lines), and selection pressure was considered separately for the complementarity determining regions and framework regions. Sequences are grouped into normal breast and breast cancer (containing two TNBC and two ER<sup>+</sup> samples). Paired Wilcoxon tests were conducted, and *P* values were corrected (Benjamini-Hochberg) for multiple comparisons. ns, nonsignificant; \*, *P* < 0.05; \*\*, *P* < 0.01.

breast cancers. When we compared variable region gene usage, we found specific V(D)J genes whose combined usage was overrepresented in clonally expanded IgG and IgA sequences in cancers. Specific combinatorial gene usages appeared to expand in TNBC but not ER<sup>+</sup> lesions, and vice versa, suggestive of clonally restricted, likely antigen-focused, Ig repertoires (Fig. 7D; Supplementary Fig. S10C). Furthermore, Ig light chain repertoire transcripts from single CD20<sup>+</sup>CD27<sup>+</sup> B lymphocytes from two matched blood and tumor samples (single-cell cohort, Supplementary Fig. S10D) showed similarities in kappa and lambda chain V genes (IGKV, IGLV) and J genes (IGKJ, IGLJ), pointing to potential common clonal origins. Furthermore, we observed a stronger positive selection pressure in the CDRs of IgG compared with their clonally related IgA in tumor samples, whereas such a relationship was absent in the framework region (FWR), and in BCRs from normal breast (Fig. 7E). This hints at different aspects of B lymphocyte responses where IgA expression may act as an early response and IgG may confer higher affinity antigen-driven responses.

Large clonal families, isotype switching within clonally expanded TIL-B, and a bias for IgG subclasses accumulating mutations on specific variable region gene combinations, together suggest a mature humoral immune response driven toward specific antigenic stimuli in breast cancer. Further understanding of these features may reveal therapeutic targets, prognostic biomarkers, and patient subpopulations upon whom to focus adaptive immune response-enhancing therapies.

## Discussion

Clinical outcomes in patients with cancer may be influenced by the initiation of effective antitumoral adaptive T lymphocyte responses, but these are likely to be significantly more effective when launched in combination with humoral immunity, including induction of isotype-switched B lymphocytes and secretion of antibodies. We undertook flow cytometric, IHC/IF, bulk GEX, scRNA-seq, and long-read Ig sequencing analyses to investigate activated, memory and isotype-switched B lymphocytes in breast cancers, including the more-aggressive and more-immunogenic TNBC subtypes. Consistent with previous reports (39, 40), the TIL-B compartment in tumor stroma is typically organized into clusters of lymphocytes, including isotype-switched memory, GC B cells, and plasma cells. Enhanced isotype-switched B lymphocytes, with an IgG-isotype bias may be part of the humoral clonal expansion mechanism, especially pronounced in TIL-B<sup>high</sup> TNBC. The accompanied narrow mature Ig variable region repertoires and enhanced BCR signaling in TIL-B strongly signify antigen-driven responses. This dynamic humoral immune profile is especially associated with immunogenic TNBC and indicative of more favorable patient outcomes.

We found a depleted memory CD19<sup>+</sup>CD20<sup>+</sup>CD27<sup>+</sup> B lymphocyte repertoire in patients' peripheral blood regardless of stage or treatment history for their carcinoma. Moreover, this effect appears to be exacerbated in patients with breast cancer who have undergone chemotherapy, possibly owing to the depletion of B lymphocytes during treatment, which may irreversibly diminish long-lived memory populations. Accordingly, patients receiving chemotherapy have lower total serum Ig titers, indicative of a depleted circulating antibody-secreting B lymphocyte population. In contrast, our flow cytometric analyses revealed an upregulated CD20<sup>+</sup>CD27<sup>+</sup>IgD<sup>-</sup> B-cell compartment among TIL-B. In agreement, single-cell transcriptomic analyses point to a bias toward

non-switched IgM transcripts in blood memory CD20<sup>+</sup>CD27<sup>+</sup> B lymphocytes and higher levels of isotype-switched IgG and IgA CD20<sup>+</sup>CD27<sup>+</sup> B lymphocytes in tumor samples. Consistent with an immunogenic signature in TNBCs, we found higher levels of isotype switching shown in single CD20<sup>+</sup>CD27<sup>+</sup> B lymphocyte transcripts in TNBC samples compared with non-TNBC tumors. These may be driven by a combination of antigen exposure and inflammation in the breast cancer microenvironment that promotes Ig class-switch recombination.

The TIL-B population is largely assembled in clusters (>30 TIL-B and >30 TIL-T aggregated) and positively associates with overall survival. Although evident across breast cancer types, transcriptomic analysis suggests that TIL-B infiltration is more pronounced in TNBC compared with non-TNBC. TNBC, especially the IM molecular subtype, featured elevated expression of B lymphocyte recruitment and lymphoid cell assembly (*CXCL13*, *CXCR4*, *DC-LAMP*) genes, compared with normal breast. Enhanced local expression of *CXCL13* in arthritic synovial fluids can draw circulating B lymphocytes to inflammation sites (41) and B lymphocytes may traffic from the blood towards lymphoid tissues via *CXCR4* stimulation (42). The evident expression of these signals within the TME may recruit B lymphocytes, including B<sup>m</sup>, from the periphery to cancer lesions. Consistent with this, we report reduced circulating and enhanced intratumoral CD20<sup>+</sup>CD27<sup>+</sup> B-cell compartments in patients. Such chemoattractant signals may also promote local B lymphocyte assembly into B-T clusters, in line with our observations of close proximity and strong correlation between tumor-infiltrating B and T lymphocytes. Although the B-T clusters we describe are not entirely equivalent to TLSs identified in routine histology (43), within these clusters, B-T lymphocyte cross-talk can lead to B lymphocyte activation, Ig isotype-switching and local clonal expansion (39, 44).

Alongside IHC evidence of spatial B-T association, an active and functional B lymphocyte compartment is also indicated by BCR signaling and isotype switching. Analyses of scRNA-seq data demonstrated that TIL-B are phenotypically distinct to those in blood, featuring upregulated BCR complex pathway molecules *FO5* and *JUN*, germinal center chemokine regulator *RGS1*, lymphocyte activation marker *CD69* and TNF $\alpha$  signaling via NFKB. These implicate active BCR engagement by immune complexes. In concordance, Ig repertoire analyses revealed IgG-skewed clonal family expansion with clonally restricted Ig variable regions. We detected significantly larger IgG and to a lesser extent IgA, clones with narrow variable region repertoires in cancers compared with normal breast, indicative of antigen-focused clonal expansion. Together, these suggest a dynamic expanded IgG-biased humoral response focused toward a small repertoire of antigenic stimuli in the TME the greater understanding of which has the potential to inform therapeutic and biomarker strategies in patients.

Several studies reported that TIL-B carry positive prognostic value (5, 26), whereas others found no significant effect (45), or even poorer survival with CD138<sup>+</sup> plasma cell infiltrates (46). However, the extent to which B lymphocyte activity may correlate with prognosis has not been addressed. In our TNBC cohort, we report positive prognostic associations of memory, but not of naive or plasma, B lymphocyte infiltration in high-TIL tumors. This may point to positive contributions of memory B lymphocytes as part of the humoral response in immunogenic breast cancers and especially in TNBC. In concordance, our findings indicate that genes that positively regulate B lymphocyte functions, particularly those involved in activation, proliferation, differentiation, and isotype switching, and especially genes associated

Harris et al.

with isotype switching to IgG, may carry positive prognostic value. Furthermore, evidence of a bidirectional functional cross-talk between B and T cells reveals expression and interaction of gene pairs associated with lymphoid assembly, costimulation, cytokine-cytokine receptor interactions, cytotoxic T-cell activation, and T-cell-dependent B-cell activation. These interactions between B and T cells may have functional relevance in driving B-cell stimulation and maturation. Positive associations with prognosis may stem from the observed cross-talk between B and T lymphocytes within TLS (47), where antigen presentation and antibody affinity maturation may occur. B lymphocyte-mediated T-helper lymphocyte activation may contribute to immunotherapy response in TNBC with high mutation burden (48) and local antigen presentation could amplify tumor antigen-specific immune responses (12). Our findings also provide support for the involvement of TIL-B in tumor immune surveillance through secretion of cytokines such as TNF $\alpha$ , which may promote differentiation of Th1 cells and polarize immune effector cells towards classically activated phenotypes (49). Tumor-associated B lymphocytes may, therefore, receive, trigger, and respond to significant T lymphocyte-mediated innate and antigenic signals, including BCR-immune complex formation and costimulation. These may induce Ig class-switch recombination and affinity maturation, especially in TNBC.

We identified an IgG-dominated clonally expanded B lymphocyte response in those breast cancers that were highly infiltrated by immune cells, and positive associations between IgG class regulator signatures and patient outcome, especially in TNBC. The Ig isotypes produced in the TME may be critical for containing tumor growth. Antibodies can directly block cancer cell signaling, and if expressed of the IgG class, and specifically IgG1, they engender immune-mediated clearance of cancer cells via complement activation and engagement of Fc receptor-expressing monocytes, macrophages, and NK cells (50). In cancer lesions, we observed a higher mutation load in the CDRs of IgG compared with their clonally related IgA, absent in the FWR, and in BCRs from normal breast. This stronger positive selection pressure on IgG<sup>+</sup> B lymphocytes may represent different aspects of humoral immunity, likely arising from a common B-cell precursor, with IgA<sup>+</sup> and IgG<sup>+</sup> B lymphocytes driven to generate highly specific but divergent BCRs. Our work suggests significant implications regarding the effectiveness of antitumor B lymphocyte responses within highly infiltrated cancers, where a higher IgG<sup>+</sup>:IgA<sup>+</sup> ratio among the expansive B lymphocyte infiltrate could engender potent antitumor responses through the increased relative proportion of IgG isotypes, featuring increased capacity to trigger antibody-dependent cellular cytotoxicity by NK cells and macrophages. Future therapeutic interventions may facilitate or take advantage of IgG<sup>+</sup> memory and plasma cell infiltrates, and thus influence the balance in favor of immune-activatory Ig isotypes in tumors.

Collectively, our findings indicate a highly activated B lymphocyte compartment in breast cancers. Intratumoral B lymphocytes are spatially associated with T lymphocytes within large stromal clusters, isotype-switch, expand into large clonal families featuring a bias toward IgG subclasses, and carry specific variable region gene combinations with narrow repertoires, all suggesting targeted humoral responses to specific antigenic stimuli. Clonally restricted IgG-expressing B cells may include *in situ* generated germinal center and activated memory B cells and terminally differentiated plasma cells. Together, these may contribute to humoral immune responses in breast cancer, likely more prominent in TNBC. These expansive and clonally skewed Ig repertoires, and in particular those switched to IgG

isotypes, may be associated with more-favorable patient survival. Although found across breast cancer types, these dynamic B lymphocyte traits are highly prominent in TNBC. Despite the usually poor prognosis and aggressive nature of TNBC, this analysis implicates considerable biological and associated prognostic heterogeneity that extends to the TME. Expansive and active B lymphocyte cancer infiltrates, in a proportion of individuals, provide a degree of antitumor activity that may, in combination with other immune responses, confer a survival benefit and may be exploited with immunotherapies to aid in tumor clearance. Elucidating the microenvironmental conditions required to initiate, sustain, and enhance these beneficial antitumor responses may be key to developing novel treatments.

#### Authors' Disclosures

D.K. Dunn-Walters reports grants from MRC during the conduct of the study. A.N.J. Tutt reports grants from Breast Cancer Now Charity and CRUK during the conduct of the study as well as reports personal fees from Imbionion, CRUK, MD Anderson, and reports other support from Tesaro/GlaxoSmithKline, AstraZeneca, AstraZeneca, Merck KGAA, as well as personal fees from Pfizer, Vertex, Artios, Prime Oncology, and reports other support from Medivation, Myriad Genetics, and reports personal fees from Gilead, other support from AstraZeneca, and grants from AstraZeneca outside the submitted work; as well as a patent for AstraZeneca with royalties paid to the Institute of Cancer Research with royalties paid from AstraZeneca. S.N. Karagiannis reports grants from Breast Cancer Now, Cancer Research UK, Medical Research Council, and National Institute for Health Research during the conduct of the study as well as reports grants from Epsilon Ltd. outside the submitted work; and patents on novel antibodies for cancer therapy. No disclosures were reported by the other authors.

#### Authors' Contributions

R.J. Harris: Conceptualization, data curation, formal analysis, validation, investigation, visualization, methodology, writing—original draft. A. Cheung: Conceptualization, data curation, formal analysis, validation, investigation, visualization, methodology, writing—original draft, writing—review and editing. J.C. Ng: Data curation, formal analysis, validation, investigation, visualization, methodology, writing—original draft, writing—review and editing. R. Laddach: Data curation, validation, investigation, visualization, methodology, writing—original draft, writing—review and editing. A.M. Chenoweth: Data curation, investigation, writing—review and editing. S. Crescibit: Conceptualization, writing—review and editing. M. Fittall: Conceptualization, data curation, validation, investigation, methodology. D. Dominguez Rodriguez: Data curation, validation, investigation. J. Roberts: Data curation, formal analysis, methodology. D. Levi: Data curation, formal analysis. F. Liu: Formal analysis, supervision. E. Alberts: Data curation, formal analysis, visualization. J. Quist: Data curation, formal analysis. A. Santalalla: Methodology. S.E. Pinder: Supervision, writing—review and editing. C. Gillett: Supervision. N. Hammar: Supervision. S. Irshad: Resources. M. Van Hemelrijck: Supervision, writing—review and editing. D.K. Dunn-Walters: Resources, supervision. F. Fraternali: Supervision, investigation, methodology. J.F. Spicer: Supervision. K.E. Lacy: Supervision. S. Tsoka: Supervision. A. Grigoriadis: Conceptualization, resources, supervision, funding acquisition, writing—review and editing. A.N.J. Tutt: Conceptualization, resources, supervision, funding acquisition, writing—review and editing. S.N. Karagiannis: Conceptualization, resources, supervision, funding acquisition, writing—original draft, writing—review and editing.

#### Acknowledgments

The authors acknowledge support by Breast Cancer Now (147; KCL-BCN-Q3); the Cancer Research UK King's Health Partners Center at King's College London (G604/A25135); Cancer Research UK (C30122/A11527; C30122/A15774); the Medical Research Council (MR/L023091/1); CR UK/NIHR in England/DoH for Scotland, Wales and Northern Ireland Experimental Cancer Medicine Center (C10355/A15587). The research was supported by the National Institute for Health Research Biomedical Research Center based at Guy's and St Thomas' NHS Foundation Trust and King's College London (IS-BRC-1215-20066). The authors are solely responsible for study design, data collection, analysis, decision to publish, and preparation of the manuscript. The views expressed are those of

Expanded Tumor-Infiltrating IgG<sup>+</sup> B Cells in TNBC

the author(s) and not necessarily those of the NHS, the NIHR or the Department of Health. The authors acknowledge the Breast Cancer Now Tissue Bank in collecting and making available samples used in the generation of this publication. They acknowledge the Biomedical Research Center Immune Monitoring Core Facility at Guy's and St Thomas' NHS Foundation Trust and the Nikon Imaging Center at Kings College London for assistance.

The costs of publication of this article were defrayed in part by the payment of page charges. This article must therefore be hereby marked *advertisement* in accordance with 18 U.S.C. Section 1734 solely to indicate this fact.

Received November 19, 2020; revised March 23, 2021; accepted June 14, 2021; published first June 15, 2021.

## References

- Erdag G, Schaefer JT, Smolkin ME, Deacon DH, Shea SM, Dengel LT, et al. Immunotype and immunohistologic characteristics of tumor-infiltrating immune cells are associated with clinical outcome in metastatic melanoma. *Cancer Res* 2012;72:1070–80.
- Ladanyi A, Kiss J, Mohos A, Somlai B, Liszkay G, Gilde K, et al. Prognostic impact of B-cell density in cutaneous melanoma. *Cancer Immunol Immunother* 2011; 60:1729–38.
- Garaud S, Zayakin P, Buisseret L, Rulle U, Silina K, de Wind A, et al. Antigen specificity and clinical significance of IgG and IgA autoantibodies produced in situ by tumor-infiltrating B cells in breast cancer. *Front Immunol* 2018;9: 2660.
- Lehmann BD, Pietenpol JA, Tan AR. Triple-negative breast cancer: molecular subtypes and new targets for therapy. *Am Soc Clin Oncol Educ Book* 2015;e31–9. DOI: 10.14694/EdBook\_AM.2015.35.e31.
- Loi S, Michiels S, Salgado R, Sirtaine N, Jose V, Fumagalli D, et al. Tumor-infiltrating lymphocytes are prognostic in triple negative breast cancer and predictive for trastuzumab benefit in early breast cancer: results from the FinHER trial. *Ann Oncol* 2014;25:1544–50.
- Schmid P, Rugo HS, Adams S, Schneeweiss A, Barrios CH, Iwata H, et al. Atezolizumab plus nab-paclitaxel as first-line treatment for unresectable, locally advanced or metastatic triple-negative breast cancer (IMpassion130): updated efficacy results from a randomised, double-blind, placebo-controlled, phase 3 trial. *Lancet Oncol* 2020;21:44–59.
- Keren L, Bosse M, Marquez D, Angostari R, Jain S, Varma S, et al. A structured tumor-immune microenvironment in triple negative breast cancer revealed by multiplexed ion beam imaging. *Cell* 2018;174:173–87.
- Ramakrishnan R, Assidani D, Nagaraj S, Hunter T, Cho HI, Antonia S, et al. Chemotherapy enhances tumor cell susceptibility to CTL-mediated killing during cancer immunotherapy in mice. *J Clin Invest* 2010;120:1111–24.
- Seow DYB, Yeong JPS, Lim JX, Chia N, Lim JCT, Ong CGH, et al. Tertiary lymphoid structures and associated plasma cells play an important role in the biology of triple-negative breast cancers. *Breast Cancer Res Treat* 2020;180: 369–77.
- Singh M, Al-Eryani G, Carswell S, Ferguson JM, Blackburn J, Barton K, et al. High-throughput targeted long-read single cell sequencing reveals the clonal and transcriptional landscape of lymphocytes. *Nat Commun* 2019;10:3120.
- Scott AM, Wolchok JD, Old LJ. Antibody therapy of cancer. *Nat Rev Cancer* 2012;12:278–87.
- Rossetti RAM, Lorenzi NPC, Yokochi K, Rosa M, Benevides L, Margarido PFR, et al. B lymphocytes can be activated to act as antigen presenting cells to promote anti-tumor responses. *PLoS ONE* 2018;13:e0199034.
- Schumacher TN, Schreiber RD. Neoantigens in cancer immunotherapy. *Science* 2015;348:69–74.
- Hu X, Zhang J, Wang J, Fu J, Li T, Zheng X, et al. Landscape of B cell immunity and related immune evasion in human cancers. *Nat Genet* 2019;51:560–7.
- Helms BA, Reddy SM, Gao J, Zhang S, Basar R, Thakur R, et al. B cells and tertiary lymphoid structures promote immunotherapy response. *Nature* 2020; 577:549–55.
- Garaud S, Buisseret L, Solinas C, Gu-Trantien C, de Wind A, Van den Eynden G, et al. Tumor-infiltrating B cells signal functional humoral immune responses in breast cancer. *JCI Insight* 2019;5:e129641.
- Braso-Maristany F, Filosto S, Catchpole S, Marlow R, Quist J, Franceschi-Domenich E, et al. PIM1 kinase regulates cell death, tumor growth and chemotherapy response in triple-negative breast cancer. *Nat Med* 2016;22: 1303–13.
- Szekely B, Bossuyt V, Li X, Wali VB, Patwardhan GA, Frederick C, et al. Immunological differences between primary and metastatic breast cancer. *Ann Oncol* 2018;29:2232–9.
- Gyorffy B, Lanczky A, Eklund AC, Denkert C, Budczies J, Li Q, et al. An online survival analysis tool to rapidly assess the effect of 22,277 genes on breast cancer prognosis using microarray data of 1,809 patients. *Breast Cancer Res Treat* 2010; 123:725–31.
- Newman AM, Liu CL, Green MR, Gentles AJ, Feng W, Xu Y, et al. Robust enumeration of cell subsets from tissue expression profiles. *Nat Methods* 2015; 12:453–7.
- Dieu-Nosjean MC, Goc J, Girakli NA, Sautes-Fridman C, Fridman WH. Tertiary lymphoid structures in cancer and beyond. *Trends Immunol* 2014; 35:571–80.
- Azizi E, Carr AJ, Plitas G, Cornish AE, Konopacki C, Prabhakaran S, et al. Single-cell map of diverse immune phenotypes in the breast tumor microenvironment. *Cell* 2018;174:1293–308.
- Butler A, Hoffman P, Smitert P, Papalexi E, Satija R. Integrating single-cell transcriptomic data across different conditions, technologies, and species. *Nat Biotechnol* 2018;36:411–20.
- Subramanian A, Tamayo P, Mootha VK, Mukherjee S, Ebert BL, Gillette MA, et al. Gene set enrichment analysis: a knowledge-based approach for interpreting genome-wide expression profiles. *Proc Natl Acad Sci U S A* 2005;102: 15545–50.
- Efremova M, Vento-Tormo M, Teichmann SA, Vento-Tormo R. CellPhoneDB: inferring cell-cell communication from combined expression of multi-subunit ligand-receptor complexes. *Nat Protoc* 2020;15:1484–506.
- Salgado R, Denkert C, Demaria S, Sirtaine N, Klauschen F, Pruneri G, et al. The evaluation of tumor-infiltrating lymphocytes (TILs) in breast cancer: recommendations by an International TILs Working Group 2014. *Ann Oncol* 2015;26: 259–71.
- Wu YC, Kipling D, Dunn-Walters D. Assessment of B-cell repertoire in humans. *Methods Mol Biol* 2015;1343:199–218.
- Brochet X, Lefranc MP, Giudicelli V. IMGT/V-QUEST: the highly customized and integrated system for IG and TR standardized V-J and V-D-J sequence analysis. *Nucleic Acids Res* 2008;36:W503–8.
- Margreitter C, Lu HC, Townsend C, Stewart A, Dunn-Walters DK, Fraternali F. BRepertoire: a user-friendly web server for analysing antibody repertoire data. *Nucleic Acids Res* 2018;46:W264–W70.
- Townsend CL, Laffy JM, Wu YB, Silva O'Hare J, Martin V, Kipling D, et al. Significant differences in physicochemical properties of human immunoglobulin kappa and lambda CDR3 regions. *Front Immunol* 2016;7:388.
- Yaari G, Uduman M, Kleinstein SH. Quantifying selection in high-throughput immunoglobulin sequencing datasets. *Nucleic Acids Res* 2012; 40:e134.
- Carpenter EL, Mick R, Rech AJ, Beatty GL, Colligon TA, Rosenfeld MR, et al. Collapse of the CD27<sup>+</sup> B-cell compartment associated with systemic plasmacytosis in patients with advanced melanoma and other cancers. *Clin Cancer Res* 2009;15:4277–87.
- Waldius G, Malmstrom H, Jungner I, de Faire U, Lambe M, Van Hemelrijck M, et al. Cohort profile: the AMORIS cohort. *Int J Epidemiol* 2017;46:1103–i.
- Lehmann BD, Bauer JA, Chen X, Sanders ME, Chakravarthy AB, Shtyr Y, et al. Identification of human triple-negative breast cancer subtypes and preclinical models for selection of targeted therapies. *J Clin Invest* 2011; 121:2750–67.
- Yin Q, Wang X, McBride J, Fewell C, Flemington E. B-cell receptor activation induces BIC/miR-155 expression through a conserved AP-1 element. *J Biol Chem* 2008;283:2654–62.
- Moratz C, Kang VH, Druey KM, Shi CS, Scheschonka A, Murphy PM, et al. Regulator of G protein signaling 1 (RGS1) markedly impairs Gi alpha signaling responses of B lymphocytes. *J Immunol* 2000;164:1829–38.
- D'Arena G, Musto P, Nunziata G, Cascavilla N, Savino L, Pistolesi G. CD69 expression in B-cell chronic lymphocytic leukemia: a new prognostic marker? *Haematologica* 2001;86:995–6.



Harris et al.

38. Liberzon A, Birger C, Thorvaldsdottir H, Ghandi M, Mesirov JP, Tamayo P. The Molecular Signatures Database (MSigDB) hallmark gene set collection. *Cell Syst* 2015;1:417–25.
39. Maletzki C, Jahnke A, Oswald C, Klar E, Prall F, Linnbacher M. Ex-vivo clonally expanded B lymphocytes infiltrating colorectal carcinoma are of mature immunophenotype and produce functional IgG. *PLoS ONE* 2012;7:e32639.
40. Silina K, Rulle U, Kalnina Z, Line A. Manipulation of tumour-infiltrating B cells and tertiary lymphoid structures: a novel anti-cancer treatment avenue? *Cancer Immunol Immunother* 2014;63:643–62.
41. Armas-Gonzalez E, Dominguez-Luis MJ, Diaz-Martin A, Arce-Franco M, Castro-Hernandez J, Danelon G, et al. Role of CXCL13 and CCL20 in the recruitment of B cells to inflammatory foci in chronic arthritis. *Arthritis Res Ther* 2018;20:114.
42. Okada T, Ngo VN, Eldand EH, Forster R, Lipp M, Littman DR, et al. Chemokine requirements for B-cell entry to lymph nodes and Peyer's patches. *J Exp Med* 2002;196:65–75.
43. Pavoni E, Monteriu G, Santapaola D, Petronzelli F, Anastasi AM, Pelliccia A, et al. Tumor-infiltrating B lymphocytes as an efficient source of highly specific immunoglobulins recognizing tumor cells. *BMC Biotechnol* 2007;7:70.
44. Buisseret L, Desmets C, Garaud S, Fornili M, Wang X, Van den Eyden G, et al. Reliability of tumor-infiltrating lymphocyte and tertiary lymphoid structure assessment in human breast cancer. *Mod Pathol* 2017;30:1204–12.
45. Song IH, Heo SH, Bang WS, Park HS, Park IA, Kim YA, et al. Predictive value of tertiary lymphoid structures assessed by high endothelial venule counts in the neoadjuvant setting of triple-negative breast cancer. *Cancer Res Treat* 2017;49:399–407.
46. Mohammed ZM, Going JJ, Edwards J, Elsberger B, McMillan DC. The relationship between lymphocyte subsets and clinic-pathological determinants of survival in patients with primary operable invasive ductal breast cancer. *Br J Cancer* 2013;109:1676–84.
47. Gamelo M, Tan A, Her Z, Yeong J, Lim CJ, Chen J, et al. Interaction between tumour-infiltrating B cells and T cells controls the progression of hepatocellular carcinoma. *Gut* 2017;66:342–51.
48. Hollern DP, Xu N, Thennavan A, Glodowski C, Garcia-Recio S, Mott KR, et al. B cells and T follicular helper cells mediate response to checkpoint inhibitors in high mutation burden mouse models of breast cancer. *Cell* 2019;179:1191–206.
49. Lund FE. Cytokine-producing B lymphocytes—key regulators of immunity. *Curr Opin Immunol* 2008;20:332–8.
50. Cheung A, Opzomeer J, Ilieva KM, Gazinska P, Hoffmann RM, Mirza H, et al. Anti-folate receptor alpha-directed antibody therapies restrict the growth of triple-negative breast cancer. *Clin Cancer Res* 2018;24:5098–111.

# Supplementary Material for (Harris et al. 2021)

## Supplementary Tables and Figures

Supplementary Table 1. Patient and control cohorts, summary.

Suppl. Table 1

<p><b>Flow cytometry data:</b> <i>KCL flow cohort</i> Peripheral blood PBMC (Fig. 1B)</p> <p><b>Breast tissue single cell extraction</b> (Fig. 1C, 1D, 1E)</p>	<p><b>Control group:</b> Healthy volunteer PBMC (N=29). Age: 50 years (+/- 12); age range: 31-81.</p> <p><b>Experimental group:</b> Breast cancer patient PBMC (N=55). Age: 55 years (+/- 13); age range: 33-83. Receptor: ER+ (N=39), ER- (N=16); HER2+ (N=13); HER2- (N=40); TNBC (N=11). Stage: 1 (N=7); 2 (N=21); 3 (N=8); 4 (N=18). Chemotherapy: none (N=10); &lt;1 year post-chemo (N=21); &gt;1 year post-chemo (N=22).</p> <p><b>Control group:</b> Normal breast (reduction surgery) (N=9). Age: 37 years (+/- 5); age range: 32-45.</p> <p><b>Experimental group:</b> Treatment naive tumor (N=17) and NANT (N=12), with matched PBMC. Age: 62 years (+/- 15); age range: 38-87. ER+ (N=11), ER- (N=6); HER2+ (N=5), HER2- (N=12); TNBC (N=3).</p>										
<p><b>IHC/IF data:</b> <i>Bart's IHC cohort</i> (Fig. 2A, 2B, 2D, 2F, 2G, 3A to 3C, 5A to 5E; Suppl. Fig. 3C, 3E, 4A, 6 and 7)</p>	<p><b>Control group:</b> Normal breast (reduction surgery/prophylactic mastectomy) (N=15). Age: 42 years (+/- 10); age range: 27-63.</p> <p><b>Experimental group:</b> Grade 3 IDC TNBC tumor (N=14 primary). Age: 64 years (+/- 10); age range: 45-86. Receptor: ER+ (N=0), ER- (N=15); HER2+ (N=0); HER2- (N=15); TNBC (N=15). Stage: 1 (N=5); 2 (N=5); 3 (N=2); 4 (N=1). Chemotherapy: none (N=13); neoadjuvant (N=1).</p>										
<p><b>Transcriptomic data:</b> <i>KCL and TCGA GEx cohorts</i> (Fig. 2A, 2B, 2E, 3D; Suppl. Fig. 4A, 4B, 4D; Suppl. Fig. 5, 8, 9)</p> <p><b>NanoString cohort</b> (GSE102818, Szekely et al.) (Fig. 2C)</p>	<p><b>Control group:</b> KCL: normal breast (N=10); TCGA: non-TNBC (N=515); KCL: TNBC (N=131); Lehmann et al. TNBC subtypes - mesenchymal, luminal androgen receptor, basal-like 1/2 and immunomodulatory (N=122); TCGA: TNBC (N=123)</p> <p><b>Control group:</b> primary tumor (N=31)</p> <p><b>Experimental groups:</b> Metastatic site (N=17)</p>										
<p><b>Survival data:</b> <i>KM plotter cohort</i> (<a href="https://kmplot.com/">https://kmplot.com/</a>; Cyörffy et al.) (Fig. 2D, 3E, 4D, 6E; Suppl. Fig. 4C)</p>	<table border="0"> <thead> <tr> <th><b>Investigated groups:</b></th> <th><b>Chemotherapy:</b></th> </tr> </thead> <tbody> <tr> <td>Basal-like (N=241)</td> <td>N=188</td> </tr> <tr> <td>Luminal A (N=611)</td> <td>N=321</td> </tr> <tr> <td>Luminal B (N=433)</td> <td>N=246</td> </tr> <tr> <td>HER2 (N=117)</td> <td>N=98</td> </tr> </tbody> </table>	<b>Investigated groups:</b>	<b>Chemotherapy:</b>	Basal-like (N=241)	N=188	Luminal A (N=611)	N=321	Luminal B (N=433)	N=246	HER2 (N=117)	N=98
<b>Investigated groups:</b>	<b>Chemotherapy:</b>										
Basal-like (N=241)	N=188										
Luminal A (N=611)	N=321										
Luminal B (N=433)	N=246										
HER2 (N=117)	N=98										
<p><b>scRNA-seq data:</b> <i>Single cell cohort</i> (GSE114725, Azizi et al.) (Fig. 2E, 4A to 4C, 4E, 6A to 6D; Suppl. Fig. 3A, 3B, 3D, 10D)</p>	<p><b>Investigated groups:</b> Breast cancer patient peripheral blood (ER, N=2): 1,476 cells.</p> <p>Treatment naive primary tumor: B cells 1,021 cells; T cells, 11,006 cells. Age: 58 years (+/- 13); age range: 38-78. Receptor: ER+ (N=5), ER- (N=3); HER2+ (N=1); HER2- (N=7); TNBC (N=2).</p>										
<p><b>B cell repertoire data:</b> <i>KCL sequencing cohort</i> Breast tissue samples (Fig. 7A to 7E, Suppl. Fig. 10A to 10C)</p>	<p><b>Control group:</b> Normal breast (N=1): 1,771 sequences. Age: 35 years old.</p> <p><b>Experimental group:</b> Treatment naive primary tumor. Age: 47 years (+/- 14); age range: 35-61. Receptor: ER+ (N=2), ER- (N=2); HER2+ (N=0); HER2- (N=4); TNBC (N=2). Stage: 1 (N=3), 2 (N=1). 5,899 sequences.</p>										
<p><b>Luminex assay data:</b> <i>KCL Luminex cohort</i> Serum samples (Suppl. Fig. 1A, 1B)</p>	<p><b>Control group:</b> Healthy volunteer serum (N=18)</p> <p><b>Experimental group:</b> Breast cancer patient serum (ER, N=9; HER2, N=3; TNBC, N=9). Chemotherapy: No chemo (N=12), Chemo (N=9).</p>										
<p><b>AMORIS data:</b> <i>AMORIS cohort</i> (Walldius et al.) (Suppl. Fig. 2)</p>	<p><b>No breast cancer-specific death:</b> Did not die from breast cancer or still alive. Mean follow-up time: 8.8 years (N=3,643)</p> <p><b>Breast cancer-specific death:</b> Death from breast cancer. Mean follow-up time: 5.2 years (N=389)</p>										

**Supplementary Table 2.** List of primary and secondary antibodies used for IHC staining.

Suppl. Table 2

**IHC Staining Panels**

Panel	Identification	Markers
1	TIL classification	DAPI, CD20, CD3, PanCK
2	Naïve B cell identification	DAPI, CD20, IgD
3	Surface Ig isotype analysis	IgM, IgA, IgG, CD27

**Primary Antibodies**

Manufacturer	Species	Target	Clone
Abcam	Ms	CD20	L26
Abcam	Rt	CD3	CD3-12
Abcam	Rb	PanCK	KRT/1877R
Abcam	Rb	CD27	EPR8569
Abcam	Rb	IgD	EPR6146
Abcam	Gt	IgM	Polyclonal
Abcam	Rb	IgG	EPR4421
Novus Biologicals	Ms	IgA	AD3
Thermo Fisher	Gt	CD138	Polyclonal
Abcam	Rb	BCL6	EPR11410-43

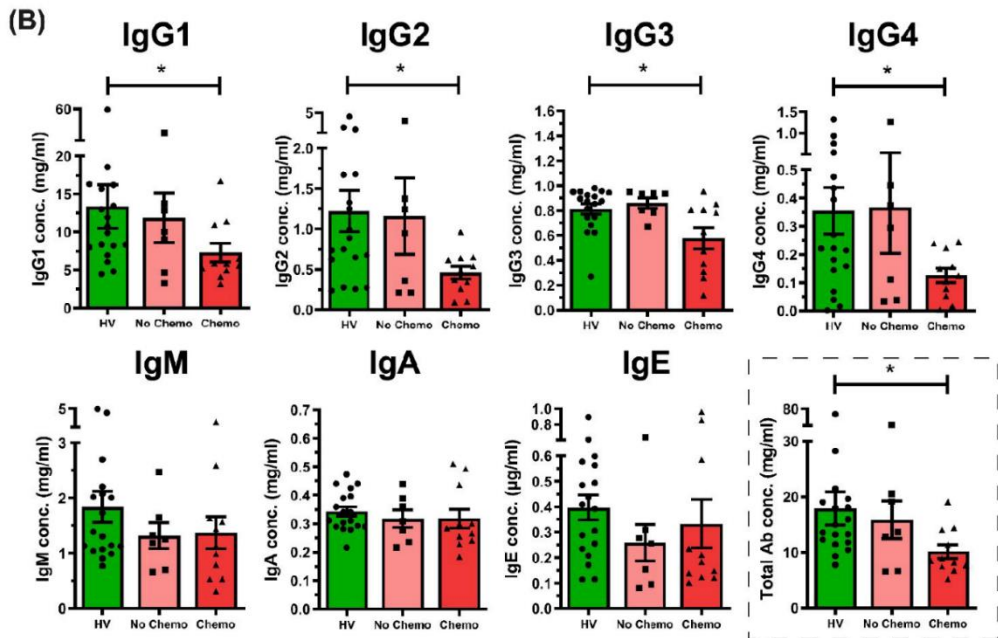
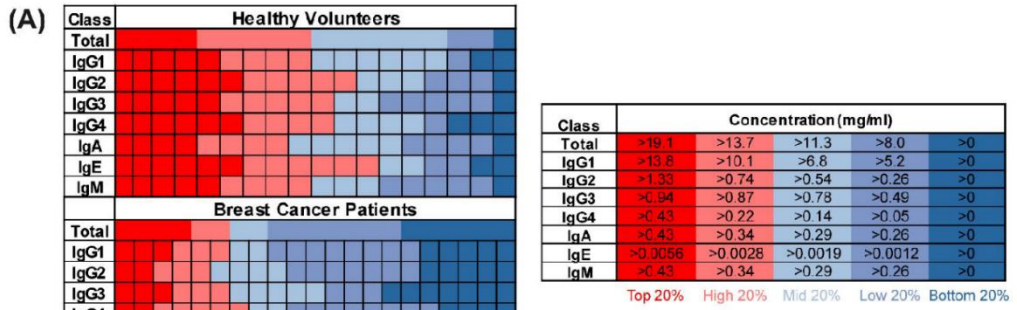
**Secondary Antibodies**

Manufacturer	Species	Target	Fluorophore
Abcam	Gt/Dnk	Ms IgG	AF488
Abcam	Gt/Dnk	Rb IgG	AF594
Abcam	Gt	Rt IgG	AF647
Abcam	Dnk	Gt IgG	AF647
Abcam	Dnk	Rb IgG	AF405
Abcam	Dnk	Gt IgG	AF594
Abcam	Dnk	Rb IgG	AF647

Ms = Mouse, Rt = Rat, Rb= Rabbit, ArH = Armenian Hamster, Gt = Goat

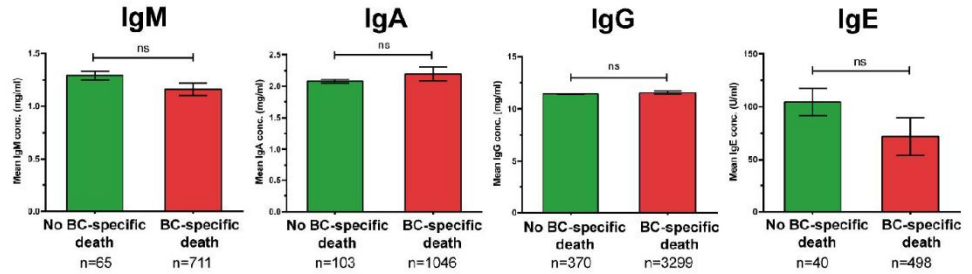
Suppl. Figure 1

Serum Immunoglobulin Isotyping



Suppl. Figure 2

AMORIS analysis: serum Ig titer and likelihood of BC-specific death



	Breast cancer-specific death N = 389 n (%)	No breast cancer-specific death N = 3,643 n (%)
<b>Mean Age (years) (SD)</b>	62.1 (13.35)	63.4 (11.88)
<b>Education</b>		
Missing	32 (8.23)	143 (3.93)
Low	104 (26.74)	1,091 (29.12)
Middle	155 (39.85)	1,532 (42.05)
High	98 (25.19)	907 (24.90)
<b>Parity</b>		
Yes	312 (80.21)	2,847 (78.15)
No	77 (19.79)	796 (21.85)
<b>Charlson Comorbidity Index</b>		
0	298 (76.61)	2,827 (77.60)
1	39 (10.03)	345 (9.47)
2	30 (7.71)	320 (8.78)
3+	22 (5.66)	151 (4.14)
<b>Mean follow-up time (years) (SD)</b>	5.2 (4.26)	8.8 (5.27)
<b>IgM (mg/mL)</b>		
Mean (SD)	1.16 (0.48)	1.29 (1.15)
< 2.08 mg/mL	61 (15.66)	635 (17.43)
≥ 2.08 mg/mL	4 (1.03)	76 (2.09)
Missing	324 (83.29)	2,932 (80.48)
<b>IgA (mg/mL)</b>		
Mean (SD)	2.19 (1.11)	2.08 (0.96)
< 3.66 mg/mL	94 (24.16)	976 (26.79)
≥ 3.66 mg/mL	9 (2.31)	70 (1.92)
Missing	286 (73.52)	2,597 (71.29)
<b>IgG (mg/mL)</b>		
Mean (SD)	11.55 (3.11)	11.42 (2.92)
< 15.00 mg/mL	320 (82.26)	2,908 (79.82)
≥ 15.00 mg/mL	50 (12.85)	391 (10.73)
Missing	19 (4.88)	344 (9.44)
<b>IgE (U/mL)</b>		
Mean (SD)	71.83 (113.34)	104.43 (287.29)
< 100 U/mL	32 (8.23)	384 (10.54)
≥ 100 U/mL	8 (2.06)	114 (3.13)
Missing	349 (89.72)	3,145 (86.33)

	Events/Total N	Hazard Ratio <sup>1</sup> (95% CI)
<b>IgM (mg/mL)</b>		
< 2.08 mg/mL	61/696	1.00 (Ref)
≥ 2.08 mg/mL	4/80	0.52 (0.19-1.40)
<b>IgA (mg/mL)</b>		
< 3.66 mg/mL	94/1,070	1.00 (Ref)
≥ 3.66 mg/mL	9/79	1.35 (0.69-2.62)
<b>IgG (mg/mL)</b>		
< 15.00 mg/mL	320/3,228	1.00 (Ref)
≥ 15.00 mg/mL	50/441	1.19 (0.88-1.80)
<b>IgE (U/mL)</b>		
< 100 U/mL	32/416	1.00 (Ref)
≥ 100 U/mL	8/122	0.84 (0.42-1.69)

<sup>1</sup> Adjusted for age, parity, education and CCI.

Suppl. Figure 3

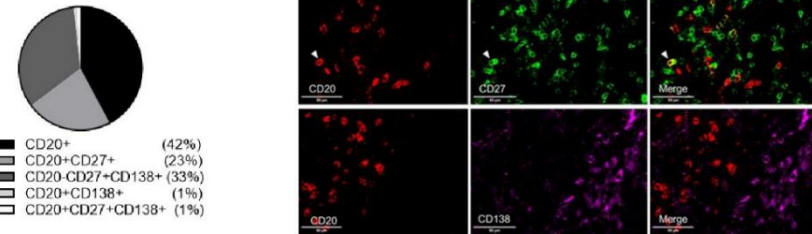
(A) CD27<sup>+</sup> cell distribution in blood (N = 66) and tumor (N = 30)



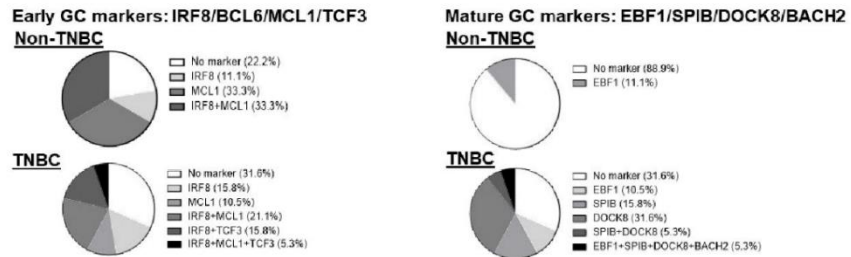
(B) CD27<sup>+</sup>IgD<sup>-</sup> cell distribution in blood (N = 37) and tumor (N = 26)



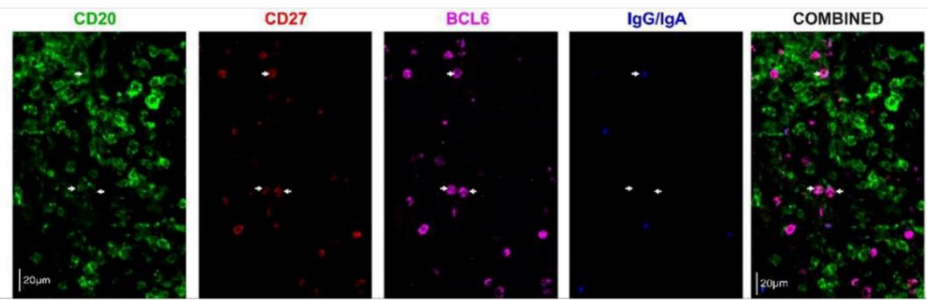
(C) B cell population in TNBC (N = 7) by IHC/IF (% of density: cells/mm<sup>3</sup>) with representative images depicting memory B cell IHC/IF staining



(D) GCB marker expression in class-switched (IgD<sup>-</sup>IgM<sup>-</sup>) CD19<sup>+</sup>/CD20<sup>+</sup>/CD22<sup>+</sup>CD27<sup>+</sup> B cell in non-TNBC (N=9) and TNBC (N=19)

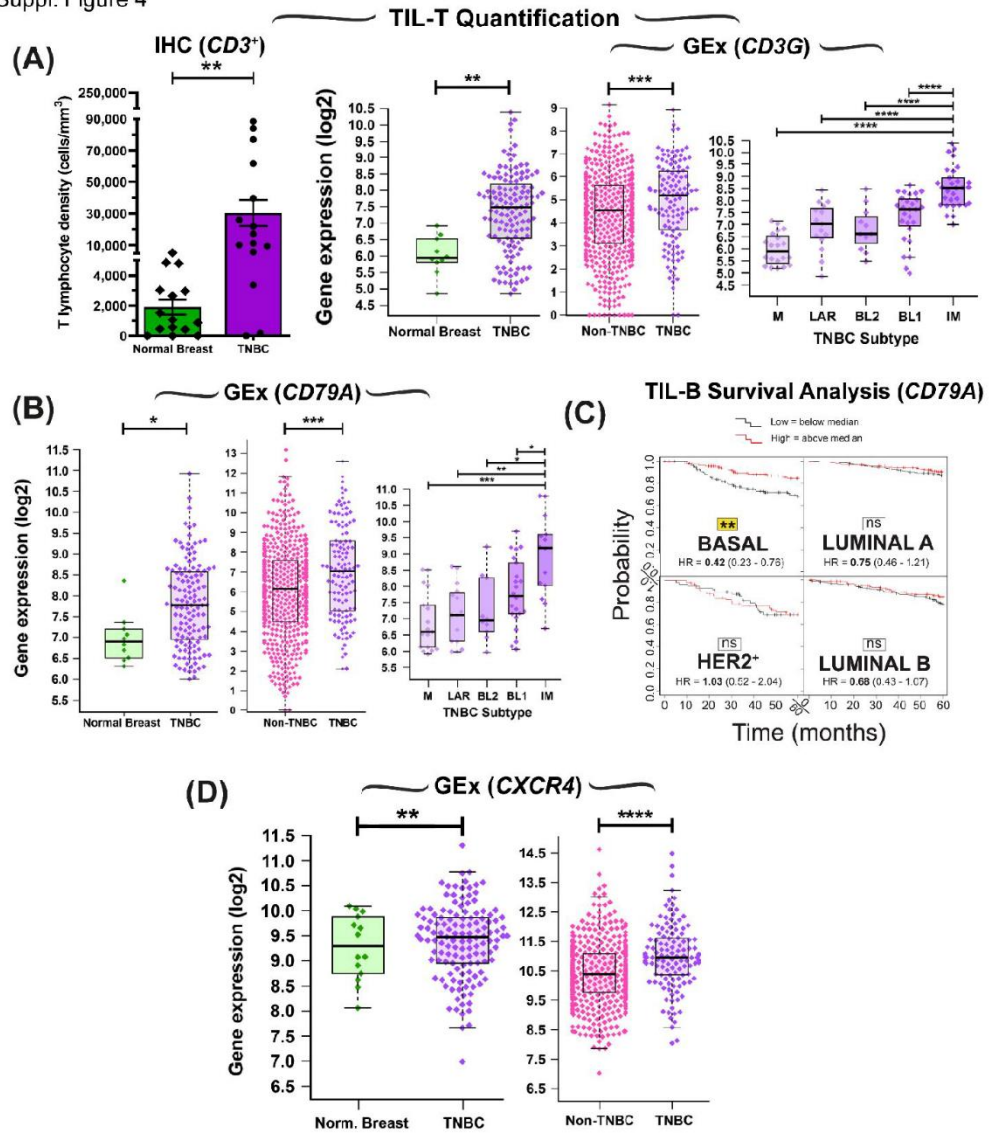


(E) Representative IHC/IF images depicting expression of GC B cell marker BCL6 among CD20<sup>+</sup>CD27<sup>+</sup> B cells within TNBC tumor

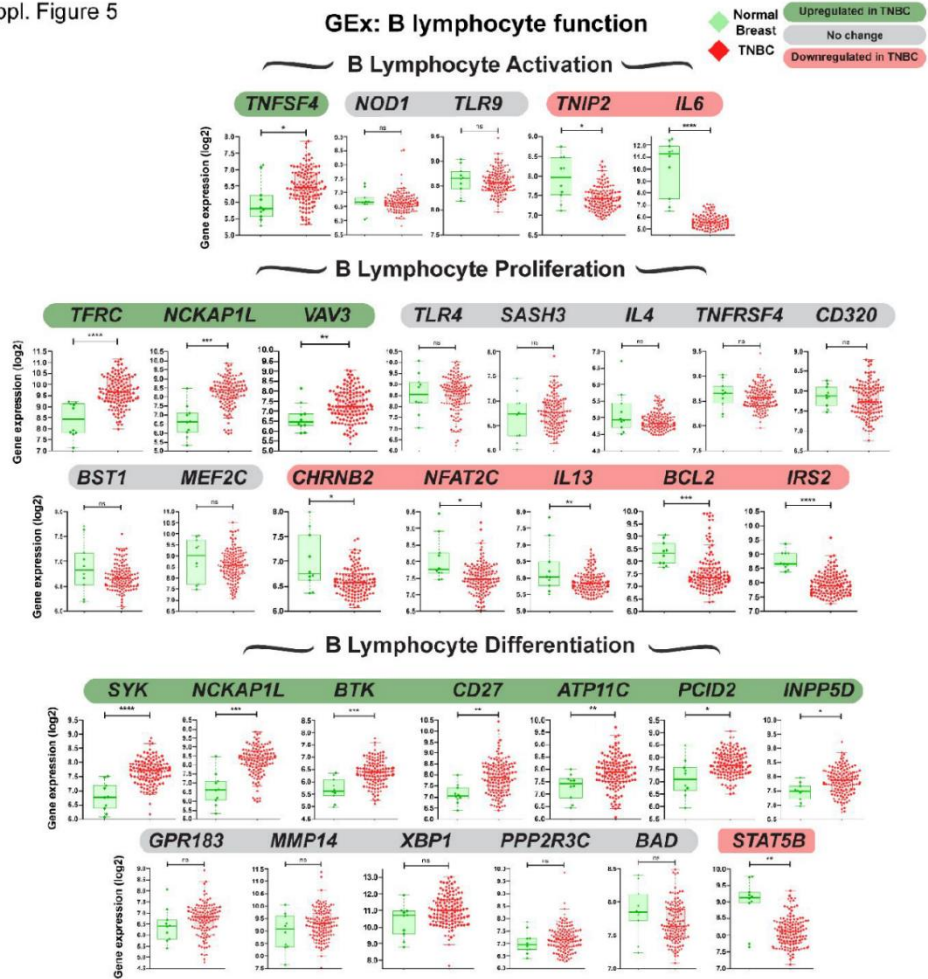


IgG/IgA<sup>+</sup> CD20<sup>+</sup>CD27<sup>+</sup>BCL6<sup>+</sup> cells indicated with white arrows

Suppl. Figure 4

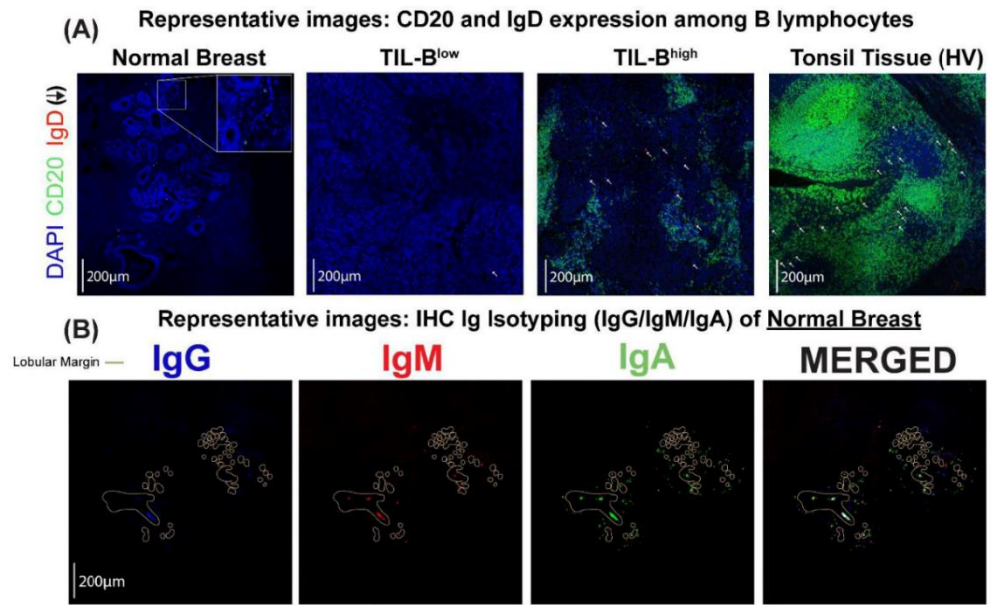


Suppl. Figure 5

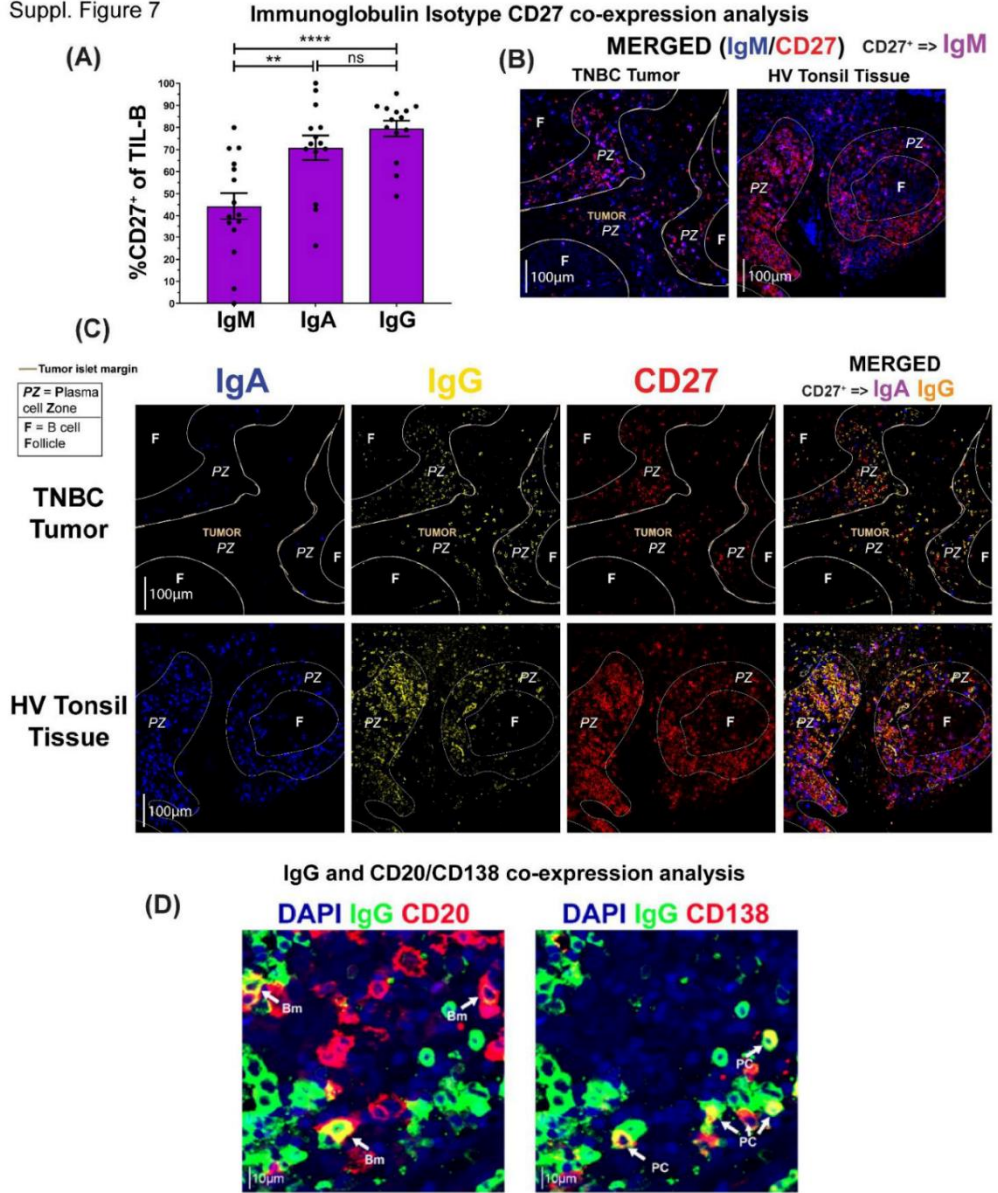




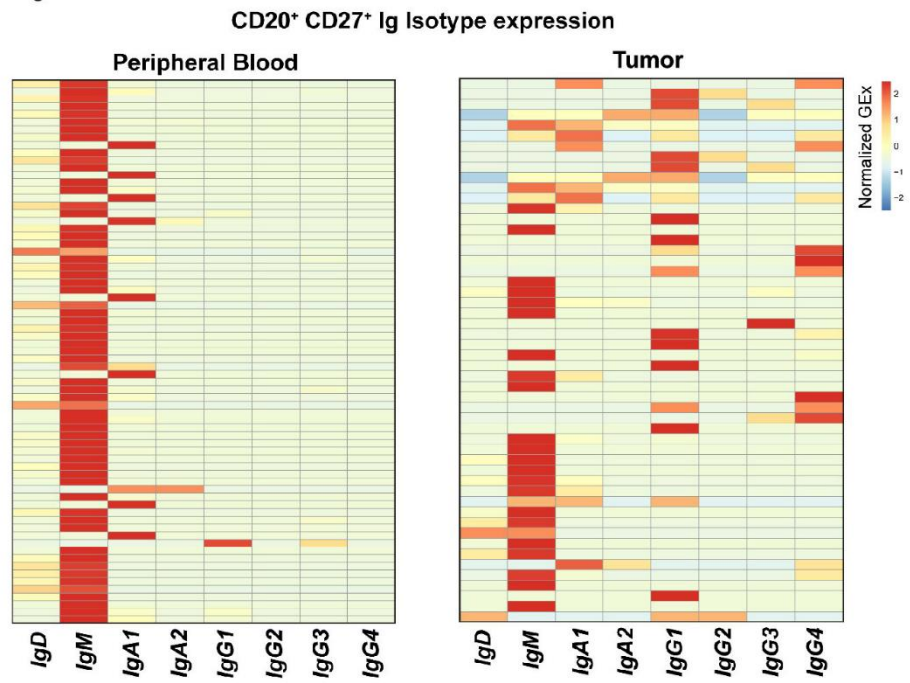
Suppl. Figure 6



Suppl. Figure 7



Suppl. Figure 8





## Supplementary Materials and Methods

### Cell isolation and flow cytometry

Surgical resection specimens of cancers and non-adjacent, non-tumor (NANT) tissues were collected, with paired blood samples. Normal tissues were obtained from breast reduction surgery and single cells were isolated as previously described (1). Peripheral blood mononuclear cells (PBMCs) were using Ficoll-Paque PLUS density gradient centrifugation and stained with LIVE/DEAD Fixable Near-IR dye (Life Technologies). Cells were incubated with fluorescently-conjugated antibodies (BioLegend): PE-Cy7  $\alpha$ -CD45, V500  $\alpha$ -CD19, FITC  $\alpha$ -CD20, PE  $\alpha$ -CD27 and BV421  $\alpha$ -IgD and analyzed using FACSCanto flow cytometer.

### Immunohistochemical/immunofluorescence (IHC/IF) evaluations of TIL-B structural formation and immunoglobulin isotype expression

Formalin-fixed paraffin embedded (FFPE) breast cancer and normal breast tissue sections (4 $\mu$ m thickness) were provided by Bart's Cancer Institute, Queen Mary University of London (Bart's IHC cohort, **Suppl. Table 1**). TIL working group guidelines (2) were used to determine the quantitative analysis methodology for TIL density quantification. For cancer specimens, the area of analysis was determined as being within the borders of the invasive lesion, guided by a trained pathologist and discerned using PanCK and DAPI staining. For normal breast sections, the area of analysis was determined as being the area surrounding normal lobules. Quantitative analysis was performed by capturing 40 randomly distributed image fields within each defined breast section using a Nikon TE 2000-U confocal microscope. TILs positive for relevant markers were counted manually using ImageJ software and the cellular density of each TIL subset (per mm<sup>3</sup> tumor/normal breast) was calculated accordingly: mean cell count per image analysed\*(1/image area)/(1/section thickness). Image area=0.42mm<sup>2</sup>; section thickness=0.004mm.

To investigate TIL-B structural formation and localisation within the TME, B lymphocytes were classified into distinct groups. TIL-B were categorised as being intratumoral or stromal, according to their location inside or outside of tumor islets respectively, defined using PanCK staining. Furthermore, the presence of B lymphocytes within TIL clusters was determined as those belonging to groups of at least thirty B lymphocytes immediately adjacent to at least thirty T lymphocytes within 100 $\mu$ m of tissue. Whole slide images (WSI) were obtained using the Olympus VS120-S5 slide scanning microscope.

1

### **KM plotter prospective cohort study**

Assignment of subtypes analysed in the KM plotter cohort are determined in KM plotter as described in (3, 4) using the expression of HER2, ESR1 and MKI67 (Basal: ESR1-/HER2-; luminal A: ESR1+/HER2-/MKI67 low; luminal B: ESR1+/HER2-/MKI67 high and HER2+/ESR1+; HER2\*: HER2+/ESR1).

### **CIBERSORT to examine tumor-infiltrating immune subpopulations**

Gene expression data for the Guy's TNBC-enriched cohort was previously described (5). Briefly, gene expression was obtained from the Affymetrix GeneChip Human Exon 1.0ST microarray (E-MTAB-5270). CIBERSORT (6) was applied to quantify the abundance of 22 immune subsets in 177 TNBC samples, including naïve B cells, plasma cells and memory B cells. Only tumors for which the CIBERSORT deconvolution was considered successful ( $P < 0.05$ ) were taken forward (N=116). Semi-quantitative TIL classification was performed by a trained histopathologist using tissue microarrays. Each tumor was scored as following: 0 (absence of lymphocytes); 1 (minimal infiltration), 2 (mild infiltration), 3 (moderate infiltration), and 4 (marked infiltration). Tumors with a semi-quantitative score  $\geq 3$  were considered to have high TILs. An iterative process to determine the optimal cut-off point by a minimal  $P$  value approach was employed to identify the cut-off for each of the immune subsets used in the outcome analyses. Univariate Cox proportional hazards regression models were used to investigate the prognostic importance of immune subsets.

### **CellPhoneDB analysis to study T cell-B cell interactions in breast cancer tumor microenvironment**

Cells originally annotated by Azizi *et al.* (7) as B or T cells were selected from tumors (Single cell cohort, **Suppl. Table 1**). All T cell subtypes (CD4<sup>+</sup>CM, CD4<sup>+</sup>EM, CD4<sup>+</sup>naive, CD8<sup>+</sup>CM, CD8<sup>+</sup>EM, CD8<sup>+</sup>naive, Treg) were combined into one category: T cells. The list of B and T cell IDs was used to subset the imputed dataset. A pseudocount of 2.591 (the minimal absolute normalized expression value) was added to shift the data to non-negative space for downstream analysis of cell-cell interactions using CellPhoneDB v2.0 (8). The statistical analysis in CellPhoneDB used default settings. False discovery rate (FDR) correction was

2

applied to identify interactions between B cells and T cells. The resulting interactions were filtered to include those with FDR<0.001, and further manually curated to include communication pathways associated with: lymphoid assembly, cytokine signalling, co-stimulation, B cell dependent T-cell activation and cytotoxic T lymphocyte (CTL) activation.

#### **GO numbers for KM plotter prospective cohort study gene sets**

Positive regulation of B lymphocyte activation: 9 genes, GO:0050871

Positive regulation of B lymphocyte differentiation: 13 genes, GO:0045579

Positive regulation of B lymphocyte proliferation: 44 genes, GO:0030890

Isotype switching mechanism: 15 genes, GO:0045190

Positive regulation of IgG-isotype switching: 10 genes, GO:0048304

Positive regulation of IgA-isotype switching: 5 genes, GO:0048298

#### **Breast cancer patient serum immunoglobulin isotyping**

To examine the modulation of serum immunoglobulin isotype profiles in breast cancer patients (KCL Luminex cohort, **Suppl. Table 1**), a high-throughput antibody isotyping magnetic bead-based Luminex assay (Thermo Fisher) was performed according to manufacturer's instructions. Titers of IgG1, IgG2, IgG3, IgG4, IgM, IgA and IgE were quantified in healthy volunteer and breast cancer patient's serum, which was stored at -80°C and thawed on ice prior to analysis.

#### **Immunoglobulin repertoire analyses**

From two ER<sup>+</sup> cancers, two TNBC and a normal breast sample (KCL sequencing cohort, **Suppl. Table 1**) cDNA was synthesized using the 5' RACE template switch method. Firstly, a 4µL reaction with min 170ng - max 2µg of RNA, mixed with 10µM of reverse transcription primer for each of IgA, IgG and IgM (0.5µL each), was run at 70°C (4min) then 42°C (2min). The product was subsequently mixed with 2µL First Strand 5x buffer (Clontech), 1µL DTT (20mM, Clontech), 1µL SmartNNN primer (10µM), 1µL dNTP solution Mix (10mM each, NEB) and 1µL SMARTScribe™ Transcriptase (Clontech), and placed at 42°C for 60 minutes.

This mixture was treated with 1  $\mu$ L of UDG (Uracil-DNA Glycosylase, NEB) enzyme and placed at 37°C (60min) then heat inactivated at 95°C (10min). A 20  $\mu$ L PCR1 reaction containing 1  $\mu$ L of cDNA, 0.2  $\mu$ L Q5 enzyme (NEB), 10  $\mu$ M each dNTP, 10  $\mu$ M each of IgA, IgG and IgM primers, 4  $\mu$ L 5x Q5 reaction buffer (NEB) and 1  $\mu$ L Smart20 (10  $\mu$ M) was run at 98°C (30s), 21 cycles of 98°C (10s); 65°C (20s); 72°C (50s), and 1 cycle of 72°C (5min). PCR2 was then performed with each isotype amplified separately, with a 20  $\mu$ L reaction using 1  $\mu$ L of PCR1 product, 0.2  $\mu$ L Q5 enzyme, 10  $\mu$ M each dNTPs, 10  $\mu$ M forward primers, 10  $\mu$ M constant gene-specific primers and 4  $\mu$ L 5x Q5 reaction buffer, at 98°C (30 s) then 12 cycles of 98°C (10s); 65°C (20s); 72°C (50s), and 1 cycle of 72°C (5min). The forward and reverse primers in PCR2 contain unique molecular barcodes. PCR2 products of identical barcodes were pooled and purified. Sequencing was carried out using the PacBio Single Molecule, Real-Time (SMRT) Sequencing platform.

Data clean-up was carried out as described (9) removing sequences with identical molecular barcodes. Ig genes and CDR3 sequences were determined using IMGT/HighV-QUEST (10). Relatedness among sequences were estimated using the BRepertoire webserver (11), by partitioning all CDR3 DNA sequences by the sample and the V gene family used, and calculating Levenshtein distances between all sequence pairs within each partition (12). Related sequence pairs were determined as having a distance of 0.18 (11). Hierarchical clustering was performed on this pairwise distance matrix to define clonotypes. Therefore the clones defined are specific to each sample, and are independent from the isotype. Modal sequences of each clonotype were determined as representatives. This representative subset (here denoted R) were compared against all the sampled sequences (denoted S) to delineate immunoglobulin isotype and subclass distributions of clonally expanded repertoire. Specifically, the number of sequences for each Ig isotype and subclass were quantified separately in R and S sequence sets, and fold change is quantified for each isotype/subtype as:

$$\text{fold difference} = \frac{\text{Number of Ig sequences in S} - \text{Number of Ig sequences in R}}{\text{Number of Ig sequences in R}}$$

A large fold difference implies sizeable clonal expansion. This method of quantification was applied to compare isotype, subtype and VDJ gene usage combination changes following clonal expansion. Data visualization was performed using the ggplot2 package in the R Statistical Programming environment (version 3.6.2).



### **Ig isotype titers in sera of patients with breast cancer**

The Swedish Apolipoprotein MOrtality-related RiSk (AMORIS) cohort consists of participants predominantly living in greater Stockholm in Sweden during the baseline period 1985–1996 (13). This study enabled a follow-up of cancer and cause-specific death until the end of 2011. We examined baseline serum immunoglobulin isotype titres (IgA, IgG, IgM and IgE) in individuals diagnosed with breast cancer, and explored their association with breast cancer-specific death. Mean follow-up time was 5.2 years patients who died of breast cancer (N=389), and 8.8 years for patients who did not die of their breast cancer during follow-up (N=3,643) (AMORIS cohort, **Suppl. Table 1**).

## Supplementary Figure legends

### **Supplementary Figure 1. Serum IgG titers are collapsed in patients following chemotherapy.**

(A) Heat map showing serum immunoglobulin isotype concentrations in healthy volunteers (HV) (N=18) and breast cancer patients (N=7 No Chemo, N=11 Chemo) (KCL Luminex cohort, **Suppl. Table 1**) determined via Luminex 7plex assay. Concentrations were split into quintiles using pooled global concentrations of each isotype, with increasing concentrations ordered from left to right within each isotype for each subject group (colored from blue (low) to red (high)). A significant overall reduction, particularly in IgG and IgE serum concentrations, can be visualised in the breast cancer group compared to the HV group. (B) Statistical comparison of serum immunoglobulin isotype concentrations within HV and patients with or without previous or ongoing chemotherapy treatment. Significant decreases in concentration of IgG subclasses but not of IgE, IgA or IgM isotypes are apparent in the chemotherapy treated patient cohort, resulting in a reduced total serum immunoglobulin titre.

### **Supplementary Figure 2. Serum immunoglobulin isotype titers do not serve as a predictive marker for breast cancer-related mortality.**

Examination of whether serum immunoglobulin isotype titers affect the overall risk of breast cancer-specific death. Mean serum immunoglobulin isotype concentrations were compared for breast cancer patients who either died specifically from breast cancer (N=389) (mean follow-up time 5.2 years) and those patients for whom no breast cancer-specific death was recorded (N=3,643) (mean follow-up time 8.8 years) (AMORIS cohort). We observed that the distribution of Ig among the breast cancer specific death group and deaths from other causes group, was not statistically significant. The Ig categories used in the analysis were selected following the medical cut-offs established by the Central Automation Laboratory (CALAB) in Stockholm, Sweden, where the samples were analysed. Moreover, the multivariate Cox Proportional Hazards regression analysis was adjusted for age, parity, education status and Charlton Comorbidity Index (CCI). The analyses did not show any

6

difference in survival based on the Ig isotype categories.

**Supplementary Figure 3. CD27<sup>+</sup> expression distribution and GC B cell marker expression across B lymphocyte populations analyzed by single-cell gene expression and IHC/IF.** The distribution of CD27<sup>+</sup> populations was investigated by scRNA-seq. **(A)** CD27<sup>+</sup> cells and **(B)** CD27<sup>+</sup>IgD<sup>-</sup> cells in patient blood and tumor samples (Single cell cohort). All transcript counts were of cells positive for either or both BCR complex CD79A and CD79B markers. **(C)** Analyses for B lymphocyte subpopulations were also performed by IHC/IF in seven TNBC tumor samples (KCL IHC cohort), with representative images for IHC/IF staining. White arrows indicate memory B lymphocytes as CD20<sup>+</sup>CD27<sup>+</sup> (visible in yellow color (merge)), while CD138<sup>+</sup> cells are mostly negative for CD20 staining. Scale bar=50µm. **(D)** Analysis of GC markers expressed by B cells using scRNA-seq. Expression of GC B cell markers in isotype-switched (IgD<sup>-</sup>IgM<sup>+</sup>) CD19<sup>+</sup>CD20<sup>+</sup>CD22<sup>+</sup>CD27<sup>+</sup> memory B cells was investigated for early (IRF8, BCL6, MCL1, TCF3) and mature (EBF1, SPIB, DOCK8, BACH2) GC markers (14) in tumor samples (Single cell cohort), consistent with initial BCR stimulation inducing GC B cells to differentiate into long-lived plasma cells and memory B cells in GCs and by subsequent antigen recall responses that may drive memory B cells to either differentiate into long-lived plasma cells or to re-enter the GC reaction (15). **(E)** Representative immunofluorescence images of a TNBC lesion showing isotype-switched CD20<sup>+</sup>CD27<sup>+</sup> (including IgG/IgA<sup>+</sup>) B cells co-expressing the early GC marker BCL6 (White arrows). Scale bar=20µm.

**Supplementary Figure 4. TIL-B, TIL-T and B lymphocyte recruitment markers in TNBC**

**(A)** Quantitative IHC analysis of CD3<sup>+</sup> T lymphocytes within normal breast tissues and TNBC lesions (N=15 each) (Bart's IHC cohort), and by GEx: normal breast vs TNBC ([left] N=10 vs 131, KCL GEx cohort); non-TNBC vs TNBC ([middle] N=515 vs 123, TCGA GEx cohort); and TNBC subtypes ([right] N=122, KCL GEx cohort) **(B)** TIL-B GEx of the BCR complex *CD79A* marker: normal breast vs TNBC ([left] N=10 vs 131, KCL GEx cohort), non-TNBC vs TNBC ([middle] N=515 vs 123, TCGA GEx

cohort) and TNBC subtypes ([right] N=122, KCL GEx cohort). **(C)** High TIL-B (*CD79A* expression) demonstrate better overall survival in basal-like subtype (N=241) (KM plotter cohort). **(D)** GEx data for the B lymphocyte recruitment marker gene *CXCR4*: normal breast vs TNBC ([left] N=10 vs 131, KCL GEx cohort); non-TNBC vs TNBC ([right] N=515 vs 123, TCGA GEx cohort).

**Supplementary Figure 5. Expression data of genes that positively regulate key B lymphocyte functions.**

GEx data (normal breast vs TNBC (N=10 vs 131, KCL GEx cohort) of individual genes evaluated in TNBC compared to normal breast. Pathways investigated include B lymphocyte activation, proliferation and differentiation.

**Supplementary Figure 6. IHC staining demonstrate CD20 and IgD expression in normal breast and TNBC tumors.**

**(A)** IF images show that naïve ( $IgD^+$ , arrows) B lymphocyte distribution in TNBC TIL-B<sup>high</sup> tumors is analogous to secondary lymphoid organs (tonsil). **(B)** As a control, IF images illustrating Ig isotype distribution in normal breast tissue (Bart's IHC cohort). Scale bar=200 $\mu$ m.

**Supplementary Figure 7. IHC staining demonstrates CD27 expression in isotype-switched TIL-B and presence of both memory/GC B and plasma IgG<sup>+</sup> B lymphocytes in TNBC.**

**(A)** Significantly-greater CD27 co-expression among  $IgA^+$  and  $IgG^+$  than  $IgM^+$  TIL-B in TNBC (N=15). **(B)** Example images illustrating the extent to which  $IgM^+$  B lymphocytes co-express CD27 in a typical TIL-B<sup>high</sup> individual and secondary lymphoid organ (tonsil) of healthy volunteer. Scale bar=100 $\mu$ m. **(C)** Representative images depicting the extent to which isotype-switched  $IgA^+$  (blue) and  $IgG^+$  (yellow) B lymphocytes co-express CD27<sup>+</sup> (red). Brown dash lines indicate margin of tumor. White lines separate distinct regions of B lymphocyte compartments (PZ=plasma cell zone; F=B cell follicle) (Bart's IHC cohort). Scale bar=100 $\mu$ m. **(D)** Representative images for  $IgG^+$  B lymphocyte populations performed by IHC/IF in TNBC samples (KCL IHC cohort). White arrows indicate IgG-expressing

memory/GC B cells (CD20) or plasma cells (CD138) (visible in yellow color (merge)). Scale bar=10µm.

**Supplementary Figure 8. IgCH transcripts of CD27<sup>+</sup> B lymphocytes.**

IgCH switch transcripts of single B cells (CD19<sup>+</sup>CD27<sup>+</sup>/CD20<sup>+</sup>CD27<sup>+</sup>/CD22<sup>+</sup>CD27<sup>+</sup> single cells) were identified in patient blood (N=71) and breast cancer tissues (N=52) (Single cell cohort).

**Supplementary Figure 9. Expression data in TNBC of key genes known to positively regulate B lymphocyte isotype-switching.**

GEx data (normal breast versus TNBC (N=10 vs 131, KCL GEx cohort) of individual genes evaluated in TNBC compared to normal breast. Pathways investigated include isotype-switching mechanism and IgG/IgA isotype-switching.

**Supplementary Figure 10. Immunoglobulin repertoire analysis of breast cancer samples.**

Clonal expansion separated by Ig isotypes and subtypes (KCL sequencing cohort). Total count of Ig sequences for (A) each isotype or (B) subtype per sample. [right panel in (A)] Mean number of sequences for each Ig subtype per clonal family. A larger number indicates greater clonal expansion. (C) Usage of V, D, and J genes in IgA and IgG sequences. The left panels depict the percentage of sequences utilising each V/D/J gene. The right panels indicate the fold change obtained by comparing the total sequence set with the representative subset. A large fold change thus indicates greater clonal expansion for sequences carrying that particular V/D/J gene. (D) The B cell repertoires in matched blood and tumor samples (Single cell cohort) from each of two patients with breast cancer show similarities in the kappa and lambda chain V genes (IGKV, IGLV) and J genes (IGKJ, IGLJ) between a patient's blood and tumor-associated CD20<sup>+</sup>CD27<sup>+</sup> B lymphocytes. Yellow circles represent light chain repertoires in blood; red circles represent the light chain repertoire in tumors. Numbers in circles indicate the raw transcript count of each gene.

### Supplementary Reference:

1. Garaud S, Gu-Trantien C, Lodewyckx JN, Boisson A, De Silva P, Buisseret L, et al. A simple and rapid protocol to non-enzymatically dissociate fresh human tissues for the analysis of infiltrating lymphocytes. *J Vis Exp*. 2014 Dec 6(94).
2. Salgado R, Denkert C, Demaria S, Sirtaine N, Klauschen F, Pruneri G, et al. The evaluation of tumor-infiltrating lymphocytes (TILs) in breast cancer: recommendations by an International TILs Working Group 2014. *Ann Oncol*. 2015 Feb;26(2):259-71.
3. Györfy B, Lanczky A, Eklund AC, Denkert C, Budczies J, Li Q, et al. An online survival analysis tool to rapidly assess the effect of 22,277 genes on breast cancer prognosis using microarray data of 1,809 patients. *Breast Cancer Res Treat*. 2010 Oct;123(3):725-31.
4. Mihaly Z, Györfy B. Improving Pathological Assessment of Breast Cancer by Employing Array-Based Transcriptome Analysis. *Microarrays (Basel)*. 2013 Aug 29;2(3):228-42.
5. Patel N, Weekes D, Drosopoulos K, Gazinska P, Noel E, Rashid M, et al. Integrated genomics and functional validation identifies malignant cell specific dependencies in triple negative breast cancer. *Nat Commun*. 2018 Mar 13;9(1):1044.
6. Newman AM, Liu CL, Green MR, Gentles AJ, Feng W, Xu Y, et al. Robust enumeration of cell subsets from tissue expression profiles. *Nat Methods*. 2015 May;12(5):453-7.
7. Azizi E, Carr AJ, Plitas G, Cornish AE, Konopacki C, Prabhakaran S, et al. Single-Cell Map of Diverse Immune Phenotypes in the Breast Tumor Microenvironment. *Cell*. 2018 Aug 23;174(5):1293-308 e36.
8. Efremova M, Vento-Tormo M, Teichmann SA, Vento-Tormo R. CellPhoneDB: inferring cell-cell communication from combined expression of multi-subunit ligand-receptor complexes. *Nat Protoc*. 2020 Apr;15(4):1484-506.
9. Wu YC, Kipling D, Dunn-Walters D. Assessment of B Cell Repertoire in Humans. *Methods Mol Biol*. 2015;1343:199-218.
10. Brochet X, Lefranc MP, Giudicelli V. IMGT/V-QUEST: the highly customized and integrated system for IG and TR standardized V-J and V-D-J sequence analysis. *Nucleic Acids Res*. 2008 Jul 1;36(Web Server issue):W503-8.
11. Margreitter C, Lu HC, Townsend C, Stewart A, Dunn-Walters DK, Fraternali F. BRepertoire: a user-friendly web server for analysing antibody repertoire data. *Nucleic Acids Res*. 2018 Jul 2;46(W1):W264-W70.
12. Townsend CL, Laffy JM, Wu YB, Silva O'Hare J, Martin V, Kipling D, et al. Significant Differences in Physicochemical Properties of Human Immunoglobulin Kappa and Lambda CDR3 Regions. *Front Immunol*. 2016;7:388.
13. Walldius G, Malmstrom H, Jungner I, de Faire U, Lambe M, Van Hemelrijck M, et al. Cohort Profile: The AMORIS cohort. *Int J Epidemiol*. 2017 Aug 1;46(4):1103-i.
14. De Silva NS, Klein U. Dynamics of B cells in germinal centres. *Nat Rev Immunol*. 2015 Mar;15(3):137-48.
15. Akkaya M, Kwak K, Pierce SK. B cell memory: building two walls of protection against pathogens. *Nat Rev Immunol*. 2020 Apr;20(4):229-38.

## **References**

1. Sung H, Ferlay J, Siegel RL, Laversanne M, Soerjomataram I, Jemal A, et al. Global Cancer Statistics 2020: GLOBOCAN Estimates of Incidence and Mortality Worldwide for 36 Cancers in 185 Countries. *CA: A Cancer Journal for Clinicians*. 2021;71(3): 209–249.
2. Carioli G, Malvezzi M, Bertuccio P, Boffetta P, Levi F, la Vecchia C, et al. European cancer mortality predictions for the year 2021 with focus on pancreatic and female lung cancer. *Annals of Oncology*. 2021;32(4): 478–487.
3. Martincorena I, Raine KM, Gerstung M, Dawson KJ, Haase K, van Loo P, et al. Universal Patterns of Selection in Cancer and Somatic Tissues. *Cell*. 2017;171(5): 1029–1041.e21.
4. Hortobagyi GN, de la Garza Salazar J, Pritchard K, Amadori D, Haidinger R, Hudis CA, et al. The Global Breast Cancer Burden: Variations in Epidemiology and Survival. *Clinical Breast Cancer*. 2005;6(5): 391–401.
5. Torre LA, Bray F, Siegel RL, Ferlay J, Lortet-Tieulent J, Jemal A. Global cancer statistics, 2012. *CA: A Cancer Journal for Clinicians*. 2015;65(2): 87–108.
6. McCormack VA, Boffetta P. Today's lifestyles, tomorrow's cancers: trends in lifestyle risk factors for cancer in low- and middle-income countries. *Annals of Oncology*. 2011;22(11): 2349–2357.
7. Verma R, Bowen RL, Slater SE, Mihaimed F, Jones JL. Pathological and epidemiological factors associated with advanced stage at diagnosis of breast cancer. *British Medical Bulletin*. 2012;103(1): 129–145.
8. Feng Y, Spezia M, Huang S, Yuan C, Zeng Z, Zhang L, et al. Breast cancer development and progression: Risk factors, cancer stem cells, signaling pathways, genomics, and molecular pathogenesis. *Genes & diseases*. 2018;5(2): 77–106.
9. Perou CM, Sørlie T, Eisen MB, van de Rijn M, Jeffrey SS, Rees CA, et al. Molecular portraits of human breast tumours. *Nature*. 2000;406(6797): 747–752.
10. Sørlie T, Perou CM, Tibshirani R, Aas T, Geisler S, Johnsen H, et al. Gene expression patterns of breast carcinomas distinguish tumor subclasses with clinical implications. *Proceedings of the National Academy of Sciences*. 2001;98(19): 10869.
11. Bauer KR, Brown M, Cress RD, Parise CA, Caggiano V. Descriptive analysis of estrogen receptor (ER)-negative, progesterone receptor (PR)-negative, and HER2-negative invasive breast cancer, the so-called triple-negative phenotype. *Cancer*. 2007;109(9): 1721–1728.
12. Prat A, Perou CM. Deconstructing the molecular portraits of breast cancer. *Molecular Oncology*. 2011;5(1): 5–23.
13. Cheang MCU, Voduc D, Bajdik C, Leung S, McKinney S, Chia SK, et al. Basal-Like Breast Cancer Defined by Five Biomarkers Has Superior Prognostic Value than Triple-Negative Phenotype. *Clinical Cancer Research*. 2008;14(5): 1368.

14. Hudis CA, Gianni L. Triple-Negative Breast Cancer: An Unmet Medical Need. *The Oncologist*. 2011;16(S1): 1–11.
15. *BioRender templates*. BioRender App. Available from: <https://app.biorender.com/biorender-templates> [Accessed: 8th November 2021]
16. Polyak K. Breast cancer: origins and evolution. *The Journal of Clinical Investigation*. 2007;117(11): 3155–3163.
17. Place AE, Jin Huh S, Polyak K. The microenvironment in breast cancer progression: biology and implications for treatment. *Breast Cancer Research*. 2011;13(6): 227.
18. Amin MB, Edge SB, Greene FL, Byrd DR, Brookland RK, Washington MK, et al. *AJCC cancer staging manual*. 8th ed. New York, NY: Springer; 2017.
19. John S, Broggio J. *Cancer survival in England - adults diagnosed*. Office for National Statistics. Available from: <https://www.ons.gov.uk/peoplepopulationandcommunity/healthandsocialcare/conditionsanddiseases/datasets/cancersurvivalratescancersurvivalinenglandadultsdiagnosed> [Accessed: 11th December 2021]
20. Koh J, Kim MJ. Introduction of a New Staging System of Breast Cancer for Radiologists: An Emphasis on the Prognostic Stage. *Korean J Radiol*. 2019;20(1): 69–82.
21. Weinstock MA. Nonmelanoma Skin Cancer Mortality in the United States, 1969 Through 1988. *Archives of Dermatology*. 1993;129(10): 1286–1290.
22. Howlader N, Noone AM, Krapcho M, Miller D, Brest A, Yu M, et al. *Seer Cancer Statistics Review, 1975-2017*. SEER. Available from: [https://seer.cancer.gov/csr/1975\\_2017](https://seer.cancer.gov/csr/1975_2017) [Accessed: 28th October 2021]
23. Scotto J, Fears TR, Fraumeni JF. Incidence of non-melanoma skin cancer in the United States. *Washington DC: U.S. Government Printing Office*. 1983;83–2433.
24. Rogers HW, Weinstock MA, Harris AR, Hinckley MR, Feldman SR, Fleischer AB, et al. Incidence Estimate of Nonmelanoma Skin Cancer in the United States, 2006. *Archives of Dermatology*. 2010;146(3): 283–287.
25. Haass NK, Smalley KSM, Li L, Herlyn M. Adhesion, migration and communication in melanocytes and melanoma. *Pigment Cell Research*. 2005;18(3): 150–159.
26. Gottardi CJ, Wong E, Gumbiner BM. E-Cadherin Suppresses Cellular Transformation by Inhibiting  $\beta$ -Catenin Signaling in an Adhesion-Independent Manner. *Journal of Cell Biology*. 2001;153(5): 1049–1060.
27. Nesbit M, Nesbit HKE, Bennett J, Andl T, Hsu MY, Dejesus E, et al. Basic fibroblast growth factor induces a transformed phenotype in normal human melanocytes. *Oncogene*. 1999;18(47): 6469–6476.
28. Bierie B, Moses HL. TGF $\beta$ : the molecular Jekyll and Hyde of cancer. *Nature Reviews Cancer*. 2006;6(7): 506–520.



29. Albini A, Sporn MB. The tumour microenvironment as a target for chemoprevention. *Nature Reviews Cancer*. 2007;7(2): 139–147.
30. Ogata D, Namikawa K, Takahashi A, Yamazaki N. A review of the AJCC melanoma staging system in the TNM classification (eighth edition). *Japanese Journal of Clinical Oncology*. 2021;51(5): 671–674.
31. Keohane SG, Proby CM, Newlands C, Motley RJ, Nasr I, Mohd Mustapa MF, et al. The new 8th edition of TNM staging and its implications for skin cancer: a review by the British Association of Dermatologists and the Royal College of Pathologists, U.K. *British Journal of Dermatology*. 2018;179(4): 824–828.
32. Umscheid CA, Margolis DJ, Grossman CE. Key Concepts of Clinical Trials: A Narrative Review. *Postgraduate Medicine*. 2011;123(5): 194–204.
33. *Early and locally advanced breast cancer: Diagnosis and management*. NICE. Available from: <https://www.nice.org.uk/guidance/ng101> [Accessed: 10th December 2021]
34. *Advanced breast cancer: Diagnosis and treatment*. NICE. Available from: <https://www.nice.org.uk/guidance/cg81> [Accessed: 11th December 2021]
35. Sparano JA, Gray RJ, Makower DF, Pritchard KI, Albain KS, Hayes DF, et al. Adjuvant Chemotherapy Guided by a 21-Gene Expression Assay in Breast Cancer. *New England Journal of Medicine*. 2018;379(2): 111–121.
36. Kurian AW, Bondarenko I, Jagsi R, Friese CR, McLeod MC, Hawley ST, et al. Recent Trends in Chemotherapy Use and Oncologists' Treatment Recommendations for Early-Stage Breast Cancer. *JNCI: Journal of the National Cancer Institute*. 2018;110(5): 493–500.
37. Untch M, Gelber RD, Jackisch C, Procter M, Baselga J, Bell R, et al. Estimating the magnitude of trastuzumab effects within patient subgroups in the HERA trial. *Annals of Oncology*. 2008;19(6): 1090–1096.
38. Lange CA, Yee D. Killing the second messenger: targeting loss of cell cycle control in endocrine-resistant breast cancer. *Endocrine-related cancer*. 2011;18(4): C19–C24.
39. Nicolini A, Carpi A, Ferrari P, Biava PM, Rossi G. Immunotherapy and hormone-therapy in metastatic breast cancer: A review and an update. *Current Drug Targets*. 2016;17(10): 1127–1139.
40. Xue M, Zhang K, Mu K, Xu J, Yang H, Liu Y, et al. Regulation of estrogen signaling and breast cancer proliferation by an ubiquitin ligase TRIM56. *Oncogenesis*. 2019;8(5): 30.
41. Liedtke C, Mazouni C, Hess KR, André F, Tordai A, Mejia JA, et al. Response to Neoadjuvant Therapy and Long-Term Survival in Patients With Triple-Negative Breast Cancer. *Journal of Clinical Oncology*. 2008;26(8): 1275–1281.
42. Nedeljković M, Damjanović A. Mechanisms of Chemotherapy Resistance in Triple-Negative Breast Cancer—How We Can Rise to the Challenge. *Cells*. 2019;8(9).
43. Cortes J, Cescon DW, Rugo HS, Nowecki Z, Im SA, Yusof MM, et al. Pembrolizumab plus chemotherapy versus placebo plus chemotherapy for previously untreated locally

recurrent inoperable or metastatic triple-negative breast cancer (KEYNOTE-355): a randomised, placebo-controlled, double-blind, phase 3 clinical trial. *The Lancet*. 2020;396(10265): 1817–1828.

44. Schmid P, Rugo HS, Adams S, Schneeweiss A, Barrios CH, Iwata H, et al. Atezolizumab plus nab-paclitaxel as first-line treatment for unresectable, locally advanced or metastatic triple-negative breast cancer (IMpassion130): updated efficacy results from a randomised, double-blind, placebo-controlled, phase 3 trial. *The Lancet Oncology*. 2020;21(1): 44–59.
45. *Genentech Provides Update on Tecentriq U.S. Indication for PD-L1-Positive, Metastatic Triple-Negative Breast Cancer*. Genentech. Available from: <https://www.gene.com/media/press-releases/14927/2021-08-27/genentech-provides-update-on-tecentriq-u> [Accessed: 12th November 2021]
46. Zhang M, Zhang L, Hei R, Li X, Cai H, Wu X, et al. CDK inhibitors in cancer therapy, an overview of recent development. *American journal of cancer research*. 2021;11(5): 1913–1935.
47. *Melanoma: Assessment and management*. NICE. Available from: <https://www.nice.org.uk/guidance/ng14> [Accessed: 10th December 2021]
48. Elder DE, Guerry D, Heiberger RM, LaRossa D, Goldman LI, Clark WH, et al. Optimal resection margin for cutaneous malignant melanoma. *Plastic and reconstructive surgery*. 1983;71(1): 66–72.
49. Kirkwood JM, Strawderman MH, Ernstoff MS, Smith TJ, Borden EC, Blum RH. Interferon alfa-2b adjuvant therapy of high-risk resected cutaneous melanoma: the Eastern Cooperative Oncology Group Trial EST 1684. *Journal of Clinical Oncology*. 1996;14(1): 7–17.
50. Lotze MT, Frana LW, Sharrow SO, Robb RJ, Rosenberg SA. In vivo administration of purified human interleukin 2. I. Half-life and immunologic effects of the Jurkat cell line-derived interleukin 2. *The Journal of Immunology*. 1985;134(1): 157.
51. Sabel MS, Sondak VK. Pros and cons of adjuvant interferon in the treatment of melanoma. *The oncologist*. 2003;8(5): 451–458.
52. Rosenberg SA, Yang JC, Topalian SL, Schwartzentruber DJ, Weber JS, Parkinson DR, et al. Treatment of 283 Consecutive Patients With Metastatic Melanoma or Renal Cell Cancer Using High-Dose Bolus Interleukin 2. *JAMA*. 1994;271(12): 907–913.
53. Krishnamoorthy M, Lenehan JG, Maleki Vareki S. Neoadjuvant Immunotherapy for High-Risk, Resectable Malignancies: Scientific Rationale and Clinical Challenges. *JNCI: Journal of the National Cancer Institute*. 2021;113(7): 823–832.
54. Hodi FS, O’Day SJ, McDermott DF, Weber RW, Sosman JA, Haanen JB, et al. Improved Survival with Ipilimumab in Patients with Metastatic Melanoma. *New England Journal of Medicine*. 2010;363(8): 711–723.

55. Hamid O, Robert C, Daud A, Hodi FS, Hwu WJ, Kefford R, et al. Safety and Tumor Responses with Lambrolizumab (Anti-PD-1) in Melanoma. *New England Journal of Medicine*. 2013;369(2): 134–144.
56. Brahmer JR, Drake CG, Wollner I, Powderly JD, Picus J, Sharfman WH, et al. Phase I study of single-agent anti-programmed death-1 (MDX-1106) in refractory solid tumors: safety, clinical activity, pharmacodynamics, and immunologic correlates. *Journal of clinical oncology: official journal of the American Society of Clinical Oncology*. 2010/06/01. 2010;28(19): 3167–3175.
57. Robert C, Long G v, Brady B, Dutriaux C, Maio M, Mortier L, et al. Nivolumab in Previously Untreated Melanoma without BRAF Mutation. *New England Journal of Medicine*. 2014;372(4): 320–330.
58. Gray-Schopfer V, Wellbrock C, Marais R. Melanoma biology and new targeted therapy. *Nature*. 2007;445(7130): 851–857.
59. Dhomen N, Marais R. BRAF Signaling and Targeted Therapies in Melanoma. *Hematology/Oncology Clinics*. 2009;23(3): 529–545.
60. Long G v, Menzies AM, Nagrial AM, Haydu LE, Hamilton AL, Mann GJ, et al. Prognostic and Clinicopathologic Associations of Oncogenic BRAF in Metastatic Melanoma. *Journal of Clinical Oncology*. 2011;29(10): 1239–1246.
61. Chapman PB, Hauschild A, Robert C, Haanen JB, Ascierto P, Larkin J, et al. Improved Survival with Vemurafenib in Melanoma with BRAF V600E Mutation. *New England Journal of Medicine*. 2011;364(26): 2507–2516.
62. Hauschild A, Grob JJ, Demidov L v, Jouary T, Gutzmer R, Millward M, et al. Dabrafenib in BRAF-mutated metastatic melanoma: a multicentre, open-label, phase 3 randomised controlled trial. *The Lancet*. 2012;380(9839): 358–365.
63. Shi H, Hugo W, Kong X, Hong A, Koya RC, Moriceau G, et al. Acquired Resistance and Clonal Evolution in Melanoma during BRAF Inhibitor Therapy. *Cancer Discovery*. 2014;4(1): 80.
64. Flaherty KT, Infante JR, Daud A, Gonzalez R, Kefford RF, Sosman J, et al. Combined BRAF and MEK Inhibition in Melanoma with BRAF V600 Mutations. *New England Journal of Medicine*. 2012;367(18): 1694–1703.
65. Fu J, Xu D, Liu Z, Shi M, Zhao P, Fu B, et al. Increased Regulatory T Cells Correlate With CD8 T-Cell Impairment and Poor Survival in Hepatocellular Carcinoma Patients. *Gastroenterology*. 2007;132(7): 2328–2339.
66. Curiel TJ, Coukos G, Zou L, Alvarez X, Cheng P, Mottram P, et al. Specific recruitment of regulatory T cells in ovarian carcinoma fosters immune privilege and predicts reduced survival. *Nature Medicine*. 2004;10(9): 942–949.
67. Murakami Y, Saito H, Shimizu S, Kono Y, Shishido Y, Miyatani K, et al. Increased regulatory B cells are involved in immune evasion in patients with gastric cancer. *Scientific Reports*. 2019;9(1): 13083.

68. Harris RJ, Cheung A, Ng JCF, Laddach R, Chenoweth AM, Crescioli S, et al. Tumor-Infiltrating B Lymphocyte Profiling Identifies IgG-Biased, Clonally Expanded Prognostic Phenotypes in Triple-Negative Breast Cancer. *Cancer Research*. 2021;81(16): 4290.
69. Akkaya M, Kwak K, Pierce SK. B cell memory: building two walls of protection against pathogens. *Nature Reviews Immunology*. 2020;20(4): 229–238.
70. Tobón GJ, Izquierdo JH, Cañas CA. B Lymphocytes: Development, Tolerance, and Their Role in Autoimmunity—Focus on Systemic Lupus Erythematosus. Anaya JM (ed.) *Autoimmune Diseases*. 2013;2013: 827254.
71. Fuxa M, Skok JA. Transcriptional regulation in early B cell development. *Current Opinion in Immunology*. 2007;19(2): 129–136.
72. Chi X, Li Y, Qiu X. V(D)J recombination, somatic hypermutation and class switch recombination of immunoglobulins: mechanism and regulation. *Immunology*. 2020;160(3): 233–247.
73. Mombaerts P, Iacomini J, Johnson RS, Herrup K, Tonegawa S, Papaioannou VE. RAG-1-deficient mice have no mature B and T lymphocytes. *Cell*. 1992;68(5): 869–877.
74. Melchers F. Checkpoints that control B cell development. *The Journal of Clinical Investigation*. 2015;125(6): 2203–2210.
75. Chung JB, Silverman M, Monroe JG. Transitional B cells: step by step towards immune competence. *Trends in Immunology*. 2003;24(6): 342–348.
76. Marshall-Clarke S, Tasker L, Parkhouse RM. Immature B lymphocytes from adult bone marrow exhibit a selective defect in induced hyperexpression of major histocompatibility complex class II and fail to show B7.2 induction. *Immunology*. 2000;100(2): 141–151.
77. Rolink AG, Andersson J, Melchers F. Characterization of immature B cells by a novel monoclonal antibody, by turnover and by mitogen reactivity. *European Journal of Immunology*. 1998;28(11): 3738–3748.
78. Coutinho A, Möller G. Thymus-Independent B-Cell Induction and Paralysis 11 The work reported in this review was supported by grants from the Swedish Cancer Society. In: Dixon FJ, Kunkel HG (eds.) *Advances in Immunology*. Academic Press; 1975. p. 113–236.
79. Pieper K, Grimbacher B, Eibel H. B-cell biology and development. *Journal of Allergy and Clinical Immunology*. 2013;131(4): 959–971.
80. Appelgren D, Eriksson P, Ernerudh J, Segelmark M. Marginal-Zone B-Cells Are Main Producers of IgM in Humans, and Are Reduced in Patients With Autoimmune Vasculitis. *Frontiers in Immunology*. 2018;9: 2242.
81. Cerutti A, Cols M, Puga I. Marginal zone B cells: virtues of innate-like antibody-producing lymphocytes. *Nature Reviews Immunology*. 2013;13(2): 118–132.
82. Victora GD, Nussenzweig MC. Germinal Centers. *Annual Review of Immunology*. 2012;30(1): 429–457.

83. Ron Y, Sprent J. T cell priming in vivo: a major role for B cells in presenting antigen to T cells in lymph nodes. *The Journal of Immunology*. 1987;138(9): 2848.
84. Akkaya M, Pierce SK. From zero to sixty and back to zero again: the metabolic life of B cells. *Current Opinion in Immunology*. 2019;57: 1–7.
85. Akkaya M, Akkaya B, Kim AS, Miozzo P, Sohn H, Pena M, et al. Toll-like receptor 9 antagonizes antibody affinity maturation. *Nature Immunology*. 2018;19(3): 255–266.
86. *Biorender*. BioRender App. Available from: <https://app.biorender.com> [Accessed: 8th November 2021]
87. Muramatsu M, Kinoshita K, Fagarasan S, Yamada S, Shinkai Y, Honjo T. Class Switch Recombination and Hypermutation Require Activation-Induced Cytidine Deaminase (AID), a Potential RNA Editing Enzyme. *Cell*. 2000;102(5): 553–563.
88. W KH, Nara O, C RJ, J CA, Gary W, A TS, et al. Single-cell analysis of human B cell maturation predicts how antibody class switching shapes selection dynamics. *Science Immunology*. 2021;6(56): eabe6291.
89. Currie CG, McCallum K, Poxton IR. Mucosal and systemic antibody responses to the lipopolysaccharide of Escherichia coli O157 in health and disease\*. *Journal of Medical Microbiology*. 2001;50(4): 345–354.
90. Chaplin DD. Overview of the immune response. *Journal of Allergy and Clinical Immunology*. 2010;125(2, Supplement 2): S3–S23.
91. Schroeder HW, Cavacini L. Structure and function of immunoglobulins. *Journal of Allergy and Clinical Immunology*. 2010;125(2, Supplement 2): S41–S52.
92. Gonzalez-Quintela A, Alende R, Gude F, Campos J, Rey J, Meijide LM, et al. Serum levels of immunoglobulins (IgG, IgA, IgM) in a general adult population and their relationship with alcohol consumption, smoking and common metabolic abnormalities. *Clinical & Experimental Immunology*. 2008;151(1): 42–50.
93. Keyt BA, Baliga R, Sinclair AM, Carroll SF, Peterson MS. Structure, Function, and Therapeutic Use of IgM Antibodies. *Antibodies*. 2020;9(4).
94. Wei X, Decker JM, Wang S, Hui H, Kappes JC, Wu X, et al. Antibody neutralization and escape by HIV-1. *Nature*. 2003;422(6929): 307–312.
95. Kim H, Hong SH, Kim JY, Kim IC, Park YW, Lee SJ, et al. Preclinical development of a humanized neutralizing antibody targeting HGF. *Experimental & Molecular Medicine*. 2017;49(3): e309–e309.
96. Lu LL, Suscovich TJ, Fortune SM, Alter G. Beyond binding: antibody effector functions in infectious diseases. *Nature Reviews Immunology*. 2018;18(1): 46–61.
97. Boross P, van Montfoort N, Stapels DAC, van der Poel CE, Bertens C, Meeldijk J, et al. FcR $\gamma$ -Chain ITAM Signaling Is Critically Required for Cross-Presentation of Soluble Antibody–Antigen Complexes by Dendritic Cells. *The Journal of Immunology*. 2014;193(11): 5506.

98. Joller N, Weber SS, Müller AJ, Spörri R, Selchow P, Sander P, et al. Antibodies protect against intracellular bacteria by Fc receptor-mediated lysosomal targeting. *Proceedings of the National Academy of Sciences*. 2010;107(47): 20441.
99. He W, Tan GS, Mullarkey CE, Lee AJ, Lam MMW, Krammer F, et al. Epitope specificity plays a critical role in regulating antibody-dependent cell-mediated cytotoxicity against influenza A virus. *Proceedings of the National Academy of Sciences*. 2016;113(42): 11931.
100. Junttila TT, Parsons K, Olsson C, Lu Y, Xin Y, Theriault J, et al. Superior *in vivo* Efficacy of Afucosylated Trastuzumab in the Treatment of HER2-Amplified Breast Cancer. *Cancer Research*. 2010;70(11): 4481.
101. Sanjay R, Lewis LA, Rice PA. Infections of People with Complement Deficiencies and Patients Who Have Undergone Splenectomy. *Clinical Microbiology Reviews*. 2010;23(4): 740–780.
102. Bonavita E, Gentile S, Rubino M, Maina V, Papait R, Kunderfranco P, et al. PTX3 Is an Extrinsic Oncosuppressor Regulating Complement-Dependent Inflammation in Cancer. *Cell*. 2015;160(4): 700–714.
103. Rodríguez-Pinto D. B cells as antigen presenting cells. *Cellular Immunology*. 2005;238(2): 67–75.
104. Guéry JC, Ria F, Adorini L. Dendritic cells but not B cells present antigenic complexes to class II-restricted T cells after administration of protein in adjuvant. *Journal of Experimental Medicine*. 1996;183(3): 751–757.
105. Yan J, Wolff MJ, Unternaehrer J, Mellman I, Mamula MJ. Targeting antigen to CD19 on B cells efficiently activates T cells. *International Immunology*. 2005;17(7): 869–877.
106. Constant S, Schweitzer N, West J, Ranney P, Bottomly K. B lymphocytes can be competent antigen-presenting cells for priming CD4<sup>+</sup> T cells to protein antigens *in vivo*. *The Journal of Immunology*. 1995;155(8): 3734.
107. Lund FE. Cytokine-producing B lymphocytes—key regulators of immunity. *Current Opinion in Immunology*. 2008;20(3): 332–338.
108. Endres R, Alimzhanov MB, Plitz T, Fütterer A, Kosco-Vilbois MH, Nedospasov SA, et al. Mature Follicular Dendritic Cell Networks Depend on Expression of Lymphotoxin  $\beta$  Receptor by Radioresistant Stromal Cells and of Lymphotoxin  $\beta$  and Tumor Necrosis Factor by B Cells. *Journal of Experimental Medicine*. 1999;189(1): 159–168.
109. Harris DP, Haynes L, Sayles PC, Duso DK, Eaton SM, Lepak NM, et al. Reciprocal regulation of polarized cytokine production by effector B and T cells. *Nature Immunology*. 2000;1(6): 475–482.
110. Barr TA, Brown S, Ryan G, Zhao J, Gray D. TLR-mediated stimulation of APC: Distinct cytokine responses of B cells and dendritic cells. *European Journal of Immunology*. 2007;37(11): 3040–3053.

111. Cariappa A, Boboila C, Moran ST, Liu H, Shi HN, Pillai S. The Recirculating B Cell Pool Contains Two Functionally Distinct, Long-Lived, Posttransitional, Follicular B Cell Populations. *The Journal of Immunology*. 2007;179(4): 2270.
112. Harris DP, Goodrich S, Gerth AJ, Peng SL, Lund FE. Regulation of IFN- $\gamma$  Production by B Effector 1 Cells: Essential Roles for T-bet and the IFN- $\gamma$  Receptor. *The Journal of Immunology*. 2005;174(11): 6781.
113. Harris DP, Goodrich S, Mohrs K, Mohrs M, Lund FE. Cutting Edge: The Development of IL-4-Producing B Cells (B Effector 2 Cells) Is Controlled by IL-4, IL-4 Receptor  $\alpha$ , and Th2 Cells. *The Journal of Immunology*. 2005;175(11): 7103.
114. Ashour HM, Seif TM. The role of B cells in the induction of peripheral T cell tolerance. *Journal of Leukocyte Biology*. 2007;82(5): 1033–1039.
115. Mizoguchi A, Mizoguchi E, Takedatsu H, Blumberg RS, Bhan AK. Chronic Intestinal Inflammatory Condition Generates IL-10-Producing Regulatory B Cell Subset Characterized by CD1d Upregulation. *Immunity*. 2002;16(2): 219–230.
116. Inoue S, Leitner WW, Golding B, Scott D. Inhibitory Effects of B Cells on Antitumor Immunity. *Cancer Research*. 2006;66(15): 7741.
117. Wei B, Velazquez P, Turovskaya O, Spricher K, Aranda R, Kronenberg M, et al. Mesenteric B cells centrally inhibit CD4<sup>+</sup> T cell colitis through interaction with regulatory T cell subsets. *Proceedings of the National Academy of Sciences of the United States of America*. 2005;102(6): 2010.
118. Zhang X. Regulatory functions of innate-like B cells. *Cellular & molecular immunology*. 2013/02/11. 2013;10(2): 113–121.
119. Duddy ME, Alter A, Bar-Or A. Distinct Profiles of Human B Cell Effector Cytokines: A Role in Immune Regulation? *The Journal of Immunology*. 2004;172(6): 3422.
120. Evans JG, Chavez-Rueda KA, Eddaoudi A, Meyer-Bahlburg A, Rawlings DJ, Ehrenstein MR, et al. Novel Suppressive Function of Transitional 2 B Cells in Experimental Arthritis. *The Journal of Immunology*. 2007;178(12): 7868.
121. Blair PA, Noreña LY, Flores-Borja F, Rawlings DJ, Isenberg DA, Ehrenstein MR, et al. CD19<sup>+</sup>CD24<sup>hi</sup>CD38<sup>hi</sup> B Cells Exhibit Regulatory Capacity in Healthy Individuals but Are Functionally Impaired in Systemic Lupus Erythematosus Patients. *Immunity*. 2010;32(1): 129–140.
122. Mauri C, Menon M. The expanding family of regulatory B cells. *International Immunology*. 2015;27(10): 479–486.
123. van de Veen W, Stanic B, Yaman G, Wawrzyniak M, Söllner S, Akdis DG, et al. IgG4 production is confined to human IL-10–producing regulatory B cells that suppress antigen-specific immune responses. *Journal of Allergy and Clinical Immunology*. 2013;131(4): 1204–1212.
124. Weill JC, Weller S, Reynaud CA. Human Marginal Zone B Cells. *Annual Review of Immunology*. 2009;27(1): 267–285.

125. de Masson A, Bouaziz JD, le Buanec H, Robin M, O'Meara A, Parquet N, et al. CD24<sup>hi</sup>CD27<sup>+</sup> and plasmablast-like regulatory B cells in human chronic graft-versus-host disease. *Blood*. 2015;125(11): 1830–1839.
126. Duddy M, Niino M, Adatia F, Hebert S, Freedman M, Atkins H, et al. Distinct Effector Cytokine Profiles of Memory and Naive Human B Cell Subsets and Implication in Multiple Sclerosis. *The Journal of Immunology*. 2007;178(10): 6092.
127. Fabian FB, Anneleen B, Dorothy N, Venkat R, R EM, A ID, et al. CD19<sup>+</sup>CD24<sup>hi</sup>CD38<sup>hi</sup> B Cells Maintain Regulatory T Cells While Limiting TH1 and TH17 Differentiation. *Science Translational Medicine*. 2013;5(173): 173ra23-173ra23.
128. Oka A, Ishihara S, Mishima Y, Tada Y, Kusunoki R, Fukuba N, et al. Role of Regulatory B Cells in Chronic Intestinal Inflammation: Association with Pathogenesis of Crohn's Disease. *Inflammatory Bowel Diseases*. 2014;20(2): 315–328.
129. Liu J, Zhan W, Kim CJ, Clayton K, Zhao H, Lee E, et al. IL-10-Producing B Cells Are Induced Early in HIV-1 Infection and Suppress HIV-1-Specific T Cell Responses. *PLOS ONE*. 2014;9(2): e89236.
130. Ingulli E. Mechanism of cellular rejection in transplantation. *Pediatric Nephrology*. 2010;25(1): 61–74.
131. Hartono C, Muthukumar T, Suthanthiran M. Immunosuppressive Drug Therapy. *Cold Spring Harbor Perspectives in Medicine*. 2013;3(9).
132. Cherukuri A, Rothstein DM, Clark B, Carter CR, Davison A, Hernandez-Fuentes M, et al. Immunologic Human Renal Allograft Injury Associates with an Altered IL-10/TNF- $\alpha$  Expression Ratio in Regulatory B Cells. *Journal of the American Society of Nephrology*. 2014;25(7): 1575.
133. Lee KM, Stott RT, Zhao G, SooHoo J, Xiong W, Lian MM, et al. TGF- $\beta$ -producing regulatory B cells induce regulatory T cells and promote transplantation tolerance. *European Journal of Immunology*. 2014;44(6): 1728–1736.
134. Hu Y, He GL, Zhao XY, Zhao XS, Wang Y, Xu LP, et al. Regulatory B cells promote graft-versus-host disease prevention and maintain graft-versus-leukemia activity following allogeneic bone marrow transplantation. *OncImmunity*. 2017;6(3): e1284721.
135. Wu WC, Sun HW, Chen HT, Liang J, Yu XJ, Wu C, et al. Circulating hematopoietic stem and progenitor cells are myeloid-biased in cancer patients. *Proceedings of the National Academy of Sciences*. 2014;111(11): 4221.
136. Gabrilovich DI, Ostrand-Rosenberg S, Bronte V. Coordinated regulation of myeloid cells by tumours. *Nature Reviews Immunology*. 2012;12(4): 253–268.
137. Templeton AJ, McNamara MG, Šeruga B, Vera-Badillo FE, Aneja P, Ocaña A, et al. Prognostic Role of Neutrophil-to-Lymphocyte Ratio in Solid Tumors: A Systematic Review and Meta-Analysis. *JNCI: Journal of the National Cancer Institute*. 2014;106(6): dju124.



138. Hiam-Galvez KJ, Allen BM, Spitzer MH. Systemic immunity in cancer. *Nature Reviews Cancer*. 2021;21(6): 345–359.
139. Meyer MA, Baer JM, Knolhoff BL, Nywening TM, Panni RZ, Su X, et al. Breast and pancreatic cancer interrupt IRF8-dependent dendritic cell development to overcome immune surveillance. *Nature Communications*. 2018;9(1): 1250.
140. Zhu YP, Padgett L, Dinh HQ, Marcovecchio P, Blatchley A, Wu R, et al. Identification of an Early Unipotent Neutrophil Progenitor with Pro-tumoral Activity in Mouse and Human Bone Marrow. *Cell Reports*. 2018;24(9): 2329-2341.e8.
141. Sagiv JY, Michaeli J, Assi S, Mishalian I, Kisos H, Levy L, et al. Phenotypic Diversity and Plasticity in Circulating Neutrophil Subpopulations in Cancer. *Cell Reports*. 2015;10(4): 562–573.
142. Filipazzi P, Valenti R, Huber V, Pilla L, Canese P, Iero M, et al. Identification of a New Subset of Myeloid Suppressor Cells in Peripheral Blood of Melanoma Patients With Modulation by a Granulocyte-Macrophage Colony-Stimulation Factor–Based Antitumor Vaccine. *Journal of Clinical Oncology*. 2007;25(18): 2546–2553.
143. Failli A, Legitimo A, Orsini G, Romanini A, Consolini R. Numerical defect of circulating dendritic cell subsets and defective dendritic cell generation from monocytes of patients with advanced melanoma. *Cancer Letters*. 2013;337(2): 184–192.
144. Manuel M, Tredan O, Bachelot T, Clapisson G, Courtier A, Parmentier G, et al. Lymphopenia combined with low TCR diversity (divpenia) predicts poor overall survival in metastatic breast cancer patients. *OncoImmunology*. 2012;1(4): 432–440.
145. Liyanage UK, Moore TT, Joo HG, Tanaka Y, Herrmann V, Doherty G, et al. Prevalence of Regulatory T Cells Is Increased in Peripheral Blood and Tumor Microenvironment of Patients with Pancreas or Breast Adenocarcinoma. *The Journal of Immunology*. 2002;169(5): 2756.
146. Mojgan A, Anna P, Li J, C DD, Sanja S, F RP, et al. Tumor-infiltrating human CD4+ regulatory T cells display a distinct TCR repertoire and exhibit tumor and neoantigen reactivity. *Science Immunology*. 2019;4(31): eaao4310.
147. Wang L, Simons DL, Lu X, Tu TY, Solomon S, Wang R, et al. Connecting blood and intratumoral Treg cell activity in predicting future relapse in breast cancer. *Nature Immunology*. 2019;20(9): 1220–1230.
148. Verronèse E, Delgado A, Valladeau-Guilemond J, Garin G, Guillemaut S, Tredan O, et al. Immune cell dysfunctions in breast cancer patients detected through whole blood multi-parametric flow cytometry assay. *OncoImmunology*. 2016;5(3): e1100791.
149. Wang L, Miyahira AK, Simons DL, Lu X, Chang AY, Wang C, et al. IL6 Signaling in Peripheral Blood T Cells Predicts Clinical Outcome in Breast Cancer. *Cancer Research*. 2017;77(5): 1119.
150. Mamessier E, Sylvain A, Thibult ML, Houvenaeghel G, Jacquemier J, Castellano R, et al. Human breast cancer cells enhance self tolerance by promoting evasion from NK cell antitumor immunity. *The Journal of Clinical Investigation*. 2011;121(9): 3609–3622.

151. Karagiannis P, Villanova F, Josephs DH, Correa I, van Hemelrijck M, Hobbs C, et al. Elevated IgG4 in patient circulation is associated with the risk of disease progression in melanoma. *OncoImmunology*. 2015;4(11): e1032492.
152. Carpenter EL, Mick R, Rech AJ, Beatty GL, Colligon TA, Rosenfeld MR, et al. Collapse of the CD27+ B-Cell Compartment Associated with Systemic Plasmacytosis in Patients with Advanced Melanoma and Other Cancers. *Clinical Cancer Research*. 2009;15(13): 4277.
153. Wu H, Xia L, Jia D, Zou H, Jin G, Qian W, et al. PD-L1+ regulatory B cells act as a T cell suppressor in a PD-L1-dependent manner in melanoma patients with bone metastasis. *Molecular Immunology*. 2020;119: 83–91.
154. Willem van de V, Anna G, Kirstin J, Alex S, Terufumi K, Daniëlle V, et al. A novel proangiogenic B cell subset is increased in cancer and chronic inflammation. *Science Advances*. 2021;6(20): eaaz3559.
155. Kai H, T EB, E PW, Mark D, Hirokazu M, Masako K, et al. Batf3 Deficiency Reveals a Critical Role for CD8 $\alpha$ + Dendritic Cells in Cytotoxic T Cell Immunity. *Science*. 2008;322(5904): 1097–1100.
156. Binnewies M, Mujal AM, Pollack JL, Combes AJ, Hardison EA, Barry KC, et al. Unleashing Type-2 Dendritic Cells to Drive Protective Antitumor CD4<sup>+</sup> T Cell Immunity. *Cell*. 2019;177(3): 556-571.e16.
157. Gabrilovich DI, Chen HL, Girgis KR, Cunningham HT, Meny GM, Nadaf S, et al. Production of vascular endothelial growth factor by human tumors inhibits the functional maturation of dendritic cells. *Nature Medicine*. 1996;2(10): 1096–1103.
158. Hardy-Werbin M, Rocha P, Arpi O, Taus Á, Nonell L, Durán X, et al. Serum cytokine levels as predictive biomarkers of benefit from ipilimumab in small cell lung cancer. *OncoImmunology*. 2019;8(6): e1593810.
159. Sanmamed MF, Perez-Gracia JL, Schalper KA, Fusco JP, Gonzalez A, Rodriguez-Ruiz ME, et al. Changes in serum interleukin-8 (IL-8) levels reflect and predict response to anti-PD-1 treatment in melanoma and non-small-cell lung cancer patients. *Annals of Oncology*. 2017;28(8): 1988–1995.
160. Alfaro C, Teijeira A, Oñate C, Pérez G, Sanmamed MF, Andueza MP, et al. Tumor-Produced Interleukin-8 Attracts Human Myeloid-Derived Suppressor Cells and Elicits Extrusion of Neutrophil Extracellular Traps (NETs). *Clinical Cancer Research*. 2016;22(15): 3924.
161. Willsmore ZN, Harris RJ, Crescioli S, Hussein K, Kakkassery H, Thapa D, et al. B Cells in Patients With Melanoma: Implications for Treatment With Checkpoint Inhibitor Antibodies. *Frontiers in Immunology*. 2021;11: 3560.
162. Capone M, Giannarelli D, Mallardo D, Madonna G, Festino L, Grimaldi AM, et al. Baseline neutrophil-to-lymphocyte ratio (NLR) and derived NLR could predict overall survival in patients with advanced melanoma treated with nivolumab. *Journal for ImmunoTherapy of Cancer*. 2018;6(1): 74.

163. Weide B, Martens A, Hassel JC, Berking C, Postow MA, Bisschop K, et al. Baseline Biomarkers for Outcome of Melanoma Patients Treated with Pembrolizumab. *Clinical Cancer Research*. 2016;22(22): 5487.
164. Hogan SA, Courtier A, Cheng PF, Jaberg-Bentele NF, Goldinger SM, Manuel M, et al. Peripheral Blood TCR Repertoire Profiling May Facilitate Patient Stratification for Immunotherapy against Melanoma. *Cancer Immunology Research*. 2019;7(1): 77.
165. Meyer C, Cagnon L, Costa-Nunes CM, Baumgaertner P, Montandon N, Leyvraz L, et al. Frequencies of circulating MDSC correlate with clinical outcome of melanoma patients treated with ipilimumab. *Cancer Immunology, Immunotherapy*. 2014;63(3): 247–257.
166. Martens A, Wistuba-Hamprecht K, Foppen MG, Yuan J, Postow MA, Wong P, et al. Baseline Peripheral Blood Biomarkers Associated with Clinical Outcome of Advanced Melanoma Patients Treated with Ipilimumab. *Clinical Cancer Research*. 2016;22(12): 2908.
167. Spitzer MH, Carmi Y, Reticker-Flynn NE, Kwek SS, Madhireddy D, Martins MM, et al. Systemic Immunity Is Required for Effective Cancer Immunotherapy. *Cell*. 2017;168(3): 487-502.e15.
168. Fairfax BP, Taylor CA, Watson RA, Nassiri I, Danielli S, Fang H, et al. Peripheral CD8+ T cell characteristics associated with durable responses to immune checkpoint blockade in patients with metastatic melanoma. *Nature Medicine*. 2020;26(2): 193–199.
169. Huang AC, Postow MA, Orlovski RJ, Mick R, Bengsch B, Manne S, et al. T-cell invigoration to tumour burden ratio associated with anti-PD-1 response. *Nature*. 2017;545(7652): 60–65.
170. Fässler M, Diem S, Mangana J, Hasan Ali O, Berner F, Bomze D, et al. Antibodies as biomarker candidates for response and survival to checkpoint inhibitors in melanoma patients. *Journal for ImmunoTherapy of Cancer*. 2019;7(1): 50.
171. Diem S, Fässler M, Bomze D, Ali OH, Berner F, Niederer R, et al. Immunoglobulin G and Subclasses as Potential Biomarkers in Metastatic Melanoma Patients Starting Checkpoint Inhibitor Treatment. *Journal of Immunotherapy*. 2019;42(3).
172. DeFalco J, Harbell M, Manning-Bog A, Baia G, Scholz A, Millare B, et al. Non-progressing cancer patients have persistent B cell responses expressing shared antibody paratopes that target public tumor antigens. *Clinical Immunology*. 2018;187: 37–45.
173. Balkwill FR, Capasso M, Hagemann T. The tumor microenvironment at a glance. *Journal of Cell Science*. 2012;125(23): 5591–5596.
174. Fridman WH, Pagès F, Sautès-Fridman C, Galon J. The immune contexture in human tumours: impact on clinical outcome. *Nature Reviews Cancer*. 2012;12(4): 298–306.
175. Milne K, Köbel M, Kalloger SE, Barnes RO, Gao D, Gilks CB, et al. Systematic Analysis of Immune Infiltrates in High-Grade Serous Ovarian Cancer Reveals CD20, FoxP3 and TIA-1 as Positive Prognostic Factors. *PLOS ONE*. 2009;4(7): e6412.

176. Tachibana T, Onodera H, Tsuruyama T, Mori A, Nagayama S, Hiai H, et al. Increased Intratumor V $\alpha$ 24-Positive Natural Killer T Cells: A Prognostic Factor for Primary Colorectal Carcinomas. *Clinical Cancer Research*. 2005;11(20): 7322.
177. Nevala WK, Vachon CM, Leontovich AA, Scott CG, Thompson MA, Markovic SN, et al. Evidence of systemic Th2-driven chronic inflammation in patients with metastatic melanoma. *Clinical cancer research : an official journal of the American Association for Cancer Research*. 2009/02/24. 2009;15(6): 1931–1939.
178. Shimato S, Maier LM, Maier R, Bruce JN, Anderson RCE, Anderson DE. Profound tumor-specific Th2 bias in patients with malignant glioma. *BMC Cancer*. 2012;12(1): 561.
179. Ellyard JI, Simson L, Parish CR. Th2-mediated anti-tumour immunity: friend or foe? *Tissue Antigens*. 2007;70(1): 1–11.
180. Paul WE. Interleukin-4: A Prototypic Immunoregulatory Lymphokine. *Blood*. 1991;77(9): 1859–1870.
181. Satoguina JS, Weyand E, Larbi J, Hoerauf A. T Regulatory-1 Cells Induce IgG4 Production by B Cells: Role of IL-10. *The Journal of Immunology*. 2005;174(8): 4718.
182. Karagiannis P, Gilbert AE, Josephs DH, Ali N, Dodev T, Saul L, et al. IgG4 subclass antibodies impair antitumor immunity in melanoma. *The Journal of Clinical Investigation*. 2013;123(4): 1457–1474.
183. Chiaruttini G, Mele S, Opzoomer J, Crescioli S, Ilieva KM, Lacy KE, et al. B cells and the humoral response in melanoma: The overlooked players of the tumor microenvironment. *OncImmunity*. 2017;6(4): e1294296.
184. Germain C, Gnjatic S, Dieu-Nosjean MC. Tertiary Lymphoid Structure-Associated B Cells are Key Players in Anti-Tumor Immunity. *Frontiers in Immunology*. 2015;6: 67.
185. Seow DY bin, Yeong JPS, Lim JX, Chia N, Lim JCT, Ong CCH, et al. Tertiary lymphoid structures and associated plasma cells play an important role in the biology of triple-negative breast cancers. *Breast Cancer Research and Treatment*. 2020;180(2): 369–377.
186. Cipponi A, Mercier M, Seremet T, Baurain JF, Théate I, van den Oord J, et al. Neogenesis of Lymphoid Structures and Antibody Responses Occur in Human Melanoma Metastases. *Cancer Research*. 2012;72(16): 3997.
187. Zhao Z, Ding H, Lin Z bin, Qiu S hui, Zhang Y ran, Guo Y guan, et al. Relationship between Tertiary Lymphoid Structure and the Prognosis and Clinicopathologic Characteristics in Solid Tumors. *International Journal of Medical Sciences*. 2021;18(11): 2327–2338.
188. Lee HJ, Park IA, Song IH, Shin SJ, Kim JY, Yu JH, et al. Tertiary lymphoid structures: prognostic significance and relationship with tumour-infiltrating lymphocytes in triple-negative breast cancer. *Journal of Clinical Pathology*. 2016;69(5): 422.

189. Cabrita R, Lauss M, Sanna A, Donia M, Skaarup Larsen M, Mitra S, et al. Tertiary lymphoid structures improve immunotherapy and survival in melanoma. *Nature*. 2020;577(7791): 561–565.
190. Dieu-Nosjean MC, Antoine M, Danel C, Heudes D, Wislez M, Poulot V, et al. Long-term survival for patients with non-small-cell lung cancer with intratumoral lymphoid structures. *Journal of clinical oncology : official journal of the American Society of Clinical Oncology*. 2008;26(27): 4410–4417.
191. Helmink BA, Reddy SM, Gao J, Zhang S, Basar R, Thakur R, et al. B cells and tertiary lymphoid structures promote immunotherapy response. *Nature*. 2020;577(7791): 549–555.
192. Sharonov G v, Serebrovskaya EO, Yuzhakova D v, Britanova O v, Chudakov DM. B cells, plasma cells and antibody repertoires in the tumour microenvironment. *Nature Reviews Immunology*. 2020;20(5): 294–307.
193. Cai C, Zhang J, Li M, Wu ZJ, Song KH, Zhan TW, et al. Interleukin 10-expressing B cells inhibit tumor-infiltrating T cell function and correlate with T cell Tim-3 expression in renal cell carcinoma. *Tumor Biology*. 2016;37(6): 8209–8218.
194. Noy R, Pollard JW. Tumor-associated macrophages: from mechanisms to therapy. *Immunity*. 2014;41(1): 49–61.
195. Iglesia MD, Parker JS, Hoadley KA, Serody JS, Perou CM, Vincent BG. Genomic Analysis of Immune Cell Infiltrates Across 11 Tumor Types. *JNCI: Journal of the National Cancer Institute*. 2016;108(11).
196. Gao Z hua, Li C xin, Liu M, Jiang J yuan. Predictive and prognostic role of tumour-infiltrating lymphocytes in breast cancer patients with different molecular subtypes: a meta-analysis. *BMC Cancer*. 2020;20(1): 1150.
197. Salgado R, Denkert C, Demaria S, Sirtaine N, Klauschen F, Pruneri G, et al. The evaluation of tumor-infiltrating lymphocytes (TILs) in breast cancer: recommendations by an International TILs Working Group 2014. *Annals of Oncology*. 2015;26(2): 259–271.
198. Razvan C, Robin M, Mark A, Andrew A, Erin M, Jennifer Y, et al. Pan-tumor genomic biomarkers for PD-1 checkpoint blockade-based immunotherapy. *Science*. 2018;362(6411): eaar3593.
199. Kolberg-Liedtke C, Gluz O, Heinisch F, Feuerhake F, Kreipe H, Clemens M, et al. Association of TILs with clinical parameters, Recurrence Score® results, and prognosis in patients with early HER2-negative breast cancer (BC)—a translational analysis of the prospective WSG PlanB trial. *Breast Cancer Research*. 2020;22(1): 47.
200. Mohammed ZMA, Going JJ, Edwards J, Elsberger B, McMillan DC. The relationship between lymphocyte subsets and clinico-pathological determinants of survival in patients with primary operable invasive ductal breast cancer. *British Journal of Cancer*. 2013;109(6): 1676–1684.

201. Mohammed ZMA, Going JJ, Edwards J, Elsberger B, McMillan DC. The relationship between lymphocyte subsets and clinico-pathological determinants of survival in patients with primary operable invasive ductal breast cancer. *British Journal of Cancer*. 2013;109(6): 1676–1684.
202. Mohammed ZMA, Going JJ, Edwards J, Elsberger B, Doughty JC, McMillan DC. The relationship between components of tumour inflammatory cell infiltrate and clinicopathological factors and survival in patients with primary operable invasive ductal breast cancer. *British Journal of Cancer*. 2012;107(5): 864–873.
203. Mahmoud SMA, Lee AHS, Paish EC, Macmillan RD, Ellis IO, Green AR. The prognostic significance of B lymphocytes in invasive carcinoma of the breast. *Breast Cancer Research and Treatment*. 2012;132(2): 545–553.
204. Xu Y, Lan S, Zheng Q. Prognostic significance of infiltrating immune cell subtypes in invasive ductal carcinoma of the breast. *Tumori Journal*. 2018;104(3): 196–201.
205. Miligy I, Mohan P, Gaber A, Aleskandarany MA, Nolan CC, Diez-Rodriguez M, et al. Prognostic significance of tumour infiltrating B lymphocytes in breast ductal carcinoma in situ. *Histopathology*. 2017;71(2): 258–268.
206. Brown JR, Wimberly H, Lannin DR, Nixon C, Rimm DL, Bossuyt V. Multiplexed Quantitative Analysis of CD3, CD8, and CD20 Predicts Response to Neoadjuvant Chemotherapy in Breast Cancer. *Clinical Cancer Research*. 2014;20(23): 5995.
207. Song IH, Heo SH, Bang WS, Park HS, Park IA, Kim YA, et al. Predictive Value of Tertiary Lymphoid Structures Assessed by High Endothelial Venule Counts in the Neoadjuvant Setting of Triple-Negative Breast Cancer. *Cancer Res Treat*. 2016;49(2): 399–407.
208. García-Martínez E, Gil GL, Benito AC, González-Billalabeitia E, Conesa MAV, García TG, et al. Tumor-infiltrating immune cell profiles and their change after neoadjuvant chemotherapy predict response and prognosis of breast cancer. *Breast Cancer Research*. 2014;16(6): 488.
209. Schmidt M, Böhm D, von Törne C, Steiner E, Puhl A, Pilch H, et al. The Humoral Immune System Has a Key Prognostic Impact in Node-Negative Breast Cancer. *Cancer Research*. 2008;68(13): 5405.
210. Schmidt M, Hellwig B, Hammad S, Othman A, Lohr M, Chen Z, et al. A Comprehensive Analysis of Human Gene Expression Profiles Identifies Stromal Immunoglobulin  $\kappa$  C as a Compatible Prognostic Marker in Human Solid Tumors. *Clinical Cancer Research*. 2012;18(9): 2695.
211. Iglesia MD, Vincent BG, Parker JS, Hoadley KA, Carey LA, Perou CM, et al. Prognostic B-cell Signatures Using mRNA-Seq in Patients with Subtype-Specific Breast and Ovarian Cancer. *Clinical Cancer Research*. 2014;20(14): 3818.
212. Charoentong P, Finotello F, Angelova M, Mayer C, Efremova M, Rieder D, et al. Pan-cancer Immunogenomic Analyses Reveal Genotype-Immunophenotype Relationships and Predictors of Response to Checkpoint Blockade. *Cell Reports*. 2017;18(1): 248–262.

213. Garaud S, Zayakin P, Buisseret L, Rulle U, Silina K, de Wind A, et al. Antigen Specificity and Clinical Significance of IgG and IgA Autoantibodies Produced in situ by Tumor-Infiltrating B Cells in Breast Cancer. *Frontiers in Immunology*. 2018;9: 2660.
214. Garaud S, Buisseret L, Solinas C, Gu-Trantien C, de Wind A, van den Eynden G, et al. Tumor-infiltrating B cells signal functional humoral immune responses in breast cancer. *JCI Insight*. 2019;4(18).
215. Schumacher TN, Schreiber RD. Neoantigens in cancer immunotherapy. *Science*. 2015;348(6230): 69–74.
216. Clemente CG, Mihm Jr. MC, Bufalino R, Zurrida S, Collini P, Cascinelli N. Prognostic value of tumor infiltrating lymphocytes in the vertical growth phase of primary cutaneous melanoma. *Cancer*. 1996;77(7): 1303–1310.
217. Ladányi A, Kiss J, Mohos A, Somlai B, Liskay G, Gilde K, et al. Prognostic impact of B-cell density in cutaneous melanoma. *Cancer Immunology, Immunotherapy*. 2011;60(12): 1729–1738.
218. Erdag G, Schaefer JT, Smolkin ME, Deacon DH, Shea SM, Dengel LT, et al. Immunotype and Immunohistologic Characteristics of Tumor-Infiltrating Immune Cells Are Associated with Clinical Outcome in Metastatic Melanoma. *Cancer Research*. 2012;72(5): 1070.
219. Garg K, Maurer M, Griss J, Brüggem MC, Wolf IH, Wagner C, et al. Tumor-associated B cells in cutaneous primary melanoma and improved clinical outcome. *Human Pathology*. 2016;54: 157–164.
220. Bolotin DA, Poslavsky S, Davydov AN, Frenkel FE, Fanchi L, Zolotareva OI, et al. Antigen receptor repertoire profiling from RNA-seq data. *Nature Biotechnology*. 2017;35(10): 908–911.
221. Bosisio FM, Wilmott JS, Volders N, Mercier M, Wouters J, Stas M, et al. Plasma cells in primary melanoma. Prognostic significance and possible role of IgA. *Modern Pathology*. 2016;29(4): 347–358.
222. Shalapour S, Font-Burgada J, di Caro G, Zhong Z, Sanchez-Lopez E, Dhar D, et al. Immunosuppressive plasma cells impede T-cell-dependent immunogenic chemotherapy. *Nature*. 2015;521(7550): 94–98.
223. Schioppa T, Moore R, Thompson RG, Rosser EC, Kulbe H, Nedospasov S, et al. B regulatory cells and the tumor-promoting actions of TNF- $\alpha$  during squamous carcinogenesis. *Proceedings of the National Academy of Sciences*. 2011;108(26): 10662.
224. Mose LE, Selitsky SR, Bixby LM, Marron DL, Iglesia MD, Serody JS, et al. Assembly-based inference of B-cell receptor repertoires from short read RNA sequencing data with V'DJer. *Bioinformatics*. 2016;32(24): 3729–3734.
225. Griss J, Bauer W, Wagner C, Simon M, Chen M, Grabmeier-Pfistershammer K, et al. B cells sustain inflammation and predict response to immune checkpoint blockade in human melanoma. *Nature Communications*. 2019;10(1): 4186.

226. Saul L, Ilieva KM, Bax HJ, Karagiannis P, Correa I, Rodriguez-Hernandez I, et al. IgG subclass switching and clonal expansion in cutaneous melanoma and normal skin. *Scientific Reports*. 2016;6(1): 29736.
227. Brase JC, Walter RFH, Savchenko A, Gusenleitner D, Garrett J, Schimming T, et al. Role of Tumor-Infiltrating B Cells in Clinical Outcome of Patients with Melanoma Treated With Dabrafenib Plus Trametinib. *Clinical Cancer Research*. 2021;27(16): 4500.
228. Sahin U, Türeci O, Schmitt H, Cochlovius B, Johannes T, Schmits R, et al. Human neoplasms elicit multiple specific immune responses in the autologous host. *Proceedings of the National Academy of Sciences*. 1995;92(25): 11810.
229. Pfreundschuh M. The genealogy of SEREX. *Cancer immunity*. 2012/05/01. 2012;12: 7.
230. Correa I, Ilieva KM, Crescioli S, Lombardi S, Figini M, Cheung A, et al. Evaluation of Antigen-Conjugated Fluorescent Beads to Identify Antigen-Specific B Cells. *Frontiers in Immunology*. 2018;9: 493.
231. Gilbert AE, Karagiannis P, Dodev T, Koers A, Lacy K, Josephs DH, et al. Monitoring the Systemic Human Memory B Cell Compartment of Melanoma Patients for Anti-Tumor IgG Antibodies. *PLOS ONE*. 2011;6(4): e19330.
232. Daveau M, Fischer JP, Rivat L, Rivat C, Ropartz C, Peter HH, et al. IgG4 Subclass in Malignant Melanoma. *JNCI: Journal of the National Cancer Institute*. 1977;58(2): 189–192.
233. Azeem N, Ajmera V, Hameed B, Mehta N. Hilar cholangiocarcinoma associated with immunoglobulin G4-positive plasma cells and elevated serum immunoglobulin G4 levels. *Hepatology Communications*. 2018;2(4): 349–353.
234. Jordakieva G, Bianchini R, Reichhold D, Piehslinger J, Groschopf A, Jensen SA, et al. IgG4 induces tolerogenic M2-like macrophages and correlates with disease progression in colon cancer. *OncoImmunology*. 2021;10(1): 1880687.
235. Aalberse RC, Schuurman J. IgG4 breaking the rules. *Immunology*. 2002;105(1): 9–19.
236. Wang H, Xu Q, Zhao C, Zhu Z, Zhu X, Zhou J, et al. An immune evasion mechanism with IgG4 playing an essential role in cancer and implication for immunotherapy. *Journal for ImmunoTherapy of Cancer*. 2020;8(2): e000661.
237. Olkhanud PB, Damdinsuren B, Bodogai M, Gress RE, Sen R, Wejksza K, et al. Tumor-Evoked Regulatory B Cells Promote Breast Cancer Metastasis by Converting Resting CD4<sup>+</sup> T Cells to T-Regulatory Cells. *Cancer Research*. 2011;71(10): 3505.
238. Wejksza K, Lee-Chang C, Bodogai M, Bonzo J, Gonzalez FJ, Lehrmann E, et al. Cancer-Produced Metabolites of 5-Lipoxygenase Induce Tumor-Evoked Regulatory B Cells via Peroxisome Proliferator-Activated Receptor  $\alpha$ . *The Journal of Immunology*. 2013;190(6): 2575.



239. Han S, Feng S, Ren M, Ma E, Wang X, Xu L, et al. Glioma cell-derived placental growth factor induces regulatory B cells. *The International Journal of Biochemistry & Cell Biology*. 2014;57: 63–68.
240. Zhang Y, Gallastegui N, Rosenblatt JD. Regulatory B cells in anti-tumor immunity. *International Immunology*. 2015;27(10): 521–530.
241. Horikawa M, Minard-Colin V, Matsushita T, Tedder TF. Regulatory B cell production of IL-10 inhibits lymphoma depletion during CD20 immunotherapy in mice. *The Journal of Clinical Investigation*. 2011;121(11): 4268–4280.
242. Lindner S, Dahlke K, Sontheimer K, Hagn M, Kaltenmeier C, Barth TFE, et al. Interleukin 21–Induced Granzyme B–Expressing B Cells Infiltrate Tumors and Regulate T Cells. *Cancer Research*. 2013;73(8): 2468.
243. Wang WW, Yuan XL, Chen H, Xie GH, Ma YH, Zheng YX, et al. CD19+CD24hiCD38hiBregs involved in downregulate helper T cells and upregulate regulatory T cells in gastric cancer. *Oncotarget*. 2015;6(32): 33486–33499.
244. Egbuniwe IU, Harris RJ, Nakamura M, Nestle FO, Akbar AN, Karagiannis SN, et al. B Lymphocytes Accumulate and Proliferate in Human Skin at Sites of Cutaneous Antigen Challenge. *Journal of Investigative Dermatology*. 2021;
245. Yanaba K, Kamata M, Ishiura N, Shibata S, Asano Y, Tada Y, et al. Regulatory B cells suppress imiquimod-induced, psoriasis-like skin inflammation. *Journal of Leukocyte Biology*. 2013;94(4): 563–573.
246. Aira LE, Debes GF. Skin-Homing Regulatory B Cells Required for Suppression of Cutaneous Inflammation. *Journal of Investigative Dermatology*. 2021;141(8): 1995-2005.e6.
247. Kobayashi T, Oishi K, Okamura A, Maeda S, Komuro A, Hamaguchi Y, et al. Regulatory B1a Cells Suppress Melanoma Tumor Immunity via IL-10 Production and Inhibiting T Helper Type 1 Cytokine Production in Tumor-Infiltrating CD8+ T Cells. *Journal of Investigative Dermatology*. 2019;139(7): 1535-1544.e1.
248. Sanz I, Wei C, Jenks SA, Cashman KS, Tipton C, Woodruff MC, et al. Challenges and Opportunities for Consistent Classification of Human B Cell and Plasma Cell Populations. *Frontiers in Immunology*. 2019;10: 2458.
249. Patel N, Weekes D, Drosopoulos K, Gazinska P, Noel E, Rashid M, et al. Integrated genomics and functional validation identifies malignant cell specific dependencies in triple negative breast cancer. *Nature Communications*. 2018;9(1): 1044.
250. Ma CX, Ellis MJ. The cancer genome atlas: clinical applications for breast cancer. *Oncology*. 2013;27(12): 1263.
251. Brasó-Maristany F, Filosto S, Catchpole S, Marlow R, Quist J, Francesch-Domenech E, et al. PIM1 kinase regulates cell death, tumor growth and chemotherapy response in triple-negative breast cancer. *Nature Medicine*. 2016;22(11): 1303–1313.

252. Thennavan A, Beca F, Xia Y, Garcia-Recio S, Allison K, Collins LC, et al. Molecular analysis of TCGA breast cancer histologic types. *Cell Genomics*. 2021;1(3): 100067.
253. Szekely B, Bossuyt V, Li X, Wali VB, Patwardhan GA, Frederick C, et al. Immunological differences between primary and metastatic breast cancer. *Annals of Oncology*. 2018;29(11): 2232–2239.
254. Györfly B, Lanczky A, Eklund AC, Denkert C, Budczies J, Li Q, et al. An online survival analysis tool to rapidly assess the effect of 22,277 genes on breast cancer prognosis using microarray data of 1,809 patients. *Breast Cancer Research and Treatment*. 2010;123(3): 725–731.
255. Mihály Z, Györfly B. Improving Pathological Assessment of Breast Cancer by Employing Array-Based Transcriptome Analysis. *Microarrays*. 2013;2(3): 228–242.
256. Dieu-Nosjean MC, Goc J, Giraldo NA, Sautès-Fridman C, Fridman WH. Tertiary lymphoid structures in cancer and beyond. *Trends in Immunology*. 2014;35(11): 571–580.
257. Newman AM, Liu CL, Green MR, Gentles AJ, Feng W, Xu Y, et al. Robust enumeration of cell subsets from tissue expression profiles. *Nature Methods*. 2015;12(5): 453–457.
258. Azizi E, Carr AJ, Plitas G, Cornish AE, Konopacki C, Prabhakaran S, et al. Single-Cell Map of Diverse Immune Phenotypes in the Breast Tumor Microenvironment. *Cell*. 2018;174(5): 1293-1308.e36.
259. Butler A, Hoffman P, Smibert P, Papalexi E, Satija R. Integrating single-cell transcriptomic data across different conditions, technologies, and species. *Nature Biotechnology*. 2018;36(5): 411–420.
260. Subramanian A, Tamayo P, Mootha VK, Mukherjee S, Ebert BL, Gillette MA, et al. Gene set enrichment analysis: A knowledge-based approach for interpreting genome-wide expression profiles. *Proceedings of the National Academy of Sciences*. 2005;102(43): 15545.
261. Efremova M, Vento-Tormo M, Teichmann SA, Vento-Tormo R. CellPhoneDB: inferring cell–cell communication from combined expression of multi-subunit ligand–receptor complexes. *Nature Protocols*. 2020;15(4): 1484–1506.
262. Li H, van der Leun AM, Yofe I, Lubling Y, Gelbard-Solodkin D, van Akkooi ACJ, et al. Dysfunctional CD8 T Cells Form a Proliferative, Dynamically Regulated Compartment within Human Melanoma. *Cell*. 2019;176(4): 775-789.e18.
263. Wu YC, Kipling D, Dunn-Walters D. Assessment of B Cell Repertoire in Humans. In: Shaw AC (ed.) *Immunosenescence: Methods and Protocols*. New York, NY: Springer New York; 2015. p. 199–218.
264. Brochet X, Lefranc MP, Giudicelli V. IMGT/V-QUEST: the highly customized and integrated system for IG and TR standardized V-J and V-D-J sequence analysis. *Nucleic Acids Research*. 2008;36(suppl\_2): W503–W508.

265. Margreitter C, Lu HC, Townsend C, Stewart A, Dunn-Walters DK, Fraternali F. BRepertoire: a user-friendly web server for analysing antibody repertoire data. *Nucleic Acids Research*. 2018;46(W1): W264–W270.
266. Townsend CL, Laffy JMJ, Wu YCB, Silva O’Hare J, Martin V, Kipling D, et al. Significant Differences in Physicochemical Properties of Human Immunoglobulin Kappa and Lambda CDR3 Regions. *Frontiers in Immunology*. 2016;7: 388.
267. Yaari G, Uduman M, Kleinstein SH. Quantifying selection in high-throughput Immunoglobulin sequencing data sets. *Nucleic Acids Research*. 2012;40(17): e134–e134.
268. Walldius G, Malmström H, Jungner I, de Faire U, Lambe M, van Hemelrijck M, et al. Cohort Profile: The AMORIS cohort. *International Journal of Epidemiology*. 2017;46(4): 1103–1103i.
269. Lehmann BD, Pietenpol JA, Tan AR. Triple-Negative Breast Cancer: Molecular Subtypes and New Targets for Therapy. *American Society of Clinical Oncology Educational Book*. 2015;(35): e31–e39.
270. Loi S, Michiels S, Salgado R, Sirtaine N, Jose V, Fumagalli D, et al. Tumor infiltrating lymphocytes are prognostic in triple negative breast cancer and predictive for trastuzumab benefit in early breast cancer: results from the FinHER trial. *Annals of Oncology*. 2014;25(8): 1544–1550.
271. Keren L, Bosse M, Marquez D, Angoshtari R, Jain S, Varma S, et al. A Structured Tumor-Immune Microenvironment in Triple Negative Breast Cancer Revealed by Multiplexed Ion Beam Imaging. *Cell*. 2018;174(6): 1373-1387.e19.
272. Ramakrishnan R, Assudani D, Nagaraj S, Hunter T, Cho HI, Antonia S, et al. Chemotherapy enhances tumor cell susceptibility to CTL-mediated killing during cancer immunotherapy in mice. *The Journal of Clinical Investigation*. 2010;120(4): 1111–1124.
273. Singh M, Al-Eryani G, Carswell S, Ferguson JM, Blackburn J, Barton K, et al. High-throughput targeted long-read single cell sequencing reveals the clonal and transcriptional landscape of lymphocytes. *Nature Communications*. 2019;10(1): 3120.
274. Scott AM, Wolchok JD, Old LJ. Antibody therapy of cancer. *Nature Reviews Cancer*. 2012;12(4): 278–287.
275. Rossetti RAM, Lorenzi NPC, Yokochi K, Rosa MBS de F, Benevides L, Margarido PFR, et al. B lymphocytes can be activated to act as antigen presenting cells to promote anti-tumor responses. *PLOS ONE*. 2018;13(7): e0199034.
276. Hu X, Zhang J, Wang J, Fu J, Li T, Zheng X, et al. Landscape of B cell immunity and related immune evasion in human cancers. *Nature Genetics*. 2019;51(3): 560–567.
277. Carpenter EL, Mick R, Rech AJ, Beatty GL, Colligon TA, Rosenfeld MR, et al. Collapse of the CD27+ B-Cell Compartment Associated with Systemic Plasmacytosis in Patients with Advanced Melanoma and Other Cancers. *Clinical Cancer Research*. 2009;15(13): 4277.

278. de Silva NS, Klein U. Dynamics of B cells in germinal centres. *Nature Reviews Immunology*. 2015;15(3): 137–148.
279. Yin Q, Wang X, McBride J, Fewell C, Flemington E. B-cell Receptor Activation Induces BIC/miR-155 Expression through a Conserved AP-1 Element \*. *Journal of Biological Chemistry*. 2008;283(5): 2654–2662.
280. Moratz C, Kang VH, Druey KM, Shi CS, Scheschonka A, Murphy PM, et al. Regulator of G Protein Signaling 1 (RGS1) Markedly Impairs  $G_{i\alpha}$  Signaling Responses of B Lymphocytes. *The Journal of Immunology*. 2000;164(4): 1829–1838.
281. D’Arena G, Musto P, Nunziata G, Cascavilla N, Savino L, Pistolese G. CD69 expression in B-cell chronic lymphocytic leukemia: a new prognostic marker? *Haematologica*. 2001;86(9): 995–996.
282. Liberzon A, Birger C, Thorvaldsdóttir H, Ghandi M, Mesirov JP, Tamayo P. The Molecular Signatures Database Hallmark Gene Set Collection. *Cell Systems*. 2015;1(6): 417–425.
283. Maletzki C, Jahnke A, Ostwald C, Klar E, Prall F, Linnebacher M. Ex-vivo Clonally Expanded B Lymphocytes Infiltrating Colorectal Carcinoma Are of Mature Immunophenotype and Produce Functional IgG. *PLOS ONE*. 2012;7(2): e32639.
284. Siliņa K, Rulle U, Kalniņa Z, Linē A. Manipulation of tumour-infiltrating B cells and tertiary lymphoid structures: a novel anti-cancer treatment avenue? *Cancer Immunology, Immunotherapy*. 2014;63(7): 643–662.
285. Armas-González E, Domínguez-Luis MJ, Díaz-Martín A, Arce-Franco M, Castro-Hernández J, Danelon G, et al. Role of CXCL13 and CCL20 in the recruitment of B cells to inflammatory foci in chronic arthritis. *Arthritis Research & Therapy*. 2018;20(1): 114.
286. Okada T, Ngo VN, Ekland EH, Förster R, Lipp M, Littman DR, et al. Chemokine Requirements for B Cell Entry to Lymph Nodes and Peyer’s Patches. *Journal of Experimental Medicine*. 2002;196(1): 65–75.
287. Pavoni E, Monteriù G, Santapaola D, Petronzelli F, Anastasi AM, Pelliccia A, et al. Tumor-infiltrating B lymphocytes as an efficient source of highly specific immunoglobulins recognizing tumor cells. *BMC Biotechnology*. 2007;7(1): 70.
288. Buisseret L, Desmedt C, Garaud S, Fornili M, Wang X, van den Eyden G, et al. Reliability of tumor-infiltrating lymphocyte and tertiary lymphoid structure assessment in human breast cancer. *Modern Pathology*. 2017;30(9): 1204–1212.
289. Garnelo M, Tan A, Her Z, Yeong J, Lim CJ, Chen J, et al. Interaction between tumour-infiltrating B cells and T cells controls the progression of hepatocellular carcinoma. *Gut*. 2017;66(2): 342.
290. Hollern DP, Xu N, Thennavan A, Glodowski C, Garcia-Recio S, Mott KR, et al. B Cells and T Follicular Helper Cells Mediate Response to Checkpoint Inhibitors in High Mutation Burden Mouse Models of Breast Cancer. *Cell*. 2019;179(5): 1191-1206.e21.

291. Cheung A, Opzoomer J, Ilieva KM, Gazinska P, Hoffmann RM, Mirza H, et al. Anti-Folate Receptor Alpha-Directed Antibody Therapies Restrict the Growth of Triple-negative Breast Cancer. *Clinical Cancer Research*. 2018;24(20): 5098.
292. Kalialis LV, Drzewiecki KT, Klyver H. Spontaneous regression of metastases from melanoma: review of the literature. *Melanoma Research*. 2009;19(5).
293. Bulkley GB, Cohen MH, Banks PM, Char DH, Ketcham AS. Long-term spontaneous regression of malignant melanoma with visceral metastases Report of a case with immunologic profile. *Cancer*. 1975;36(2): 485–494.
294. Shimamura T, Hashimoto K, Sasaki S. Feedback suppression of the immune response in vivo: I. Immune B cells induce antigen-specific suppressor T cells. *Cellular Immunology*. 1982;68(1): 104–113.
295. Fillatreau S, Sweenie CH, McGeachy MJ, Gray D, Anderton SM. B cells regulate autoimmunity by provision of IL-10. *Nature Immunology*. 2002;3(10): 944–950.
296. Mauri C, Gray D, Mushtaq N, Londei M. Prevention of Arthritis by Interleukin 10-producing B Cells. *Journal of Experimental Medicine*. 2003;197(4): 489–501.
297. Mizoguchi A, Mizoguchi E, Takedatsu H, Blumberg RS, Bhan AK. Chronic Intestinal Inflammatory Condition Generates IL-10-Producing Regulatory B Cell Subset Characterized by CD1d Upregulation. *Immunity*. 2002;16(2): 219–230.
298. Iyer SS, Cheng G. Role of interleukin 10 transcriptional regulation in inflammation and autoimmune disease. *Critical reviews in immunology*. 2012;32(1): 23–63.
299. de Jonge K, Tillé L, Lourenco J, Maby-El Hajjami H, Nassiri S, Racle J, et al. Inflammatory B cells correlate with failure to checkpoint blockade in melanoma patients. *OncImmunity*. 2021;10(1): 1873585.
300. Hanahan D, Weinberg RA. Hallmarks of Cancer: The Next Generation. *Cell*. 2011;144(5): 646–674.
301. Nenu I, Tudor D, Filip AG, Baldea I. Current position of TNF- $\alpha$  in melanomagenesis. *Tumor Biology*. 2015;36(9): 6589–6602.
302. Agematsu K, Hokibara S, Nagumo H, Komiyama A. CD27: a memory B-cell marker. *Immunology Today*. 2000;21(5): 204–206.
303. Ticchioni M, Deckert M, Mary F, Bernard G, Brown EJ, Bernard A. Integrin-associated protein (CD47) is a comitogenic molecule on CD3-activated human T cells. *The Journal of Immunology*. 1997;158(2): 677.
304. Bogoevska V, Nollau P, Lucka L, Grunow D, Klampe B, Uotila LM, et al. DC-SIGN binds ICAM-3 isolated from peripheral human leukocytes through Lewis x residues. *Glycobiology*. 2007;17(3): 324–333.
305. Shen H, Wu N, Nanayakkara G, Fu H, Yang Q, Yang WY, et al. Co-signaling receptors regulate T-cell plasticity and immune tolerance. *Frontiers in bioscience (Landmark edition)*. 2019;24: 96–132.

306. Wu C, Thalhamer T, Franca RF, Xiao S, Wang C, Hotta C, et al. Galectin-9-CD44 Interaction Enhances Stability and Function of Adaptive Regulatory T Cells. *Immunity*. 2014;41(2): 270–282.
307. Pereira BI, Devine OP, Vukmanovic-Stejic M, Chambers ES, Subramanian P, Patel N, et al. Senescent cells evade immune clearance via HLA-E-mediated NK and CD8+ T cell inhibition. *Nature Communications*. 2019;10(1): 2387.
308. Kale A, Sharma A, Stolzing A, Desprez PY, Campisi J. Role of immune cells in the removal of deleterious senescent cells. *Immunity & Ageing*. 2020;17(1): 16.
309. Mistry AR, O’Callaghan CA. Regulation of ligands for the activating receptor NKG2D. *Immunology*. 2007;121(4): 439–447.
310. Li DY, Xiong XZ. ICOS+ Tregs: A Functional Subset of Tregs in Immune Diseases. *Frontiers in Immunology*. 2020;11: 2104.
311. Wikenheiser DJ, Stumhofer JS. ICOS Co-Stimulation: Friend or Foe? *Frontiers in Immunology*. 2016;7: 304.
312. Parnes JR, Pan C. CD72, a negative regulator of B-cell responsiveness. *Immunological reviews*. 2000;176: 75–85.
313. Correa-Rocha R, Lopez-Abente J, Gutierrez C, Pérez-Fernández VA, Prieto-Sánchez A, Moreno-Guillen S, et al. CD72/CD100 and PD-1/PD-L1 markers are increased on T and B cells in HIV-1+ viremic individuals, and CD72/CD100 axis is correlated with T-cell exhaustion. *PLOS ONE*. 2018;13(8): e0203419.
314. Taga K, Tosato G. IL-10 inhibits human T cell proliferation and IL-2 production. *The Journal of Immunology*. 1992;148(4): 1143.
315. Baitsch L, Baumgaertner P, Devêvre E, Raghav SK, Legat A, Barba L, et al. Exhaustion of tumor-specific CD8+ T cells in metastases from melanoma patients. *The Journal of Clinical Investigation*. 2011;121(6): 2350–2360.
316. Yi JS, Cox MA, Zajac AJ. T-cell exhaustion: characteristics, causes and conversion. *Immunology*. 2010;129(4): 474–481.
317. Moir S, Fauci AS. B-cell exhaustion in HIV infection: the role of immune activation. *Current Opinion in HIV and AIDS*. 2014;9(5).
318. Aruffo A, Kanner SB, SgROI D, Ledbetter JA, Stamenkovic I. CD22-mediated stimulation of T cells regulates T-cell receptor/CD3-induced signaling. *Proceedings of the National Academy of Sciences*. 1992;89(21): 10242.
319. Ghods A, Ghaderi A, Shariat M, Talei AR, Mehdipour F. TNFR2 but not TNFR1 is the main TNFR expressed by B and T lymphocytes in breast cancer draining lymph nodes. *Immunology Letters*. 2019;209: 36–44.
320. Qu Y, Zhao G, Li H. Forward and Reverse Signaling Mediated by Transmembrane Tumor Necrosis Factor-Alpha and TNF Receptor 2: Potential Roles in an Immunosuppressive Tumor Microenvironment. *Frontiers in Immunology*. 2017;8: 1675.

321. Chen X, Oppenheim JJ. Contrasting effects of TNF and anti-TNF on the activation of effector T cells and regulatory T cells in autoimmunity. *FEBS Letters*. 2011;585(23): 3611–3618.
322. Yang S, Wang J, Brand DD, Zheng SG. Role of TNF–TNF Receptor 2 Signal in Regulatory T Cells and Its Therapeutic Implications. *Frontiers in Immunology*. 2018;9: 784.
323. Ye LL, Wei XS, Zhang M, Niu YR, Zhou Q. The Significance of Tumor Necrosis Factor Receptor Type II in CD8+ Regulatory T Cells and CD8+ Effector T Cells. *Frontiers in Immunology*. 2018;9: 583.
324. Oppenheim JJ. IL-2: More Than a T Cell Growth Factor. *The Journal of Immunology*. 2007;179(3): 1413.
325. Chazen GD, Pereira GM, LeGros G, Gillis S, Shevach EM. Interleukin 7 is a T-cell growth factor. *Proceedings of the National Academy of Sciences*. 1989;86(15): 5923.
326. Steel JC, Waldmann TA, Morris JC. Interleukin-15 biology and its therapeutic implications in cancer. *Trends in Pharmacological Sciences*. 2012;33(1): 35–41.
327. Shang B, Liu Y, Jiang S, Juan, Liu Y. Prognostic value of tumor-infiltrating FoxP3+ regulatory T cells in cancers: a systematic review and meta-analysis. *Scientific Reports*. 2015;5(1): 15179.
328. McDaniel JR, Pero SC, Voss WN, Shukla GS, Sun Y, Schaetzle S, et al. Identification of tumor-reactive B cells and systemic IgG in breast cancer based on clonal frequency in the sentinel lymph node. *Cancer Immunology, Immunotherapy*. 2018;67(5): 729–738.
329. Gu-Trantien C, Loi S, Garaud S, Equeter C, Libin M, de Wind A, et al. CD4+ follicular helper T cell infiltration predicts breast cancer survival. *The Journal of Clinical Investigation*. 2013;123(7): 2873–2892.
330. Tangye SG, Ferguson A, Avery DT, Ma CS, Hodgkin PD. Isotype Switching by Human B Cells Is Division-Associated and Regulated by Cytokines. *The Journal of Immunology*. 2002;169(8): 4298.
331. Sorenmo KU, Krick E, Coughlin CM, Overley B, Gregor TP, Vonderheide RH, et al. CD40-Activated B Cell Cancer Vaccine Improves Second Clinical Remission and Survival in Privately Owned Dogs with Non-Hodgkin’s Lymphoma. *PLOS ONE*. 2011;6(8): e24167.
332. Wennhold K, Shimabukuro-Vornhagen A, von Bergwelt-Baildon M. B Cell-Based Cancer Immunotherapy. *Transfusion Medicine and Hemotherapy*. 2019;46(1): 36–46.
333. Egbuniwe IU, Karagiannis SN, Nestle FO, Lacy KE. Revisiting the role of B cells in skin immune surveillance. *Trends in Immunology*. 2015;36(2): 102–111.
334. Haro MA, Littrell CA, Yin Z, Huang X, Haas KM. PD-1 Suppresses Development of Humoral Responses That Protect against Tn-Bearing Tumors. *Cancer Immunology Research*. 2016;4(12): 1027.

335. Mercogliano MF, Bruni S, Mauro F, Elizalde PV, Schillaci R. Harnessing Tumor Necrosis Factor Alpha to Achieve Effective Cancer Immunotherapy. *Cancers*. 2021;13(3).
336. Harada K, Shimoda S, Kimura Y, Sato Y, Ikeda H, Igarashi S, et al. Significance of immunoglobulin G4 (IgG4)-positive cells in extrahepatic cholangiocarcinoma: Molecular mechanism of IgG4 reaction in cancer tissue. *Hepatology*. 2012;56(1): 157–164.
337. Kimura Y, Harada K, Nakanuma Y. Pathologic significance of immunoglobulin G4–positive plasma cells in extrahepatic cholangiocarcinoma. *Human Pathology*. 2012;43(12): 2149–2156.



## Articles

**Harris RJ**, Cheung A, Ng JCF, Laddach R, Chenoweth AM, Crescioli S, et al. **Tumor-Infiltrating B Lymphocyte Profiling Identifies IgG-Biased, Clonally Expanded Prognostic Phenotypes in Triple-Negative Breast Cancer.** *Cancer Research.* 2021;81(16): 4290. (Summarised in Chapter 3, Full manuscript and Supplementary material found in **Appendix**).

Willsmore ZN, **Harris RJ**, Crescioli S, Hussein K, Kakkassery H, Thapa D, et al. **B Cells in Patients With Melanoma: Implications for Treatment With Checkpoint Inhibitor Antibodies.** *Frontiers in Immunology.* 2021;11: 3560.

Egbuniwe IU, **Harris RJ**, Nakamura M, Nestle FO, Akbar AN, Karagiannis SN, et al. **B Lymphocytes Accumulate and Proliferate in Human Skin at Sites of Cutaneous Antigen Challenge.** *Journal of Investigative Dermatology.* 2021.

Roulstone V, Mansfield D, **Harris RJ**, Twigger K, White C, de Bono J, et al. **Antiviral antibody responses to systemic administration of an oncolytic RNA virus: the impact of standard concomitant anticancer chemotherapies.** *Journal for ImmunoTherapy of Cancer.* 2021;9(7): e002673.

Nakamura M, Bax HJ, Scotto D, Souri EA, Sollie S, **Harris RJ**, et al. **Immune mediator expression signatures are associated with improved outcome in ovarian carcinoma.** *Oncoimmunology.* 2019;8(6): e1593811

Willsmore ZN, Coumbe BGT, Crescioli S, Reci S, Gupta A, **Harris RJ**, et al. **Combined anti-PD-1 and anti-CTLA-4 checkpoint blockade: Treatment of melanoma and immune mechanisms of action.** *European Journal of Immunology.* 2021;51(3): 544–556.

Khair DO, Bax HJ, Mele S, Crescioli S, Pellizzari G, Khiabany A, Nakamura M, **Harris RJ**, et al. **Combining Immune Checkpoint Inhibitors: Established and Emerging Targets and Strategies to Improve Outcomes in Melanoma.** *Frontiers in Immunology*. 2019;10: 453.



## B Cells in Patients With Melanoma: Implications for Treatment With Checkpoint Inhibitor Antibodies

Zena N. Willmore<sup>1</sup>, Robert J. Harris<sup>1</sup>, Silvia Crescioli<sup>1</sup>, Khuluud Hussein<sup>1</sup>, Helen Kakkassery<sup>1</sup>, Deepika Thapa<sup>1</sup>, Anthony Cheung<sup>1,2</sup>, Jitesh Chauhan<sup>1</sup>, Heather J. Bax<sup>1,3</sup>, Alicia Chenoweth<sup>1,2</sup>, Roman Laddach<sup>1,4</sup>, Gabriel Osborn<sup>1</sup>, Alexa McCraw<sup>1</sup>, Ricarda M. Hoffmann<sup>1</sup>, Mano Nakamura<sup>1</sup>, Jenny L. Geh<sup>5</sup>, Alastair MacKenzie-Ross<sup>6</sup>, Ciaran Healy<sup>5</sup>, Sophia Tsoka<sup>4</sup>, James F. Spicer<sup>3</sup>, Sophie Papa<sup>6,7</sup>, Linda Barber<sup>3</sup>, Katie E. Lacy<sup>1</sup> and Sophia N. Karagiannis<sup>1,2\*</sup>

### OPEN ACCESS

#### Edited by:

Maria Manuela Rosado,  
Independent Researcher,  
Rome, Italy

#### Reviewed by:

Andrea Picchianti-Diamanti,  
Sapienza University, Italy  
Gordon Cook,  
University of Leeds, United Kingdom

#### \*Correspondence:

Sophia N. Karagiannis  
sophia.karagiannis@kcl.ac.uk

#### Specialty section:

This article was submitted to  
B Cell Biology,  
a section of the journal  
Frontiers in Immunology

Received: 28 October 2020

Accepted: 04 December 2020

Published: 25 January 2021

#### Citation:

Willmore ZN, Harris RJ, Crescioli S,  
Hussein K, Kakkassery H, Thapa D,  
Cheung A, Chauhan J, Bax HJ,  
Chenoweth A, Laddach R, Osborn G,  
McCraw A, Hoffmann RM,  
Nakamura M, Geh JL,  
MacKenzie-Ross A, Healy C, Tsoka S,  
Spicer JF, Papa S, Barber L, Lacy KE  
and Karagiannis SN (2021) B  
Cells in Patients With Melanoma:  
Implications for Treatment With  
Checkpoint Inhibitor Antibodies.  
Front. Immunol. 11:622442.  
doi: 10.3389/fimmu.2020.622442

<sup>1</sup> St. John's Institute of Dermatology, School of Basic & Medical Biosciences, King's College London, Tower Wing, Guy's Hospital, London, United Kingdom, <sup>2</sup> Breast Cancer Now Research Unit, School of Cancer & Pharmaceutical Sciences, King's College London, Guy's Cancer Centre, London, United Kingdom, <sup>3</sup> School of Cancer & Pharmaceutical Sciences, King's College London, Guy's Hospital, London, United Kingdom, <sup>4</sup> Department of Informatics, Faculty of Natural and Mathematical Sciences, King's College London, London, United Kingdom, <sup>5</sup> Department of Plastic Surgery at Guy's, King's, and St. Thomas' Hospitals, London, United Kingdom, <sup>6</sup> Department of Medical Oncology, Guy's and St Thomas' NHS Foundation Trust, London, United Kingdom, <sup>7</sup> ImmunoEngineering, School of Cancer and Pharmaceutical Sciences, Faculty of Life Sciences and Medicine, King's College London, London, United Kingdom

The contributions of the humoral immune response to melanoma are now widely recognized, with reports of positive prognostic value ascribed to tumor-infiltrating B cells (TIL-B) and increasing evidence of B cells as key predictors of patient response to treatment. There are disparate views as to the pro- and anti-tumor roles of B cells. B cells appear to play an integral role in forming tumor-associated tertiary lymphoid structures (TLSs) which can further modulate T cell activation. Expressed antibodies may distinctly influence tumor regulation in the tumor microenvironment, with some isotypes associated with strong anti-tumor immune response and others with progressive disease. Recently, B cells have been evaluated in the context of cancer immunotherapy. Checkpoint inhibitors (CPIs), targeting T cell effector functions, have revolutionized the management of melanoma for many patients; however, there remains a need to accurately predict treatment responders. Increasing evidence suggests that B cells may not be simple bystanders to CPI immunotherapy. Mature and differentiated B cell phenotypes are key positive correlates of CPI response. Recent evidence also points to an enrichment in activatory B cell phenotypes, and the contribution of B cells to TLS formation may facilitate induction of T cell phenotypes required for response to CPI. Contrastingly, specific B cell subsets often correlate with immune-related adverse events (irAEs) in CPI. With increased appreciation of the multifaceted role of B cell immunity, novel therapeutic strategies and biomarkers can be explored and translated into the clinic to optimize CPI immunotherapy in melanoma.

**Keywords:** melanoma, B cell, checkpoint inhibition therapy, antibody, humoral immune response

## B Lymphocytes Accumulate and Proliferate in Human Skin at Sites of Cutaneous Antigen Challenge

JID Open

Journal of Investigative Dermatology (2021) ■, ■-■; doi:10.1016/j.jid.2021.06.038

### TO THE EDITOR

B cells play important roles in skin diseases (Egbuniwe et al., 2015) and in cutaneous homeostasis (Geherin et al., 2016, 2012; Nihal et al., 2000). Mature class-switched IgG<sup>+</sup> B cells have been detected in normal human skin (Saul et al., 2016) featuring clonally restricted B-cell receptors, indicating narrow antigenic repertoires (Nihal et al., 2000). However, the involvement of B cells during an antigenic stimulus in human skin remains unexplored. B cells are relatively scarce in normal human skin (Supplementary Figure S1), explaining why past studies have primarily focused on T cells, which constitute the major skin-resident lymphocyte population (Clark et al., 2006b; Jiang et al., 2012; Sanchez Rodriguez et al., 2014).

We investigated the dynamics of B-cell infiltration in the skin after local antigen challenge with varicella-zoster virus (VZV; provided by Prof A.N. Akbar, University College London, UK) and candida (Candin) antigens (Allermid Laboratories, San Diego, CA) by taking skin biopsies from and inducing suction blisters over the site of intradermal injection in human skin in vivo. The induction of skin suction blisters has been reproducibly employed in examining the cellular kinetics of skin-infiltrating immune subsets, including T cells in delayed-type hypersensitivity responses after intradermal injection of recall antigens (Vukmanovic-Stejic et al., 2013); innate lymphoid cells after challenge with house dust mite (Salimi et al., 2013); and different leukocyte subsets (including B cells) during acute inflammation (Akbar et al., 2013; Jenner et al., 2014).

Flow cytometric analysis (FACSCanto II or LSRFortessa Cell Analyser - Becton Dickinson, Franklin Lakes, NJ) showed CD19<sup>+</sup>CD20<sup>+</sup> B cells in low numbers (mean percentage of total lymphocyte population) in fluid from skin suction blisters induced without antigen challenge (mean = 0.05%, n = 3) (Figure 1a and b). This, in addition to immunofluorescence studies on normal skin (Supplementary Figure S1), confirmed that B cells were scarce under homeostatic conditions in unperturbed skin. After intradermal challenge with VZV antigen, CD20<sup>+</sup> B cells (percentage of total live lymphocytes) were detected on day 3 (mean = 0.26%, n = 3) and day 7 (mean = 5.07%, n = 3) blisters (Figure 1c). Blister fluid obtained from sites injected with sterile saline (Advanz Pharma, London, UK) contained lower percentages of B cells on both day 3 and day 7 compared with VZV blisters (Figure 1c). A trend toward lower absolute numbers of cells extracted from saline blister fluid (n = 5, mean = 5.1 cells per ml) than that from VZV blister fluid (n = 5, mean = 48.1 cells per ml) was seen, although this did not reach statistical significance.

Markers of skin-homing B cells remain undefined, although cutaneous lymphocyte antigen (CLA) is expressed on circulating B cells after percutaneous immunization with tetanus toxoid toxin (Kantele et al., 2003). We examined circulating CD20<sup>+</sup> B cells by flow cytometry for expression of classical T-cell skin-homing markers CLA, CCR4, and CCR10 (Clark et al., 2006a; McCully et al., 2012). The percentages of CLA<sup>+</sup>CD20<sup>+</sup> B cells were significantly greater than those of CCR4<sup>+</sup>CD20<sup>+</sup> B cells (no significant

differences between CCR10<sup>+</sup>CD20<sup>+</sup> and CLA<sup>+</sup>CD20<sup>+</sup> cells) (Supplementary Figure S2). CLA<sup>+</sup>CD20<sup>+</sup> B cells were identified within VZV blister aspirates on day 3 after challenge (mean = 19.5%, n = 3) and persisted within cutaneous blisters on day 7 after VZV challenge (mean = 0.71%, n = 3). CLA<sup>+</sup>CD3<sup>+</sup> T cells were present (day 3: mean = 64.6%, day 7: mean = 57.7%, n = 3) (Figure 1e and f) as described (Clark et al., 2006a).

We next investigated antibody production from cutaneous B cells. Flow cytometric analyses revealed populations of mature (CD22<sup>+</sup>CD27<sup>-</sup>) and memory (CD22<sup>+</sup>CD27<sup>+</sup>) B cells within suction blister aspirates on days 3 and 7 after VZV challenge (Figure 1g and h). Steady-state circulating plasma cells lose expression of CD20 but retain high expression of CD27 and CD38, with or without CD138 expression (Caraux et al., 2010). We detected distinct populations of CD38<sup>hi</sup>CD138<sup>+</sup> in CD3<sup>-</sup>CD27<sup>+</sup> circulating plasma cells in blood but not in blister fluids of two donors (one assessed on day 3 and one on day 7) after VZV injection (Figure 1i and j). CD38<sup>int</sup>CD138<sup>+</sup> B cells were also identified within the blister fluid and peripheral blood (day 3 and day 7; Figure 1j), likely representing short-lived plasmablasts known to have antibody-secreting capabilities (Nutt et al., 2015).

VZV-specific IgA and IgG antibodies are produced in response to primary VZV infection, with IgG persisting long term (Arvin, 1996). We detected IgG antibodies (ImmunoCAP assay and Total IgG ELISA; Supplementary Materials and Methods) at higher mean titres within VZV (n = 10, mean = 3.705 mg/ml) and candida (n = 4, mean = 3.688 mg/ml) blister fluids than within saline controls (n = 4, mean = 2.142 mg/ml), although statistical significance was not achieved (Figure 1k). IgG titres within VZV blisters were greater than IgA, IgE,

Abbreviations: CLA, cutaneous lymphocyte antigen; VZV, varicella-zoster virus

Accepted manuscript published online XXX; corrected proof published online XXX

© 2021 The Authors. Published by Elsevier, Inc. on behalf of the Society for Investigative Dermatology. This is an open access article under the CC BY license (<http://creativecommons.org/licenses/by/4.0/>).



# Antiviral antibody responses to systemic administration of an oncolytic RNA virus: the impact of standard concomitant anticancer chemotherapies

Victoria Roulstone,<sup>1</sup> David Mansfield <sup>1</sup>, Robert J Harris,<sup>2</sup> Katie Twigger,<sup>1</sup> Christine White,<sup>1</sup> Johann de Bono,<sup>1</sup> James Spicer <sup>2</sup>, Sophia N Karagiannis <sup>2</sup>, Richard Vile,<sup>3</sup> Hardev Pandha,<sup>4</sup> Alan Melcher,<sup>1</sup> Kevin Harrington <sup>1</sup>

**To cite:** Roulstone V, Mansfield D, Harris RJ, et al. Antiviral antibody responses to systemic administration of an oncolytic RNA virus: the impact of standard concomitant anticancer chemotherapies. *Journal for ImmunoTherapy of Cancer* 2021;**9**:e002673. doi:10.1136/jitc-2021-002673

► Additional supplemental material is published online only. To view, please visit the journal online (<http://dx.doi.org/10.1136/jitc-2021-002673>).

Accepted 05 July 2021



© Author(s) (or their employer(s)) 2021. Re-use permitted under CC BY. Published by BMJ.

<sup>1</sup>Radiotherapy and Imaging, The Institute of Cancer Research, London, UK

<sup>2</sup>St John's Institute of Dermatology, Guy's Hospital, London, UK

<sup>3</sup>Department of Molecular Medicine, Mayo Clinic, Rochester, Minnesota, USA

<sup>4</sup>Faculty of Health and Medical Sciences, University of Surrey, Guildford, UK

**Correspondence to**  
Mr David Mansfield;  
david.mansfield@icr.ac.uk

## ABSTRACT

**Background** Oncolytic reovirus therapy for cancer induces a typical antiviral response to this RNA virus, including neutralizing antibodies. Concomitant treatment with cytotoxic chemotherapies has been hypothesized to improve the therapeutic potential of the virus. Chemotherapy side effects can include immunosuppression, which may slow the rate of the antiviral antibody response, as well as potentially make the patient more vulnerable to viral infection.

**Method** Reovirus neutralizing antibody data were aggregated from separate phase I clinical trials of reovirus administered as a single agent or in combination with gemcitabine, docetaxel, carboplatin and paclitaxel doublet or cyclophosphamide. In addition, the kinetics of individual antibody isotypes were profiled in sera collected in these trials.

**Results** These data demonstrate preserved antiviral antibody responses, with only moderately reduced kinetics with some drugs, most notably gemcitabine. All patients ultimately produced an effective neutralizing antibody response.

**Conclusion** Patients' responses to infection by reovirus are largely unaffected by the concomitant drug treatments tested, providing confidence that RNA viral treatment or infection is compatible with standard of care treatments.

## INTRODUCTION

Mammalian orthoreovirus type 3 Dearing (hereafter referred to as reovirus) is a wild-type double-stranded RNA virus. While reovirus is non-pathogenic in humans, it has been shown to replicate selectively in cells that have an activated or mutated Ras signaling pathway<sup>1</sup> and this inspired research into its use as an oncolytic virus. Later research indicated that the oncolytic activity of reovirus may be contingent on a more complex and nuanced mechanism than simply being Ras enabled.<sup>2,3</sup>

It has been suggested that antireoviral antibody responses may hinder the anti-tumor efficacy of reovirus. It has also been

postulated that frequent, high doses of virus given before an antibody response peaks or cytotoxic chemotherapy-mediated attenuation of the antibody titer might enhance systemic delivery of virus to tumor tissue.<sup>4</sup> More recently, preclinical data have suggested that the antireovirus neutralizing antibody response may, paradoxically, enhance therapy in mouse models.<sup>5,6</sup> This effect, which occurs after cotreatment with granulocyte-macrophage colony-stimulating factor, was predicated on enhanced monocyte/macrophage virus carriage and delivery to tumor. It is not known if this phenomenon occurs in patients.

Reovirus has been tested as a single agent in multiple clinical trials in patients with advanced cancers, initially intratumorally<sup>7</sup> and then intravenously.<sup>8,9</sup> No dose-limiting toxicities were observed, and clear signs of single-agent activity were observed, with a 37% response rate in the first trial of intratumoural administration<sup>10</sup> and a 45% response rate in the first trial of intravenous administration, improving to 67% in patients with confirmed viral shedding.<sup>11</sup> Subsequently, preclinical and clinical studies combining reovirus with standard anticancer chemotherapies were conducted in an attempt to further improve responses.<sup>12-17</sup> These phase I trials, which variously involved combinations with gemcitabine, platinum and taxanes, primarily looked for safety, tolerability and signals of efficacy, but data were also collected on the effect of chemotherapy on antiviral humoral immune responses. In particular, studies on cyclophosphamide were conducted with the premeditated intention of blunting antiviral antibody responses to allow more effective systemic delivery. Promising preclinical data<sup>18-20</sup> underpinned that phase I trial of

## Immune mediator expression signatures are associated with improved outcome in ovarian carcinoma

Mano Nakamura<sup>a</sup>, Heather J. Bax<sup>a,b</sup>, Daniele Scotto<sup>a</sup>, Elmira Amiri Souri<sup>c</sup>, Sam Sollie<sup>d</sup>, Robert J. Harris<sup>a</sup>, Niklas Hammar<sup>e</sup>, Goran Walldius<sup>f</sup>, Anna Winship<sup>g</sup>, Sharmistha Ghosh<sup>g</sup>, Ana Montes<sup>g</sup>, James F. Spicer<sup>b</sup>, Mieke Van Hemelrijck<sup>d,e</sup>, Debra H. Josephs<sup>a,b</sup>, Katie E. Lacy<sup>a</sup>, Sophia Tsoka<sup>a</sup>, and Sophia N. Karagiannis<sup>a</sup>

<sup>a</sup>St. John's Institute of Dermatology, School of Basic and Medical Biosciences, King's College London, London, UK; <sup>b</sup>School of Cancer and Pharmaceutical Sciences, King's College London, London, UK; <sup>c</sup>Department of Informatics, Faculty of Natural and Mathematical Sciences, King's College London, London, UK; <sup>d</sup>King's College London, School of Cancer and Pharmaceutical Sciences, Translational Oncology & Urology Research (TOUR), London, UK; <sup>e</sup>Unit of Epidemiology, Institute of Environmental Medicine, Karolinska Institutet, Stockholm, Sweden; <sup>f</sup>Unit of Cardiovascular Epidemiology, Institute of Environmental Medicine, Karolinska Institutet, Stockholm, Sweden; <sup>g</sup>Departments of Medical Oncology and Clinical Oncology, Guy's and St Thomas' NHS Foundation Trust, London, UK

### ABSTRACT

Immune and inflammatory cascades may play multiple roles in ovarian cancer. We aimed to identify relationships between expression of immune and inflammatory mediators and patient outcomes. We interrogated differential gene expression of 44 markers and marker combinations ( $n = 1,978$ ) in 1,656 ovarian carcinoma patient tumors, alongside matched 5-year overall survival (OS) data *in silico*. Using machine learning methods, we investigated whether genomic expression of these 44 mediators can discriminate between malignant and non-malignant tissues in 839 ovarian cancer and 115 non-malignant ovary samples. We furthermore assessed inflammation markers in 289 ovarian cancer patients' sera in the Swedish Apolipoprotein MOrtality-related RiSk (AMORIS) cohort. Expression of the 44 mediators could discriminate between malignant and non-malignant tissues with at least 96% accuracy. Higher expression of classical Th1, Th2, Th17, anti-parasitic/infection and M1 macrophage mediator signatures were associated with better OS. Contrastingly, inflammatory and angiogenic mediators, CXCL-12, C-reactive protein (CRP) and platelet-derived growth factor subunit A (PDGFA) were negatively associated with OS. Of the serum inflammatory markers in the AMORIS cohort, women with ovarian cancer who had elevated levels of haptoglobin ( $\geq 1.4$  g/L) had a higher risk of dying from ovarian cancer compared to those with haptoglobin levels  $< 1.4$  g/L (HR = 2.09, 95% CI: 1.38–3.16). Our findings indicate that elevated "classical" immune mediators, associated with response to pathogen antigen challenge, may confer immunological advantage in ovarian cancer, while inflammatory markers appear to have negative prognostic value. These highlight associations between immune protection, inflammation and clinical outcomes, and offer opportunities for patient stratification based on secretome markers.

### ARTICLE HISTORY

Received 18 December 2018  
Revised 17 February 2019  
Accepted 2 March 2019

### KEYWORDS




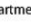
Immune activation; ovarian cancer; immune mediators; inflammation; Th1/Th2/Th17; M1/M2; inflammation; biomarkers


### Introduction

Ovarian cancer is a lethal gynecological malignancy with 5-year survival rates of  $< 48\%$  and few improvements in clinical outcomes in the last decade.<sup>1,2</sup> Complex interactions between immune and cancer cells in the tumor microenvironment involve multifaceted contributions of associated secretomes,<sup>3</sup> including critical roles in cancer progression and survival.<sup>4,5</sup> However, comprehensive evaluations of immune mediator signatures in relation to disease progression are still required to help inform prognostic or predictive algorithms for disease management.<sup>6</sup>

The immune system is capable of locating, recognizing and ultimately eliminating tumor cells,<sup>7</sup> and leukocytes play a major role in these processes. For example, T helper lymphocytes

stimulate antigen-specific effector cells, enhance cytotoxic immunity and recruit inflammatory cells to tumor sites.<sup>8</sup> Macrophages can destroy cancerous cells by innate mechanisms that involve secreted mediators such as interferon gamma (IFN $\gamma$ ), granulocyte-macrophage colony-stimulating factor (GM-CSF), and tumor necrosis factor alpha (TNF $\alpha$ ).<sup>9</sup> Macrophages can also be activated by antibodies to trigger antibody-dependent cellular cytotoxicity (ADCC) or phagocytosis (ADCP).<sup>10–12</sup> On the other hand, tumors evolve strategies to evade immunological control, including reduced antigen presentation, upregulation of anti-apoptotic molecules, modified cancer antigens arising from genomic instability and co-opting immune cells to promote tumor proliferation and spread. Ovarian cancer cells and tumor-associated fibroblasts may also secrete mediators (e.g. IL-10, VEGF, TGF $\beta$ ) which may


**CONTACT** Sophia N. Karagiannis  [sophia.karagiannis@kcl.ac.uk](mailto:sophia.karagiannis@kcl.ac.uk)  St. John's Institute of Dermatology, School of Basic & Medical Biosciences, King's College London & NIHR Biomedical Research Centre at Guy's and St. Thomas's Hospitals and King's College London, Guy's Hospital, Tower Wing, 9th Floor, London SE1 9RT, United Kingdom; Sophia Tsoka  [sophia.tsoka@kcl.ac.uk](mailto:sophia.tsoka@kcl.ac.uk)  Department of Informatics, Faculty of Natural and Mathematical Sciences, King's College London, Bush House, London WC2B 4BG, United Kingdom

 Supplemental data for this article can be accessed on the publisher's website.

© 2019 The Author(s). Published with license by Taylor & Francis Group, LLC.  
This is an Open Access article distributed under the terms of the Creative Commons Attribution License (<http://creativecommons.org/licenses/by/4.0/>), which permits unrestricted use, distribution, and reproduction in any medium, provided the original work is properly cited.

## REVIEW

**Combined anti-PD-1 and anti-CTLA-4 checkpoint blockade: Treatment of melanoma and immune mechanisms of action**

Zena N. Willmore<sup>1</sup>, Ben G. T. Coumbe<sup>1</sup>, Silvia Crescioli<sup>1</sup>, Sara Reci<sup>1</sup>, Ayushi Gupta<sup>1</sup>, Robert J. Harris<sup>1</sup>, Alicia Chenoweth<sup>1,2</sup>, Jitesh Chauhan<sup>1</sup>, Heather J. Bax<sup>1,3</sup>, Alexa McCraw<sup>1</sup>, Anthony Cheung<sup>1,2</sup>, Gabriel Osborn<sup>1</sup>, Ricarda M. Hoffmann<sup>1</sup>, Mano Nakamura<sup>1</sup>, Roman Laddach<sup>1,4</sup>, Jenny L. C. Geh<sup>5</sup>, Alastair MacKenzie-Ross<sup>5</sup>, Ciaran Healy<sup>5</sup>, Sophia Tsoka<sup>4</sup>, James F. Spicer<sup>3</sup>, Debra H. Josephs<sup>1,3</sup>, Sophie Papa<sup>6,7</sup>, Katie E. Lacy<sup>1</sup> and Sophia N. Karagiannis<sup>1,2</sup> 

<sup>1</sup> St. John's Institute of Dermatology, School of Basic & Medical Biosciences, King's College London, London, SE1 9RT, United Kingdom

<sup>2</sup> Breast Cancer Now Research Unit, School of Cancer & Pharmaceutical Sciences, King's College London, Guy's Cancer Centre, London, United Kingdom

<sup>3</sup> School of Cancer & Pharmaceutical Sciences, King's College London, London, United Kingdom

<sup>4</sup> Department of Informatics, Faculty of Natural and Mathematical Sciences, King's College London, London, United Kingdom

<sup>5</sup> Department of Plastic Surgery at Guy's, King's, and St. Thomas' Hospitals, London, United Kingdom

<sup>6</sup> Department of Medical Oncology, Guy's and St. Thomas' NHS Foundation Trust, London, United Kingdom

<sup>7</sup> ImmunoEngineering, School of Cancer and Pharmaceutical Sciences, Faculty of Life Sciences and Medicine, King's College London, London, United Kingdom

Cytotoxic T-lymphocyte associated protein-4 (CTLA-4) and the Programmed Death Receptor 1 (PD-1) are immune checkpoint molecules that are well-established targets of antibody immunotherapies for the management of malignant melanoma. The monoclonal antibodies, Ipilimumab, Pembrolizumab, and Nivolumab, designed to interfere with T cell inhibitory signals to activate immune responses against tumors, were originally approved as monotherapy. Treatment with a combination of immune checkpoint inhibitors may improve outcomes compared to monotherapy in certain patient groups and these clinical benefits may be derived from unique immune mechanisms of action. However, treatment with checkpoint inhibitor combinations also present significant clinical challenges and increased rates of immune-related adverse events. In this review, we discuss the potential mechanisms attributed to single and combined checkpoint inhibitor immunotherapies and clinical experience with their use.

**Keywords:** PD-1 · CTLA-4 · Cancer · Immunotherapy · Melanoma

Correspondence: Prof. Sophia N. Karagiannis  
e-mail: sophia.karagiannis@kcl.ac.uk

© 2021 The Authors. *European Journal of Immunology* published by Wiley-VCH GmbH

www.eji-journal.eu

This is an open access article under the terms of the Creative Commons Attribution License, which permits use, distribution and reproduction in any medium, provided the original work is properly cited.



# Combining Immune Checkpoint Inhibitors: Established and Emerging Targets and Strategies to Improve Outcomes in Melanoma

Duaa O. Khair<sup>1</sup>, Heather J. Bax<sup>1,2</sup>, Silvia Mele<sup>1</sup>, Silvia Crescioli<sup>1</sup>, Giulia Pellizzari<sup>1</sup>, Atousa Khiabany<sup>1</sup>, Mano Nakamura<sup>1</sup>, Robert J. Harris, Elise French<sup>1</sup>, Ricarda M. Hoffmann<sup>1,2</sup>, Iwan P. Williams<sup>1</sup>, Anthony Cheung<sup>1,3</sup>, Benjamin Thair<sup>1</sup>, Charlie T. Beales<sup>1</sup>, Emma Touizer<sup>1</sup>, Adrian W. Signell<sup>1</sup>, Nahrin L. Tasnova<sup>1</sup>, James F. Spicer<sup>2</sup>, Debra H. Josephs<sup>1,2</sup>, Jenny L. Geh<sup>4</sup>, Alastair MacKenzie Ross<sup>4</sup>, Ciaran Healy<sup>4</sup>, Sophie Papa<sup>2</sup>, Katie E. Lacy<sup>1</sup> and Sophia N. Karagiannis<sup>1\*</sup>

## OPEN ACCESS

### Edited by:

Christian Ostheimer,  
Martin Luther University of  
Halle-Wittenberg, Germany

### Reviewed by:

Nicole Joller,  
University of Zurich, Switzerland  
Daniel Olive,  
Aix Marseille Université, France

### \*Correspondence:

Sophia N. Karagiannis  
sophia.karagiannis@kcl.ac.uk

### Specialty section:

This article was submitted to  
Cancer Immunity and Immunotherapy,  
a section of the journal  
Frontiers in Immunology

**Received:** 30 August 2018

**Accepted:** 20 February 2019

**Published:** 19 March 2019

### Citation:

Khair DO, Bax HJ, Mele S, Crescioli S,  
Pellizzari G, Khiabany A, Nakamura M,  
Harris RJ, French E, Hoffmann RM,  
Williams IP, Cheung A, Thair B,  
Beales CT, Touizer E, Signell AW,  
Tasnova NL, Spicer JF, Josephs DH,  
Geh JL, MacKenzie Ross A, Healy C,  
Papa S, Lacy KE and Karagiannis SN  
(2019) Combining Immune  
Checkpoint Inhibitors: Established and  
Emerging Targets and Strategies to  
Improve Outcomes in Melanoma.  
*Front. Immunol.* 10:453.  
doi: 10.3389/fimmu.2019.00453

<sup>1</sup> St. John's Institute of Dermatology, School of Basic & Medical Biosciences, Guy's Hospital, King's College London, London, United Kingdom, <sup>2</sup> School of Cancer & Pharmaceutical Sciences, Guy's Hospital, King's College London, London, United Kingdom, <sup>3</sup> Breast Cancer Now Research Unit, School of Cancer & Pharmaceutical Sciences, Guy's Cancer Centre, King's College London, London, United Kingdom, <sup>4</sup> Department of Plastic Surgery at Guy's, King's, and St. Thomas' Hospitals, London, United Kingdom

The immune system employs several checkpoint pathways to regulate responses, maintain homeostasis and prevent self-reactivity and autoimmunity. Tumor cells can hijack these protective mechanisms to enable immune escape, cancer survival and proliferation. Blocking antibodies, designed to interfere with checkpoint molecules CTLA-4 and PD-1/PD-L1 and counteract these immune suppressive mechanisms, have shown significant success in promoting immune responses against cancer and can result in tumor regression in many patients. While inhibitors to CTLA-4 and the PD-1/PD-L1 axis are well-established for the clinical management of melanoma, many patients do not respond or develop resistance to these interventions. Concerted efforts have focused on combinations of approved therapies aiming to further augment positive outcomes and survival. While CTLA-4 and PD-1 are the most-extensively researched targets, results from pre-clinical studies and clinical trials indicate that novel agents, specific for checkpoints such as A2AR, LAG-3, IDO and others, may further contribute to the improvement of patient outcomes, most likely in combinations with anti-CTLA-4 or anti-PD-1 blockade. This review discusses the rationale for, and results to date of, the development of inhibitory immune checkpoint blockade combination therapies in melanoma. The clinical potential of new pipeline therapeutics, and possible future therapy design and directions that hold promise to significantly improve clinical prognosis compared with monotherapy, are discussed.

**Keywords:** checkpoint inhibitors, combination immunotherapy, immunoncology therapeutics, melanoma, CTLA-4, PD-1, PD-L1, antibody engineering